INTEGRATED BIOLOGICAL, CHEMICAL AND PHYSICAL PROCESSES KINETIC MODEL FOR THE ANAEROBIC DIGESTION OF PRIMARY SEWAGE SLUDGE

By

Pierre van Rensburg

Thesis submitted for the degree of
Master of Science in Engineering
at the University of Cape Town

University of Cape Town
Department of Civil Engineering

September 2001

DECLARATION BY CANDIDATE

I, Pierre van Rensburg, hereby declare that
this thesis is my own work and has not
been submitted for a degree at another University

September 2001

ACKNOWLEDGEMENTS

I wish to express my sincere gratitude and thanks to:

Professor M.C. Wentzel, Department of Civil Engineering, University of Cape Town, for his unremitting interest, patience, guidance and support. His sound advice and critical review of this thesis is very much appreciated.

Professor G.A. Ekama, Department of Civil Engineering, University of Cape Town, for his sustained interest, guidance and support at all times.

Professor R.E. Loewenthal, Department of Civil Engineering, University of Cape Town, for his incisive suggestions and invaluable inputs.

Mr. N.E. Ristow, fellow postgraduate student, for his willingness to share his experience and knowledge throughout the duration of this study.

The Water Research Commission for providing financial support for the research.

My parents, for their love, support and never - ending believe in me.

THE ALMIGHTY – this was possible through his grace, love and guidance alone!

SYNOPSIS

BACKGROUND AND MOTIVATION

Anaerobic digestion has developed technologically to such an extent, that it has established itself as a reliable method for sludge stabilization. Furthermore, it has proven itself technologically feasible in reducing the volumes of sludge with the production of energy rich biogas (methane). Accordingly, the application of anaerobic digestion to the stabilization of sewage sludges (primary and waste activated) is widespread worldwide, and this research project focuses on this application.

Despite its widespread application, the design, operation and control of anaerobic digesters treating sewage sludges still is largely based on experience, or empirical guidelines. To aid the design, operation and control of (and research into) anaerobic digestion, a mathematical model would be an invaluable process evaluation tool. Mathematical models provide quantitative descriptions of the treatment system of interest. By providing quantitative descriptions, they allow predictions of the system response and performance to be made. From the predictions, design and operational criteria can be identified for optimization of the system performance. Also, mathematical models are very useful as research tools. By evaluating the model predictions, it is possible to test hypothesis on the behaviour of the system (e.g. biological processes, their response to system constraints, etc.) in a consistent and integrated fashion.

Recognising the potential usefulness of mathematical models various researchers have developed such models for anaerobic digestion. However, the vast majority of these models have focussed almost exclusively on the biological processes operative in the anaerobic digester. (e.g. Hill and Barth, 1977; Gujer and Zehnder, 1983; Sam-Soon *et al.*, 1991; Kiely *et al.*, 1996). By focussing on the biological processes it is implicitly accepted that: (i) the biological processes take place within a regime of constant pH, (ii) chemical and physical processes (e.g. precipitation and gas stripping respectively) play an

insignificant role compared to the biological processes and accordingly can be neglected or rudimentarily incorporated, and (iii) compounds not directly involved in the biological processes of interest, even though present, do not significantly influence their behaviour.

In anaerobic digestion, however, pH does play a very important role in regulating the processes, especially as many of the processes have been shown to be extremely sensitive to pH changes. Since acetic acid is produced as the main intermediary product in anaerobic digestion, the assumption of a constant pH regime clearly becomes invalid. Furthermore, as alkalinity is routinely used as a measure of predicting the state of health of anaerobic digesters by many operators, compounds not part of the anaerobic processes, but influencing alkalinity become important. Additionally, in some anaerobic digestion systems precipitation of minerals is significant, either within the digester itself, or in pipework leading from the digester (e.g. Borgerding, 1972; Mamais *et al.*, 1994). Accordingly, a complete kinetic model for anaerobic digesters should include the biological processes, aqueous phase weak acid/base chemistry with pH explicitly included, aqueous/gas phase gas exchange (in particular CO_2) and solid/aqueous phase mineral precipitation.

Musvoto *et al.* (1997; 1998) have developed a kinetic weak acid/base chemistry model aimed at integration with existing biological models. This model is based on general principles according to which any weak acid/base specie can be added, to form a complete pH interlinked weak acid/base chemistry system. The model was also extended to include the full three phase gas/aqueous/solid weak acid/base chemistry. As the entire model used kinetic rate equations to describe the different processes taking place, it is ideally suited for integration with any existing kinetic model describing biological processes.

Thus, the Musvoto *et al.* (1996; 1998) model can form a useful starting point for the development of a kinetic model that completely describes the three phase (solid/aqueous/gas) biological, chemical and physical processes operative in anaerobic digestion of sewage sludge – this is the main objective of this research project.

PRINCIPAL AIM

The principal aim of this research project was to:

- Develop a three phase (aqueous/gas/solid) kinetic model describing the anaerobic digestion of sewage sludges, which integrates the biological, chemical and physical processes.

To achieve the aim above, the research project was divided into two main phases:

- Development and evaluation of a kinetic model that describes the three phase chemical and physical processes possibly operative in the anaerobic digestion of sewage sludges, and
- Develop an integrated two phase (aqueous/gas) biological, chemical and physical model aimed at describing the anaerobic digestion system, with SCFA and alkalinity as two prominent components describing the stability of the digester.

If the above two phases could be completed, then the two kinetic models could be readily integrated, to form a complete three phase model describing anaerobic digestion of sewage sludges. However, due to the lack of available comprehensive data in the literature, and the constraints of time the integration of the two models falls beyond the scope of this research project.

MODEL DEVELOPMENT

As set out above, the research project was divided into two main phases towards developing the model.

Phase I: Three phase chemical and physical processes kinetic model

First, it was decided to evaluate the kinetic model (as developed by Musvoto *et al.*, 1998; 2000a, b, c) that describes the three phase (aqueous/solid/gas) chemical and physical processes likely to be operative in the anaerobic digestion of sewage sludges. The mineral precipitation problems in units treating sludge from anaerobic digesters being

experienced by the Cape Flats Wastewater Treatment Plant (Cape Town), presented an ideal opportunity to gather data against which the model of Musvoto *et al.* could be evaluated extensively, and to use the model to gain insight into the mineral precipitation problem. A series of experimental investigations were carried out on ADS drawn from the anaerobic digesters at the Cape Flats Wastewater Treatment Plant. These included batch aeration tests, pH controlled experiments and extended pH controlled experiments. The kinetic model of Musvoto *et al.* (1998; 2000a, b and c) was then applied to the experimental results to address the tasks above. From this investigation, with regard to the mineral precipitation the following conclusions could be made:

- The dominant mineral that precipitates is struvite. For the batch test conducted, struvite was dominant (516 mg/ℓ as $MgNH_4PO_4.6H_2O$ = 97% of mass of precipitant), followed by ACP (16.8 mg/ℓ as $Ca_3(PO_4)_2$ = 3% of the mass of precipitant), and negligible newberyite, calcite and magnesite precipitate. Similarly, for the extended pH change test, the dominant mineral that precipitates is struvite (217mg/ℓ as $MgNH_4PO_4.6H_2O$ = 99.8% of mass of precipitant), followed by very small amount of ACP (0.36 mg/ℓ as $Ca_3(PO_4)_2$ = 0.2% of the mass of precipitant), and negligible newberyite, calcite and magnesite precipitate. These observations are similar to those of Musvoto *et al.* With the large volumes of ADS passing to the pelletization plant, this represents substantial precipitation potential.
- The precipitation of struvite is stimulated by the increase in pH when CO_2 is lost from the ADS. Within the anaerobic digester, the partial pressure of CO_2 is high due to anaerobic processes acting in the digester. When the ADS leaves the digester it comes into contact with atmospheric conditions where the partial pressure of CO_2 is much lower than inside the digester. This causes CO_2 loss from the ADS to the air, until equilibrium between the CO_2 concentration in the ADS and the air is reached. Loss of CO_2 can also be caused by pressure drops at pipe bends, pumps, etc. The loss of CO_2 represents an increase in acidity which means that the pH of the ADS will increase. This increase in pH causes struvite to become supersaturated, and hence it precipitates. Increasing the pH by addition

of NaOH also results in struvite precipitation and confirms that the increase in pH is the primary process driving the struvite precipitation.

- When the ADS leaves the digester, it is initially undersaturated with respect to struvite. Depending on the initial conditions in the ADS, significant struvite only starts precipitating when the pH increases above pH = 7.3 to 7.7. This indicates that if the pH of the ADS can be maintained below about 7.3 along the sludge treatment line, then significant struvite precipitation will not take place.
- With aeration, the critical pH for struvite precipitation is reached after 40 to 60 minutes aeration. However, this time will depend on a number of factors, including aeration rate, initial pH, buffer capacity, initial P and Mg concentrations, etc.
- With aeration, the loss of CO_2 from the ADS causes the pH to increase which stimulates struvite precipitation. Initially, the rate of CO_2 loss is rapid. However, as the partial pressure of CO_2 in the ADS approaches that in the atmosphere, the rate of CO_2 loss and consequent pH increase slows, and this effectively slows the rate of struvite precipitation with time. The maximum pH reached with aeration was about pH = 8. However, from about pH = 7.8 the rate of pH increase with time was very low, and consequently, the struvite precipitation effectively ceased. The pH = 7.8 was reached after about 80 minutes. However, this time will depend on a number of factors, including aeration rate, initial pH, buffer capacity, initial P and Mg concentrations, etc.
- The rate of struvite precipitation is very fast, so that essentially, in the aeration of the ADS from Cape Flats, struvite is at equilibrium between the precipitant and soluble species at all times. Thus, in this case the rate of struvite precipitation is not limited by the precipitation kinetics, but rather by the rate in increase in pH through aeration.
- The amount of struvite that precipitates is limited by two factors: With aeration to increase pH, the struvite precipitating is limited by the final pH reached and the initial Mg concentration present - if the initial Mg concentration is increased, then more struvite precipitates. With addition of NaOH, the struvite precipitating is limited by the initial Mg concentration present - after precipitation the Mg

concentration is very low, while significant concentrations of P and N are still present.

- The initial concentrations of P and Mg in the ADS were variable, with P ranging from 89 to 190 mgP/ℓ and Mg from 29 to 67 mgMg/ℓ This is probably indicative of the variable performance of the activated sludge system with regard to BEPR. The higher P concentrations are in agreement with values measured for anaerobically digested BEPR sludges in Johannesburg, at 150 to 250 mgP/ℓ (Pitman, 1995). Should BEPR become more reliable in the activated sludge system at Cape Flats, consistently higher P and Mg concentrations can be expected, with the resultant larger masses of struvite precipitating.
- The change in FSA due to struvite precipitation is insignificant compared with the amount of FSA present. Thus, FSA does not provide a reliable assessment of struvite precipitation, and will not limit the amount of struvite that potentially can precipitate.
- The increase in pH with aeration also stimulates precipitation of ACP. However, as noted above, the mass of ACP precipitating is relatively small compared with struvite. The ADS is initially undersaturated with respect to ACP, and ACP precipitation initiates only after the pH increases above 7.7.
- In running experiments on the ADS, the solids concentrations were so high that the ADS could not be effectively filtered. Accordingly, the ADS was allowed to settle for 5 days and the supernatant used for the experimental investigations. Accordingly, the effect of solids concentration on mineral precipitation could not be evaluated, e.g. factors such as surface area for nucleation of minerals, inhibition or poisoning of crystal growth. However, the effect of solids is not expected to be significant, because theoretical modelling of the precipitation gave close correspondence with measured values.
- In the experimental investigation it was found that filtering samples through 0.45µm filters caused significant CO_2 loss, which resulted in increase in pH. To counter this, the samples should be acidified prior to filtration with these filters.
- The pH change tests provide a simple rapid method to assess struvite precipitation potential.

With regard to the kinetic model of Musvoto *et al.*:

- Keeping the default values for the model constants except for the struvite precipitation rate (increased from 300/d to 1000/d), close agreement was obtained between theoretically measured and predicted values, for pH, Mg, Ca, C_T, FSA and P_T.
- The kinetic model of Musvoto *et al.* adequately describes integrated three phase chemical and physical processes modelling.
- The inherent value of such a model was clearly demonstrated.

Phase II: Two phase biological, chemical and physical processes kinetic model.

This phase was aimed at developing a two phase (aqueous/gas) integrated biological, chemical and physical processes kinetic model for the anaerobic digestion of primary sewage sludge. Accordingly, the following tasks were identified towards completion of this phase:

- Develop a kinetic model for describing the biological processes operative in the anaerobic digestion of primary sewage sludges.
- Integrate the weak acid/base chemistry and CO_2 gas exchange model developed by Musvoto *et al.*, (1997; 1998; 2000a, b) with the biological model above, for a complete description of the two phases in the anaerobic digestion of primary sewage sludges.
- Calibrate and validate the model using experimental data available in the literature.

The proposed model was developed in stages. First, the biological processes kinetic model was set up. Then the weak acid/base chemistry kinetic model as developed by Musvoto *et al.* (2000) was integrated with the biological reactions. The complete model was then calibrated and validated against the experimental data set of Izzet *et al.* (1992). Finally, the model was modified and applied to examine anaerobic digester failure.

Biological processes kinetic model

The biological processes kinetic model was based on a modification and simplification of the Gujer and Zehnder (1983) reaction scheme. In setting up the biological processes kinetic model, of note were:

- The primary sludge was formulated as a generic organic representing the combined carbohydrates, lipids and proteins.
- The primary sludge was hydrolysed to the intermediate organic glucose, since the anaerobic pathways with glucose are well established.
- The effect of hydrogen partial pressure ($\overline{p}H_2$) on the anaerobic pathways was incorporated.
- With the exception of the hydrolysis process, formulations for the kinetic rates of the processes were in terms of the appropriate organism group growth rates.
- Where possible, formulations for the kinetic rates were drawn from literature.
- For the hydrolysis processes, the conventional first order rate formulation was rejected, and replaced by planar surface saturation kinetics, similar to that used for the hydrolysis of slowly biodegradable COD in activated sludge systems (Dold *et al.* 1980). This was to eliminate the shortcoming of the first order expression, of varying specific rate constants for different systems.
- The stoichiometry for the processes was developed from the established biochemical reactions.

Weak acid/base chemistry kinetic model

This section of the model was taken directly from that developed by Musvoto *et al.* (1998; 2000c). However, since propionic acid is a key intermediate in the anaerobic digestion process, this weak acid/base was added to the model, by following the approach of Musvoto *et al.*

Model calibration

Where possible, values for model constants were drawn from the literature. However, due to the novel formulation of the hydrolysis process, three aspects required calibration:

- Stoichiometric formulation of the primary sludge

- Hydrolysis process maximum specific rate and half saturation constant.
- Unbiodegradable fraction of the primary sludge.

Values for these were determined from the experimental data set of Izzet *et al.* (1992). In this calibration exercise, it became evident that:

- The stoichiometrical chemical formulation used for the primary sludge is crucial. This formulation in effect determines the amount of N and C contained in the influent per measured COD, and hence determines (i) the total N and C that leaves the system, (ii) the production of NH_3 in the hydrolysis and therefore H^+ consumption (alkalinity generation), (iii) the relative amounts of CH_4 and CO_2 in the gas, and (iv) the amount of inorganic C dissolved in the effluent. For the N, this could be determined from measurements on the influent TKN and FSA, as the organic N content of the primary sludge (TKN – FSA). However, for the C this had to be determined from a C mass balance on the experimental data. Accepting these, the formulation for the primary sludge was found to be $C_{3.5}H_7O_2N_{0.196}$. However, it is not certain whether this formulation is general or restricted to the Izzet *et al.* (1992) data. Recognising the importance of the formulation in the modelling efforts, clearly this is an area that requires further investigation.
- A single pair of hydrolysis rate constants could adequately describe the data of Izzet *et al.* (1992), see Chapter 6, Section 6.3.6.
- The unbiodegradable fraction of the primary sludge in the Izzet *et al.* (1992) experiments was 36%. This corresponds to the value determined by O'Rourke *et al.* (1968) in an independent investigation.

Model validation

The model was validate by application to the data set of Izzet *et al.* (1992). From this application:

- With a single set of constants, close correlation could be achieved between predicted and measured results for:
  - effluent COD
  - effluent free and saline ammonia (FSA)
  - effluent short chain fatty acids (SCFA)

- effluent $H_2CO_3^*$ alkalinity
- effluent pH
- CO_2 gas production
- CH_4 gas production
- $\overline{p}CO_2$

This lends substantive support to validating the model.

- The advantage of the proposed planar surface saturation kinetics for the hydrolysis rate over the conventional first order kinetics was clearly demonstrated – with a single pair of hydrolysis rate constants the observed behaviour could be correctly predicted for all retention times (7 to 20 days), whereas the first order kinetics requires different rate constants for each retention time. This indicates that the proposed hydrolysis kinetics are more general.
- The interactions between the biological processes and weak acid/base chemistry could be correctly predicted for stable steady stae operation of anaerobic digesters.
- It was recognized that the same data set was used for calibrating the hydrolysis process (Chapter 6, Section 6.3.5) and validating the model. Accordingly it was proposed that future work should examine application of the model to other data sets in the literature. However, sufficiently comprehensive data sets are not readily available.

Digester failure

Having shown that the model can accurately predict stable anaerobic digester behaviour, the model was modified to incorporate literature reported sensitivities of acetoclastic and hydrogenotrophic methanogens to pH. This proved possible since weak acid/base chemistry, particularly pH, were explicitly included in the model. The resultant model was then used to simulate digester failure, caused by temporary inhibition of the acetoclastic methanogens. The resultant failure process correlates well with observations reported in the literature. This demonstrates the usefulness of the developed kinetic model.

TABLE OF CONTENTS

LIST OF SYMBOLS AND ABBREVIATIONS

SYMBOL	DESCRIPTION
Ac^-	Acetate
Acetyl – CoA	Acetyl coenzyme A
ACP	Amorphous calcium phosphate
ADL	Anaerobic digester liquor
ADP	Adenosine diphosphate
ADS	Anaerobic digester supernatant
Alk	Alkalinity
ATP	Adenosine triphosphate
BEPR	Biological excess phosphorus removal
Ca^{2+}	Calcium ion
$CaCO_3$	Calcium carbonate (Calcite)
CH_4	Methane
CMC	Cape Metropolitan Council
CO_2	Carbon dioxide
CO_3^{2-}	Carbonate ion
COD	Chemical oxygen demand (g/m^3)
COD_p	Sewage sludge biodegradable organics
COD_{pu}	Sewage sludge unbiodegradable organics
COD_s	Soluble glucose
C_T	Total inorganic carbonate species (mol/l)
DCP	Monenite
DCPD	Dicalcium phosphate dihydrate (brushite)
EMP	Embden - Meyerhof pathway
f_m	Monovalent activity coefficient
f_d	Divalent activity coefficient
f_t	Trivalent activity coefficient
Fe	Iron

FSA	Free and saline ammonia
h	Hours
H^+	Hydrogen ion
H_2	Molecular hydrogen
HAc	Undissociated acetic acid
HAP	Hydroxyapatite
HCl	Hydrochloric acid
HCO_3^-	Bicarbonate ion
H_2CO_3	Undissociated carbonic acid
$H_2CO_3^*$	Sum of molecularly dissolved carbon dioxide and undissociated carbonic acid
HNLC	High nutrient low organic carbon
HNO_3	Nitric acid
HPO_4^{2-}	Hydrogen orthophosphate ion
$H_2PO_4^-$	Dihydrogen orthophosphate ion
H_3PO_4	Orthophosphoric acid
HPr	Undissociated propionic acid
ICP	Inductively coupled plasma
K^+	Potassium ion
K, K'	General symbol for the thermodynamic and apparent equilibrium constant for the dissociation of weak acid/bases and ion association reaction for the formation of ion pairs.
K_f, K'_f	General symbol for the thermodynamic and apparent specific rate constant for the forward reaction of the dissociation of weak acid/bases and ion association reaction for the formation of ion pairs.
k_h	First order rate constant
k_{max}	Maximum specific rate constant
K_r, K'_r	General symbol for the thermodynamic and apparent specific rate constant for the forward reaction of the dissociation of weak

	acid/bases and ion association reaction for the formation of ion pairs.
Ks	Half saturation constant
Mg^{2+}	Magnesium ion
MLE	Modified Ludzack Ettinger
N	Nitrogen
Na^{+}	Sodium ion
NAD^{+}	Nicotinamide adenine dinucleotide
NaOH	Sodium hydroxide
NH_3	Ammonia
NH_4^{+}	Ammonium ion
N_T	Total inorganic nitrogen species (mol/l)
OCP	Octacalcium phosphate
P	Phosphorus
PAO	Phosphate accumulating organisms
$\bar{p}CO_2$	Partial pressure of carbon dioxide
$\bar{p}H_2$	Hydrogen partial pressure
pK	General symbol for the negative logarithm of an equilibrium constant, subscript denotes the particular reaction.
pKs	General symbol for the negative logarithm of the solubility product, subscript denotes the particular compound
PO_4^{3-}	orthophosphate
Pr^{-}	Propionate
PS	Primary sludge
P_T	Total inorganic phosphate species concentration (mol/l)
R	Universal gas constant
s	Seconds
SCFA	Short-chain fatty acids
SRP	Soluble reactive phosphate
TCP	Tricalcium phosphate
TKN	Total Kjeldahl Nitrogen

UASB	Upflow anaerobic sludge bed
UCT	University of Cape Town
V	Volume
WAS	Waste activated sludge
WRC	Water Research Commission
X_a	Acidogen active biomass
X_{AM}	Acetoclastic methanogen active biomass
X_{HM}	Hydrogenotrophic methanogen active biomass
X_p	Acetogen active biomass
Y_{Ac}	Biomass yield from the growth of acidogens
Y_{AP}	Biomass yield from the growth of acetogens
Y_{AM}	Biomass yield from the growth of acetoclastic methanogens
YH_{AM}	Biomass yield from the growth of hydrogenotrophic methanogens

CHAPTER 1

INTRODUCTION

1.1 RESEARCH BACKGROUND

Anaerobic digestion is one of the oldest biological wastewater treatment processes, dating back more than a century. With the development of digester heating and mixing, anaerobic digestion has established itself as the most common method of sludge stabilization, and has proven to be technological feasible also in reducing the volumes of sludge with the production of energy rich biogas. Anaerobic digestion has been shown to work for a number of organic sludges, ranging from municipal waste activated and primary sludges (Kayhanian and Tchobanoglous, 1992; Cout *et al.*, 1994) to industrial organic sludges and agricultural slurries (Hill and Barth, 1977). In particular, the application of anaerobic digestion to the stabilization of sewage sludges (primary and waste activated) is widespread worldwide, and this research project focuses on this application.

Despite its widespread application, the design, operation and control of anaerobic digesters treating sewage sludges still is largely based on experience, or empirical guidelines. To aid the design, operation and control of (and research into) anaerobic digestion, a mathematical model would be an invaluable process evaluation tool. Mathematical models provide quantitative descriptions of the treatment system of interest. By providing quantitative descriptions, they allow predictions of the system response and performance to be made. From the predictions, design and operational criteria can be identified for optimization of the system performance. Also, mathematical models are very useful as research tools. By evaluating the model predictions, it is possible to test hypothesis on the behaviour of the system (e.g. biological processes, their response to system constraints, etc.) in a consistent and integrated fashion. This may direct attention to issues not so obvious from the physical system, and lead to a deeper

understanding of the fundamental behavioural patterns controlling the system response. In essence, mathematical models can provide a refined framework which can direct thinking (design, operation or research).

Recognising the potential usefulness of mathematical models, in the literature various researchers have developed such models to describe anaerobic digestion, aimed at improving understanding of the process (e.g. Hill and Barth, 1977; Gujer and Zehnder, 1983; Sam-Soon *et al.*, 1991; Kiely *et al.*, 1997). However, the vast majority of these models have focussed almost exclusively on the biological processes operative in the anaerobic digester. By focussing on the biological processes it is implicitly accepted that: (i) the biological processes take place within a regime of constant pH, (ii) chemical and physical processes (e.g. precipitation and gas stripping respectively) play an insignificant role compared to the biological processes and accordingly can be neglected, and (iii) compounds not directly involved in the biological processes of interest, even though present, do not significantly influence their behaviour.

In anaerobic digestion, however, pH does play a very important role in regulating the processes, especially as many of the processes have been shown to be extremely sensitive to pH changes. Since acetic acid is produced as the main intermediary product in anaerobic digestion, the assumption of a constant pH regime clearly becomes invalid. Furthermore, as alkalinity is routinely used as a measure of predicting the state of health of anaerobic digesters by many operators, compounds not part of the anaerobic processes, but influencing alkalinity become important. Additionally, in some anaerobic digestion systems precipitation of minerals is significant, either within the digester itself, or in pipework leading from the digester (e.g. Borgerding, 1972; Mamais *et al.*, 1994). Accordingly, a complete kinetic model for anaerobic digesters should include the biological processes, aqueous phase weak acid/base chemistry with pH explicitly included, aqueous/gas phase gas exchange (in particular CO_2) and solid/aqueous phase mineral precipitation.

Musvoto *et al.* (1997; 1998; 2000a, b and c) have developed a kinetic weak acid/base chemistry model aimed at integration with existing biological models. This model is based on general principles according to which any weak acid/base specie can be added, to form a complete pH interlinked weak acid/base chemistry system. The model was also extended to include the full three phase gas/aqueous/solid weak acid/base chemistry. As the entire model used kinetic rate equations to describe the different processes taking place, it is ideally suited for integration with any existing kinetic model describing biological processes.

Thus, the Musvoto *et al.* (1997; 1998; 2000a, b and c) model can form a useful starting point for the development of a kinetic model that completely describes the three phase (solid/aqueous/gas) biological, chemical and physical processes operative in anaerobic digestion of sewage sludge. The development of such a model is the main objective in this research project.

1.2 PRINCIPAL AIM

The principal aim of this research project was to:

- Develop a three phase (aqueous/gas/solid) kinetic model describing the anaerobic digestion of sewage sludges, which integrates the biological, chemical and physical processes.

To achieve the aim above, the research project was divided into two main phases:

- Development and evaluation of a kinetic model that describes the three phase chemical and physical processes possibly operative in the anaerobic digestion of sewage sludges, and

- Develop an integrated two phase (aqueous/gas) biological, chemical and physical model aimed at describing the anaerobic digestion system, with SCFA and alkalinity as two prominent components describing the stability of the digester.

The two kinetic models would be evaluated with data from the literature where possible; where data are not available, this will be collected through experimental investigations.

If the above two phases could be completed, then the two kinetic models could be readily integrated, to form a complete three phase model describing anaerobic digestion of sewage sludges. Due to the lack of available data in the literature, and the constraints of time the integration of the two models falls beyond the scope of this research project.

1.3 RESEARCH APPROACH

The research was divided into a two main phases, and in each a number of tasks were identified for completion of the project:

Phase I: Three phase chemical and physical processes kinetic model.

Musvoto *et al.* (1998; 2000a, b) have developed a kinetic model describing the aeration treatment of anaerobic digester supernatant. This model includes the three phase chemical and physical processes operative in such a treatment scheme. Since the model is based on kinetics, it can be readily integrated with a kinetic model describing the biological processes. Accordingly, it was decided to accept this model for this phase of the research project. However, the model would be extensively evaluated against experimental data, and modified if necessary. The Cape Flats Wastewater Treatment Plant (Cape Town, South Africa) was experiencing mineral precipitation difficulties in unit processes treating sludges from the anaerobic digesters, e.g. in the centrifuges and pipelines. This presented an ideal opportunity to evaluate the Musvoto *et al.* (1998; 2000a, b) model, and to gain greater insight into the mineral precipitation problem at the Cape Flats Wastewater Treatment Plant. Thus, specific tasks identified for this phase were:

- Evaluating the kinetic model of Musvoto *et al.* (1998; 2000a,b), and

- Gaining insight into the mineral precipitation problem at the Cape Flats Wastewater Treatment Plant and providing possible solutions to resolving the problem.

The above would be achieved through:

- Experimental tests on the anaerobic digester supernatant (aeration and chemical)
- Modelling the test results to determine:
    - The ability of the kinetic model to correctly predict the observed behaviour
    - From the predictions to determine:
        - ◊ the types of minerals that precipitate
        - ◊ the concentrations of the different minerals that form
        - ◊ the mineral precipitation and gas stripping rates
        - ◊ mineral precipitation potential and rates.

Phase II: Two phase biological, chemical and physical processes kinetic model

In this phase, the following specific tasks were identified:

- Develop a kinetic model to describe the biological processes operative in the anaerobic digestion of sewage sludges.

- Integrate the weak acid/base chemistry model developed by Musvoto *et al.*, (1997; 1998; 2000a, b) with the biological model, above for a complete description of the two phases in the anaerobic digestion of sewage sludges.

- Calibrate the model using experimental data available in the literature.

1.4 REPORT LAYOUT

To address the objectives above, the research report details:

- Chapter 2 - Literature review of the biological processes in anaerobic digestion, as well as the three phase chemical and physical processes model developed by Musvoto *et al.* (1997; 1998; 2000a, b).

- Chapter 3 - Application of the three phase chemical and physical model of Musvoto *et al.* to investigate mineral precipitation in anaerobic digester supernatant from the Cape Flats Wastewater Treatment Plant.

- Chapter 4 - Development of an integrated two phase (aqueous/gas) biological, chemical and physical processes kinetic model for the description of anaerobic digestion of sewage sludges.

- Chapter 5 - Calibration and validation of the model developed in Chapter 4 using experimental data from the literature.

CHAPTER 2

LITERATURE SURVEY

2.1 INTRODUCTION

Anaerobic digestion is among the oldest biological wastewater treatment processes, having first been used more than a century ago (McCarty, 1981). The development of digester heating and mixing, has led to anaerobic digestion establishing itself as one of the most common methods of sludge treatment. Advances made in the area of anaerobic digestion has seen the process also being applied to include agricultural wastes (e.g. plant residues, animal waste) and food processing wastewaters, all of which are considered concentrated wastes (i.e. high content of biodegradable organics).

Among the advantages of anaerobic treatment is the production of methane gas, a useable source of energy. In contrast, aerobic processes require energy input in operation for oxygen supply. In addition, the synthesis of biological cells during anaerobic treatment is considerably lower than with aerobic processes, tending to minimize sludge disposal problems and nutrient requirements. Recognition of the advantages of anaerobic processes over those of aerobic processes, has led to the development of new anaerobic process configurations capable of treating medium and low strength soluble and colloidal wastes (e.g. municipal wastewater) (Jewell, 1987).

Process kinetics plays a central role in the development and operation of anaerobic treatment systems; incorporated in an appropriate model, kinetics provide a rational basis for process analysis, control and design. In this research project, the objective is to develop such a kinetic model, to describe the processes operative in anaerobic digestion of sewage sludges. In the anaerobic digestion of sewage sludges, biological, weak acid/base chemistry, gas exchange/loss and mineral precipitation processes will be of importance. Accordingly the kinetic model should incorporate these processes. In this Chapter, a brief review of these processes is presented.

2.2 BIOLOGICAL PROCESSES

To ensure surety in kinetic model application, the biological processes incorporated should be based on an understanding of the biochemistry and microbiology of the biologically mediated reactions. This section presents an overview of the biological processes common to anaerobic digestion systems.

The anaerobic degradation of complex, particulate organic materials has been described as a multistep scheme of series and parallel reactions/processes (Kaspar and Wuhrmann, 1987; Gujer and Zehnder, 1983). The 6 step reaction scheme as adapted from Gujer and Zehnder (1983) is shown in Fig 2.1.

First, complex polymeric materials such as polysaccharides, proteins and lipids (fats and grease) are hydrolyzed (Step 1) by extra cellular enzymes to soluble products of a size small enough to allow their transport across the cell membrane. These relative simple, soluble compounds are fermented (Step 2) or anaerobically oxidized (Step 3) to short chain fatty acids, alcohols, carbon dioxide, hydrogen and ammonia. Some of the products of hydrolysis also end up as intermediary products (propionate, butyrate, etc.). The intermediate short chain fatty acids (other than acetate) are converted to acetate, hydrogen gas and carbon dioxide through a process called acetogenesis (Step 4). Lastly, methanogenesis occurs from carbon dioxide reduction by hydrogen (Step 6) and from acetate cleavage (Step 5).

The above reactions are all biologically mediated by micro-organisms. Microbiological reactions are autocatalytic; meaning the catalyst for the biologically mediated reaction (i.e. micro-organisms, a microbial population) will be produced by the reaction itself. Therefore, in a complex biological system, such as an anaerobic digester at steady state, the size of each distinct group of micro-organisms mediating specific biological reactions will be proportional to the flux of its corresponding substrate in the system, the constant of proportionality being the organism yield.

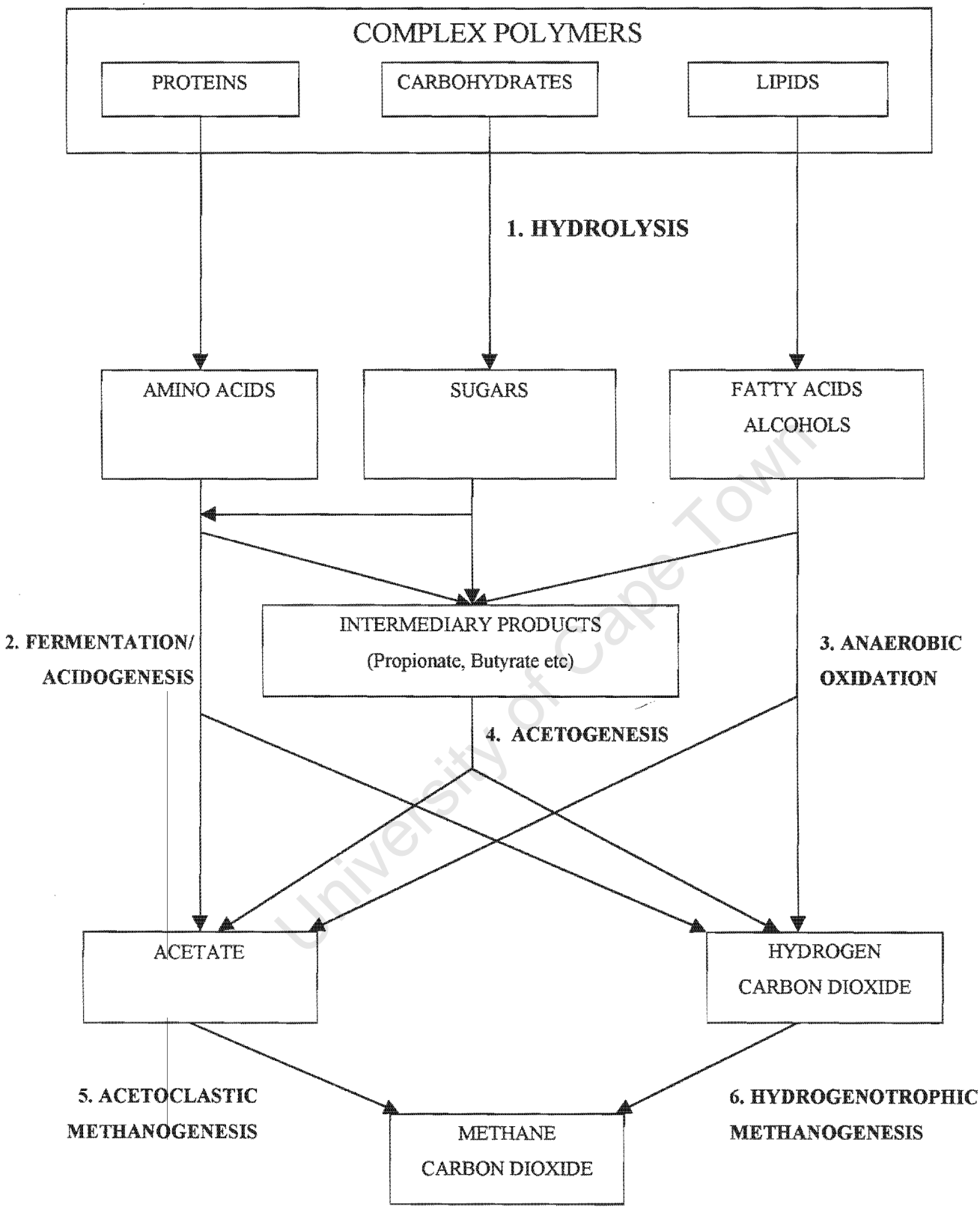

Fig 2.1: Reaction scheme for the anaerobic digestion of polymeric materials.

Therefore, the composition of the microbial population of a reactor will depend greatly on the feed material and its composition. However, since micro-organisms are also sensitive to the operating conditions (e.g. pH, temperature, residence time) their populations will depend on these also, as well as the stoichiometry of the reactions involved. In the reaction scheme as described in Figure 2.1, four distinct microbial groups are identified (Massé and Droste, 1999). The major groups of bacteria and the reactions they mediate are as follows:

- Fermentative (acidogenic) bacteria – hydrolysis, fermentation and anaerobic oxidation (Steps 1-3)
- Hydrogen producing acetogenic bacteria – acetogenesis (Step 4)
- Acetoclastic methanogens – acetoclastic methanogenesis (Step 5)
- Hydrogen-reducing methanogens – hydrogenotrophic methanogenesis (Step 6)

It is very important to note that, because of the slow growth rate of some of these micro-organisms, it may take a considerable period of time for the digester to reach steady state, and establish a "mature" microbial population. Interpreting results where some of the populations have not reached steady state may lead to gross misunderstanding of the system.

2.2.1 Step 1 – Hydrolysis

It is not possible for micro-organisms to utilize complex organic polymeric material unless it has first been broken down (hydrolysed) to soluble compounds (usually simple polymers or monomers) which can then pass through the cell membrane. Thus, solubilization is the first step required for microbial utilization of complex biopolymers

and is carried out extra cellularly by a group of organisms collectively called the acidogens.

In terms of chemical composition, three groups of organics are considered to be the major components of complex organics: carbohydrates, proteins and lipids. The separate hydrolysis of each of these different components has been studied and a summary of the findings are given by Pavlostathis *et al.* (1991). Generally the kinetic rates for hydrolysis have been assumed as first order with respect to substrate concentration, with different kinetic constants for the different components (i.e. carbohydrates proteins, lipids). The end products of the hydrolysis of proteins, carbohydrates and lipids are short chain compounds, the amino acids, sugars and fatty acids and alcohols respectively.

2.2.2 Step 2 - Acidogenesis/Fermentation

Acidogenesis or fermentation is the process whereby substrate molecules from hydrolysis (i.e. fatty acids, amino acids and sugars) are converted intracellularly by the acidogenic organisms to short chain fatty acids (SCFA) (e.g. acetic, propionic and butyric acids), carbon dioxide and hydrogen gas. The biochemical pathways by which the substrate is fermented and the nature of the end product (i.e. type of SCFA produced) will depend primarily on the type of substrate and the hydrogen partial pressure ($\overline{p}H_2$). For example, fatty acids usually are fermented only under low $\overline{p}H_2$ via β–oxidation, either to acetic acid and hydrogen if the fatty acid contains an even number of carbons, or to acetic and propionic acids if it contains an odd number of carbons. Sugars are usually fermented via the Embden-Meyerhof pathway to SCFA (such as acetate, butyrate and propionate), hydrogen and carbon dioxide (CO_2). The relative fractions of the various SCFA, however, are dependent on the $\overline{p}H_2$ in the medium. At low $\overline{p}H_2$, glucose is fermented to acetic acid, butyric acid, hydrogen and carbon dioxide (Sam-Soon *et al.* (1990a) put forward a theory for the non-appearance of butyrate in real systems). Under conditions of high $\overline{p}H_2$, glucose is fermented to acetic acid, propionic acid, butyric acid and carbon

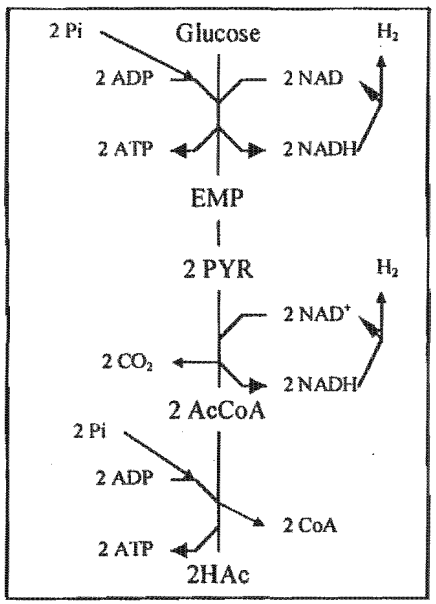

(a) Acetic acid generation

($\overline{p}H_2 < 10^{-3.7}$ atm)

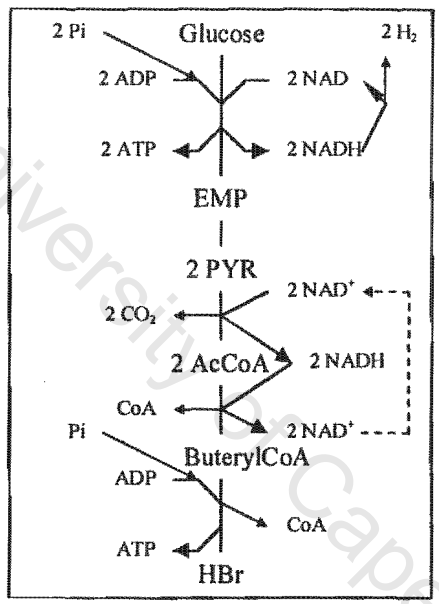

(b) Butyric acid generation

($\overline{p}H_2 < 10^{-3.7}$ atm and $> 10^{-3.7}$ atm)

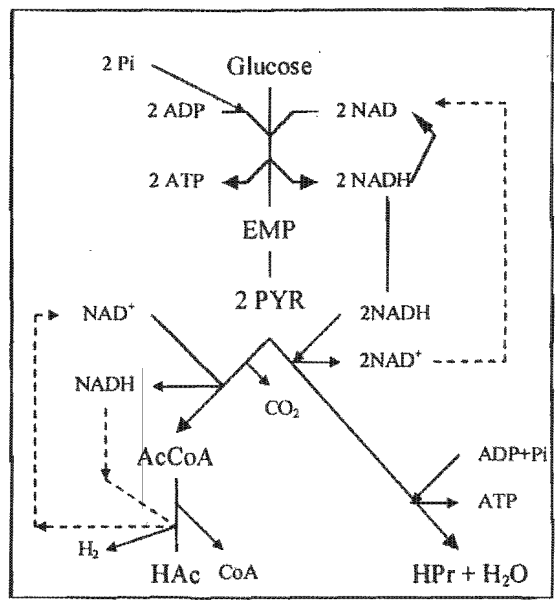

(c) Acetic and propionic acid generation

($\overline{p}H_2 > 10^{-3.7}$ atm)

Fig 2.2: Acidogenic phase of glucose fermentation under low and high H_2 partial pressures to form acetic acid, butyric acid and propionic acid (after Sam-Soon *et al.*, 1990)

dioxide. The detailed fermentation pathways for glucose under low and high $\overline{p}H_2$, are shown in Fig 2.2 (a, b and c). Under both low and high $\overline{p}H_2$, glucose is fermented first to pyruvic acid and intracellular generated electrons (attached to the electron accepting co-enzyme NAD^+, forming NADH) via the Embden-Meyerhof Pathway (EMP), see Fig 2.2; thereafter the pathways differ depending on the electron sink utilised to dehydrogenate the NADH: under low $\overline{p}H_2$, only intracellular protons (H^+) act as the terminal electron acceptor (i.e. H^+ is the electron sink), under high $\overline{p}H_2$, pyruvic, acetyl-CoA and protons act as electron acceptors. The sequences whereby the electron transfer takes place in the respective acidogenic stages are described below:

Sequence 1: (Embden-Meyerhof pathway, both high and low $\overline{p}H_2$)

Glucose is fermented to pyruvic acid and hydrogen via the Embden-Meyerhof pathway (EMP). The hydrogen is attached to the electron-carrying co-enzyme, NAD^+, and 2 moles ATP per mole glucose are obtained by the organisms, i.e.

$$C_6H_{12}O_6\,(\text{glucose}) + 2NAD^+ + 2ADP + 2P \Rightarrow 2CH_3COCOOH\,(\text{pyruvic acid}) + 2\text{NADH} + 2\text{ATP} \qquad (2.1)$$

That is, one mole of glucose generates 2 moles of pyruvic acid. Sequence 1 is common to both low and high $\overline{p}H_2$; Fig 2.2 (a, b and c).

Sequence 2: (Dehydrogenation)

The NADH formed in sequence 1 needs to be dehydrogenated to maintain a high level of NAD^+ in order that the Embden-Meyerhof pathway remains operative (NAD^+ acts as the electron acceptor in the EMP). Dehydrogenation can take place in one of three ways depending on the $\overline{p}H_2$:

Under low $\overline{p}H_2$ ($\overline{p}H_2$ of less than $10^{-3.7}$ atm, calculated from Lehninger, 1972) (see Fig 2.2a) oxidation of NADH is a downhill reaction, i.e. NADH is oxidised spontaneously to NAD^+ and hydrogen gas, i.e.

$$2NADH \Rightarrow 2NAD^{+} + 2H_2 \qquad (2.2)$$

The NAD^{+} thus regenerated acts as electron acceptor for further oxidation of glucose to pyruvic acid via the EMP (sequence 1, Eq 2.1). The two moles pyruvic acid generated in sequence 1, Eq (2.1) are oxidised further to acetyl CoA and carbon dioxide (Fig 2.2a):

$$2CH_3COCOOH + 2NAD^{+} \Rightarrow 2CH_3CoA + 2CO_2 + 2NADH \qquad (2.3)$$

The 2 moles NADH formed from this step again are dehydrogenated spontaneously to form hydrogen gas, as in Eq (2.2); the two moles of acetyl-CoA are converted to 2 moles acetic acid with concomitant of 2 moles ATP, i.e.

$$2CH_3CoA + 2ADP + 2P \Rightarrow 2CH_3COOH + 2ATP \qquad (2.4)$$

Hence, under low $\overline{p}H_2$ the overall fermentation of 1 mole glucose is:

$$C_6H_{12}O_6 + 2H_2O + 4ADP + 4P \Rightarrow CH_3COOH + 2CO_2 + 4H_2 + 4ATP \qquad (2.5)$$

The overall reaction depicted by Eq (2.5) is only slightly downhill; a small change in $\overline{p}H_2$, for example, will cause the reaction to become thermodynamically unfavourable. Noting from Eq (2.5) that H_2 is released, the rate of H_2 removal must be at least as fast as H_2 generation in order to maintain the low $\overline{p}H_2$ condition required for acetate generation only. In the production of H_2, if the $\overline{p}H_2$ increases only slightly, the reaction could become thermodynamically unfeasible until H_2 is removed, i.e. $\overline{p}H_2$ declines again.

It would seem that in the intermediate $\overline{p}H_2$ state the acidogens utilise an alternative pathway (Fig 2.2b) in which butyric acid is produced. Experimental investigations have shown that during acidogenic fermentation of glucose under low $\overline{p}H_2$ conditions, acetate

is not the only SCFA generated, butyrate also is generated (Thauer *et al.*, 1977; Jones and Woods, 1986):

In the fermentation of 1 mole glucose to acetate as the only SCFA, hydrogen and carbon dioxide, 4 moles ATP are generated; this implies an 85 percent energy conversion approximately (Thauer *et al.*, 1977). This percentage energy conversion implies that the reaction (glucose to acetate) is only slightly downhill ($\approx$-2 Kcal/mole glucose oxidised). The conversion of glucose to butyric acid is energetically strongly downhill at the expense that only 3 moles ATP are produced per mole of glucose oxidised (cf 4 moles of ATP in acetic acid production). The possible overall pathway for butyric acid production is shown in Fig 2.2b. The overall reaction of butyric acid formation is as follows:

$$C_6H_{12}O_6 + 3ADP + 3P \Rightarrow CH_3CH_2CH_2COOH + 2CO_2 + 2H_2 + 3ATP \qquad (2.6)$$

In summary, the classification of butyric acid formation in a low $\overline{p}H_2$ system arises from the experimental difficulty of effecting glucose oxidation to acetate only (with generation of H_2 and CO_2) in pure culture systems in the absence of H_2 utilising bacteria to maintain low $\overline{p}H_2$. As noted by Sam – Soon *et al.* (1990a), in practical mixed culture systems, butyric acid usually is not observed as it is readily converted to acetic acid via acetogenesis (see below)

Under high $\overline{p}H_2$ (see Fig 2.2c), the forward reaction in Eq (2.2) is no longer thermodynamically feasible. Consequently an alternative method for oxidising the NADH generated in the EMP is needed. This effected in two ways, which may take place simultaneously, or alternatively (by the same or different groups of acidogens):

Alternative 1 – The two moles of acetyl-CoA are reduced to butyric acid, see Fig 2.2b, (Wolin, 1974; Thauer *et al.*, 1977).

$$2Ac - CoA + 2NADH + ADP + P \Rightarrow CH_3CH_2CH_2COOH + 2NAD^+ + 2H_2 + ATP \qquad (2.7)$$

This reaction is thermodynamically favourable, but at the cost of producing a less oxidised SCFA and only one ATP (cf. 2 ATP produced when 2 moles acetyl-CoA are converted to acetic acid under low $\overline{p}H_2$, Eq (2.4)).

Alternative 2 – One of the 2 moles of pyruvic acid, Eq (2.1), is reduced to propionic acid so as to oxidise the NADH produced from the EMP (Wood, 1982), see Fig 2.2c:

$$CH_3COCOOH + 2NADH + ADP + P \Rightarrow CH_3CH_2COOH + 2NAD^+ + 2H_2 + ATP \quad (2.8)$$

The remaining mole of pyruvic acid is oxidised to acetyl-CoA as in Eq (2.3), i.e.

$$CH_3COCOOH + NAD^+ \Rightarrow CH_3CoA + CO_2 + NADH \quad (2.9)$$

The NADH cannot be spontaneously oxidised to NAD^+ as the reaction is not thermodynamically favourable at high $\overline{p}H_2$. However, the organism can achieve dehydrogenation of NADH by coupling this reaction with the thermodynamically favourable reaction in which acetyl-CoA is converted to acetic acid, but at the cost that no ATP is generated (cf the low $\overline{p}H_2$ reaction where 2 moles ATP are generated, Eq (2.4)). The coupled reaction is as follows:

$$CH_3 - CoA + NADH \Rightarrow CH_3COOH + H_2 + NAD^+ \quad (2.10)$$

Hence, for alternative 2 under high $\overline{p}H_2$, the overall fermentation of glucose becomes:

$$C_6H_{12}O_6 + 2H_2O + 3ADP + 3P \Rightarrow CH_3CH_2COOH + CH_3COOH + CO_2 + H_2 + 3ATP \quad (2.11)$$

in which only 3 ATP are produced.

Fermentative bacteria, or acidogens, are generally faster growing than the other bacteria involved in anaerobic digestion, and are more resistant to inhibition than the other bacteria. For this reason, acidogenesis has sometimes been omitted from model development, since it will not limit the rate of the overall process, and will thus have little influence on the system. Similarly amino acids are fermented to a variety of end products.

2.2.3 Step 3 - Anaerobic oxidation

Domestic sludge usually has a high content of lipids and free long chain fatty acids. The free long chain fatty acids or those produced by the hydrolysis of lipids are subject to anaerobic oxidation via β – oxidation by anaerobic bacteria commonly found in anaerobic environments. Anaerobic oxidation is the process in which these long chain fatty acids are anaerobically oxidised to acetic acid and hydrogen or acetic acid, propionate and hydrogen, depending on whether the long chain fatty acids are even carbon or odd carbon acids (McInerney and Bryant, 1981). Although the rate of anaerobic oxidation has been extensively discussed by Gujer and Zehnder (1983), little emphasis has been placed on this reaction in the literature, as it follows roughly the same kinetics and reaction scheme as the acidogenesis. Accordingly, up to now this step has generally been included with the acidogenic process.

2.2.4 Step 4 – Acetogenesis

Several sources in literature report on the anaerobic oxidation of short chain fatty acids (e.g. propionate, butyrate, e.g. McInerney *et al.* (1979)). These reactions are usually termed acetogenesis, since acetate is the major carbon product. The acetogenic organisms have an important intermediate role between acidogenesis and methanogenesis. Methanogenic organisms use substrate source, formic acid, acetic acid (by cleavage), hydrogen, methanol and methylamines to form methane. However, short chain fatty acids with more than 2 carbon atoms (i.e. > C_2) (such as propionic and butyric acids) cannot be fermented directly to methane (McInerney *et al.*, 1979). Hydrogen-producing acetogenic bacteria are capable of converting short chain fatty acids longer than C_2, to acetic acid,

carbon dioxide and hydrogen gas, provided the hydrogen partial pressure is low (McInerney *et al.*, 1979). Therefore the efficient removal of hydrogen gas produced is of utmost important for the successful degradation of the intermediary products (Figure 2.1) formed during anaerobic digestion.

The limits of hydrogen partial pressure ($\overline{p}H_2$) for the degradation of butyric and propionic acids are below $10^{-2.7}$ atm and $10^{-4.1}$ atm respectively. Propionic acid is oxidised as follows (for $\overline{p}H_2 < 10^{-4.1}$ atm):

$$CH_3CH_2COOH + 2H_2O \Rightarrow CH_3COOH + CO_2 + 3H_2 \qquad (2.12)$$

and butyric acid is oxidised as follows (for $\overline{p}H_2 < 10^{-2.7}$ atm.):

$$CH_3CH_2COOH + 2H_2O \Rightarrow 2CH_3COOH + 2H_2 \qquad (2.13)$$

Under high $\overline{p}H_2$ (i.e. $> 10^{-2.7}$atm) the forward reactions for the oxidation of both propionic and butyric acids becomes thermodynamically unfavourable so that they remain unaltered.

2.2.5 Steps 5 and 6 – Methanogenesis

Methanogenesis is the final step in anaerobic digestion and for a carbohydrate type substrate the two main sources for methane production are:

1. Acetate cleavage, and
2. Hydrogen oxidation.

Methane can also be formed from formic acid, methanol and methylamines by specific groups of methanogens. However, their production tends to be insignificant in the fermentation of carbohydrates, and hence is not considered.

2.2.5.1 Acetoclastic methanogenesis

The majority of methane produced in a digester, about seventy percent, comes from acetate cleavage, according to the following reaction:

$$CH_3COOH \Rightarrow CH_4 + CO_2 \qquad (2.14)$$

Therefore, acetate is the primary precursor for methane production. Huser *et al.* (1982) showed that acetoclastic bacteria (mostly *Methanothrix*) are pH sensitive with an optimum pH of between 7.4 and 7.8 and are inactive below a pH of 6.7. Extreme temperature sensitivity was also established, with an increase in growth rate by a factor of 2.05 per 10° C increase in the temperature range of 15° C to 35° C.

2.2.5.2 Hydrogenotrophic methanogenesis

H_2-utilising (hydrogenotrophic) methanogens use hydrogen as sole energy source and CO_2 as carbon source, to produce methane. Many archaea species can utilize H_2 in anaerobic systems treating (e.g. *Methanobrevibacter aboriphilus* Gujer *et al.*, 1983; Dubourguier *et al.*, 1985). Hydrogenotrophic methanogenesis take place according to the following reaction:

$$CO_2 + 4H_2 \Rightarrow CH_4 + 2H_2O \qquad (2.15)$$

Variations in $\overline{p}H_2$ do not appear to affect either the hydrogenotrophs or the acetoclastic methanogens; however, H_2 does serve as energy source for the hydrogenotrophic methanogens, and so must be present for this methanogenic step. Both however, appear to be sensitive to pH and temperature changes (Gujer and Zehnder, 1983).

2.2.6 Kinetics of biological processes

Although considerable information exists in the literature on the kinetics of the biological processes outlined above as operative in anaerobic digestion systems (e.g. Sam-Soon *et al.*, 1991; Ristow 1999), no single model provides a complete description. Accordingly, it was decided to develop such a model, drawing information of relevance from the literature. The relevant literature and the model development are described in Chapter 4.

2.3 MATHEMATICAL MODELLING OF WEAK ACID/BASE CHEMISTRY PROCESSES

A number of mathematical models of biological waste-water treatment systems for the purpose of design, operation and research have been developed (e.g. Dold *et al.*, 1980; 1991; Van Haandel *et al.*, 1981; Henze *et al.*, 1987; Costello *et al.*, 1991; Siegriest *et al.*, 1993). In these models it is usually implicitly assumed that the biological processes dominate the system response and that the chemical and physical processes (e.g. precipitation and gas stripping respectively) play an insignificant role compared to the biological processes and accordingly can be neglected. It is also assumed that the biological processes take place within a regime of constant pH. This has restricted the application of these models to situations where these assumptions remain valid. However, in the treatment of a number of wastewaters the assumptions are not valid and the models cannot be applied. Of importance to this research project, is the anaerobic treatment of wastes (sewage sludges) where the generation and utilisation of SCFA (e.g. acetic, propionic) are significant. Hence, the assumption that the pH remains essentially constant can not be accepted. Furthermore, if the pH does not remain constant, this will impact on the biological processes since these are pH sensitive, and chemical and physical processes can become significant (in any event, in anaerobic digesters significant CO_2 is produced and the physical process of CO_2 loss is fundamental). To include chemical and physical processes requires that the pH is incorporated in the model and accurately determined, as pH is of fundamental importance in these processes. Hence, the parameter

pH should form an integral part of any kinetic model for anaerobic digestion, i.e. the chemistry of mixed weak acid/bases needs to be included.

Traditionally, an equilibrium chemistry based approach that includes the mass parameter of alkalinity for the weak acid/bases species, has formed the basis on which most chemical conditioning (determining the chemical type and dosing to achieve a final state or conversely to determine the final state of a water after addition/removal of a known amount of a specified chemical) algorithms have been developed (e.g. Loewenthal *et al.*, 1991). However, in reviewing this approach to develop an integrated chemical/physical/biological kinetic model for the treatment of high nutrient (N and P) low organic (COD) wastes, Musvoto *et al.* (1997) noted that the equilibrium chemistry approach, although possibly feasible, presented a number of practical difficulties in implementation. These arose because of the presence of a number of weak acid/bases and a number of processes acting simultaneously on the species concentrations of the weak acid/bases. They therefore concluded that this makes selection of reference species required for the solution procedure to solve the repeated calculations necessary to reach steady state very difficult and cumbersome. The kinetic model being developed here is similar to that envisaged by Musvoto *et al.*, and hence will have the same constraints in utilizing equilibrium chemistry detailed above.

To overcome these difficulties, Musvoto *et al.* (1997) developed a kinetic approach to modelling mixed weak acid/base systems. In this approach, the weak acid/base equilibria are formulated in terms of the kinetics of the forward and reverse reactions for dissociation. This enabled the parameter (H^+) and all the individual weak acid/base systems to be explicitly in the model so that pH could be calculated directly from pH = - log (H^+). Musvoto *et al.* (1997) noted that the advantages of the kinetic approach over the more traditional equilibrium based approach are:

- kinetics are used throughout and this expedites integration of weak acid/base processes with existing biological kinetic models, and

- the approach is general and can be applied to include any weak acid/base of interest.

Musvoto *et al.* evaluated the kinetic approach to modelling mixed weak acid/base systems by comparing the predicted results with such a model to predictions with equilibrium chemistry based models; very close correspondence was achieved.

Since in this research project the aim was to develop a kinetic model for anaerobic digestion, in which the biological processes would be integrated with weak acid/base chemistry, the approach followed by Musvoto *et al.* to deal with the weak acid/base chemistry would seem ideally suitable. The kinetic model of Musvoto *et al.* can be readily integrated with biological kinetic models to completely describe the chemical background within which the biological reactions take place. Accordingly this approach was selected for modelling weak acid/base chemistry in the model being developed here. The approach is reviewed in more detail below.

2.3.1 The Musvoto *et al.* kinetic model for mixed weak acid/base systems

From the discussion above, it is evident that the principle requirement for a mixed weak acid/base chemistry model is that the pH is explicitly incorporated and accurately determined. In the kinetic based model, $[H^+]$ is included explicitly in the model as a compound (in mole units); pH can be calculated directly from H^+ via $pH = -\log(H^+) = -\log f_m.[H^+]$. Further all weak acid/base species that significantly influence the pH are included as compounds (in mole units). The weak acid/base equilibria are described in terms of the kinetics of the forward and the reverse dissociation reactions. For example, consider the acetate/acetic acid weak acid/base. The dissociation equation is given by:

$$HAc \Leftrightarrow H^+ + Ac^- \qquad (2.16)$$

The rate of the reverse reaction is:

$$r_r = K_r(Ac^-)(H^+) = K_r f_m[Ac^-] f_m[H^+] = K_r'[Ac^-][H^+] \quad (2.17)$$

where:

r_r	=	rate of reverse reaction
K_r	=	specific rate constant for the reverse reaction
()	=	activity
f_m	=	monovalent activity coefficient (see Loewenthal *et al.*, 1989)
[]	=	molar concentration
K_r'	=	apparent specific rate constant for the reverse reaction

Similarly, the rate of the forward reaction is:

$$r_f = K_f'[HAc] \quad (2.18)$$

where:

r_f	=	rate of forward reaction
K_f'	=	specific rate constant for the forward reaction

The dissociation equation for the acetate/acetic acid weak acid/base can be represented by these two half-reactions and both kinetic equations are modelled as separate processes. Similarly, the kinetics of the forward and reverse dissociation equations for all the weak acid/base species of importance are included. The apparent specific rate constants of the forward and reverse dissociation reactions are selected such that the rates are so rapid that equilibrium can be considered to be reached effectively instantaneously. Since (H^+) (and correspondingly pH) is included as a compound in the model, and also is included in the kinetic equations for the forward and reverse dissociation reactions, its value can be calculated at any given time. If any of the weak acid/base species is added or removed from the solution (including H^+), the kinetic equations for the forward and the reverse dissociation reactions will cause the relative species concentrations (including H^+) to

Table 2.1: Matrix presentation of the kinetic model for an aqueous mixture of acid/base systems. Exchange of CO_2 has also been included.

Compound → / **Process ↓**	**1** H_3PO_4	**2** $H_2PO_4^-$	**3** HPO_4^{2-}	**4** PO_4^{3-}	**5** NH_4^+	**6** NH_3	**7** $H_2CO_3^*$	**8** HCO_3^-	**9** CO_3^{2-}	**10** $CO_2(g)$	**11** H^+	**12** OH^-	**13** HA	**14** A^-	**Rate**
Forward dissociation of H_3PO_4	-1	1									1				$K'_{fp1}[H_3PO_4]$
Reverse dissociation of H_3PO_4	1	-1									-1				$K'_{rp1}[H_2PO_4^-][H^+]$
Forward dissociation of $H_2PO_4^-$		-1	1								1				$K'_{fp2}[H_2PO_4^-]$
Reverse dissociation of $H_2PO_4^-$		1	-1								-1				$K'_{rp2}[HPO_4^{2-}][H^+]$
Forward dissociation of HPO_4^{2-}			-1	1							1				$K'_{fp3}[HCO_4^{2-}]$
Reverse dissociation of HPO_4^{2-}			1	-1							-1				$K'_{rp3}[PO_4^{3-}][H^+]$
Forward dissociation of NH_4^+					-1	1					1				$K'_{fn}[NH_4^+]$
Reverse dissociation of NH_4^+					1	-1					-1				$K'_{rn}[NH_3][H^+]$
Forward dissociation of $H_2CO_3^*$							-1	1			1				$K'_{fc1}[H_2CO_3^*]$
Reverse dissociation of $H_2CO_3^*$							1	-1			-1				$K'_{rc1}[HCO_3^-][H^+]$
Forward dissociation of HCO_3^-								-1	1		1				$K'_{fc2}[HCO_3^-]$
Reverse dissociation of HCO_3^-								1	-1		-1				$K'_{rc2}[CO_3^{2-}][H^+]$
Dissolution of CO_2							1			-1					$K'_{fCO2}[CO_2(g)]$
Expulsion of CO_2 from solution							-1			1					$K'_{rCO2}[H_2CO_3^*]$
Forward dissociation of HA											1		-1	1	$K'_{fa}[HA]$
Reverse dissociation of HA											-1		1	-1	$K'_{ra}[A^-][H^+]$
Forward dissociation of water											1	1			K'_{fw}
Reverse dissociation of water											-1	-1			$K'_{rw}[H^+][OH^-]$
Units	mol/ℓ	mol/ℓ	mol/ℓ	mol/ℓ	mol/ℓ	mol/ℓ	mol/ℓ	mol/ℓ	mol/ℓ	mol/ℓ	mol/ℓ	mol/ℓ	mol/ℓ	mol/ℓ	

Table 2.2(a): Kinetic constants for weak acids/bases in mixed acid/base model

PROCESS	SPECIFIC RATE CONSTANTS					
	FORWARD DISSOC. REACTION		REVERSE DISSOC. REACTION		EQUILIBRIUM CONSTANT	
	SYMBOL	VALUE	SYMBOL	VALUE	SYMBOL	VALUE
Ammonia $NH_4^+ \Leftrightarrow NH_3 + H^+$	K'_{fn}	$K'_m.K'_n$	K'_{rn}	10^{12} (/s)	K'_n	10^{-pKn}
Phosphate 1 $H_3PO_4 \Leftrightarrow H_2PO_4^- + H^+$	K'_{fp1}	$K'_{rp1}.K'_{p1}$	K'_{rp1}	10^{8} (/s)	K'_{p1}	$\frac{10^{-pKp1}}{f_m^{\,2}}$
Phosphate 2 $H_2PO_4^- \Leftrightarrow HPO_4^{2-} + H^+$	K'_{fp2}	$K'_{rp2}.K'_{p2}$	K'_{rp2}	10^{12} (/s)	K'_{p2}	$\frac{10^{-pKp2}}{f_d}$
Phosphate 3 $HPO_4^{2-} \Leftrightarrow PO_4^{3-} + H^+$	K'_{fp3}	$K'_{rp3}.K'_{p3}$	K'_{rp3}	10^{15} (/s)	K'_{p3}	$\frac{10^{-pK_{p3}}.f_d}{f_t.f_m}$
Carbonate 1 $H_2CO_3^* \Leftrightarrow HCO_3^- + H^+$	K'_{fc1}	$K'_{rc1}.K'_{c1}$	K'_{rc1}	10^{7} (/s)	K'_{c1}	$\frac{10^{-pKc1}}{f_m^{\,2}}$
Carbonate 2 $HCO_3^- \Leftrightarrow CO_3^{2-} + H^+$	K'_{fc2}	$K'_{rc2}.K'_{c2}$	K'_{rc2}	10^{10} (/s)	K'_{c2}	$\frac{10^{-pKc2}}{f_d}$
SCFA $HAc \Leftrightarrow Ac^- + H^+$	K'_{fa}	$K'_{ra}.K'_a$	K'_{ra}	10^{7} (/s)	K'_a	$\frac{10^{-pKa}}{f_m^{\,2}}$
Water $H_2O \Leftrightarrow OH^- + H^+$	K'_{fw}	$K'_{rw}.K'_w$	K'_{rw}	10^{17} (/s)	K'_w	$\frac{10^{-pKw}}{f_m^{\,2}}$

Table 2.2(b): Values for pK constants in the mixed weak acid/base model (Temperature in Kelvin)

pK CONSTANT	FORMULATION
1940's Data base (Loewenthal and Marais, 1976;Loewenthal *et al.*, 1989)	
pK_n	2 835.8/T – 0.6322 + 0.00123.T
pK_{c1}	3 404.7/T – 14.8435 + 0.03279.T
pK_{c2}	2 909.4/T – 6.498 + 0.02379.T
pK_a	1 170.5/T – 3.165 + 0.0134.T
pK_{p1}	799.3/T-4.5535+0.01349.T
pK_{p2}	1979.5/T-5.3541+0.01984.T
pK_{p3}	12.023
1980's Data base (Friend and Loewenthal, 1992)	
pK_{c1}	$356.309 + 0.0609196.T - 21\,834.4/T - 126.834.\log(T) + 1.68492 \times 10^6/T^2$
pK_{c2}	$107.887 + 0.0325285.T - 5\,151.79/T - 38.9256.\log(T) + 563\,714/T^2$
$pK_{H,CO2}$	-2 025.3/T – 0.104.T + 11.365
pK_w	14.00

readjust very rapidly (effectively instantaneous) to the new condition. Since all the weak acid/bases have the (H^+) species in common, all would be influenced and thus readjust. The values of the apparent specific rate constants for the forward and reverse dissociation reactions that give rise to weak acid/base species concentrations that correspond to true equilibrium chemistry are determined from the equilibrium constants. From the law of mass action, for the same acetate/acetic acid system, at equilibrium:

$$r_f = r_r \tag{2.19}$$

So,

$$K_f'[HAc] = K_r'[Ac^-][H^+] \tag{2.20}$$

$$\therefore K_f^{'} / K_r^{'} = [Ac^-][H^+]/[HAc] = K_a^{'} \qquad (2.21)$$

where:

$K_a^{'}$ = apparent equilibrium constant for the acetate system

The forward and reverse reactions are very rapid, and the true reaction rates cannot be measured. However, the exact values are of little importance and the values for the apparent specific rate constants are selected so that the reactions are effectively instantaneous. One of the rate constants (the reverse rate $K_r^{'}$) would be given a very high theoretical value such that the new equilibrium is achieved in as short as 3 seconds. To ensure that kinetically established equilibrium corresponds to true equilibrium chemistry, the rate of the forward rate constant ($K_f^{'}$) is calculated through the relationship with the apparent equilibrium constant, i.e. $K_f^{'} = K_a^{'}.K_r^{'}$.

Using the kinetic based approach above, Musvoto *et al.* developed a model to describe aqueous mixtures of the carbonate, ammonium, phosphate and SCFA (represented by acetate) weak acid/bases. This model is illustrated in matrix format (Henze *et al.*, 1987) in Table 2.1; values for kinetic constants obtained from literature by Musvoto *et al.* are listed in Tables 2.2(a) and (b). The approach of Musvoto *et al.* is general, and can be applied to include (or exclude) any weak acid/base in the model. This makes it ideally suited to the application in this research project.

2.4 MODELLING OF TWO PHASE SYSTEMS

In addition to the single phase (aqueous) processes described above (biological and mixed weak acid/base chemistry), in anaerobic digestion two phase processes can also be expected:

- gaseous/aqueous – significant CO_2 ,CH_4 and H_2 are produced within anaerobic digesters and will be expelled to the atmosphere; NH_3 loss may occur if the pH is sufficiently high
- solid/aqueous – mineral precipitation may be of importance, particularly where waste activated sludges from biological nutrient (N and P) removal systems are anaerobically digested.

Accordingly, any kinetic model for anaerobic digestion systems should consider these processes also. In this section, these processes are reviewed.

2.4.1 Gaseous/aqueous systems

2.4.1.1 Stripping/exchange of carbon dioxide (CO_2)

The rate of CO_2 stripping needed to be integrated with the weak acid/base reactions as described above (Section 2.3) to give a gaseous/aqueous system model. Exchange of CO_2 between the atmosphere and an aqueous system does not only occur when aeration is the driving force, but it occurs whenever there is a pressure difference between the CO_2 in the atmosphere and the dissolved CO_2 (e.g. when an underground water is exposed to the atmosphere or in this case when significant CO_2 is generated by biological reactions). In such situations the pressure difference is the driving force and CO_2 exchange occurs between the aqueous and gas phases until equilibrium is reached. Such a situation is best represented by considering the equilibrium between the dissolved and gaseous carbon dioxide as outlined below.

Since the ratio of CO_2 dissolved and H_2CO_3 is fixed, these two species can be dealt with as a single combined species, $H_2CO_3^*$ (Stumm and Morgan, 1970), where $[H_2CO_3^*] = [CO_2 \text{ dissolved}] + [H_2CO_3]$. The CO_2 dissolved, and hence $H_2CO_3^*$, tends to equilibrium with the partial pressure of CO_2 (gas) outside the liquid, i.e.:

$$CO_2(g) \Leftrightarrow CO_2 \text{dissolved} \qquad (2.22)$$

or equivalently:

$$CO_2(g) \Leftrightarrow H_2CO_3^* \tag{2.23}$$

This gives rise to CO_2 exchange at the liquid/gas interface, resulting in loss or gain of $H_2CO_3^*$ in the solution, and accordingly in total carbonate weak acid/base species concentration. Thus, CO_2 loss or gain should be included in the model, and linked to the carbonate species. This can be done by following the same approach as for the weak acid/base dissociation reactions, i.e. by modelling separately the rate of the forward and reverse reactions of Eq. (2.23). The forward reaction is:

$$r_f = K'_{fCO_2}[CO_2(g)] \tag{2.24}$$

where

r_f = rate of forward reaction

K'_{fCO_2} = apparent specific rate constant for forward reaction

Similarly for the reverse reaction:

$$r_r = K'_{rCO_2}[H_2CO_3^*] \tag{2.25}$$

where

r_r = rate of reverse reaction

K'_{rCO_2} = apparent specific rate constant for reverse reaction

The formulation in Eqns (2.24) and (2.25) were accepted as describing the kinetics of CO_2 exchange between the aqueous and gas phases, and hence were incorporated in the model (Table 2.1). In Eq (2.24), $[CO_2(g)]$ is explicitly included. The concentration of

$CO_2(g)$ was accepted to be constant, and can be calculated from the partial pressure of CO_2 with Daltons' law of partial pressure (Stumm and Morgan, 1970):

$$[CO_2(g)] = \frac{\rho CO_2}{RT} \tag{2.26}$$

where:

ρCO_2	=	partial pressure of CO_2 (atm)
R	=	universal gas constant
	=	8.20575×10^{-2} (ℓ atm/K/mol)
T	=	temperature (K)

In Eqs. (2.24) and (2.25) values are required for the apparent specific rate constants for the forward (K'_{fCO_2}) and reverse (K'_{rCO_2}) reactions respectively. If only the equilibrium condition is being considered, exact values for K'_{fCO_2} and K'_{rCO_2} are not required, however, the relative values are important since the relative values will establish the equilibrium concentration of $H_2CO_3^*$. If the rate of CO_2 exchange is of importance then both the exact values for K'_{fCO_2} and K'_{rCO_2} and their relative values need to be determined. At equilibrium:

$$r_f = r_r \tag{2.27}$$

Substituting Eqs. (2.24) and (2.25) into (2.27) and rearranging gives:

$$\frac{K'_{fCO_2}}{K'_{rCO_2}} = \frac{[H_2CO_3^*]}{[CO_2(g)]} = K'_{eqCO_2} \tag{2.28}$$

where:

K'_{eqCO_2}	=	apparent equilibrium constant for CO_2 exchange

From Eq. (2.28):

$$K'_{fCO_2} = K'_{eqCO_2} K'_{rCO_2} \qquad (2.29)$$

Thus if K'_{eqCO_2} is known, by selecting a value for K'_{rCO_2}, the relative value for K'_{fCO_2} can be calculated and the correct equilibrium condition will be established giving the correct equilibrium concentration of $[H_2CO_3^*]$. K'_{eqCO_2} is determined by noting that at equilibrium (Stumm and Morgan, 1981):

$$K'_{H,CO_2} = \frac{K'_{eqCO_2}}{RT} \qquad (2.30)$$

where:

K'_{H,CO_2} = Henry's law constant for CO_2 (mol/ℓ/atm)

K'_{eqCO_2} = K'_{D,CO_2}

K'_{D,CO_2} = distribution (mass law) constant

Values for Henry's law constant for CO_2 (K'_{H,CO_2}) with temperature are available in the literature (Friend and Loewenthal, 1992, See Table 2.2(b)). From K'_{H,CO_2} the equilibrium constant (K'_{eqCO2}) can be calculated with Eq. (2.30), and for a selected value of K'_{rCO_2}, K'_{fCO_2} can be calculated with Eq. (2.29). The value for K'_{H,CO_2} used in constructing the model is from (Musvoto *et al.*, 1998) and is given in Table 2.2(b). The value for K'_{rCO_2} was calibrated in the model application to fit the experimental data available (see Chapters 3 and 5).

In terms of the approach followed above to derive kinetic equations for CO_2 exchange, the net rate of CO_2 loss/gain is given by the sum of the forward and reverse reaction rates used in the model (Table 2.1):

$$r_{H_2CO_3} = +K'_{fCO_2}[CO_2(g)] - K'_{rCO_2}[H_2CO_3^*] \quad (2.31)$$

In Eq (2.31) above, noting that from Eq (2.28) $K'_{eqCO_2} = \frac{K'_{fCO_2}}{K'_{rCO_2}}$, from Eq (2.26) $[CO_2(g)] = \frac{\rho CO_2}{RT}$ and from Eq (2.30) $K'_{H,CO_2} = \frac{K'_{eqCO_2}}{RT}$, then

$$-r_{H_2CO_3} = K'_{rCO_2}\left([H_2CO_3^*] - K'_{H,CO_2}.\rho CO_2\right) \quad (2.32)$$

An identical formulation to Eq (2.32) above can be derived from the theory of interphase mass transfer, by noting $K'_{rCO_2} = K'_{La,CO_2}$ (Musvoto *et al.*, 1997). Hence, the approach above is acceptable for incorporating CO_2 exchange in the model.

In calibrating their model, from the work of Munz and Roberts (1989), Musvoto *et al.* (1998; 2000c) assumed that the K_{La} values for oxygen and CO_2 are proportional and only the former needs to be calibrated. However, in application of the model Musvoto *et al.* did not determine values for $K_{La,O2}$ but effectively calibrated this from CO_2 loss determined from C_T measurements (See Table 2.5). For application envisaged here, it was noted that $K_{La,CO2}$ would be specific to the conditions prevailing and would require calibration, either independently or via the relationship with $K_{La,O2}$ (see Chapters 3 and 5).

2.4.1.2 Stripping of NH_3

If the pH is sufficiently high (e.g. on aeration treatment of ADS, Musvoto *et al.*, 2000c), then NH_3 loss may become significant. To include this in their model, Musvoto *et al.* (1998; 2000c) assumed that for NH_3 the atmosphere acts as an infinite sink. Thus, the

Table 2.3:Matrix representation of the processes of precipitation and gas stripping included in the three phase mixed weak acid/base kinetic model. The single phase aqueous forward and reverse dissociation processes of weak acid/base species and the three phase processes of the carbonate system are given in Table 1 of Musvoto *et al.* (1997) with the same numbering of the compounds.

No	Compound	1	2	3	4	5	7	8	9	10	11	12	13	13	15	16	Rate
	Process	NH_4^+	NH_3	$H_2CO_3^*$	HCO_3^-	CO_3^{2-}	H^+	OH^-	H_3PO_4	$H_2PO_4^-$	HPO_4^-	PO_4^{3-}	HA	A^-	Ca^{2+}	Mg^{2+}	
42	Precipitation of $MgNH_4PO_4$	-1										-1				-1	$K'_{ppt,Struv}\left([Mg^{2+}]^{\frac{1}{3}}[NH_4^+]^{\frac{1}{3}}[PO_4^{3-}]^{\frac{1}{3}} - K'^{\frac{1}{3}}_{sp,Struv}\right)^3$
43	Precipitation of $MgHPO_4$										-1					-1	$K'_{ppt,Newb}\left([Mg^{2+}]^{\frac{1}{2}}[HPO_4^{2-}]^{\frac{1}{2}} - K'^{\frac{1}{2}}_{sp,Newb}\right)^2$
44	Precipitation of $Ca_3(PO_4)_2$											-2/3			-1		$K'_{ppt,ACP}\left([Ca^{2+}]^{\frac{3}{5}}[PO_4^{3-}]^{\frac{2}{5}} - K'^{\frac{1}{5}}_{sp,ACP}\right)^2$
45	Precipitation of $MgCO_3$					-1										-1	$K'_{ppt,MgCO_3}\left([Mg^{2+}]^{\frac{1}{2}}[CO_3^{2-}]^{\frac{1}{2}} - K'^{\frac{1}{2}}_{spMgCO_3}\right)^2$
46	Stripping of NH_3		-1														$K'_{rNH_3}[NH_3]$
	Units	mol/ℓ	mol/ℓ	mol/ℓ	mol/ℓ	mol/ℓ	mol/ℓ	mol/ℓ	mol/ℓ	mol/ℓ	mol/ℓ	mol/ℓ	mol/ℓ	mol/ℓ	mol/ℓ	mol/ℓ	

dissolution of NH_3 from the atmosphere into the solution was not included, only NH_3 expulsion as given in Table 2.3, with specific loss rate K'_{rNH_3}. In application of their model, Musvoto *et al.* found that this rate had to be determined by independent calibration. In application in this research work (Chapters 3 and 5), NH_3 loss was not significant due to the pH values or short time periods at higher pHs.

2.4.1.3 CH_4 and H_2

The gasses CH_4 and H_2 are considered relatively insoluble gasses and therefore it was assumed that they automatically go into the gas phase without the specific stripping rate being modelled. This assumption remains valid in a steady state situation, however the stripping of CH_4 and H_2 to the gas phase were modelled explicitly when a dynamic situation (failure) was considered (See Chapter 5).

2.4.2 Solid/aqueous systems: precipitation of sparingly soluble salts

In anaerobic digestion, the precipitation of minerals may be of importance. The minerals likely to precipitate fall into the sparingly soluble salts group. The precipitation of sparingly soluble salts as such has been extensively reviewed (Musvoto *et al.*, 1998). Only those parts relevant to the work presented in this project are briefly reviewed below.

2.4.2.1 The kinetics and mechanisms of precipitation of sparingly soluble salts

The first requirement for a solid phase to form from a liquid solution is some degree of supersaturation, and the degree of supersaturation is the main factor controlling the precipitation process. The precipitation process usually takes place in three steps, namely nucleation, crystal growth and ripening:

2.4.2.1.1 *Nucleation*

Nucleation is the formation of the new centres from which spontaneous crystal growth can occur. Thus, the condition of supersaturation alone is not sufficient to start crystallisation and a number of minute solid bodies known as the centres of

crystallisation, seeds or nuclei, must exist in the solution (Mullin, 1972). The mechanism of nucleation is believed to take place initially by bimolecular attraction and then addition of single molecules which leads to the formation of critical clusters. Further addition of molecules to the critical clusters would then result in nucleation. If a nucleus grows beyond a certain critical size, it becomes stable. The critical size of a nucleus therefore represents the minimum size of a stable nucleus. Particle sizes smaller than the critical size redissolve and those larger continue to grow.

2.4.2.1.2 *Growth of crystals*

The growth of crystals is a process which takes place in successive reaction steps; the transport of ions to the crystal/solution interface, the adsorption of ions at the interface and the incorporation of the crystal constituents into the lattice.

2.4.2.1.3 *Ripening*

Ripening (also called ageing or particle coarsening) is the eventual formation of large crystals from fine crystallites and occurs after crystal growth, if sufficient time is allowed to elapse. Ripening occurs due to the tendency of smaller particles in their own saturated or supersaturated solution to dissolve and the solute to be deposited later on the larger particles (Mullin, 1972). The particle size distribution gradually changes to that of a monosized distribution. The speed with which ripening occurs depend largely on the particle size and the solubility of the salt. Smaller particles of a more soluble salt will age much faster than those of a sparingly soluble salt.

Kinetics of precipitation applied to modelling of solid/aqueous systems

From the discussion above, in order to effect crystallisation the solution must be supersaturated to a certain degree with respect to a particular salt. When small concentrations of seed crystals are present, such as in conventional precipitation processes, then both nucleation and crystal growth take place simultaneously. However, it is the crystal growth process that is invariably rate limiting and so limits the overall rate of crystallisation/precipitation. Accepting this, then the equation put forward by

Nanchollas and Purdie (1964) best describes the crystal growth kinetics of sparingly soluble salts from solutions of unequal cation and anion concentration, and accordingly can be used to describe the overall crystallisation/precipitation process:

$$-\frac{dm}{dt} = k.s\left\{\left([M^{y+}]^x[A^{x-}]^y\right)^{\frac{1}{x+y}} - K_{sp}^{\frac{1}{x+y}}\right\}^{x+y} \qquad (2.33)$$

where:

m	=	mass of salt precipitated (mol/ℓ)
k	=	rate constant (mol/m^{2}s)
s	=	surface area of crystals (m^2/mol)
K_{sp}	=	solubility product of salt M_xA_y (molar form)

Koutsoukos *et al.* (1980) accepted the validity of this equation to describe the rate of precipitation of many sparingly soluble salts, i.e. for a salt $M_{v+}A_{v-}$ the rate of crystallisation can be expressed by a general form:

$$\frac{d}{dt}M_{v^+}A_{v^-} = -k's\left\{\left([M^{m+}]^{v^+}[A^{a-}]^{v^-}\right)^{\frac{1}{v}} - \left([M^{m+}]_0^{v^+}[A^{a-}]_0^{v^-}\right)^{\frac{1}{v}}\right\}^n \qquad (2.34)$$

where:

- $[M^{m+}]$, $[A^{a+}]$ and $[M^{m+}]_0$, $[A^{a+}]_0$ are the concentrations in (mol/ℓ) of crystal lattice ions in solution at time t and at equilibrium respectively. At equilibrium $[M^{m+}]_0[A^{a+}]_0 = K'_{sp}$ where K'_{sp} is the apparent solubility product of the salt.
- k' is the apparent precipitation rate constant (mol/m^{2}s)
- s is proportional to the total number of available growth sites on the added seed material (m^2/mol)
- v^+ is the number of cationic species
- v^- is the number of anionic species
- $v = v^+ + v^-$

- the exponent n is determined experimentally and is available in the literature (Stumm and Morgan, 1981 and Gunn, 1976).

Due to the general acceptance of Eq (2.34) in precipitation kinetics research, this equation was utilized in the model developed by Musvoto *et al.*(1998) for mineral precipitation. However, they did note that the term "s" represents the surface area of seed material inoculated into the solution. In the cases considered by Musvoto *et al.* (1998), no seed material of the crystal type precipitating was added. Accordingly, the rate of precipitation could be represented by an overall crystal growth rate, with the term "k's" in Eq (2.34) replaced by an apparent precipitation rate constant K'. The formulation and modification were applied by Musvoto *et al.* (1998) to successfully predict precipitation of a variety of minerals, and accordingly were accepted for application in the model being developed here. However, it must be remembered that the general formulation applies only to precipitation and not to dissolution; in the model the equation is valid only if the ionic product is greater than the solubility product – this condition must be verified.

2.4.2.2 Minerals precipitating in anaerobic digesters

In anaerobic digester supernatant, magnesium and calcium can be present at concentrations sufficient to precipitate considerable amounts of P and N without external cation addition. The main phosphate salts precipitated are magnesium phosphates and the various calcium phosphates. The carbonates of calcium and magnesium are also precipitated under the same conditions as their phosphates. The solids most likely to precipitate are set out in Table 2.4.

Magnesium phosphates

Four possible species can crystallise from solutions containing Mg, N and P species; magnesium phosphate or struvite ($MgNH_4PO_4.6H_2O$), magnesium hydrogen phosphate trihydrate or newberyite ($MgHPO_4.3H_2O$) and trimagnesium phosphate in two states of hydration $Mg_3(PO_4)_2.22H_2O$ and $Mg_3(PO_4)_2.8H_2O$, see Table 2.3.

Studies have identified the regions for precipitation of these minerals: Struvite is the most abundant of the magnesium phosphates found in nature, either precipitating alone or with other magnesium phosphates. It precipitates at neutral and higher pH. In wastewater treatment, the precipitation of struvite has been widely reported in anaerobic digesters, sludge handling equipment and side streams from anaerobic digesters causing operational problems through pipe and pump blockages (Borgerding, 1972; Mohajit *et al.*, 1989; Mamais *et al.*, 1994). Newberyite precipitates at lower pH (< 6.0), while trimagnesium phosphate has never been observed in the pH ranges common to anaerobic digestion (6 < pH < 9). Accordingly, struvite and newberyite precipitation were included in the model.

Calcium phosphates

Five calcium phosphate crystalline species can precipitate from solutions containing calcium and phosphate (Heugebaert and Nanchollas, 1984; Abbona *et al.*, 1986), and in order of increasing solubility, these are

- Hydroxyapatite (HAP) $Ca_5(PO_4)_3OH$
- Tricalcium phosphate (whitlockite, TCP) $Ca_3(PO_4)_2$
- Octacalcium phosphate (OCP) $Ca_8(HPO_4)_2(PO_4)_4.5H_2O$
- Monenite (DCP) $CaHPO_4$
- Dicalcium phosphate dihydrate (brushite, DCPD) $CaHPO_4.2H_2O$

Thermodynamically HAP is the most stable phase and is expected to precipitate. However, it has been established that a number of species act as precursors to precipitation of HAP, such as amorphous calcium phosphate (ACP, with approximate formulation $Ca_3(PO_4)_2.xH_2O$, similar to TCP, but no structured crystalline order, Blumenthal *et al.*, 1977; Betts *et al.*, 1981), OCP and DCPD. With time these species may transform to HAP. The precursor species which first precipitate and their transformation are significantly affected by the interaction between pH, Ca and Mg concentrations in the wastewater, as well as the alkalinity and organic material present. From experimental investigations of these processes, it can be concluded that in highly supersaturated solutions containing Ca, Mg and P, DCPD and ACP are the phases that

precipitates first, with DCPD precipitating at low pH (< 7.0) and ACP at higher pH (Abbona *et al.*, 1986; 1988). Precipitation follows Oswald's rule of stages (when a number of similar solids are highly supersaturated, the least stable solid will precipitate) with the initially formed metastable precursor species ACP and DCPD converting with time to the more thermodynamically stable species of DCP, HAP or TCP. The presence of Mg in solution strongly affects the conversion process (Arvin, 1983). Conversion of ACP to the thermodynamically stable species HAP does not take place in solutions with high Mg/Ca molar ratios (> 4.0). Other factors such as high pH, high ionic strength, high HCO_3^-/PO_4^{3-} molar ratio, presence of pyrophosphates as well as certain proteins, and lack of HAP seed material also stabilize ACP. Therefore, ACP can be expected to precipitate in high nutrient low organic carbon (HNLC) wastewaters such as sewage effluents, anaerobic digester liquor (ADL) and sludge dewatering liquors which have the characteristics that suppress the precipitation of HAP, but promote and stabilize the formation of ACP. Furthermore, in such wastewaters the transformation of ACP to HAP will be retarded; thus within the timescale of typical treatment systems , significant HAP is unlikely. For these reasons, Musvoto *et al.* (1998) included ACP in their model as the calcium phosphate mineral most likely to precipitate.

Calcium carbonates

Three crystalline structure varieties of $CaCO_3$ can precipitate namely calcite, aragonite and vaterite. The species that precipitate have been shown to depend on the temperature, degree of supersaturation, presence of foreign ions as well as the nucleation and growth rates of crystals. From the literature, calcite is the thermodynamically stable form at ambient temperature and atmospheric pressure (Roques and Girou, 1974). Accordingly, precipitation of the $CaCO_3$ mineral calcite was included in the model.

2.4.2.3 Kinetic model for precipitants to be included

From the discussion above, mineral precipitants that should be included in the model are struvite ($MgNH_4PO_4$), newberyite ($MgHPO_4$), amorphous calcium phosphate ($Ca_3(PO_4)_2$), calcite ($CaCO_3$) and magnesite ($MgCO_3$), see Table 2.4. The matrix representation of the kinetic model for precipitation of these minerals as extracted from Musvoto *et al.* (2000) is shown in Table 2.3.

Table 2.4: Minerals that could possibly precipitate on aeration of ADS; values of solubility products at 25°C and infinite dilution obtained form databases in the literature. The five compounds marked with an * were included in the kinetic model adapted from Musvoto *et al.* (1998)

Solubility equilibria		pK_s at 25°C			
Mineral	Reaction	Stumm and Morgan (1981)	Nordstrom *et al.* (1990)	JESS(Murray and May, 1996)	Other Sources
*Calcite/Aragonite	$CaCO_3 \Leftrightarrow Ca^{2+} + CO_3^{2-}$	8.42;8.22	8.48;8.34	8.5;8.22	8.3[e];7.8[f];6.7[h]
Nesquehonite	$MgCO_3.3H_2O \Leftrightarrow Mg^{2+} + CO_3^{2-} + 3H_2O$	5.19		4.67;5.19	
*Magnesite	$MgCO_3 \Leftrightarrow Mg^{2+} + CO_3^{2-}$	7.46;8.2		7.46;8.2	5.9[e];7.9[f]
Dolomite (disordered)	$CaMg(CO_3)_2 \Leftrightarrow Ca^{2+} + Mg^{2+} + 2CO_3^{2-}$	16.7	16.54	16.5	
Dolomite (ordered)	$CaMg(CO_3)_2 \Leftrightarrow Ca^{2+} + Mg^{2+} + 2CO_3^{2-}$		17.09	16.98	17[f]
Huntite	$CaMg(CO_3)_4 \Leftrightarrow Ca^{2+} + Mg^{2+} + 4CO_3^{2-}$				N/A
Calcium hydroxide	$Ca(OH)_2(s) \Leftrightarrow Ca^{2+} + 2OH^-$	5.2	5.2		
Brucite	$Mg(OH)_2(s) \Leftrightarrow Mg^{2+} + 2OH^-$	11.16	11.16		10.7[e]
DCP	$CaHPO_4(s) \Leftrightarrow Ca^{2+} + HPO_4^{2-}$	6.6		6.6;6.5	
OCP	$Ca_8(HPO_4)_2(PO_4)_4.5H_2O \Leftrightarrow 8Ca^{2+} + 2HPO_4^{2-} + 4PO_4^{3-} + 5H_2O$				94.16[i];72.53[i]
DCPD	$CaHPO_4.2H_2O \Leftrightarrow Ca^{2+} + HPO_4^{2-} + 2H_2O$	6.6		6.6	
HAP	$Ca_{10}(PO_4)_6(OH)_2(s) \Leftrightarrow 10Ca^{2+} + 6PO_4^{3-} + 2OH^-$	114		57.5;48.6	
TCP	$Ca_3(PO_4)_2 \Leftrightarrow 4Ca^{2+} + 2PO_4^{3-}$			32.63;32.7	
*ACP	$Ca_3(PO_4)_2.xH_2O \Leftrightarrow 3Ca^{2+} + 2PO_4^{3-} + xH_2O$	31.45			26.0[a];25.46[g]; 25.2[b]; 24[e]
*Struvite	$MgNH_4PO_4.6H_2O(s) \Leftrightarrow Mg^{2+} + NH_4^+ + PO_4^{3-} + 6H_2O$	12.6		13.16	12.6[a];12.72[c]; 13.2[d]; 13[e]
*Newberyite	$MgHPO_4.3H_2O(s) \Leftrightarrow Mg^{2+} + 2PO_4^{3-} + 3H_2O$			5.8	5.51[c];5.8[d]
Bobierrite	$Mg_3(PO_4)_2.8H_2O(s) \Leftrightarrow 3Mg^{2+} + 2PO_4^{3-} + 8H_2O$			25.2	25.2[d]
Trimagnesium phosphate	$Mg_3(PO_4)_2.22H_2O(s) \Leftrightarrow 3Mg^{2+} + 2PO_4^{3-} + 22H_2O$				23.1[d]

Note: 1. Temperature dependency of solubility products for some of the reactions has been given by Stumm and Morgan (1981) and Nordstrom *et al.* (1990).

2. Lettered references apply to the following: [a]Butler (1964);[b]Meyer and Eanes (1978) cited by Moutin *et al.* (1992); [c]Abbona *et al.* (1982); [d]Taylor *et al.* (1963) cited by Scot *et al.* (1991); [e]Mamais *et al.* (1994); [f]Ferguson and McCarty (1971). [g]Hoffmann and Marais (1977)-value from Butler (1964) corrected for ionic strength. [h]Wiechers *et al.* (1980); [i]Verbeek and Devenyns (1992).

2.4.2.4 Data for solubility products

A database containing solubility products for the various precipitants from literature is given in Table 2.4. The values as used by Musvoto *et al.* (2000c) in application of the kinetic model to aeration treatment of anaerobic digester supernatant are given in Table 2.5. Also listed are the specific precipitation rate constants found by Musvoto *et al.* (2000c).

Table 2.5: The solubility product (pK_{sp})and precipitation rate constant (K'_{ppt}) values found by Musvoto *et al.* (2000c) on aeration treatment of supernatant from sewage sludge (SS) and upflow anaerobic sludge bed (UASB) anaerobic digesters.

Mineral	pK_{sp}	K'_{ppt}	
		SS	UASB
Calcite – $CaCO_3$	6.45	50	0.5
Magnesite – $MgCO_3$	7.00	50	50
ACP – $Ca_3(PO_4)_2.xH_2O$	26.0	150	350
Newberyite – $MgHPO_4.3H_2O$	5.8	0.05	0.05
Struvite – $MgNH_4PO_4.6H_2O$	13.16	300	3000
Rate of aeration/gas stripping		K'_r	
NH_3		0.9 – 1.2	1.92 – 2.5
CO_2		204 - 545	610

2.4.2.5 Ion pairing effects

The most important equilibria in aqueous systems that affect the solubility of salts are ion pairing. Ion pairs are either positively charged, negatively charged or neutral species that are formed between ions of opposite charge. Ion pairs reduce the amount of free ions in

solutions (thereby reducing the ions available to form precipitants) as well as the ionic strength of the solution (thus changing the theoretical activity coefficients of free ions in solution). This effectively increases the solubility of the salt. In order to accurately predict the amount of free ions in solution (and hence the precipitation/dissolution potential) ion pairing has to be taken into account.

Table 2.6: Common ion pairs formed in solutions containing calcium and magnesium with carbonate, phosphate and ammonia weak acid/bases present and their stability constants (pK_{ST}) at 25° C (activity scale).

Reaction	Stumm and Morgan (1981)	Nordstrom *et al.* (1990)	JESS(Murray and May, 1996)	Other Sources
$Ca^{2+} + OH^- \Leftrightarrow CaOH^-$	-1.15	-1.22		-1.37[a]
$Ca^{2+} + CO_3^{2-} \Leftrightarrow CaCO_3(aq)$		-3.21		-3.2[a]
$Ca^{2+} + HCO_3^- \Leftrightarrow CaHCO_3^+$		-2.71		-1.26[a]
$Ca^{2+} + PO_4^{3-} \Leftrightarrow CaPO_4^-$	-6.5			-6.46[b]
$Ca^{2+} + HPO_4^{2-} \Leftrightarrow CaHPO_4(aq)$	-2.7			-2.73[b]
$Ca^{2+} + H_2PO_4^- \Leftrightarrow CaH_2PO_4^+$	-1.4			-1.41[b]
$Mg^{2+} + OH^- \Leftrightarrow MgOH^-$	-2.56	-2.56		-2.2[a]
$Mg^{2+} + CO_3^{2-} \Leftrightarrow MgCO_3(aq)$		-2.98		-3.4[a]
$Mg^{2+} + HCO_3^- \Leftrightarrow MgHCO_3^+$		-4.9		-1.16[a]
$Mg^{2+} + HPO_4^{2-} \Leftrightarrow MgHPO_4(aq)$	-2.5			-2.5[a]
$Mg^{2+} + PO_4^{3-} \Leftrightarrow MgPO_4^-$				-3.13[a]

Note: Lettered references apply to the following:

[a] Sillen and Martell (1964) cited by Ferguson and McCarthy (1971)

[b] Chugtai *et al.* (1968) cited by Ferguson and McCarthy (1971)

The most common ion pairs formed in solution containing calcium and magnesium in the presence of carbonate, phosphate and ammonia weak acid/base system species are listed in Table 2.6 together with their stability constants. To include ion pairing in the kinetic

Table 2.7: Matrix representation of the ion pairing reactions of the most common Ca^{2+} and Mg^{2+} ion pairs in solutions containing carbonate and phosphate species. Ion pair stability constants and equilibrium equations are given in Tables 2.6 and 2.8 respectively.

Compound Number		5	8	11	12	15	16	17	18	19....	.....	25	26	27	
Process Number		CO_3^{2-}	OH^-	HPO_4^{2-}	PO_4^{3-}	Ca^{2+}	Mg^{2+}	$CaOH^+$	$CaCO_3^0$	A^{X+}	B^{Y-}	AB^{X+Y-}	$MgHPO_4$	$MgPO_4^-$	Process Rate
20	Assoc. of Ca^{2+}, OH^-		-1			-1		+1							$K'_{fca1}[Ca^{2+}][OH^-]$
21	Dissoc. of $CaOH^+$		+1			+1		-1							$K'_{rca1}[CaOH^+]$
22	Assoc. of Ca^{2+}, CO_3^{2-}	-1				-1			+1						$K'_{fca2}[Ca^{2+}][CO_3^{2-}]$
23	Dissoc. of $CaCO_3^0$	+1				+1			-1						$K'_{rca2}[CaCO_3^0]$
.....	Assoc. of A^{X+}, B^{Y-}									-1	-1	+1			$K'_{fST}[A^{X+}][B^{Y-}]$
.....	Dissoc. of AB^{X+Y-}									+1	+1	-1			$K'_{rST}[AB^{X+Y-}]$
38	Assoc. of Mg^{2+}, HPO_4^{2-}			-1			-1						+1		$K'_{fmg4}[Mg^{2+}][HPO_4^{2-}]$
39	Dissoc. of $MgHPO_4^0$			+1			+1						-1		$K'_{rmg4}[MgHPO_4](aq)$
40	Assoc. of Mg^{2+}, PO_4^{3-}				-1		-1							+1	$K'_{fmg5}[Mg^{2+}][PO_4^{3-}]$
41	Dissoc. of $MgPO_4^-$				+1		+1							-1	$K'_{rmg5}[MgPO_4^-]$
	Units	mol/ℓ	mol/ℓ	mol/ℓ	mol/ℓ	mol/ℓ	mol/ℓ	mol/ℓ	mol/ℓ	mol/ℓ	mol/ℓ	mol/ℓ	mol/ℓ	mol/ℓ	

Table 2.8: Specific rate constants for ion pair reactions in Tables 2.6 and 2.7. See Loewenthal *et al.* (1989) for calculation of activity coefficients (f_i) for the different ionic species. The stability constants pK_{ST} values at infinite dilution are given in Table 2.6 (after Musvoto *et al.*, 1998).

No	Process	Specific rate constants					
		Ion pair association reaction		Ion pair dissociation reaction		Stability constant pK_{ST}	
		Symbol	Value	Symbol	Value	Symbol	Value
20..21	$Ca^{2+} + OH^- \quad CaOH^+$	K_{fca1}	$K_{rca1} K_{CaOH+}$	K_{rca1}	10^7 (/s)	K_{CaOH+}	$10^{-pKCaOH+} \cdot f_m \cdot f_d / f_m$
22..23	$Ca^{2+} + CO_3^{2-} \quad CaCO_3^0$	K_{fca2}	$K_{rca2} K_{CaCO3}$	K_{rca2}	10^7 (/s)	K_{CaCO3}	$10^{-pKCaCO3} \cdot f_d \cdot f_d$
24..37	$A^{X+} + B^{Y-} \quad AB^{X+Y-}$	K_{fST}	$K_{rST} K_{ST}$	K_{rST}	10^7 (/s)	K_{ST}	$10^{-pKST} \cdot f_{A(X+)} \cdot f_{B(Y-)} / f_{AB(X+Y-)}$
38..39	$Mg^{2+} + HPO_4^{2-} \quad MgHPO_4^0$	K_{fmg4}	$K_{rmg4} K_{MgHPO4}$	K_{rmg4}	10^7 (/s)	K_{MgHPO4}	$10^{-pKMgHPO4} \cdot f_d \cdot f_d$
40..41	$Mg^{2+} + PO_4^{3-} \quad MgPO_4^-$	K_{fmg5}	$K_{rmg5} K_{MgPO4-}$	K_{rmg5}	10^7 (/s)	K_{MgPO4-}	$10^{-pKMgPO4-} \cdot f_d \cdot f_t / f_m$

model, it was noted by Musvoto *et al.* (1998) that the equilibrium equations for ion pair formation are similar to those representing the dissociation equilibria of weak acid/bases.

Accordingly, the ion pair equilibria were described in terms of the kinetics of the forward and reverse reactions and included in the model in the same manner as outlined in Section 2.3 above for weak acid//bases (Musvoto *et al.*, 2000). Matrix representation of the ion pairs for inclusion in the model is shown in Table 2.7 and specific rate constants in Table 2.8.

2.5 CLOSURE

In this research project, the principal aim is to develop a kinetic model to describe the three phase (solid/gas/aqueous) processes operative in the anaerobic digestion of sewage sludge. In such a model, processes of importance include:

- biological
- weak acid/base chemistry
- gas exchange
- mineral precipitation

In this Chapter these processes have been reviewed. From this review it can be concluded:

For the biological processes;

- the kinetic model should include the steps of
    - hydrolysis
    - acidogenesis, both under high and low $\overline{pH}_2$
    - acetogenesis
    - acetoclastic methanogenesis
    - hydrogenotrophic methanogenesis

- no complete kinetic model of the above is available, and this will have to be developed from information contained in the literature.

For the weak acid/base chemistry;

- the kinetic approach of Musvoto *et al.* (1998) to modelling mixed weak acid/base systems offers considerable advantages over the more traditional equilibrium chemistry based approach, in particular;
    - the use of kinetics allows ready integration with both biological and precipitation models, and
    - the parameter pH is explicitly included, an advantage, as this parameter is of crucial importance in anaerobic systems.

For gas exchange;

- CO_2 loss/gain needs to be included in the model
- kinetic approach of modelling separately the rates of dissolution and expulsion of CO_2 would appear the most suitable, as
    - kinetics facilitates integration with the other kinetic processes
    - the approach is effectively identical to that derived from gas transfer theory.

For mineral precipitation;

- the general kinetic expression for precipitation of Koutsoukos *et al.* (1980) can be followed, but with the two constants "k's" replaced with a single precipitation rate constant "K'"
- minerals to be included are struvite, newberyite, calcite, amorphous calcium phosphate and magnesite
- solubility products for the above minerals are available in the literature.

Recognizing the above, the model was built in stages:

- Chapter 3 describes application of the integrated weak acid/base chemistry, gas exchange and mineral precipitation derived as above, to the aeration treatment of anaerobic digester supernatant.
- Chapter 4 describes the development of the kinetic model for the biological processes, and its integration with the weak acid/base chemistry model.
- Chapter 5 describes application of the above model to data sets in the literature.

CHAPTER 3

MINERAL PRECIPITATION FROM THE ANAEROBIC DIGESTER SUPERNATANT AT THE CAPE FLATS TREATMENT PLANT

3.1 INTRODUCTION

As described in Chapter 1, the first phase of this research investigation focussed on the development and evaluation of a kinetic model that describes the three phase (aqueous/gas/solid) chemical and physical processes likely to be operative in the anaerobic digestion of sewage sludges. Musvoto *et al.* (1998; 2000a, b) have developed such a kinetic model, and this model has been reviewed in Chapter 2. Accordingly, it was decided to accept the kinetic model of Musvoto *et al.* for this phase of the investigation. However, the model was to be extensively evaluated against experimental data, and modified if necessary. At the time, the Cape Flats Wastewater Treatment Plant (Cape Town, South Africa) was experiencing mineral precipitation problems in unit processes treating sludges from anaerobic digesters. This presented an ideal opportunity to evaluate the Musvoto *et al.* model, and to use the model to gain greater insight into the mineral precipitation problem at the Cape Flats Wastewater Treatment Plant. This Chapter describes this application.

3.2 BACKGROUND

At the Cape Flats (CF) Wastewater Treatment Plant, waste activated sludge (WAS) and primary sludge (PS) are thickened separately, the WAS by dissolved air flotation and the PS by gravity thickening. The two thickened sludge streams are blended and the blend is anaerobically digested in a high rate anaerobic digester (sludge age = ± 10d). The anaerobically digested sludge is degritted mechanically and then passes to a collection sump. The sludge is drawn from the sump, thickened/dewatered in centrifuges and the thickened/dewatered sludge passes to a thermal drying pelletization plant.

In operation of this sludge treatment scheme, problems have been experienced with mineral precipitation in the centrifuges, and in the pipework leading from the centrifuges to the pelletization plant. Precipitation inside the centrifuges reduces the capacity of the centrifuges to lower the moisture content of the output to the pelletization plant, which means that the moisture content of the sludge to the pelletization plant exceeds the suppliers specifications, and the thermal drying process is not optimal. Precipitation within the pipe network causes pipe blockages and reduced maximum flow rates.

Mineral precipitation from anaerobic digester supernatant (ADS) usually is the result of an increase in pH caused by the loss of CO_2 (Loewenthal *et al.*, 1994): Within the digester, anaerobic processes acting on the sludge cause evolution of CO_2 which results in an increase in the partial pressure of CO_2. When the ADS leaves the digester it comes into contact with atmospheric conditions where the partial pressure of CO_2 is much lower than inside the digester. This causes CO_2 loss from the ADS to the air, until equilibrium between the CO_2 concentration in the ADS and the air is reached. Loss of CO_2 can also be caused by pressure drops at pipe bends, pumps, etc. The loss of CO_2 represents an decrease in acidity which means that the pH of the ADS will increase. Inevitably the rise in pH causes some minerals to become supersaturated, which triggers the precipitation of these minerals; minerals likely to precipitate include struvite ($MgNH_4PO_4 \cdot 6H_2O$), calcium carbonate (calcite, $CaCO_3$) and amorphous calcium phosphate ($Ca_3(PO_4)_2 \cdot XH_2O$) (Musvoto *et al.*, 2000a; b).

From the above, the precipitation of minerals from ADS is a multi-phase (solid/liquid/gas) multi-mineral problem. From the experimental and theoretical framework developed by Musvoto *et al.* (1998) it is possible to examine systems with this type of mineral precipitation. This chapter details application of these methods to examine the precipitation of minerals from the ADS at the Cape Flats Treatment Plant, to evaluate the model itself and to gain insight into the precipitation processes.

This part of the research project consisted of an experimental investigation to gather appropriate data, and then the application of the Musvoto *et al.* kinetic model to the experimental data. In addition, a steady state model describing struvite precipitation was developed, and applied to the experimental data.

3.3 EXPERIMENTAL INVESTIGATION

Three types of experiments were undertaken; batch test, pH controlled experiments and extended pH controlled experiments.

3.3.1 Batch test

The aim of the batch test was to examine the effect of CO_2 loss on the ADS, in particular the effect on pH and the resultant precipitation of minerals.

3.3.1.1 Test Method

Anaerobically digested sludge was drawn from the anaerobic digesters at the Cape Flats Treatment Plant. The sludge was drawn directly from the digesters into a closed container in a manner which limited loss of CO_2 to the atmosphere, thereby preserving the *in situ* conditions inside the digesters. The sludge was transported to the laboratory at the University of Cape Town. Samples drawn from the container could not be filtered as the solids concentrations of the sludge were high and caused immediate blinding of the filters. Accordingly, the sludge in the sealed container was left to settle before samples were drawn for the batch test; initially the settling period was 24h, but tests showed that separation was not adequate after such a short settling period. Therefore, the settling period was increased to 5 days before samples were drawn for the batch experiment.

After 5 days settling, a 10ℓ sample was drawn from the sealed container and placed in a stirred batch reactor, maintained at a constant temperature of 20°C. To facilitate CO_2 loss to the atmosphere, the contents of the batch reactor were aerated by low pressure air passing through a "fish stone" diffuser placed at the bottom of the batch reactor. The pH in the reactor was monitored continually. At regular intervals 50mℓ samples were drawn from the reactor. The samples were immediately vacuum filtered through Whatman's No 1 filter papers; tests indicated that this filtration did not significantly influence the pH. The filtrate was divided into three. One filtrate sample was acidified by adding 2-3 drops (≈1mℓ) of concentrated nitric acid (HNO_3) to terminate the precipitation reactions; these acidified

samples were then stored until the end of the batch test when they were further filtered through 0.45µm filters. The second filtrate sample was not acidified and was also stored until the end of the batch test, when it was further filtered through 0.45µm filters. The third filtrate sample was acidified by adding 2-3 drops (≈1mℓ) of concentrated hydrochloric acid to preserve FSA. This sample was not filtered further, but stored for analysis at the end of the batch test.

The HNO_3 acidified 0.45µm filtered samples were analysed by an external laboratory for:

- Ca, Mg and Fe by inductively coupled plasma (ICP) emission spectroscopy (Standard Methods, 1985).
- Free (NH_3) and saline (NH_4^+) ammonia (FSA) and orthophosphate (PO_4) by autoanalyser.

The non-acidified 0.45µm filtered samples were analysed in house for:

- $H_2CO_3^*$ alkalinity and short chain fatty acid concentrations using the 5 pH point titration method (Moosbrugger *et al.*, 1992). The total inorganic carbon species concentrations ($C_T = H_2CO_3^* + HCO_3^- + CO_3^{2-}$) with time in the batch reactor were calculated from the measured $H_2CO_3^*$ alkalinities and the pH's measured in the batch reactor at the time the specific sample was taken.

The HCl acidified samples were analysed in house for:

- FSA by steam distillation method (Standard Methods, 1985).

3.3.1.2 Results

Detailed results are tabulated in Appendix A. The batch test data are shown plotted in Fig. 3.1 (a, b, c, d, e and f):

pH: From Fig. 3.1(a), the initial pH in the batch test is pH = 6.58. This pH is slightly lower than expected and is probably the result of the digester not functioning correctly, causing that short chain fatty (volatile) acids are still present in the ADS. With aeration, the pH of the batch test increases with time, to reach a value of pH = 8.0 by the end of the test (121

minutes). The pH increases because aeration strips CO_2 from the ADS, decreasing acidity. In the course of the batch test, after about 45 minutes the pH stabilises at pH = 7.6 for 20 minutes. This corresponds to the time where struvite starts precipitating (see below). Most likely this stabilisation of pH is due to the struvite precipitation decreasing the pH (due to removal of PO_4^{3-} species), while aeration and CO_2 stripping increases the pH. When the rate of struvite precipitation slows, the pH increases again.

Conductivity: From Fig. 3.1(b), conductivity which is a measure of the ionic strength of the solution, decreases slowly by a small amount as the test progresses. This decrease in conductivity is due to the precipitation of minerals as the test progresses (see below). However, the decrease in conductivity is not significant compared with the absolute value for conductivity.

SCFA, $H_2CO_3^*$ alkalinity and C_T: From Fig. 3.1(c), the SCFA concentration at the start of the batch test is high (± 4 000mg/ℓ as HAc) and remains approximately constant throughout the test. The high SCFA concentrations confirm the conclusion above that the initial low pH in the batch test is due to the presence of SCFA as a result of the digester not functioning correctly. That this concentration does not decrease in the batch test with aeration indicates the absence of biological activity in the batch test, probably due to the absence of aerobic micro-organisms. The C_T decreases throughout the batch test due to loss of CO_2 by gas stripping.

Na, K and Fe: From Fig. 3.1(d), the concentrations of Na, K and Fe do not change appreciably. This indicates that these species did not participate significantly in the precipitation reactions.

Mg and P: From Fig 3.1(e), Mg and P remain approximately constant at about 177mgP/ℓ and 65mgMg/ℓ respectively for the first 40 minutes while pH increases. Thereafter, both Mg

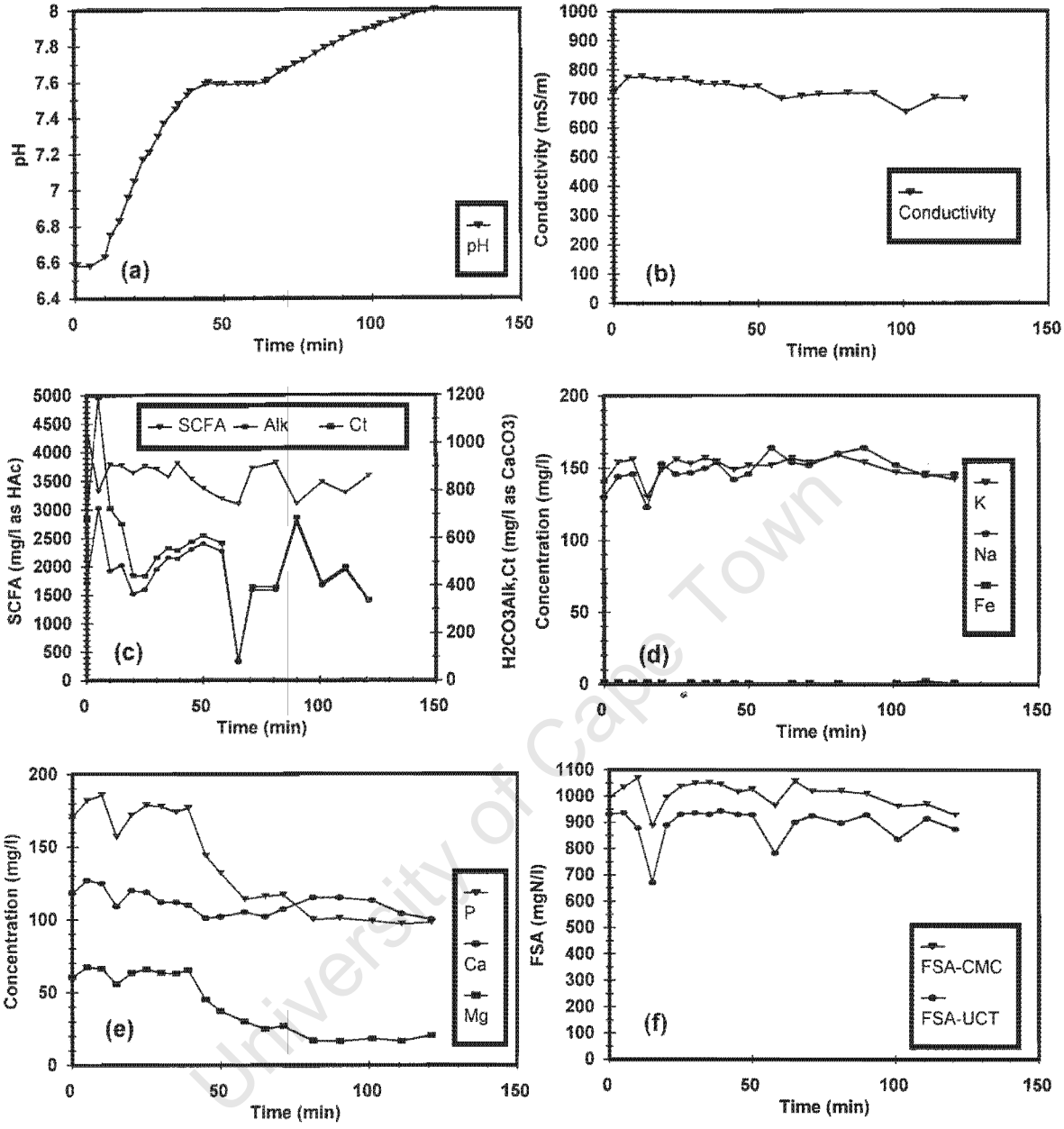

Fig 3.1: Measured soluble concentrations for pH (Fig 3.1a, top left); conductivity (Fig 3.1b, top right); total short chain fatty acids (SCFA), $H_2CO_3^*$ alkalinity (Alk) and total inorganic carbon species (C_T) (Fig 3.1c, middle left); potassium (K), sodium (Na) and iron (Fe) (Fig 3.1d, middle right); total phosphate species (P_T), calcium (Ca) and magnesium (Mg) (Fig 3.1e bottom left); free and saline ammonia (FSA) from external (CMC) and internal (UCT) analysis (Fig 3.1f, bottom right) for batch aeration of anaerobic digester liquor from Cape Flats (Cape Town, South Africa) digester treating a blend of primary and waste activated sludge.

and P concentrations decrease with time, and then level off after 80 minutes at about 99 mgP/ℓ and 17 mgMg/ℓ respectively, and thereafter remain constant at these values for the rest of the test. The molar decreases in P and Mg correspond to 2.5 mmol/ℓ and 2.0 mmol/ℓ respectively, giving a P/Mg ratio of 1.26. This is close to the theoretical molar ratio for struvite precipitation of 1. The slightly higher molar mass of P precipitating than Mg may be due to a small amount of calcium phosphate precipitation. The precipitation of the various minerals is dealt with more extensively in the theoretical analysis of the batch test (see Section 3.4 below).

Ca: From Fig 3.1(e), Ca concentrations are quite variable and so it is not possible to determine the exact amount of calcium precipitation. However, from the data it is evident that only a small quantity of Ca precipitates, probably as calcium phosphate or calcite. Determination of possible Ca precipitation is dealt with more extensively in the theoretical analysis of the batch test results (see Section 3.4 below).

FSA: Fig 3.1(f) shows the FSA determined by both the external (CMC) and internal (UCT) laboratories; results correspond reasonably closely, with the CMC FSA being about 10% greater than those from UCT, but following very similar trends. The FSA concentrations are high, at about 1 000mgN/ℓ. Accepting the P and Mg concentration changes to be primarily due to struvite precipitation, the expected decrease in FSA due to struvite precipitation is about 2mmol/ℓ = 28mgN/ℓ. Compared to the absolute concentrations, this change is so small that it can not be reliably detected with the analytical methods used. This observation is supported in the theoretical analysis of the batch test (see Section 3.4 below).

Minerals precipitating: From the results above, the dominant mineral precipitating is struvite, with possibly minor calcium phosphate. This was confirmed from theoretical simulations with a kinetic multi-precipitation weak acid/base model (see Section 3.4 below). For the state of the ADS drawn from the full-scale anaerobic digester at Cape Flats and used in the batch test, a maximum of approximately 2 to 2.5mmol/ℓ of struvite can be expected to precipitate. This corresponds to 274 to 343 mg/ℓ as $MgNH_4PO_4$, and taking into account the water of hydration 490 to 613 mg/ℓ as $MgNH_4PO_4{\cdot}6H_2O$. With the large volumes of ADS passing to the pelletization plant, this represents substantial precipitation potential. The exact

amount of struvite that will precipitate as the ADS passes along the sludge treatment line, or in a specialized reactor dedicated to struvite precipitation, will depend on the CO_2 loss and pH established, and on the initial concentrations of the reactants in the precipitation - principally Mg and P.

***Critical pH for struvite precipitation*:** The critical pH for struvite precipitation is pH = 7.6. Below this pH the solution is undersaturated with respect to struvite, and above the solution is supersaturated. Also, when a pH = 7.8 is reached the struvite precipitation reaction is essentially complete; further aeration does not stimulate significant further struvite precipitation compared to the mass precipitating when aeration increases the pH from pH 7.6 to 7.8. It is not possible to determine from the batch test whether struvite precipitation ceases because of the pH reached, or whether it ceases because aeration cannot significantly increase the pH further, or whether it ceases because initial Mg is limiting. However, from the theoretical investigation (Section 3.4 below) it appears that the latter is true.

***Time taken to reach critical pH for struvite precipitation*:** In the batch test conducted here, the critical pH for struvite precipitation is reached after 45 minutes aeration, and the precipitation is essentially complete after 80 minutes. However, these times will depend on a number of factors, including aeration rate, initial pH, buffer capacity, initial species concentrations, maximum pH reached with aeration, etc.

3.3.2 pH change tests

From the batch test above, aeration strips CO_2 from the ADS, causing the pH to increase. The increase in pH results in the precipitation of struvite from the bulk solution. Accordingly, it was decided to increase the pH by addition of NaOH to confirm that it is the increase in pH that is the primary process causing struvite precipitation. These tests also allow the struvite precipitation potential to be rapidly assessed.

3.3.2.1 Test Set 1

3.3.2.1.1 - *Test Method*

The ADS was again obtained from the anaerobic digesters at the Cape Flats Treatment Plant, as described above for the batch tests. The ADS was allowed to settle in the sealed container for a period of 5 days. One sample was drawn from the container and divided into three. The pH in one sample was decreased to pH = 2 by addition of a few drops of concentrated hydrochloric acid, to establish the baseline for mineral species concentrations before precipitation occurs. The pH in the second sample was increased to pH = 9.2 by addition of a few drops of concentrated NaOH; the batch test above indicated that this pH would exceed the pH where struvite precipitation initiates (pH = 7.6) and the theoretical investigation (Section 3.4 below) indicated that it would exceed the pH where no further significant struvite precipitation occurs (pH = ± 8.6) - accordingly increasing the pH to 9.2 would allow quantification of the struvite precipitation potential. The pH in the third sample was not adjusted.

The three samples above were then filtered through Whatman's No 1 filter paper, and this filtrate immediately filtered through 0.45µm filters. These filtrate samples were then acidified as for the batch test above, and analysed for ortho P (also called soluble reactive P, SRP) using the molybdate vanadate colorimetric method (Standard Methods, 1985). No metals analyses were done, as the test was in the development stage.

In the test it was found that filtering the samples through 0.45µm filters caused substantial CO_2 loss which resulted in the pH of the filtrate increasing to pH = 8, which deviates significantly from the sample pH = ±7. To take account of this observation, the test should be modified and the samples acidified prior to 0.45µm filtration.

3.3.2.1.2 *Results*

Results from two parallel tests on the same ADS obtained from the Cape Flats Treatment Plant anaerobic digesters, but run on different days are shown plotted in Fig. 3.2. Results

from the two tests correspond closely. In both tests, there is little difference in P concentration between samples at pH = 8 and pH = 9.2; essentially the precipitation reaction is complete at pH = 8. This is in agreement with the theoretical investigation results (see Section 3.4) where it was found that by far the vast majority of struvite precipitated when the pH increased to pH = 8, and only a small additional amount precipitated when pH increased from 8 to 9. From the theoretical investigation (Section 3.4), it was found that, with respect to mineral precipitation, the solution state at pH = 2 and pH = 7 (the initial pH of the ADS) was the same, i.e. no significant precipitation of struvite and ACP occurred between pH 2 and 7. Accordingly, the solution state at pH 2 and 9 could be used to assess the precipitation potential.

In Test 1, (92 - 74.5) = 17.5 mgP/ℓ = 0.56 mmolP/ℓ precipitated, and in test 2 (89 - 70) = 19 mgP/ℓ = 0.61 mmolP/ℓ. These values are in close agreement, but are substantially less than the precipitation in the batch test (2.5 mmol/ℓ). This reduced precipitation is because the initial P concentrations in these tests are significantly lower than those in the batch test, ±90 mgP/ℓ and ±180 mgP/ℓ respectively, and more than likely the initial Mg concentrations were

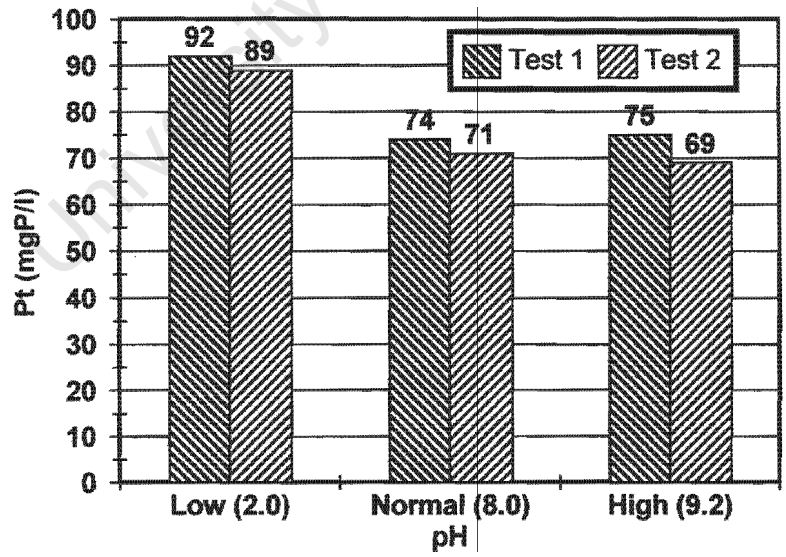

Fig 3.2: Effect of pH on soluble orthophosphate concentrations in anaerobic digester liquor from Cape Flats (Cape Town, South Africa) digester treating a blend of primary and waste activated sludge; pH change effected by HCl or NaOH addition.

similarly reduced (not measured for this test). This variation in initial conditions would indicate that the conditions in the Cape Flats digesters vary considerably. This observation is confirmed in subsequent experimental work (see below).

From the above, the pH change tests provide a simple rapid method to determine precipitation potential in ADS.

3.3.2.2 Test Set 2

In Test Set 1 above, a simple rapid method to determine precipitation potential in ADS was developed. In this set of tests the reproducibility of the method was examined.

3.3.2.2.1 *Test Method*

The ADS was obtained from the anaerobic digesters at Cape Flats Treatment Plant, as described above for the batch test. The ADS was allowed to settle in the sealed container for a period of 5 days. One sample was drawn from the container and divided into eight. In four of these samples the pH was reduced to pH = 2.0, and in the remaining four samples the pH was increased to pH = 9.0, as described above. The samples were filtered as described above and analysed for ortho P as above. At the two extreme pHs, loss of CO_2 during filtration will not alter the pH significantly, so no measures had to be taken to control pH on filtration.

3.3.2.2.2 *Results*

Results from two parallel tests on two different ADSs obtained from Cape Flats anaerobic digesters are shown in Figs. 3.3 and 3.4 respectively. It is evident that the results from the test method are reproducible. Averaging the pH =2 and pH = 9 results from the two tests, for the first test (Fig. 3) (156 - 106.3) = 49.7 mgP/ℓ = 1.60mmolP/ℓ precipitated and for the second test (Fig. 4) (190 - 110.8) = 79.2 mgP/ℓ = 2.55mmolP/ℓ precipitated. Again these values differ considerably due to the different initial P concentrations (and presumably Mg concentrations) in the two tests, averages 156 and 190 mgP/ℓ respectively. This variation in ADS initial state conforms to observations in previous tests above.

For the first test (Fig. 3.3), analyses for Mg on one sample set from the same ADS batch were available, and the measured concentrations gave Mg = 45 and 1.8 mgMg/ℓ at pH = 2 and 9 respectively. This indicates that (45 - 1.8) = 43.2 mgMg/ℓ = 1.8 mmolMg/ℓ precipitated.

This gives a P/Mg ratio of 0.9 which is close to the theoretical molar ratio for struvite precipitation of 1, which would indicate that struvite precipitation dominated with little calcium phosphate precipitation. This was confirmed in the theoretical investigation (see Section 3.4 below).

3.3.2.3 Test Set 3

Having demonstrated above that the test method is reproducible and having identified possible problems with the test method, the method was applied with metals analysis.

3.3.2.3.1 ***Test Method***

The ADS was obtained from the anaerobic digesters at Cape Flats Treatment Plant, as described above for the batch test. The ADS was allowed to settle in the sealed container for a period of 5 days. One sample was drawn from the container and divided into three. The pH in one sample was decreased to pH = 2 by addition of a few drops of concentrated hydrochloric acid, to determine whether precipitation had already occurred in the anaerobic digesters. The pH in the second sample was increased to pH = 9.0 by addition of a few drops of concentrated NaOH; the batch test above indicated that this pH would exceed the pH where struvite precipitation initiates (pH = 7.6) and the theoretical investigation (Section 3.4 below) indicated that it would exceed the pH where no further significant struvite precipitation occurs (pH = ± 8.6) - accordingly increasing the pH to 9.0 would allow quantification of the struvite precipitation potential. The pH in the third sample was not adjusted.

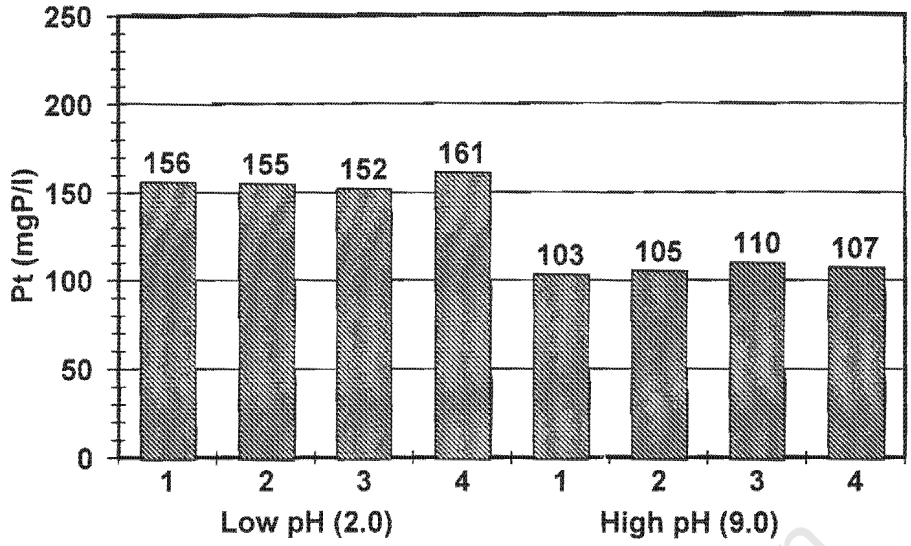

Fig 3.3: Effect of pH on soluble orthophosphate concentrations in anaerobic digester liquor from Cape Flats (Cape Town, South Africa) digester treating a blend of primary and waste activated sludge; pH change effected by HCl or NaOH addition, samples are duplicates on the same anaerobic digester liquor.

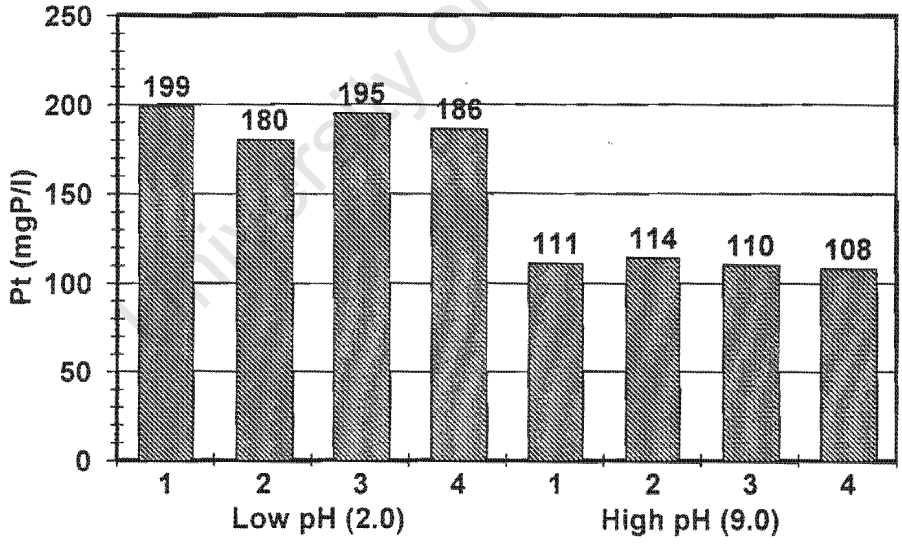

Fig 3.4: Effect of pH on soluble orthophosphate concentrations in anaerobic digester liquor from Cape Flats (Cape Town, South Africa) digester treating a blend of primary and waste activated sludge; pH change effected by HCl or NaOH addition, samples are duplicates on the same anaerobic digester liquor.

The three samples above were then filtered through Whatman's No 1 filter paper, and this filtrate immediately filtered through 0.45μm filters. These filtrate samples were then acidified as for the batch test above, and analysed for:

- Ca, Mg and Fe by inductively coupled plasma (ICP) emission spectroscopy (Standard Methods, 1985) at an external laboratory (CMC).
- Free (NH_3) and saline (NH_4^+) ammonia (FSA) and orthophosphate (PO_4) by autoanalyser at an external laboratory (CMC).
- ortho P (also called soluble reactive P, SRP) using the molybdate vanadate colorimetric method (Standard Methods, 1985) at internal laboratory (UCT).

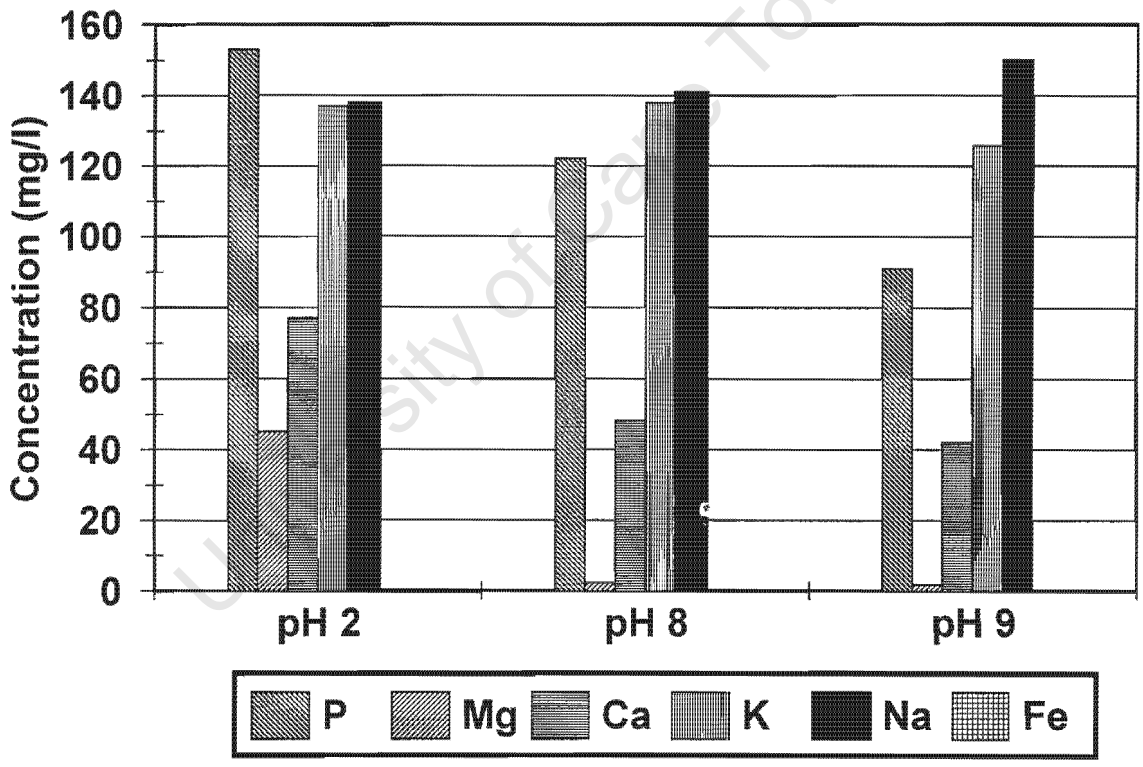

Fig 3.5: Effect of pH on soluble orthophosphate (P), magnesium (Mg), calcium (Ca), potassium (K), sodium (Na), and iron (Fe) concentrations in anaerobic digester liquor from Cape Flats (Cape Town, South Africa) digester treating a blend of primary and waste activated sludge; pH change effected by HCl or NaOH addition.

In the test it was found that filtering the samples through 0.45μm filters caused substantial CO_2 loss which resulted in the pH of the filtrate increasing to pH = 8, which deviates significantly from the sample pH = ±7. To take account of this observation, the test method should be modified and the samples acidified prior to 0.45μm filtration.

3.3.2.3.2 *Results*

Detailed results are tabulated in Appendix A. The test data are shown plotted in Fig. 3.5.

Na, K and Fe: From Fig. 3.5, the concentrations of Na, K and Fe do not change appreciably with change in pH. This indicated that, in agreement with the batch test results (Section 3.3.1 above), these species did not participate significantly in the precipitation reactions.

Mg: Mg concentrations are 45, 2.3 and 1.8 mgMg/ℓ at pH 2, 8 and 9 respectively. This gives a change from pH 2 to 9 of (45 - 1.8) = 43.2 mgMg/ℓ = 1.8 mmolMg/ℓ. Also, the Mg concentration at pH 8 is close to the concentration at pH 9 , indicating little struvite precipitation from pH 8 to 9.

P: P concentrations are 153, 122 and 91 mgP/ℓ at pH 2, 8 and 9 respectively. This gives a change from pH 2 to 9 of (153 - 91) = 62 mgP/ℓ = 2 mmolP/ℓ. The P/Mg molar ratio for this test is 1.1, which is close to the theoretical molar ratio for struvite precipitation of 1. This would indicate that struvite is the dominant precipitating mineral; the slightly higher measured P/Mg ratio than the theoretical value for struvite would indicate that some calcium phosphate did precipitate, but in small amounts. This was confirmed in the theoretical investigation (Section 3.4 below).

Ca: Ca concentrations are 77, 48 and 42 mgCa/ℓ at pH 2, 8 and 9 respectively. This gives a change from pH 2 to 9 of (77 - 42) = 35 mgCa/ℓ = 0.88 mmolCa/ℓ. This represents significant Ca precipitation and does not agree with the other tests, and the theoretical

simulations (see Section 3.4 below). Possibly an error was made in measurement of Ca at pH 2.

3.3.2.4 Discussion

From the results above for the pH change tests, it is evident that:

- Struvite is the dominant precipitating mineral.
- Increase in pH is the primary process causing struvite precipitation.
- The initial Mg and P concentrations determine to a large extent the mass of struvite that will precipitate, when the pH is increased to pH = 9.
- The pH change tests provide a method that allows the struvite precipitation potential to be rapidly assessed.
- In the pH change tests, filtering the original sample through 0.45μm filters caused substantial CO_2 loss which resulted in the pH of the filtrate increasing to pH = 8, which deviates significantly from the sample pH = ±7. To take account of this observation, the test method should be modified and the samples acidified prior to 0.45□m filtration.

3.3.3 Extended pH change tests

The pH change tests above only provide information at the pH extremes so that an assessment of precipitation potential can be obtained. No information is provided on the state of the solution in moving from the existing pH to the higher pH. Accordingly it was decided to do extended pH change tests in which the solution state at pHs between the existing pH and the higher pH would be obtained.

3.3.3.1 Test Method

The test method was a combination of the batch test and pH change tests above. The objective was to measure the state of the solution at multiple pH values, from the initial pH of the ADS to pH = 9. To achieve change in pH, the ADS was aerated as in the batch test, but with samples being drawn from the test at specific pH values rather than at specific time intervals.

The ADS was obtained from the anaerobic digesters at Cape Flats Treatment Plant, as described above for the batch test. The ADS was allowed to settle in the sealed container for a period of 5 days. A 10ℓ supernatant sample was drawn from the sealed container and placed in a stirred batch reactor, maintained at a constant temperature of 20°C. To facilitate pH change via CO_2 loss to the atmosphere, the contents of the batch reactor were aerated by low pressure air passing through a "fish stone" diffuser placed at the bottom of the batch reactor. Conductivity was measured at the start of the test - the batch test above indicated that this does not change significantly as the test progresses and thus only the initial value is adequate. The pH in the reactor was monitored continually. At specific pH values the aeration was stopped and 50mℓ samples were drawn from the reactor. The samples were immediately vacuum filtered through Whatman's No 1 filter papers. These samples were then stored until the end of the test. Aeration of the test then recommenced. At the end of the test, the pH in each stored sample was adjusted to the pH in the batch test at the time the sample was taken by addition of HCl or NaOH. The pH adjusted samples were then filtered through 0.45μm filters, the filtrates acidified with nitric acid and analysed as for the batch test. Due to problems in the analysis of Mg from the external laboratory (CMC), additionally samples were sent to another external laboratory (Department of Chemistry at UCT) for analysis of Mg via inductively coupled plasma (ICP) emission spectroscopy (Standard Methods, 1985).

During the course of the test it was found that aeration did not increase the pH adequately. Accordingly, prior to filtration the pH in samples 5 to 10 were increased by

addition of NaOH, to the desired pH values. Thus, this test is not time dependent, but rather related to pH.

3.3.3.2 Results

Detailed results are listed in Appendix A. From Appendix A, the one external laboratory (CMC) analysis for Mg gave negligible concentrations, even in the original ADS sample at time = 0, whereas the analysis by the other external laboratory (UCT) gave significant Mg (29.1 mgMg/ℓ) at time = 0. Accordingly, the UCT Mg values were accepted. The test data are shown plotted in Fig. 3.6 (a to d). The results are similar to those obtained in the batch test (Section 3.3.1 above), but the pH towards the end of the test was much higher than in the batch test due to artificially increasing this by NaOH addition.

pH: From Fig. 3.6(a), the initial pH in the batch test is pH = 7.1. This pH is higher than the initial pH for the previous batch test, and is the value expected for digesters functioning correctly. With aeration, the pH of the batch test increases with time, to reach a value of pH = 7.6 after 70 min. The pH increases because aeration strips CO_2 from the liquor, increasing acidity. Thereafter, the pH in the samples were increased by addition of NaOH prior to filtration. This increases the pH above the values recorded in the previous batch test (Section 3.3.1 above).

Due to the above artificial increase in pH, the rest of the data are shown plotted against pH and not time.

Conductivity: Conductivity was not monitored throughout the test as the results from the batch test (Section 3.3.1 above) indicated that, although conductivity decreases slowly by a small amount as the test progresses (due to the precipitation of minerals), the decrease in conductivity is not significant compared with the absolute value for conductivity. Initial conductivity was measured at 720mS/m, which is similar to the batch test (Section 3.3.1 above).

***Na, K and Fe*:** From Fig. 3.6(b), the concentrations of Na, K and Fe do not change appreciably as the pH increases. This indicates that these species did not participate significantly in the precipitation reactions, in agreement with the observations in the previous batch test (Section 3.3.1).

Mg and P: From Fig. 3.6(c), P remains approximately constant at about 116mgP/ℓ while pH increases to about pH 7.4 (at about 70 minutes). Thereafter, P concentrations decrease as the pH increases further, and then level off at about 95mgP/ℓ when the pH reaches about 8.7, and thereafter remain constant at this value when the pH is increased to 9. Unfortunately, Mg values during the course of the test are not available due to analytical problems. However, values are available for the start and end of the test, at 29.1 and 2.3 mgMg/ℓ for pH = 7.1 and 9 respectively. The molar decreases in P and Mg correspond to 0.74mmol/ℓ and 1.12mmol/ℓ respectively, giving a P/Mg ratio of 0.7. This deviates from the theoretical molar ratio for struvite precipitation of 1. The small difference cannot be ascribed to calcium phosphate precipitation, since the Mg decrease exceeds the P decrease. The precipitation of the various minerals is dealt with more extensively in the theoretical analysis of the batch test (see Section 3.4 below).

***Ca*:** From Fig. 3.6(c), Ca concentrations do not change significantly during the test, indicating little or no calcium precipitation, as calcium phosphate or calcite. Determination of possible Ca precipitation is dealt with more extensively in the theoretical analysis of the batch test results (see Section 3.4 below).

***FSA*:** From Fig. 3.6(d), the FSA concentrations are high, at about 730mgN/ℓ. Accepting the P and Mg concentration changes to be primarily due to struvite precipitation, the expected decrease in FSA due to struvite precipitation is about 1mmol/ℓ = 14mgN/ℓ. As observed in the batch test above, compared to the absolute concentrations, this change is so small it can not be reliably detected with the analytical methods used. This observation is supported in the theoretical analysis of the batch test (see Section 3.4 below).

***Minerals precipitating*:** From the results above, the dominant mineral precipitating is struvite, with possibly minor calcium phosphate. This was confirmed from theoretical simulations with a kinetic multi-precipitation weak acid/base model (see Section 3.4 below). For the state of the ADS drawn from the full-scale anaerobic digester at Cape Flats and used in the extended pH change test, a maximum of approximately 0.7 to 1.1mmol/ℓ of struvite can be expected to precipitate. This corresponds to 96 to 151 mg/ℓ as $MgNH_4PO_4$, and taking into account the water of hydration 172 to 270 mg/ℓ as $MgNH_4PO_4 \cdot 6H_2O$. With the large volumes of liquor passing to the pelletization plant, this represents substantial precipitation potential. The exact amount that will precipitate on treatment of the liquors will depend on the CO_2 loss and pH established, and on the initial concentrations of the reactants in the precipitation - principally Mg and P.

***Critical pH for struvite precipitation*:** In this test the critical pH for struvite precipitation is pH = 7.4, which closely corresponds to the value of pH = 7.6 measured in the batch test. Below this pH the solution is undersaturated with respect to struvite, and above the solution is supersaturated. Also, when a pH = 8.7 is reached the struvite precipitation reaction is essentially complete; further increase in pH does not stimulate further struvite precipitation. This latter value of 8.7 for struvite precipitation completion is considerably higher than the pH = 7.8 measured in the batch test (pH = 7.8, Section 3.3.1). However, in the batch test the increase in pH is limited to that possible through aeration, whereas in this extended pH change test the pH was adjusted by NaOH addition. In the theoretical investigation (Section 3.4 below), it was found that in the previous batch test the completion of struvite precipitation was primarily due to the inability of aeration to increase pH much above 7.8 - in the model if the pH were increased further, additional struvite precipitation would result, which is in agreement with this extended pH change test. However, the additional struvite precipitation for pH > 7.8 would be limited by the concentration of Mg available for precipitation, because Mg is the ultimate limit on the concentration of struvite that can potentially precipitate.

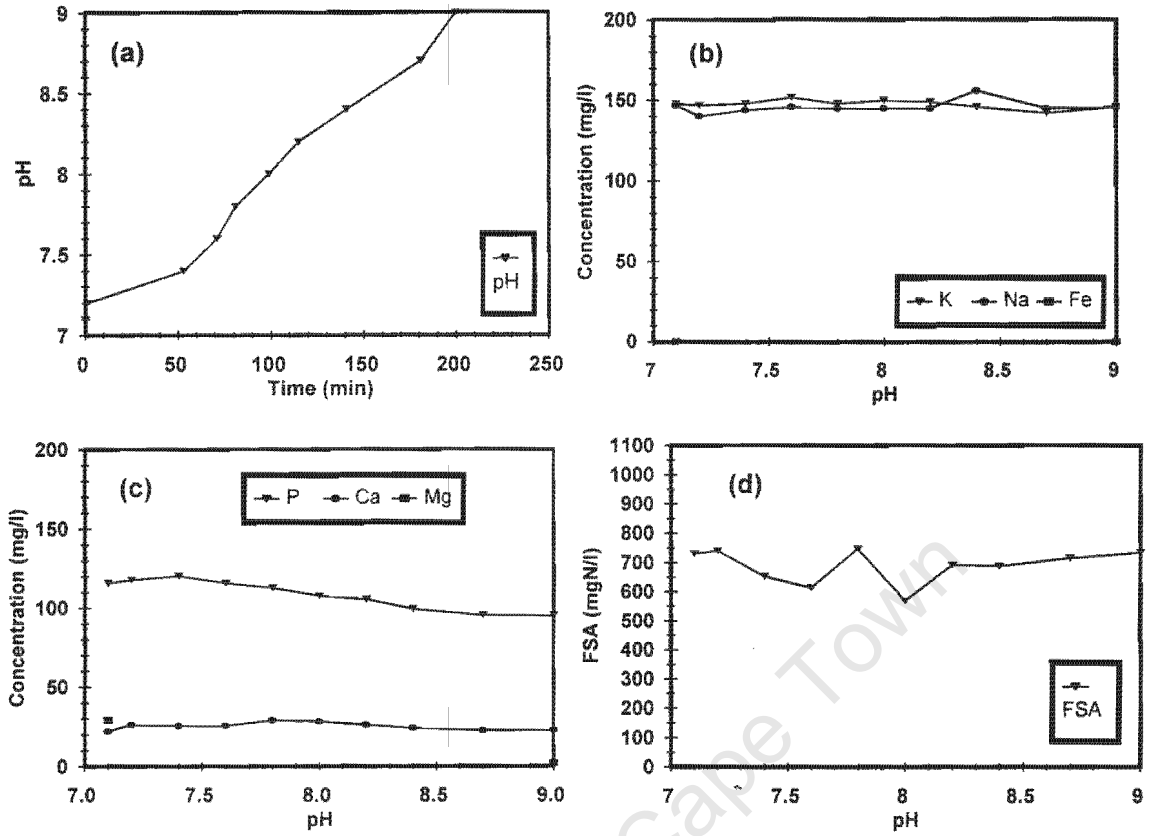

Fig 3.6: Measured soluble concentrations for pH with time (Fig 3.6a, top left) and potassium (K), Sodium (Na) and iron (Fe) (Fig 3.6b, top right); total phosphates species (PT), calcium (Ca) and magnesium (Mg) (Fig 3.6c bottom left); free and saline ammonia (FSA) (Fig 3.6d, bottom right) with pH for extended pH change test on anaerobic digester liquor form Cape Flats (Cape Town, South Africa) digester treating a blend of primary and waste activated sludge; note that form sample 5 NaOH was added to increase the pH.

***Time taken to reach critical pH for struvite precipitation*:** In the extended pH change test conducted here, the critical pH for struvite precipitation is reached after 60 minutes aeration. This value is longer than that measured in the batch test (Section 3.3.1) of 45 minutes (Fig. 3.1e). However, this time will depend on a number of factors, including aeration rate, initial pH, buffer capacity, etc. The time to reach complete precipitation in the two tests can not be compared as the pH adjustment procedures differed between the two tests.

3.4 THEORETICAL INVESTIGATION

Based on the experimental results obtained, a theoretical investigation of the precipitation in the Cape Flats ADS was also undertaken. This involved the application of kinetic and steady state models.

3.4.1 Kinetic model application

From the experimental investigation above, the precipitation of minerals from ADS is a multi-phase (solid/liquid/gas) multi-mineral problem. Musvoto *et al.* (1998) has developed a kinetic based modelling approach to simulate systems with this type of mineral precipitation. Following this approach, a kinetic model was developed to simulate the reactions that occur on ADS aeration (Musvoto *et al.*, 2000a, b). This model incorporates:

- Forward and reverse dissociation reactions for the weak acid/base systems water, carbonate, phosphate, ammonium and short chain fatty acids.
- Precipitation of the minerals struvite ($MgNH_4PO_4$ $6H_2O$), amorphous calcium phosphate (ACP, $Ca_3(PO_4)_2$ xH_2O), newberyite ($MgHPO_4$ $3H_2O$), calcite ($CaCO_3$) and magnesite ($MgCO_3$); from the literature and experimental investigations, these are the minerals most likely to precipitate on aeration of ADS.
- Gas stripping of NH_3 and gas exchange of CO_2.
- Ion pairing reactions for $CaOH^+$, $CaCO_3(aq)$, $CaHCO_3^+$, $CaPO_4^-$, $CaHPO_4(aq)$, $CaH_2PO_4^+$, $MgOH^+$, $MgCO_3(aq)$, $MgHCO_3^+$, $MgHPO_4(aq)$ and $MgPO_4^-$; from the literature, these are the ion pairs commonly found in systems dominated by the various carbonate, Mg, Ca, P and N species at pHs typical of ADS.

The model has been reviewed in more detail in Chapter 2 and is presented in Tables 2.1, 2.3, and 2.7. The model was validated by means of aeration batch tests on upflow anaerobic sludge bed (UASB) liquors and sewage sludge ADS (Musvoto *et al.*, 2000b). The weak acid/base dissociation constants, ion pairing stability constants and mineral

solubility products were kept constant at typical literature values. By curve fitting the predicted to the measured experimental batch test results for inorganic carbon (C_T), Mg, Ca, free and saline ammonia (FSA), orthoP and pH over 24h or longer, the mineral precipitation and gas stripping rates were determined for the UASB and sewage sludge ADS. From the simulations, a deeper understanding of the processes operating in the batch tests could be developed, to identify *inter alia* the dominant precipitating minerals, the conditions that cause these minerals to precipitate and the rates of precipitation of the minerals.

Although the kinetic model was applied by Musvoto *et al.* (2000b) to batch aeration experiments on ADS from the Cape Flats Treatment Plant, these experiments were not applicable to the present problem at the plant. At the time (1996/1997) the Cape Flats Treatment plant did not exhibit biological excess P removal (BEPR) and so the ADS had Mg and P concentrations much lower (Mg = 20 - 30mg/ℓ; P = 15 - 30mgP/ℓ) than ADS from plants that exhibit BEPR (P = 150 - 250 mgP/ℓ, Pitman, 1995). Since the objective in the experiments was to examine ADS from BEPR plants, the initial Mg and P concentrations were increased artificially by adding chemicals. The addition of chemicals to the ADS from Cape Flats in predetermined molar ratios would cause that the precipitation behaviour in the batch tests would deviate from the "usual" behaviour. From the above, the kinetic model forms a useful analytical tool to evaluate multi-phase (solid/liquid/gas) multi-mineral problems, and accordingly was applied to the ADS from Cape Flats Treatment Plant. Three sets of simulation were undertaken. The kinetic model was applied to:

1. the batch test described above (Section 3.3.1),
2. the extended pH change test described above (Section 3.3.3), and
3. theoretically examine the effect on mineral precipitation of changing initial concentrations of Mg and P, and the aeration rate.

All simulations were using AQUASIM ver. 2.0 (Reichert, 1994).

3.4.1.1 Batch test

The model as developed by Musvoto *et al.* (2000a, b) and described in Chapter 2 (Tables 2.1, 2.3, and 2.7) was applied to the batch test described in Section 3.3.1 above.

Model preparation

The model was given as input the eight dissociation constants (pK) and their temperature sensitivities for the 16 forward and reverse dissociation processes for the water, carbonate, phosphate, SCFA and ammonia weak acid/base systems (Tables 2a and 2c in Musvoto *et al.*, 1997; Tables 2.1 and 2.2 in Chapter 2) and the 11 stability constants (pK_{ST}) for the 22 forward and reverse dissociation processes for the ion pairs (Tables 1a and 1c in Musvoto *et al.*, 2000c; Tables 2.6 and 2.8 in Chapter 2). Also given as input were the solubility product (pK_{SP}) values from the literature for the five minerals identified to precipitate (Table 7, Musvoto *et al.*, 2000; Table 2.5 in Chapter 2). These pK, pK_{ST} and pK_{SP} values were accepted to be model constants (not changed). With the measured initial conductivity, also given as input and converted internally in the model to an ionic strength value with the formulae given by Loewenthal *et al.* (1989) (ionic strength μ = conductivity.1.68×10^{-4}), the input pK, pK_{ST} and pK_{SP} values were internally corrected for ionic strength with the appropriate mono-, di- and trivalent ion activity coefficients, as indicated in the above mentioned tables. The input pK values were also internally adjusted for temperature; the pK_{ST} and pK_{SP} values could not be adjusted as information on temperature sensitivities for these is not available in the literature. Also given as input were the specific rate constants for weak acid/bases (Table 2.2a in Chapter 2), precipitation (Table 2.5 in Chapter 2) and ion pairs (Table 2.8 in Chapter 2); the last had to be changed from 10^7 (/s) to 10^6 (/s) for computational stability. However, the rates remain effectively instantaneous. The initial total species concentrations (C_T, P_T, N_T, Ca and Mg) and pH values measured in the batch test were also given as input to the model, as initial conditions.

Model calibration - determination of mineral precipitation and gas stripping rates

In validating their model Musvoto *et al.* (2000c) changed only the precipitation rate constants (K_{ppt}) for the five minerals and the specific gas stripping rate constants (K_r) for CO_2 and NH_3 (the calibration constants); these seven rate constants were determined by trial and error fitting of theoretical model predictions to the experimental data. Values are listed in Table 2.5. In the initial simulations of the batch test reported here, the values for these constants found by Musvoto *et al.* (2000c) were accepted. In the simulations it was found that only one constant required adjustment - the gas stripping rate for CO_2. In the model this rate is calculated from the specific rate for O_2; the value for this rate had to be changed from the range 225 - 600/d reported by Musvoto *et al.* to 130/d. This change is not unexpected since the specific gas stripping rates depend on the aeration conditions (gas flow rates, mixing, solids, etc.) applied in the specific test, and this differed between the test reported here and those reported by Musvoto *et al.* Also, in the simulations the specific rate constant for struvite precipitation was changed to improve the fit between predicted and measured Mg results; changing the value for this rate constant from the "default" value of 300/d to 1 000/d improved the fit, see below.

Results

Predicted and measured batch test concentrations are shown plotted in Fig. 3.7(a to f). For all concentrations reasonably close correlation was obtained.

Minerals precipitated: Accepting that the predictions are reasonable, the predicted concentrations of the different minerals that precipitate can be determined, see Fig 3.8. From Fig. 3.8, the dominant mineral that precipitates is struvite (516mg/ℓ as $MgNH_4PO_4$ $6H_2O$ = 97% of mass of precipitant after 2 hours), followed by ACP (16.5 mg/ℓ as $Ca_3(PO_4)_2$ = 3% of the mass of precipitant after 2 hours), and negligible newberyite, calcite and magnesite precipitate. These observations are similar to those of Musvoto *et al.*, but with less ACP precipitation. The lower ACP precipitation is due to the short duration of the test here with final pH reached about pH = 8, whereas in the Musvoto *et*

al. tests the tests ran for > 48 hours with final pH = ± 8.8; significant ACP precipitation only occurs at higher pHs, see below.

Critical pH for struvite precipitation: As noted in Section 3.3.1 above, precipitation of struvite does not commence immediately on aeration. From the predictions (Fig. 3.7e), struvite precipitation only starts after approximately 30 minutes, becoming significant after about 35 to 40 minutes (Fig. 3.8); this indicates that the solution is initially undersaturated with respect to struvite, but as the pH increases the solution becomes supersaturated causing struvite precipitation. This is illustrated in Fig. 3.9, where minerals precipitated are plotted against pH; the pH at which the solution becomes supersaturated is about pH = 7.2, but significant precipitation only occurs at pH > 7.3. Comparing Figs. 3.8 and 3.9, it is evident that the struvite precipitation slows significantly after about 60 minutes. This reduction in precipitation is not primarily due to the higher pH, but is due to the rate of pH increase slowing (Fig. 3.7a) caused by the reducing rate of CO_2 loss as the solution approaches CO_2 equilibrium with the atmosphere. This becomes evident after about 90 minutes (Fig. 3.8) by which time 88% of the struvite that precipitates in the test has already precipitated.

Critical pH for ACP precipitation: Similarly to struvite, ACP precipitation only starts after about 60 minutes (pH = ± 7.7), but then, unlike struvite, increases monotonically with time (Fig. 3.8) and exponentially with pH (Fig. 3.9). However, at the end of the test with the maximum pH reached of about 8, ACP precipitation is not significant.

Effect of changing struvite specific precipitation rate constant: To provide a closer fit between predicted and measured Mg, the specific struvite precipitation rate constant was increased from the "default" value of 300/d to 1 000/d. This change influenced only Mg, P and struvite precipitation. Predicted and measured concentration time profiles for these parameters are shown in Fig. 3.10 (a to d). Comparing the predictions with the specific struvite precipitation rate constant of 300/d (Figs 3.7e, 3.7f, 3.8 and 3.9) with those for the specific struvite precipitation rate constant of 1 000/d, increasing the rate constant improves the correlation between predicted and measured Mg and P. However, the effect

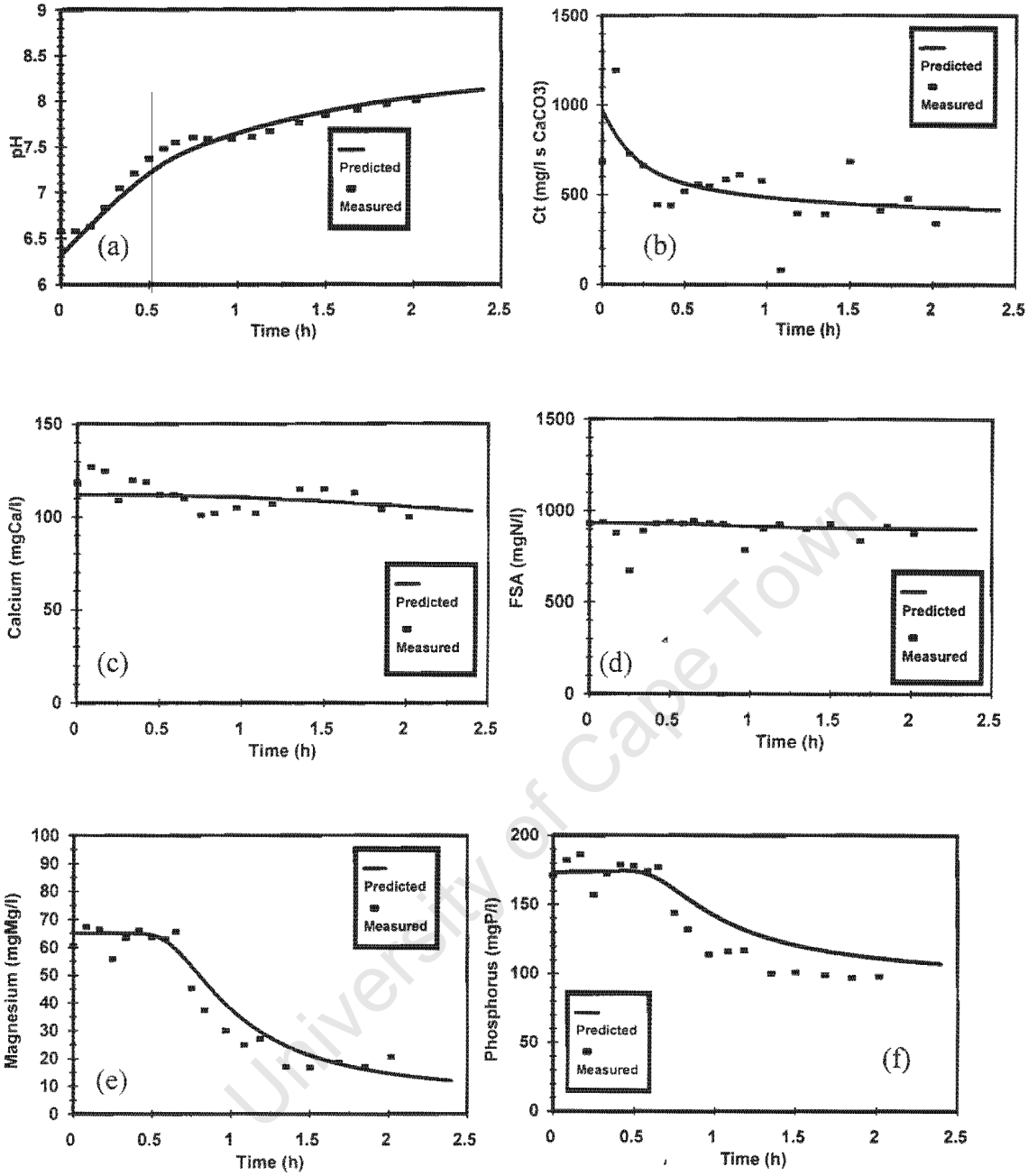

Fig. 3.7: Predicted and measured soluble concentrations for pH (Fig 3.7a, top left); total inorganic carbon species (C_T)(Fig 3.7b, top right); calcium (Ca) (Fig 3.7c, middle left); free and saline ammonia (FSA) (Fig 3.7d, middle right); magnesium (Mg) (Fig 3.7e, bottom left); total phosphate species (P_T) (Fig 3.7f, bottom right) for batch aeration of anaerobic digester liquor from Cape Flats (Cape Town, South Africa) digester treating a blend of primary and waste activated sludge; predictions using kinetic model of Musvoto *et al.*

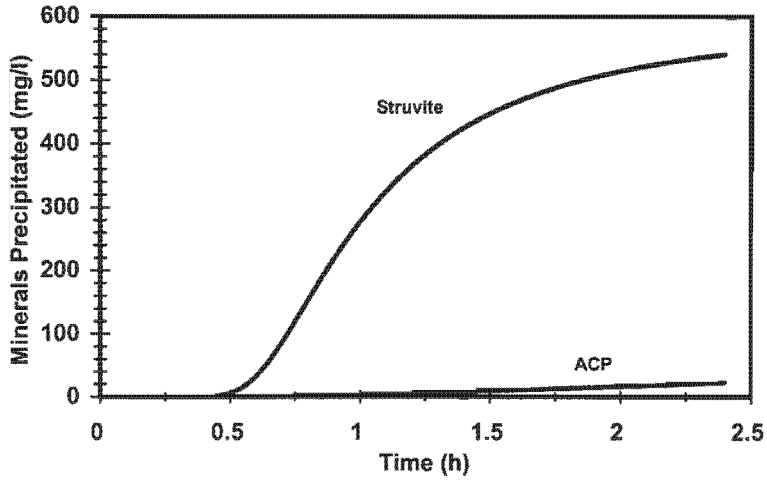

Fig 3.8: Predicted struvite and amorphous calcium phosphate (ACP) precipitation with time for batch aeration of anaerobic digester liquor from Cape Flats (Cape Town, South Africa) digester treating a blend of primary and waste activated sludges. Experimental data in Fig 3.7; predictions with kinetic model of Musvoto *et al.* (2000a, b and c).

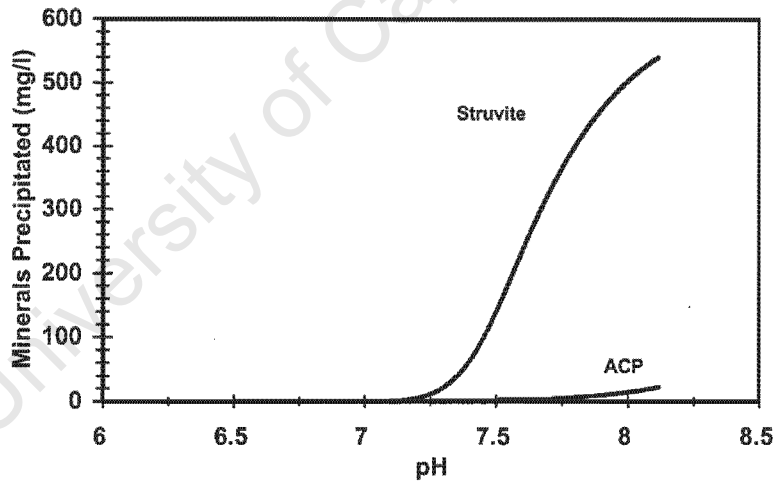

Fig 3.9: Predicted struvite and amorphous calcium phosphate (ACP) precipitation with pH for batch aeration of anaerobic digester liquor from Cape Flats (Cape Town, South Africa) digester treating a blend of primary and waste activated sludges. Experimental data in Fig 3.7; predictions with kinetic model of Musvoto *et al.* (2000a, b and c).

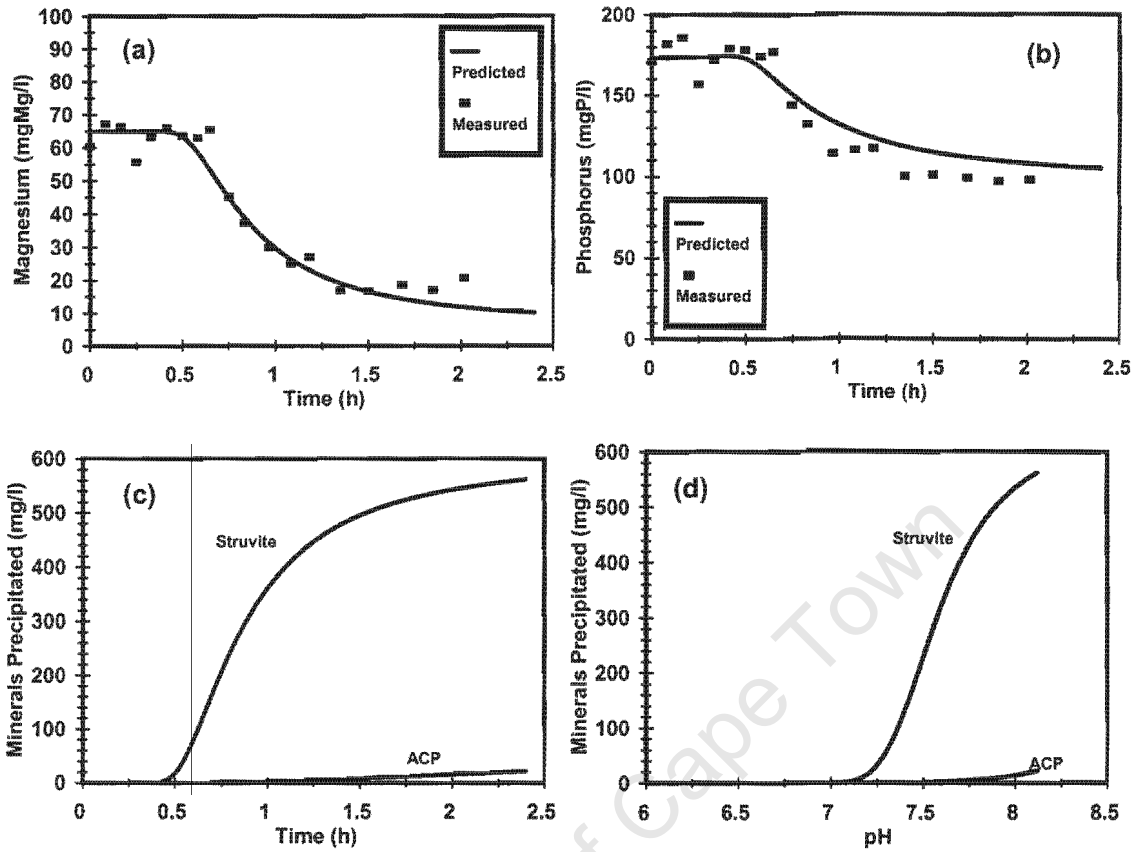

Fig 3.10: Predicted and measured soluble concentrations for magnesium (Mg) (Fig 3.10a, top left); total phosphate species (P_T) (Fig 3.10b, top right); struvite and amorphous calcium phosphate (ACP) precipitation with time (Fig 3.10c, bottom left); struvite and amorphous calcium phosphate (ACP) precipitation with pH (Fig 3.10d, bottom right) for batch aeration of anaerobic digester liquor form Cape Flats (Cape Town, South Africa) digester treating a blend of primary and waste activated sludge; predictions using kinetic model of Musvoto *et al.*, (2000a, b and c) with specific rate for struvite precipitation increased form "default" 300/d (Figs. 3.7, 3.8 and 3.9) to 1000/d.

on struvite precipitation is relatively small, with only an additional 5% struvite precipitating after 2 hours aeration. This confirms the observation that the precipitation of struvite with time is primarily linked to the rate of change of pH caused by aeration; the kinetics of precipitation have a relatively small influence. This implies that the solution is effectively continually at equilibrium as the pH changes. This indicated that equilibrium chemistry could also be used to analyse the data (see below).

3.4.1.2 Extended pH change test

The model developed by Musvoto *et al.* (2000) was applied to the extended pH change test described in Section 3.3.3 above.

Model preparation

Model preparation was the same as for the batch test, as described in Section 3.4.1.1 above; the same values for the pK, pK_{ST} and pK_{SP} constants were used, and the same corrections for ionic strength and temperature were applied. The initial total species concentrations (C_T, P_T, N_T, Ca and Mg) and pH values measured in the extended pH change test were also given as input to the model, as initial conditions.

Model calibration

The same values for the specific precipitation rate constants adopted from Musvoto *et al.* (2000) for the batch test above served as input for the extended pH change test. Again, the specific rate constant for struvite precipitation was changed from the "default" value of 300/d to 1 000/d, to assess whether this change implemented to improve the fit between predicted and measured data in the batch test improved the fit here also.

The strategy to facilitate pH change for this test differed from that for the batch test, in that aeration was implemented continually but additionally NaOH was added to the sample numbers 5 to 10 to increase pH further. To accommodate the aeration it was found that specific gas stripping rate for CO_2 had to be changed - in the model this rate is calculated from the specific rate for O_2; the value for this rate had to be changed from the range 225 - 600/d reported by Musvoto *et al.* and the value of 130/d for the batch test

above, to 50/d. This change is not unexpected since the specific gas stripping rates depend on the aeration conditions (gas flow rates, mixing, solids, etc.) applied in the specific test, and this differed between the test reported here and those reported by Musvoto *et al.* To accommodate NaOH addition, in the simulations OH was dosed to the test from sample number 5, at quantities that matched the predicted to the measured pHs; the volume of OH dose was kept small so that dilution would not have a significant influence on concentrations.

Results

Predicted and measured batch test concentrations are shown plotted in Fig. 3.11(a to e). For all concentrations reasonably close correlation was obtained; predicted final Mg is higher than the measured final value (Fig. 3.11d), but this is only one measurement and the predicted and measured P concentrations match closely (Fig. 3.11e). Note that the predicted pH time profile is obtained by continual aeration and theoretically dosing OH from sample number 5 (1.3 hours) into the test such that a match with the measured pH profile is obtained (Fig. 3.11a).

Minerals precipitated: Accepting that the predictions are reasonable, the predicted concentrations of the different minerals that precipitate can be determined, see Fig. 3.12. From Fig. 3.12, the dominant mineral that precipitates is struvite (217mg/ℓ as $MgNH_4PO_4$ $6H_2O$ = 99.8% of mass of precipitant), followed by very small amount of ACP (0.36 mg/ℓ as $Ca_3(PO_4)_2$ = 0.2% of the mass of precipitant), and negligible newberyite, calcite and magnesite precipitate. These observations conform to the batch test and are similar to those of Musvoto *et al.*, but with less ACP precipitation. The lower ACP precipitation compared to the batch test is due to the lower initial Ca concentration, 26 and 112 mgCa/ℓ respectively.

Critical pH for struvite precipitation: As noted in Section 3.3.1 above, precipitation of struvite does not commence immediately on aeration. From the predictions (Fig. 3.11d), struvite precipitation only starts after approximately 80 minutes, becoming significant after about 90 minutes; this indicates that the solution is initially undersaturated with

after about 90 minutes; this indicates that the solution is initially undersaturated with

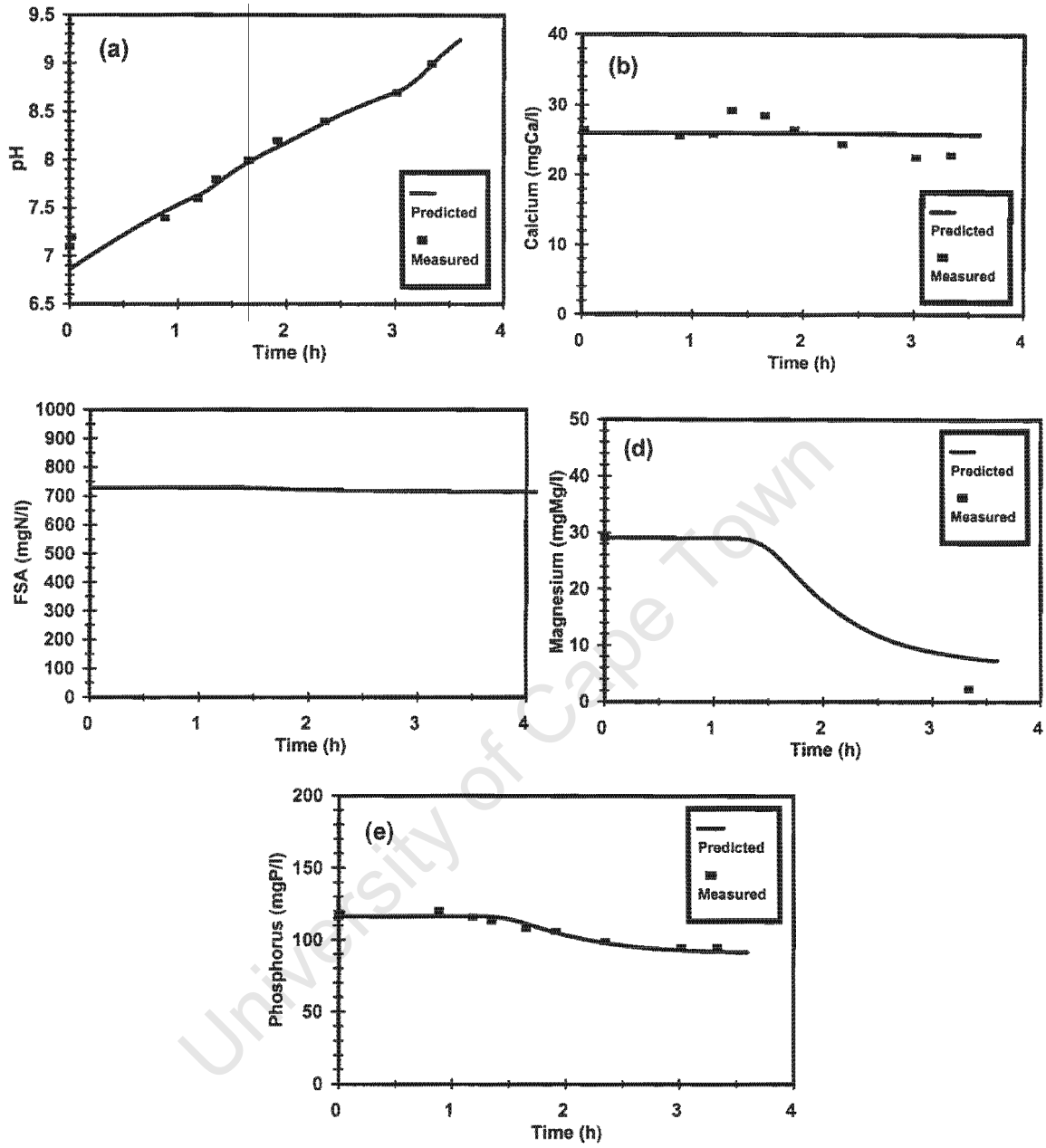

Fig 3.11: Predicted and measured soluble concentrations for pH (Fig 3.11a, top left); calcium (Ca) (Fig 3.11, top right); free and saline ammonia (FSA) (Fig 3.11c, middle left); magnesium (Mg) (Fig 3.11d, middle right); total phosphate species (P_T) (Fig 3.11e, bottom) for extended pH tests on anaerobic digester liquor form Cape Flats (Cape Town, South Africa) digester treating a blend of primary and waste activated sludge; predictions using kinetic model of Musvoto *et al.* (2000); note that form sample 5 the pH was increased with NaOH addition.

respect to struvite, but as the pH increases the solution becomes supersaturated causing struvite precipitation. This is illustrated in Fig. 3.13, where minerals precipitated are plotted against pH; the pH at which the solution becomes supersaturated is about pH = 7.7, but significant precipitation only occurs at pH > 7.8. These pH values are higher than the values measured in the batch test, and this is due to the lower initial Mg concentration measured in the extended pH change test compared with the batch test, 29 and 65 mgMg/ℓ respectively.

Critical pH for ACP precipitation: From Figs. 3.12 and 3.13, significant ACP precipitation does not occur in this test, due to the low initial Ca concentration.

Effect of changing struvite specific precipitation rate constant: In the batch test simulations above, to provide a closer fit between predicted and measured Mg, the specific struvite precipitation rate constant was increased from the "default" value of 300/d (Fig. 7) to 1 000/d (Fig. 10). This change improved the correlation between predicted and measured Mg and P. Accordingly, a similar change was implemented to examine the effect on the extended pH change test. This change influenced only Mg, P and struvite precipitation. Predicted and measured concentration time profiles for these parameters are shown in Fig. 3.14 (a to d). Comparing the predictions with the specific struvite precipitation rate constant of 300/d (Figs. 3.11d, 3.11e, 3.12 and 3.13) with those for the specific struvite precipitation rate constant of 1 000/d, increasing the rate constant improves the correlation between predicted and measured Mg, but the correlation between predicted and measured P is slightly worse. However, the effect on struvite precipitation is relatively small, with only an additional 4.5% struvite precipitating at the end of the test. This confirms the observation that the rate of precipitation of struvite is primarily linked to the rate of change of pH caused by aeration; the kinetics of precipitation have a relatively small influence. This implies that the solution is effectively continually at equilibrium as the pH changes. This indicated that equilibrium chemistry could also be used to analyse the data (see below).

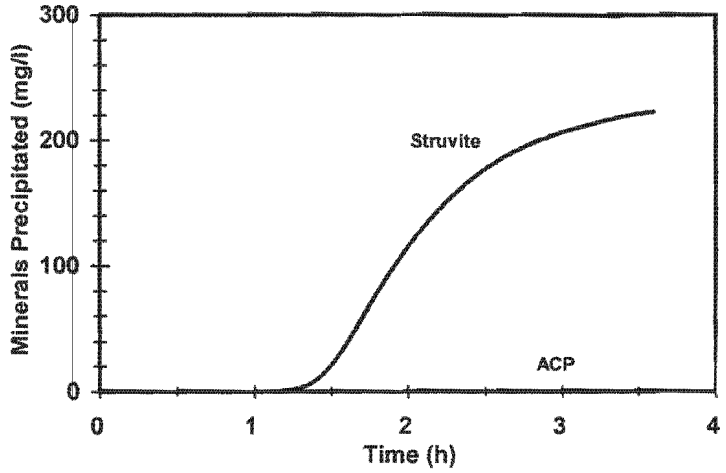

Fig 3.12: Predicted struvite and amorphous calcium phosphate (ACP) precipitation with time for extended pH change test on anaerobic digester liquor from Cape Flats (Cape Town, South Africa) digester treating a blend of primary and waste activated sludges. Experimental data in Fig 3.11; predictions with kinetic model of Musvoto *et al.* (2000a).

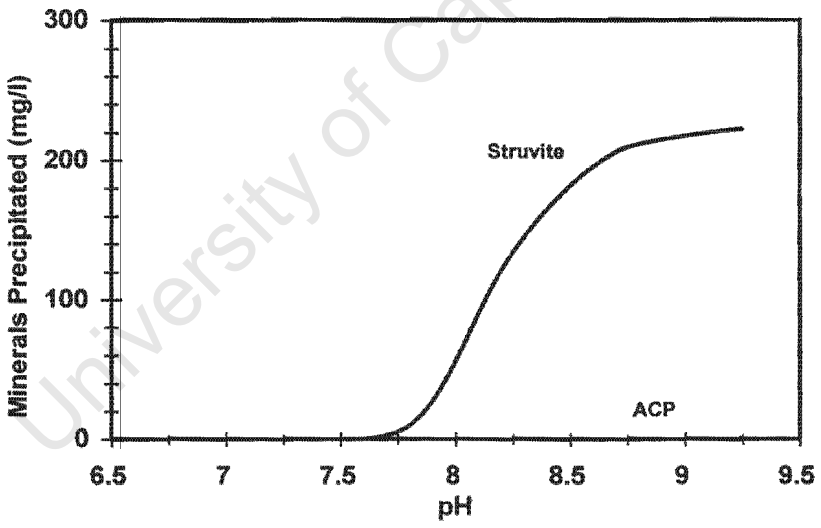

Fig 3.13: Predicted struvite and amorphous calcium phosphate (ACP) precipitation with pH for extended pH change test on anaerobic digester liquor from Cape Flats (Cape Town, South Africa) digester treating a blend of primary and waste activated sludges. Experimental data in Fig 3.11; predictions with kinetic model of Musvoto *et al.* (2000a).

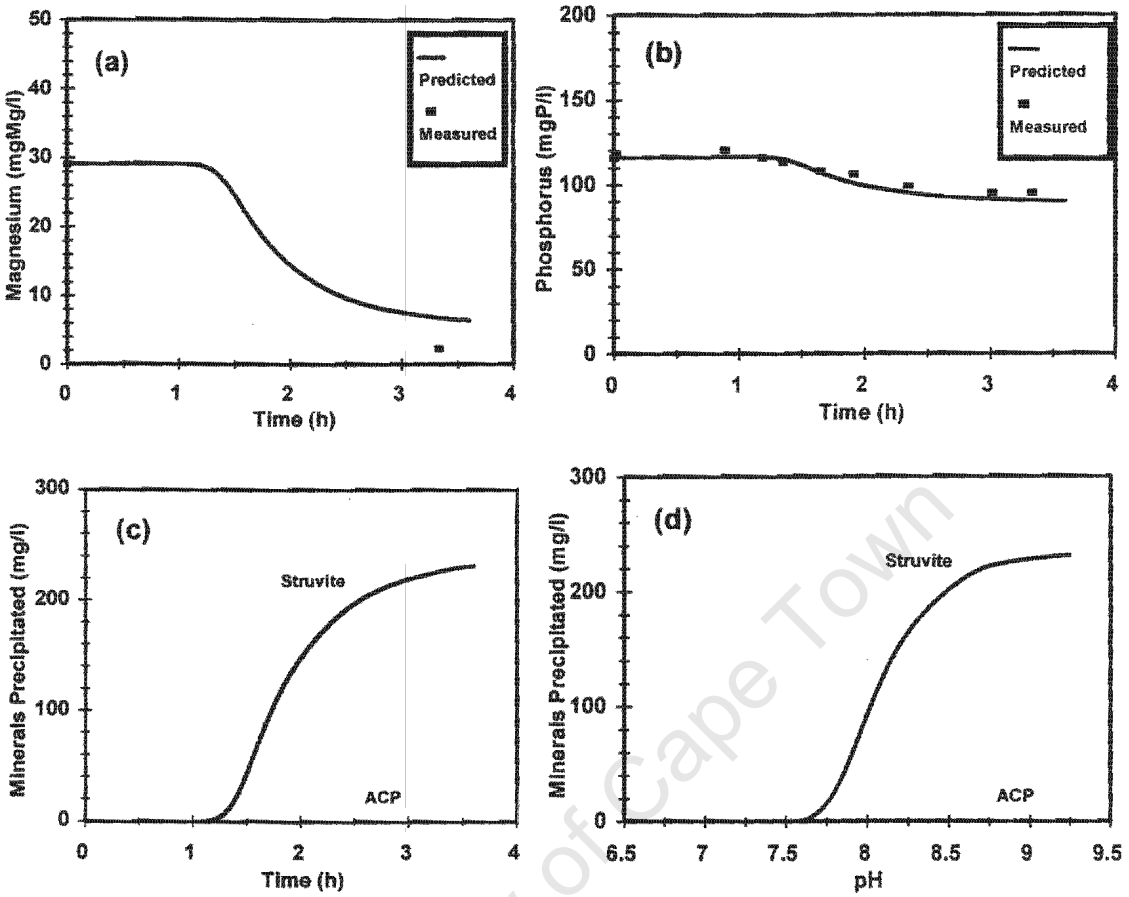

Fig 3.14: Predicted and measured soluble concentrations for magnesium (Mg) (Fig 3.14a, top left); total phosphate species (P_T) (Fig 3.14b, top right); struvite and amorphous calcium phosphate (ACP) precipitation with time (Fig 3.14c, bottom left); struvite and amorphous calcium phosphate (ACP) precipitation with pH (Fig 3.14d, bottom right) for extended pH change test on anaerobic digester liquor form Cape Flats (Cape Town, South Africa) digester treating a blend of primary and waste activated sludge; predictions using kinetic model of Musvoto *et al.*, (2000a) with specific rate for struvite precipitation increased form "default" 300/d (Figs. 3.11, 3.12 and 3.13) to 1000/d.

3.4.1.3 Change in conditions

The kinetic model was applied to theoretically simulate the effect of changes of selected parameters on the predictions for the batch test above. The following parameters were changed:

- initial concentration of Mg
- initial concentration of P
- aeration rate, via the specific rate for oxygen exchange ($K_{LA,O2}$)

The values for each of these parameters were changed to ½ x, 1x and 2x the values measured in the batch test (Mg and P) or determined from the simulations ($K_{LA,O2}$). These changes influence only the predictions for pH, Mg, P and struvite, and the change in ($K_{LA,O2}$) also has a small influence on ACP. Accordingly, only these results will be presented below.

3.4.1.3.1 *Initial concentration of Mg*

The effect of changing the initial Mg concentration from the measured value of 65 mgMg/ℓ to ½ x = 32 mgMg/ℓ and 2x = 130 mgMg/ℓ on pH, Mg, P and struvite precipitated are shown in Figs. 3.15(a, b, c and d) respectively. From Fig. 3.15(a), the effect on pH is small, and is due to the change in precipitation of struvite. The effect on Mg, P and struvite precipitated is large, with the quantity of struvite precipitating increasing significantly with higher initial Mg concentrations. This indicates that the mass of Mg initially present will significantly influence the mass of struvite that will precipitate when the pH increases. This implies that Mg rather than P or NH_4^+ is the limiting species in the struvite precipitation. Also, the results indicate that if the initial concentration of Mg can be reduced, the mass of struvite precipitating can be similarly reduced. Of interest is that the simulations with initial Mg = 32 and 65 mgMg/ℓ predict that the final Mg concentrations will approach similar values. This Mg concentration is

the result of equilibrium between the soluble "free" Mg and the struvite precipitant and various Mg ion pairs.

3.4.1.3.2 *Initial concentration of P*

The effect of changing the initial P concentration from the measured value of 170 mgP/ℓ to ½ x = 85 mgP/ℓ and 2x = 340 mgP/ℓ on pH, Mg, P and struvite precipitated are shown

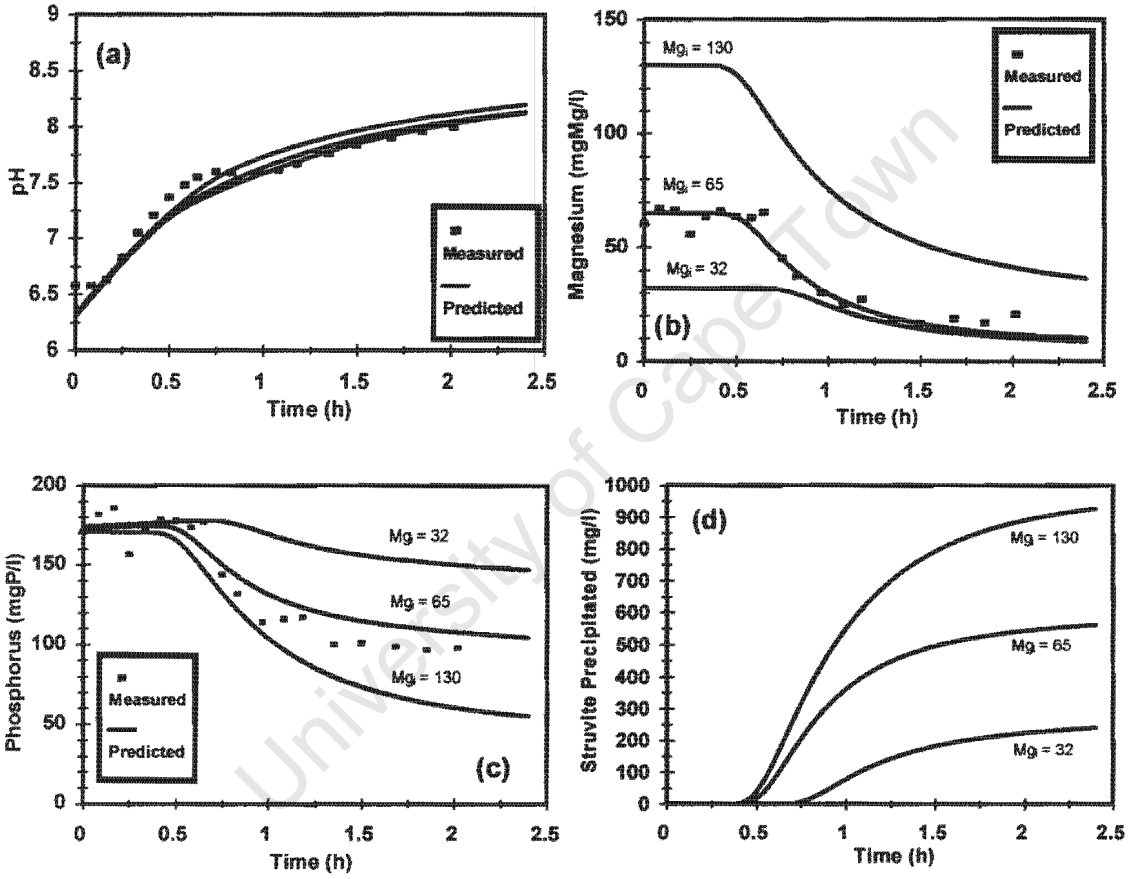

Fig 3.15: Predicted and measured soluble concentrations for pH (Fig 3.15a, top left); magnesium (Mg) (Fig 3.15b, top right); total phosphate species (P_T) (Fig 3.15c, bottom left); struvite and amorphous calcium phosphate (ACP) precipitation with time (Fig 3.15d, bottom right) for batch aeration of anaerobic digester liquor form Cape Flats (Cape Town, South Africa) digester treating a blend of raw sewage and waste activated sludge; predictions using kinetic model of Musvoto *et al.*, (2000) with varying initial Mg concentrations (Mg_i)

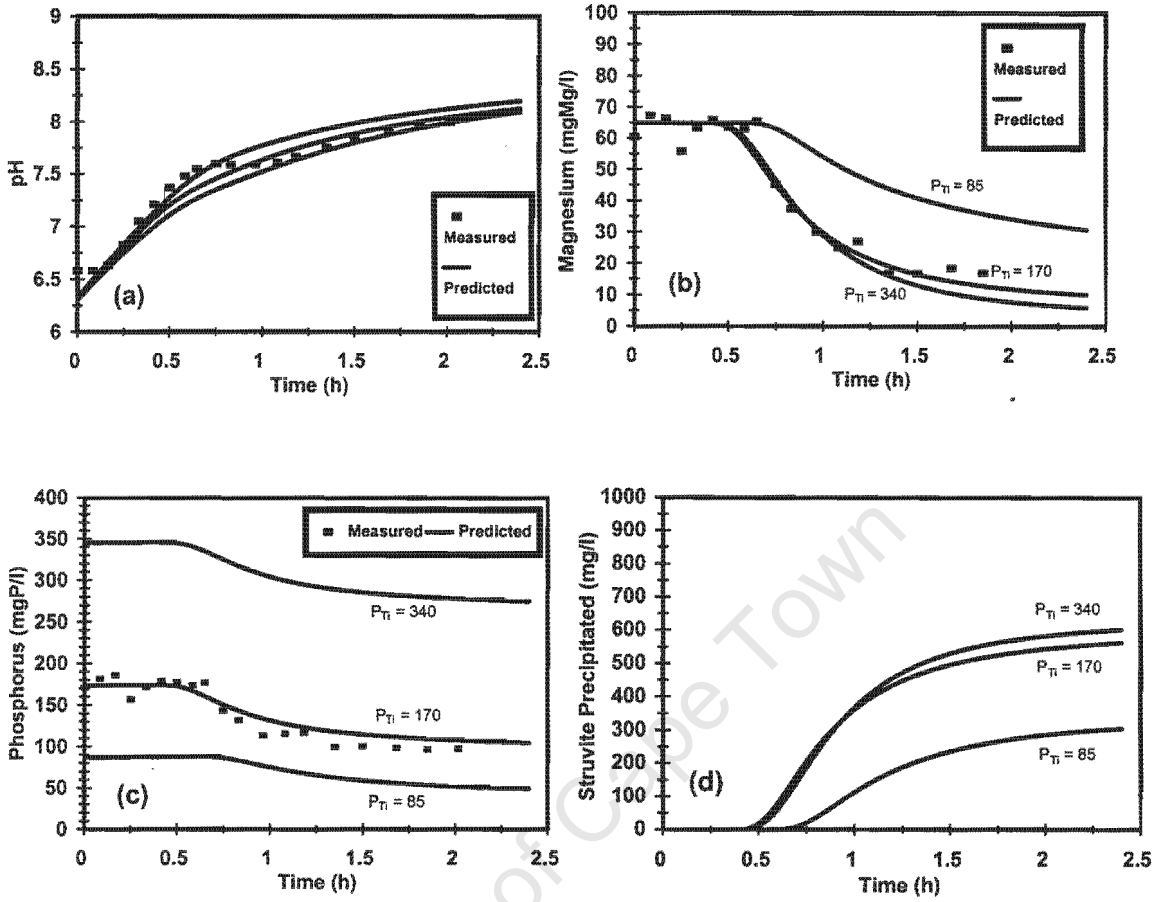

Fig 3.16: Predicted and measured soluble concentrations for pH (Fig 3.16a, top left); magnesium (Mg) (Fig 3.16b, top right); total phosphate species (P_T) (Fig 3.16c, bottom left); struvite and amorphous calcium phosphate (ACP) precipitation with time (Fig 3.16d, bottom right) for batch aeration of anaerobic digester liquor form Cape Flats (Cape Town, South Africa) digester treating a blend of raw sewage and waste activated sludge; predictions using kinetic model of Musvoto *et al.*, (2000) with varying initial P_T concentrations ($P_{T\,i}$).

in Figs. 3.16(a, b, c and d) respectively. From Fig. 3.16(a), the effect on pH is small, and is due to the change in precipitation of struvite. The effect on Mg, P and struvite precipitated is variable. When the initial P concentration is halved, the mass of struvite precipitating reduces significantly; this indicates that for this condition the quantity of P influences the struvite precipitation. However, when the initial concentration is doubled, negligible additional struvite precipitates; for this condition the quantity of Mg dominates the struvite precipitation. The results do indicate that if the initial concentration of P can be reduced significantly, then the mass of struvite precipitating can be reduced.

3.4.1.3.3 *Aeration rate, via the specific rate for oxygen exchange ($K_{LA,O2}$)*

In the kinetic model, the specific rate for CO_2 exchange is calculated from the specific rate for oxygen exchange ($K_{LA,O2}$). The effect of changing the specific rate for oxygen exchange ($K_{LA,O2}$) from the value of 130/d (determined from fitting predicted to measured data for the batch test), to ½ x = 65/d and 2x = 260/d on pH, Mg, P and struvite and ACP precipitated are shown in Figs. 3.17(a, b, c , d and e) respectively. Changing the value for $K_{LA,O2}$ has a significant influence on the pH (Fig. 3.17a). As the value for $K_{LA,O2}$ is increased, the rate of increase in pH is more rapid, and the final pH reached after 2 hours similarly increases. This increase in the rate of pH increase is due to a more rapid loss of CO_2 with the higher aeration rates. When the pH increases more rapidly, struvite starts precipitating earlier in the test (Fig. 3.17b and d), since the critical pH for struvite precipitation is reached earlier. Similarly, the struvite precipitation reaction reaches completion earlier in the test, because the pH increases faster. However, with $K_{LA,O2}$ = 130 and 260/d, the same equilibrium condition is reached at the end of the test in terms of Mg, P and struvite precipitated. This was not expected; since the final pH reached with $K_{LA,O2}$ = 260 is higher than that with $K_{LA,O2}$ = 130/d, pH = 8.5 and 8.15 respectively, it was expected that more struvite would precipitate at the faster aeration rate. That the same amount of struvite precipitates indicates that the total mass of precipitation of struvite in this test is limited by the mass of Mg available for precipitation, rather than the final pH reached. The final concentration of Mg is the result

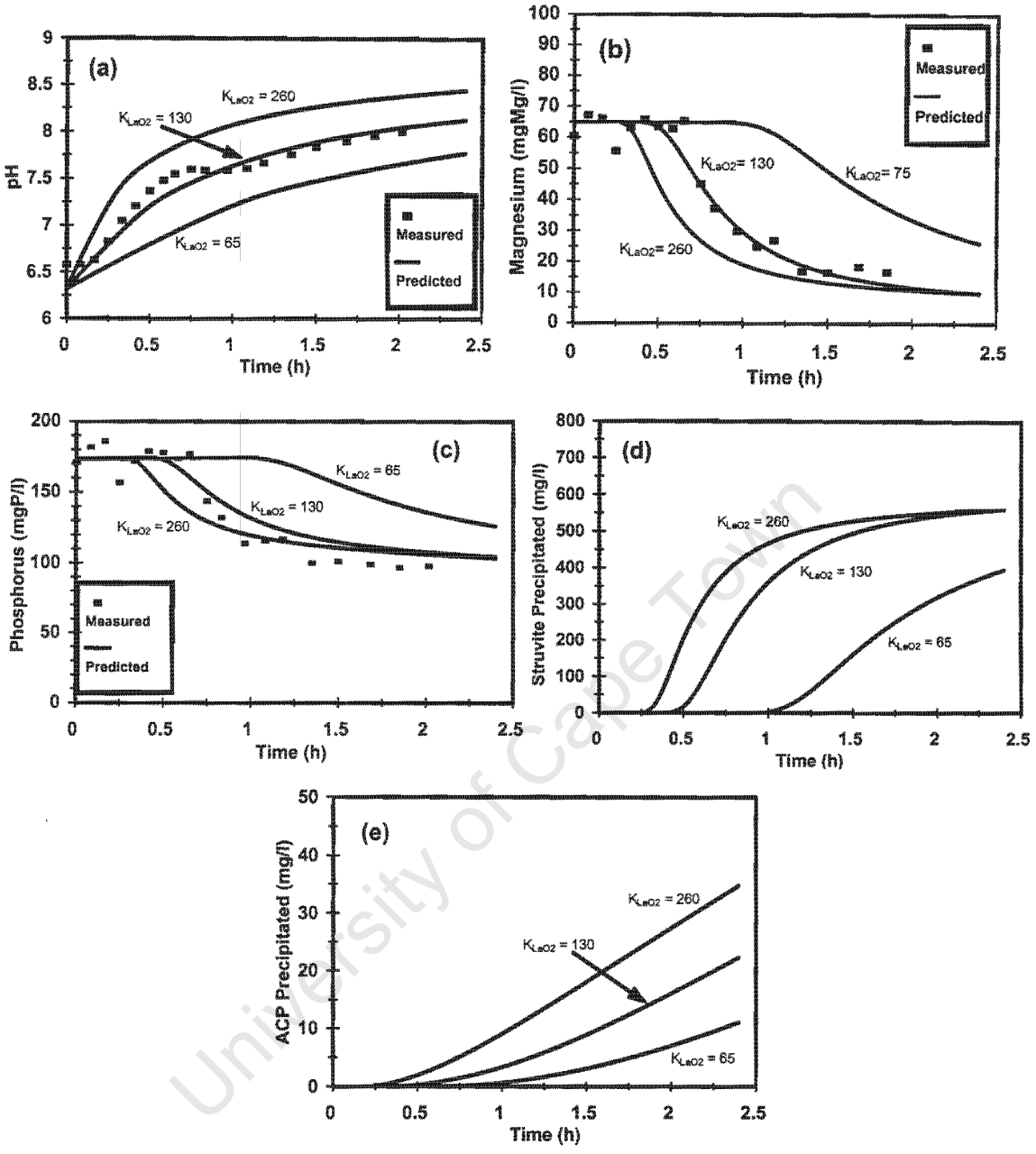

Fig 3.17: Predicted and measured soluble concentrations for pH (Fig 3.17a, top left); magnesium (Mg) (Fig 3.17b, top right); total phosphate species (P_T) (Fig 3.17c, middle left); struvite precipitation with time (Fig 3.17e, middle right); and amorphous calcium phosphate (ACP) precipitation with time (Fig 3.17e, bottom) for batch aeration of anaerobic digester liquor form Cape Flats (Cape Town, South Africa) digester treating a blend of primary and waste activated sludge; predictions using kinetic model of Musvoto *et al.*, (2000) with a varying aeration rate (K_{LaO2}).

of equilibrium between the soluble "free" Mg and the struvite precipitant and various Mg ion pairs.

The effect of changing the aeration rate on ACP precipitation is shown in Fig. 3.17e. As the aeration rate increases, the mass of ACP precipitation increases. This is due to the increased pH - ACP precipitation only occurs at higher pH. However, the mass of ACP precipitation remains small compared to the mass of struvite precipitation.

3.4.2 Steady State Model Application

Accepting from the kinetic model simulations above that (i) the dominant mineral precipitating was struvite and (ii) the rate of pH change governs the precipitation rate so that effectively a solid/liquid species equilibrium is achieved at each time step, an equilibrium chemistry based spreadsheet was developed to calculate the precipitation of struvite from initial conditions and a determined final pH. The spreadsheet considers only precipitation of struvite, takes account of Debye-Hückel ionic effects, but does not consider ion pairing effects.

For the predictions, the spreadsheet model requires as input the eight equilibrium constants (pK) and their temperature sensitivities for the 16 forward and reverse dissociation processes for the water, carbonate, phosphate, SCFA and ammonia weak acid/base systems. Also required as input is the solubility product (pK_{SP}) value for struvite. Values for these constants were taken directly from the kinetic model above. These pK and pK_{SP} values were accepted to be model constants (not changed). With the measured initial conductivity, also given as input and converted internally in the model to an ionic strength value with the formulae given by Loewenthal *et al.* (1989) (ionic strength μ = conductivity.1.68 x 10^{-4}), the input pK and pK_{SP} values were internally corrected for ionic strength with the appropriate mono-, di- and tri-valent ion activity coefficients. The input pK values were also internally adjusted for temperature; the pK_{SP} value for struvite could not be adjusted as information on temperature sensitivity for this

is not available in the literature. The initial total species concentrations (C_T[1], A_T, P_T, N_T and Mg) measured in the appropriate tests were also given as input to the model as initial conditions; for the pH change tests these were the values measured at pH = 2. The spreadsheet model then calculates the equilibrium weak acid/base species concentrations for given pH values from the initial total species concentrations. From these concentrations the ionic product for struvite is calculated and compared to the solubility product. Struvite is then precipitated until the ionic and solubility products are equal, taking due account to respeciate the weak acid/bases at the changed total species concentrations. In this manner the amount of struvite precipitated can be calculated, as well as the remaining total species concentrations.

The spreadsheet model was applied to predict struvite precipitation for four sets of experimental data.

3.4.2.1 Prediction 1 - pH change test, Test Set 2

Predicted and measured P and Mg concentrations versus pH are shown in Fig. 3.18 for the first test in this data set (see Fig. 3.3). Close correlation between measured and predicted data was found. From the prediction, for this data set the struvite precipitation was limited by the initial Mg concentration. The predicted critical pH for struvite precipitation to initiate is pH = 7.4. This value is very similar to that observed in the batch test (pH = 7.6, Section 3.3.1) and extended pH change test (pH = 7.4, Section 3.3.3) and the values predicted with the kinetic model for the batch test (pH = 7.3, Section 3.4.1.1) and extended pH change tests (pH = 7.7, Section 3.4.1.2). It should be noted that the pH of 9 would not be reached by aeration.

---

[1]Note that C_T and A_T are not required for the prediction of struvite precipitation.

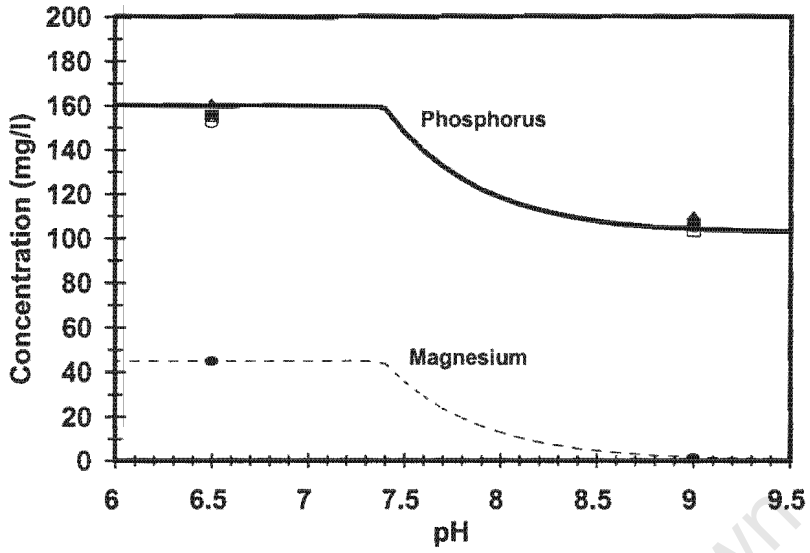

Fig 3.18: Predicted and measured soluble concentrations of magnesium (Mg) and total phosphate species (P_T) with pH for pH change test (Test Set 2, Section 3.3.2.2) on anaerobic digester supernatant from Cape Flats (Cape Town, South Africa) digester treating a blend of primary and waste activated sludge; predictions using spreadsheet equilibrium chemistry model.

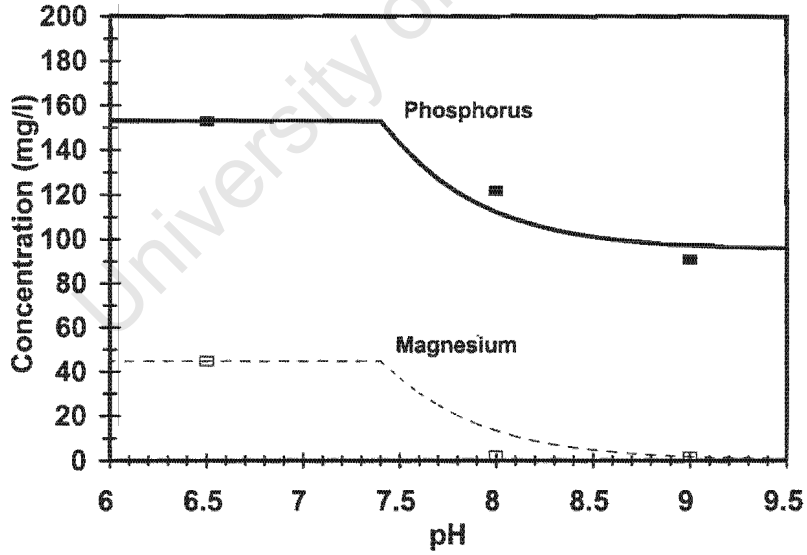

Fig 3.19: Predicted and measured soluble concentrations of magnesium (Mg) and total phosphate species (P_T) with pH for pH change test (Test Set 3, Section 3.3.2.3) on anaerobic digester supernatant from Cape Flats (Cape Town, South Africa) digester treating a blend of primary and waste activated sludge; predictions using spreadsheet equilibrium chemistry model.

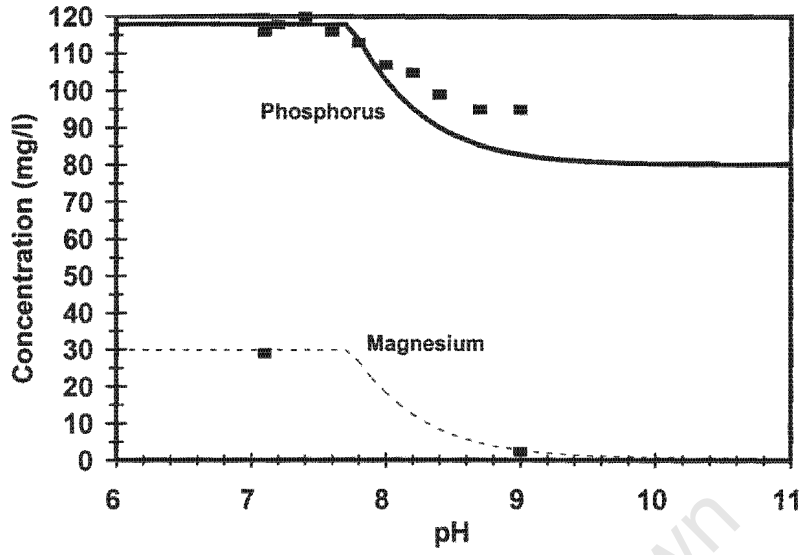

Fig 3.20: Predicted and measured soluble concentrations of magnesium (Mg) and total phosphate species (P_T) with pH for extended pH change test (Section 3.3.3) on anaerobic digester supernatant from Cape Flats (Cape Town, South Africa) digester treating a blend of primary and waste activated sludge; predictions using spreadsheet equilibrium chemistry model.

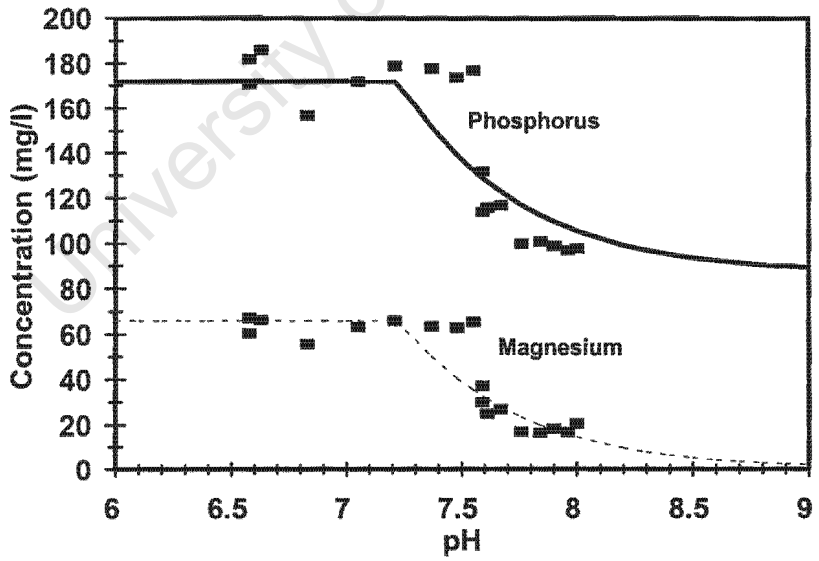

Fig 3.21: Predicted and measured soluble concentrations of magnesium (Mg) and total phosphate species (P_T) with pH for batch test (Section 3.3.1) on anaerobic digester supernatant from Cape Flats (Cape Town, South Africa) digester treating a blend of primary and waste activated sludge; predictions using spreadsheet equilibrium chemistry model.

3.4.2.2 Prediction 2 - pH change test, Test Set 3

Predicted and measured P and Mg concentrations versus pH are shown in Fig. 3.19 for the data from Fig. 3.5. Reasonably close correlation was obtained. Again struvite precipitation is limited by initial Mg concentration, and again the critical pH for struvite precipitation is pH = 7.4.

3.4.2.3 Prediction 3 - Extended pH change test

The spreadsheet was used to predict the data from the extended pH change test (Section 3.3.3 above, Fig. 3.6). Predicted and measured P and Mg concentrations are shown plotted in Fig. 3.20. Mg concentrations correlate closely. Also, the spreadsheet correctly predicts the pH where struvite precipitation is observed to start (pH = 7.6) and the pH where it effectively stops (pH = 8.8 to 9). However, the mass of P precipitating is over predicted. This over prediction is not due to calcium phosphate precipitation not being included in the spreadsheet model - including this would result in additional P precipitation being predicted. As for the predictions above, the precipitation of struvite is limited by the initial Mg concentration.

3.4.2.4 Prediction 4 - Batch test

The spreadsheet model was also applied to predict the data in the batch test (steady state) (Section 3.3.1 above, Fig. 3.1). Predicted and measured P and Mg concentrations are shown plotted in Fig. 3.21. Mg concentrations correlate reasonably closely - pH at which struvite precipitation starts is slightly under predicted (predicted pH = 7.2, measured pH = 7.6, kinetic model predicted pH = 7.3). Also, mass of P precipitated tends to be under predicted. Similar under prediction of P concentrations was observed with the kinetic model simulations of this test. The predictions indicate in agreement with those above, that should the pH be increased further, a small amount of additional struvite will precipitate.

3.5 CONCLUSIONS ON MINERAL PRECIPITATION FROM CAPE FLATS ADS.

From the investigation the following conclusions can be drawn with regards to the Cape Flats ADS:

- The dominant mineral that precipitates is struvite. For the batch test conducted, struvite was dominant (516 mg/ℓ as $MgNH_4PO_4$ $6H_2O$ = 97% of mass of precipitant), followed by ACP (16.8 mg/ℓ as $Ca_3(PO_4)_2$ = 3% of the mass of precipitant), and negligible newberyite, calcite and magnesite precipitate. Similarly, for the extended pH change test, the dominant mineral that precipitates is struvite (217mg/ℓ as $MgNH_4PO_4$ $6H_2O$ = 99.8% of mass of precipitant), followed by very small amount of ACP (0.36 mg/ℓ as $Ca_3(PO_4)_2$ = 0.2% of the mass of precipitant), and negligible newberyite, calcite and magnesite precipitate. These observations are similar to those of Musvoto *et al*. With the large volumes of ADS passing to the pelletization plant, this represents substantial precipitation potential.

- It appears that the precipitation of struvite is stimulated by the increase in pH when CO_2 is lost from the ADS. Within the anaerobic digester, the partial pressure of CO_2 is high due to anaerobic processes acting in the digester. When the ADS leaves the digester it comes into contact with atmospheric conditions where the partial pressure of CO_2 is much lower than inside the digester. This causes CO_2 loss from the ADS to the air, until equilibrium between the CO_2 concentration in the ADS and the air is reached. Loss of CO_2 can also be caused by pressure drops at pipe bends, pumps, etc. The loss of CO_2 represents an increase in acidity which means that the pH of the ADS will increase. This increase in pH causes struvite to become supersaturated, and hence it precipitates. Increasing the pH by addition of NaOH also results in struvite precipitation and confirms that the increase in pH is the primary process driving the struvite precipitation.

- When the ADS leaves the digester, it is initially undersaturated with respect to struvite. Depending on the initial conditions in the ADS, significant struvite only starts precipitating when the pH increases above pH = 7.3 to 7.7. This indicates that if the pH of the ADS can be maintained below about 7.3 along the sludge treatment line, then significant struvite precipitation will not take place.

- With aeration, the critical pH for struvite precipitation is reached after 40 to 60 minutes aeration. However, this time will depend on a number of factors, including aeration rate, initial pH, buffer capacity, initial P and Mg concentrations, etc.

- With aeration, the loss of CO_2 from the ADS causes the pH to increase which stimulates struvite precipitation. Initially, the rate of CO_2 loss is rapid. However, as the partial pressure of CO_2 in the ADS approaches that in the atmosphere, the rate of CO_2 loss and consequent pH increase slows, and this effectively slows the rate of struvite precipitation with time. The maximum pH reached with aeration was about pH = 8. However, from about pH = 7.8 the rate of pH increase with time was very low, and consequently, the struvite precipitation effectively ceased. The pH = 7.8 was reached after about 80 minutes. However, this time will depend on a number of factors, including aeration rate, initial pH, buffer capacity, initial P and Mg concentrations, etc.

- The rate of struvite precipitation is very fast, so that essentially, in the aeration of the ADS from Cape Flats, struvite is at equilibrium between the precipitant and soluble species at all times. Thus, in this case the rate of struvite precipitation is not limited by the precipitation kinetics, but rather by the rate in increase in pH through aeration which in turn is limited by the gas liquid transfer rate for CO_2.

- The amount of struvite that precipitates is limited by two factors: With aeration to increase pH, the struvite precipitating is limited by the final pH reached and the

more struvite precipitates. With addition of NaOH, the struvite precipitating is limited by the initial Mg concentration present - after precipitation the Mg concentration is very low, while significant concentrations of P and N are still present.

- The initial concentrations of P and Mg in the ADS were variable, with P ranging from 89 to 190 mgP/ℓ, and Mg from 29 to 67 mgMg/ℓ. This is probably indicative of the variable performance of the activated sludge system with regard to BEPR. The higher P concentrations are in agreement with values measured for anaerobically digested BEPR sludges in Johannesburg, at 150 to 250 mgP/ℓ (Pitman, 1995). Should BEPR become more reliable in the activated sludge system at Cape Flats, consistently higher P and Mg concentrations can be expected, with the resultant larger masses of struvite precipitating.

- The change in FSA due to struvite precipitation is insignificant compared with the amount of FSA present. Thus, FSA does not provide a reliable assessment of struvite precipitation, and will not limit the amount of struvite that potentially can precipitate.

- The increase in pH with aeration also stimulates precipitation of ACP. However, as noted above, the mass of ACP precipitating is relatively small compared with struvite. The ADS is initially undersaturated with respect to ACP, and ACP precipitation initiates only after the pH increases above 7.7.

- In running experiments on the ADS, the solids concentrations were so high that the ADS could not be effectively filtered. Accordingly, the ADS was allowed to settle for 5 days and the supernatant used for the experimental investigations. Accordingly, the effect of solids concentration on mineral precipitation could not be evaluated, e.g. factors such as surface area for nucleation of minerals, inhibition or poisoning of crystal growth. However, the effect of solids is not

expected to be significant, because theoretical modelling of the precipitation gave close correspondence with measured values.

- In the experimental investigation it was found that filtering samples through 0.45μm filters caused significant CO_2 loss, which resulted in increase in pH. To counter this, the samples should be acidified prior to filtration with these filters.

- The pH change tests provide a simple rapid method to assess struvite precipitation potential.

3.6 RECOMMENDATIONS TO CONTROL PRECIPITATION AT CAPE FLATS

Essentially there are four methods to control the struvite precipitation problem at the Cape Flats Treatment Works:

- Prevent BEPR in the activated sludge system.
- Removing Mg or P from the ADS.
- Maintain the pH along the sludge treatment line at less than the critical pH for struvite precipitation, pH $< \pm 7.3$.
- Increasing pH in a controlled fashion, in a specifically designated area.

3.6.1 Prevent BEPR in the activated sludge system

The high concentrations of Mg and P released into the Cape Flats ADS are due to the process of BEPR in the activated sludge system. In BEPR, the P is taken up from solution by phosphate accumulating organisms (PAO) and stored as polyphosphate (polyP). Mg is taken up with K to serve as a counter ions to neutralize the charge on the polyP molecule, and hence stabilise it. If BEPR were prevented from operating in the

activated sludge system, the sludge would not accumulate significant P and Mg, and these would not be released into solution at such high concentrations on anaerobic digestion. The theoretical investigation (Section 3.4) clearly demonstrates that reduced initial P and Mg concentrations in the ADS reduces the struvite precipitation on pH increase due to CO_2 loss.

BEPR in activated sludge systems is stimulated by the presence of an anaerobic reactor with the influent fed to the anaerobic reactor. Accordingly, if the activated sludge system configuration is changed to eliminate the anaerobic reactor, BEPR can be prevented. Changing the activated sludge system configuration from the present 5-stage Modified Bardenpho to a Modified Ludzack Ettinger (MLE) would achieve this. The feasibilty of this option will depend on the effluent quality required for the activated sludge system. If P removal from the wastewater must be achieved, an option is to use simultaneous chemical addition to the activated sludge system.

3.6.2 Removing Mg or P from the ADS

From the above, if the Mg and/or P concentrations in the ADS can be reduced, then reduced struvite precipitation will occur on aeration (deliberate or inadvertent). One method to reduce the Mg and P concentrations would be to precipitate these within the anaerobic digester. Of the two, precipitating P would be the more feasible. Precipitation of P within the digester can be achieved by adding metal salts, probably iron or aluminium. Addition of ferric chloride to anaerobic digesters to precipitate P, and hence control struvite precipitation, has been successfully demonstrated at full-scale (Mamais *et al.*, 1994). They also found that, if the P were precipitated with iron, this did not resolubilise when the pH increased with CO_2 loss and hence the P did not become available for struvite precipitation. With aluminium addition, waste alum sludge from water treatment plants is an option for addition.

3.6.3 Maintain the pH along the sludge treatment line at less than the critical pH for struvite precipitation, pH < ± 7.3

The experimental and theoretical investigations indicate that the ADS from the Cape Flats anaerobic digesters is undersaturated with respect to struvite when it leaves the digester. For struvite precipitation to initiate, the pH has to increase to pH > ± 7.3. If the pH can be maintained at values less than this critical pH, then struvite precipitation will not occur. Possible strategies to prevent increase in pH (via controlling CO_2 loss) are to limit exposure to atmospheric conditions, minimise pressure drops, provide CO_2 atmosphere at critical unit processes (e.g. centrifuges). A rapid assessment of whether this proposal holds merit can be obtained by monitoring the pH along the line of flow of the ADS in the treatment process, to identify where significant CO_2 loss occurs.

3.6.4 Increasing pH in a controlled fashion

From the experimental and theoretical investigations, the primary cause for struvite precipitation is the increase in pH resulting from CO_2 loss. If the pH is increased under controlled conditions, this will allow struvite precipitation in designated places rather than in undesirable places. The pH can be increased by addition of chemicals (such as caustic) or by aeration. The latter option (aeration) is probably preferable as this would eliminate the expense (and danger) associated with caustic addition. If aeration is considered, a more detailed theoretical investigation of the effect of aeration rate on CO_2 loss can be undertaken.

3.7 CLOSURE

In this Chapter, the three phase (aqueous/gas/solid) chemical and physical processes kinetic model of Musvoto *et al.* (1998; 2000a, b) has been applied to simulate the behaviour on aeration of anaerobic digester supernatant (ADS) from the Cape Flats Wastewater Treatment Plant anaerobic digesters. The theoretical predictions from the

model were compared with data collected in an extensive experimental investigation on this ADS. Keeping default values for the model suggested by Musvoto *et al.*, except for the struvite specific precipitation constant (which was increased form the default value of 300/d to 1000/d), close agreement was obtained between theoretically predicted and experimentally measured data. This would indicate that the kinetic model of Musvoto *et al.* adequately describes integrated three phase chemical and physical processes. The inherent value of such a model has clearly been demonstrated in this Chapter, by providing insight into the precipitation of minerals from ADS at the Cape Flats Wastewater Treatment Plant. From this deeper understanding, recommendations on controlling mineral precipitation (principally struvite) at this treatment plant could be identified.

Accordingly, for this research project the kinetic model of Musvoto *et al.* can be accepted for the three phase chemical and physical processes. What is still required is a kinetic model describing the biological processes – the development of this model is described in the following chapter.

CHAPTER 4

DEVELOPMENT OF A TWO PHASE BIOLOGICAL, CHEMICAL AND PHYSCIAL PROCESSES KINETIC MODEL FOR ANAEROBIC DIGESTION OF SEWAGE SLUDGES: MODEL DEVELOPMENT

4.1 INTRODUCTION

As described in Chapter 1, the primary objective in this research project was to develop a kinetic model that describes the behaviour of the processes in the anaerobic digestion of sewage sludges. In such a system, three phase behaviour (gas/liquid/solid) can be expected and the processes operative will include chemical, physical and biological reactions. In Chapter 3, the kinetic model of Musvoto *et al.* (1998; 2000a, b and c) has been successfully applied to describe the three phase chemical and physical processes that occur in aeration of anaerobic digester supernatant from the Cape Flats Wastewater Treatment Plant anaerobic digesters. What remains is to develop a kinetic model that describes the biological processes that are operative within the anaerobic digester itself. This Chapter describes the development of such a model.

Since the biological processes in anaerobic systems produce and consume significant weak acid/base species (e.g. acetic acid), these will have a significant impact on the background weak acid/base chemistry matrix of the solution. In turn, the background weak acid/base chemistry matrix has a significant impact on the biological processes, by determining the relevant concentrations of specific weak acid/base species required for utilization and the pH (i.e. water weak acid/base relative species concentrations) to which the anaerobic organisms and the processes they mediate are relatively sensitive.

Accordingly, any substantive kinetic model describing the biological processes in anaerobic systems should include the background weak acid/base chemistry. Furthermore, in anaerobic systems significant CO_2 is produced (and consumed), and

the possibility exists for NH_3 loss via gas stripping. Since these two species form part of the carbonate and ammonia weak acid/base systems respectively, the physical processes of gas exchange between air/liquid of CO_2 and NH_3 should also be considered for inclusion. Also, the possibility does exist that mineral precipitation reactions will take place in the anaerobic digester, particularly if the digester is treating waste activated sludges from a biological phosphorus removal system. In Chapter 3, the successful application of a two phase chemical and physical processes kinetic model to aeration of ADS has been detailed. To completely describe anaerobic digester behaviour for all sewage sludges as influent, this kinetic model should be incorporated also. However, in initial development of the biological processes kinetic model, it was decided to restrict application to anaerobic digesters treating primary sludge. In such systems, mineral precipitation reactions are unlikely to be of major importance and accordingly these were excluded from the kinetic model formulated here. Since both the model developed here and that described in Chapter 3 are based on kinetics, and would include the weak acid/base chemistry as common, integration of the two sets of models at a later date was not expected to present any difficulty.

Thus, required for inclusion in the two phase (aqueous/gas) kinetic model for anaerobic digesters are:

- biological processes
- chemical processes – weak acid/base chemistry
- physical processes – CO_2 and NH_3 gas exchange

These diverse processes need to be integrated in a consistent and seamless manner. In Chapter 2, the approach of Musvoto *et al.* (1998; 2000a, b and c) to kinetic modelling of such integrated systems has been reviewed. In Chapter 3 the kinetic model based on this approach for two phase chemical and physical processes and its successful application have been described. Accordingly, this approach will be followed here also.

4.2 BIOLOGICAL PROCESSES

To formulate a kinetic model describing the biological processes operative in anaerobic digestion, a number of tasks needed to be completed:

- Describe conditions within which the model is to operate.
- Conceptualize a mechanistic model that qualitatively describes the behaviour of the biological processes.
- From the mechanistic model, identify the essential compounds utilized and formed, and the processes acting on these compounds.
- Formulate mathematically the process rates, stoichiometry and transport relationships.
- Calibrate the model and test its response against that observed experimentally.

These tasks can not be completed sequentially, but are interactive, with the resultant model evolving through successive formulation and application.

4.2.1 Model conditions

The kinetic model was limited to the following conditions:

- Anaerobic digestion of sewage sludges; in the model development it was further decided to restrict application to anaerobic digestion of primary sewage sludges, due primarily to the availability of data.
- The anaerobic digester is completely mixed; should plugflow reactors be used, partial phase separation of the anaerobic process may occur leading to a change in behavioural patterns, e.g. pelletization in UASB type systems (Sam – Soon *et al.*, 1991).

- Oxidising agents (e.g. sulphate) are not present in significant concentrations in the influent, i.e. sulphate reduction and similar processes are not considered.

4.2.2 Conceptual model

From Chapter 2, in reviewing various literature sources available, a considerable variation in conceptual schemes was found for describing the biological processes of anaerobic digestion with sewage sludge as influent, from simple 2 stage reaction schemes including only hydrolysis/acidogenesis and acetoclastic methanogenesis (Kiely *et al.*, 1997), to the most commonly used 6 step reaction scheme as proposed by Gujer and Zehnder (1983) (See Fig 2.1).

In this research project, the conceptual model is based on the Gujer and Zehnder (1983) reaction scheme, but with a number of modifications:

- In the reaction scheme of Gujer and Zehnder, the hydrolysis process acts separately on the three main groupings of organic material, namely proteins, carbohydrates and lipids. Recognising that such detailed measurements on primary sludges are unlikely to be routinely available, this was modified to a single hydrolysis process acting on a generic organic material representing primary sludge. This simplification is not unreasonable since the end products of hydrolysis (and subsequent acidogenesis) of the three organic material groups are essentially the same, namely short chain fatty acids (SCFA).

- In the reaction scheme of Gujer and Zehnder, as a consequence of the separate hydrolysis processes above, the end products of hydrolysis are amino acids, sugars and fatty acids respectively. With the proposed single hydrolysis process, including three separate hydrolysis products was not feasible, or in fact desirable. Accordingly, it was proposed to include a single hydrolysis end product. The end product was chosen to be glucose for a number of reasons:

    - The subsequent biological processes on glucose are well established.

- The subsequent acidogenic/fermentation process acting on glucose to convert it to short chain fatty acids (SCFA) is extremely unlikely ever to be rate limiting. Accordingly, in model application accumulation of glucose will not occur, even under digester failure conditions. This implies that the glucose merely acts as an intermediate compound, which is acidified to SCFA as soon as it is produced. Since in the more detailed scheme of Gujer and Zehnder, the end products of hydrolysis and acidogenesis are the same as in the proposed simplified scheme, namely H_2, CO_2 and SCFA, the net result will be the same in both schemes.

- As a consequence of the single hydrolysis process, the anaerobic oxidation of fatty acids does not need to be included.

- In the reaction scheme of Gujer and Zehnder (1983), a fixed proportion of hydrolysis end products go to the intermediate SCFA (propionate, butyrate, etc) and the balance directly to acetate. As an alternative, the influence of hydrogen partial pressure ($\overline{p}H_2$) on acidogenesis of glucose to SCFA as proposed by Sam – Soon *et al.* (1991) was included (see Chapter 2). This scheme appears to provide a better description of the acidogenesis process, and would be more suitable to predict behaviour under failure conditions. To include the proposals of Sam – Soon *et al.* (1991), the acidogenesis was divided into two processes:
  - Under high $\overline{p}H_2$ conditions, acetic and propionic acids are generated together with H_2 and CO_2.
  - Under low $\overline{p}H_2$ conditions, the SCFA acetic acid only is generated together with H_2 and CO_2.

In this scheme, generation of butyrate and higher SCFA were not considered, as these usually are only found in minor concentrations, even under digester failure conditions.

Accepting the modifications above, the general proposed reaction scheme is shown in Fig 4.1. From Fig 4.1, the following general biological processes need to be considered for inclusion in the model:

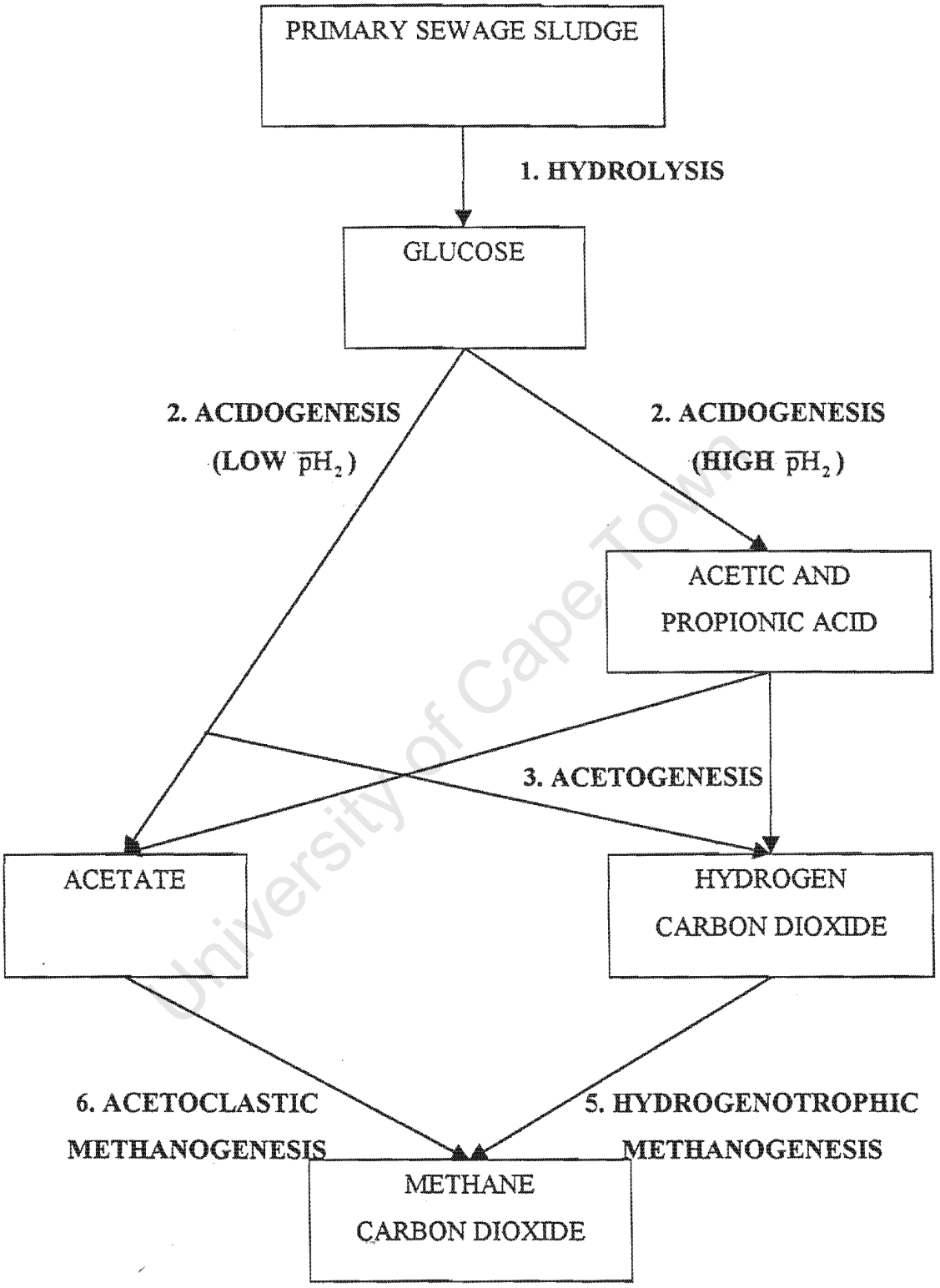

Fig 4.1: Proposed reaction scheme for the conceptual model developed as modified from Gujer and Zehnder (1983)

- Hydrolysis of particulate primary sludge to "glucose"
- Acidogenesis of glucose under,
    - high $\overline{p}H_2$
    - low $\overline{p}H_2$
- Acetogenesis
- Acetoclastic methanogenesis
- Hydrogenotrophic methanogenesis

From the literature, the above processes are mediated by four groups of organisms:

- acidogens – hydrolysis and acidogenesis
- acetogens – acetogenesis
- acetoclastic methanogens – acetoclastic methanogenesis
- hydrogenotrophic methanogens – hydrogenotrophic methanogenesis

Accordingly, the above organism groups need to be included in the model. It was recognized that the organism groups are not representative of a single organism species, but rather are "surrogates" representing all organism species performing a particular relevant function of interest; this is similar to the approach followed for modelling of activated sludge systems (e.g. Dold *et al.*, 1980, 1991).

With the exception of the hydrolysis process, as noted by Gujer and Zehnder (1983), in the processes growth of the relevant surrogate organism will occur from energy derived in the process. Accordingly, the model needs to include an associated growth of the surrogate organism mediating the specific process. Since growth of the different organism biomass are included, their deaths needs to be included also.

4.2.3 Processes

From the conceptual model above, the following essential biological processes were identified for inclusion in the model:

Hydrolyis:

- Hydrolysis of particulate sewage sludge to soluble "glucose", mediated by acidogens.

Growth:

- Acidogens on glucose under high $\overline{pH}_2$
- Acidogens on glucose under low $\overline{pH}_2$
- Acetogens on propionic acid
- Acetoclastic methanogens on acetic acid
- Hydrogenotrophic methanogens on H_2

Death/endogenous decay:

- Acidogens
- Acetogens
- Acetoclastic methanogens
- Hydrogenotrophic methanogens

4.2.4 Compounds

The processes above act on the compounds, to cause changes in the concentrations of these. The changes in some concentrations may be directly observable, but with others the compounds and their changes in concentrations are inferred from the understanding of the processes or from mass balance requirements. For inclusion in the model, the following compounds were identified:

- Sewage sludge biodegradable organics (COD_p)
- Sewage sludge unbiodegradable organics (COD_{pu})
- Soluble glucose (COD_s)
- Acidogen active biomass (X_a)
- Acetogen active biomass (X_p)
- Acetoclastic methanogen active biomass (X_{AM})
- Hydrogenotrophic methanogen active biomass (X_{HM})
- Methane (CH_4)

- Molecular hydrogen (H_2)
- Protons (H^+)
- Carbonic acid ($H_2CO_3^*$)
- Acetic acid (HAc)
- Propionic acid (HPr)
- Ammonia (NH_3)
- Ammonium (NH_4^+)

For the compounds, with the exception of sewage sludge biodegradable and unbiodegradable organics, all concentration units were mol/ℓ; sewage sludge organics units were accepted as gCOD/ℓ since this measurement would be the one available.

Furthermore, since weak acid/base chemistry and associated pH would be incorporated in the model (see Section 4.3 below), all weak acid/base system species would have to be included, i.e. water (H^+, OH^-), carbonate ($H_2CO_3^*$, HCO_3^-, CO_3^{2-}), acetic acid (HAc, Ac^-), propionic acid (HPr, Pr^-), ammonia (NH_3, NH_4^+) and phosphate (H_3PO_4, $H_2PO_4^-$, HPO_4^{2-}, PO_4^{3-}). Accordingly, the specific weak acid/base species influenced by the biological processes were included as compounds here. The other corresponding weak acid/base species will be included when the weak acid/base chemistry processes model is developed.

4.2.5 Stoichiometry

The stoichiometry in the model was deduced directly from the biochemical stoichiometric equations for the process reactions taking place. The metabolic pathways used by fermentative bacteria to convert proteins and lipids to short chain fatty acids (SCFA) and micro organisms are not very well known. Only the metabolic pathways for the degradation of carbohydrate to SCFA are well understood. As noted above, for this reason amongst others, the biodegradable particulate COD entering the system was directly transformed to glucose from which the rest of the products were formed.

4.2.5.1 Hydrolysis

In the hydrolysis process, the biodegradable particulate organics (COD_p) in the sewage sludge are transformed to the intermediate, organic glucose (COD_s). This process is crucial in anaerobic digestion modelling, as the amount of glucose formed will determine the amount of end products (CH_4, CO_2, biomass) in a stable digester. To develop the stoichiometry for the process, the stoichiometric reaction was separated into two half reactions, which are effectively the redox half reactions, which then were added based on an electron balance. In setting up the half reactions, a chemical formulation for the primary sludge is required. No such formulation was available in the literature. Accordingly, initially it was accepted that the formulation would be the same as for activated sludge biomass, namely $C_5H_7O_2N$. However, in application of the model this gave model predictions that deviated significantly from observed results (see Chapter 5). Accordingly, by tracing C and N in observed and predicted results, the chemical formulation for the primary sludge was changed to correctly reflect observed behaviour (this is described in detail in Chapter 5). This gave the chemical formulation for primary sludge of $C_{3.5}H_7O_2N_{0.196}$. Accepting the formulation, the stoichiometry for hydrolysis is as follows:

For the oxidation half reaction:

$$C_{3.5}H_7O_2N_{0.196} \Rightarrow 3.5CO_2 + 0.196NH_3 + 16.412H^+ + 16.412e^- \quad (4.1)$$

The corresponding reduction half reaction is:

$$6CO_2 + 24H^+ + 24e^- \Rightarrow C_6H_{12}O_6 + 6H_2O \quad (4.2)$$

Changing the stoichiometry of the reduction half reaction to give the same number of electrons as the oxidation half reaction, yields:

$$4.103CO_2 + 16.412H^+ + 16.412e^- \Rightarrow 0.68383C_6H_{12}O_6 + 4.103H_2O \quad (4.3)$$

Adding the two half reactions, the final equation then is:

$$C_{3.5}H_7O_2N_{0.196} + 0.603CO_2 \Rightarrow 0.196NH_3 + 0.68383C_6H_{12}O_6 + 4.103H_2O \qquad (4.4)$$

From this equation, the stoichiometric relationship for the hydrolysis reaction can be summarised as follows:

Table 4.1: Stoichiometric relationship for hydrolysis

CODp	$C_6H_{12}O_6$	NH_3	CO_2	H^+
gCOD	moles	moles	moles	moles
-1	0.00521	0.00149281	-0.00459268	0.00055

Note that in the stoichiometric reaction, the N is released as NH_3. This is possible in the model because the weak acid/base chemistry would be included, i.e at operating pH's the NH_3 released would automatically combine with a proton to form NH_4^+.

The resultant glucose enters the biological processes following.

4.2.5.2 Acidogenesis

The acidogenic reaction converts glucose (COD_s) to SCFA (Chapter 2), and can be described by the following stoichiometric equations:

Under conditions of low $\overline{pH}_2$ the SCFA formed is acetic acid (HAc):

$$C_6H_{12}O_6 + 2H_2O \Rightarrow 2CH_3COOH + 2CO_2 + 4H_2 \qquad (4.5)$$

Under conditions of high $\overline{pH}_2$, from Chapter 2 the SCFA formed are acetic (HAc) and propionic acids (HPr):

$$C_6H_{12}O_6 \Rightarrow CH_3COOH + CH_3CH_2COOH + CO_2 + H_2 \qquad (4.6)$$

For simplicity in modelling the reaction in Eq (4.6) can be separated into two reactions:

$$\tfrac{1}{2}C_6H_{12}O_6 + H_2O \Rightarrow CH_3COOH + CO_2 + 2H_2 \quad (4.7)$$

$$\tfrac{1}{2}C_6H_{12}O_6 + H_2 \Rightarrow CH_3CH_2COOH + H_2O \quad (4.8)$$

The first reaction above is identical to that for low $\overline{p}H_2$. Accordingly, Eq (4.5) for low $\overline{p}H_2$ can apply for both high and low $\overline{p}H_2$ and additionally under high $\overline{p}H_2$ Eq (4.8) will be operative.

In the acidogenesis process, growth of the acidogens (X_a) will take place. Accepting the formulation for biomass as $C_5H_7O_2N$, the synthesis of acidogenic bacteria is described as follows:

$$5C_6H_{12}O_6 + 6NH_4^+ \Rightarrow 6C_5H_7O_2N + 18H_2O + 6H^+ \quad (4.9)$$

Note that in the acidogen growth above (Eq. (4.9)), NH_4^+ is utilized instead of NH_3. This was done because in the pH range of anaerobic digesters ($6.5 < pH < 7.5$) the concentration of NH_3 species is very low and its use in the model may lead to instability during computer simulations. In the model being developed here, since weak acid/base chemistry is to be included, the exact weak acid/base species utilized is of minor importance as the weak acid/base reactions will rapidly (effectively instantaneously) re-establish the correct equilibrium weak acid/base species distribution.

Accepting that the yield of acidogens in the process above is Y_{Ac}, then Eq. (4.9) can be modified to give:

$$\tfrac{5}{6}Y_{Ac}C_6H_{12}O_6 + Y_{Ac}NH_4^+ \Rightarrow Y_{Ac}C_5H_7O_2N + 3Y_{Ac}H_2O + Y_{Ac}H^+ \quad (4.10)$$

Adding Eqs (4.5) or (4.6) and (4.10) and dividing by Y_{Ac} gives the relevant resultant net equation in terms of acidogen growth; for example, under low $\overline{p}H_2$ adding Eqs (4.5) and (4.10) and dividing by Y_{Ac} gives:

$$\frac{(1+\frac{5}{6}Y_{Ac})}{Y_{Ac}}C_6H_{12}O_6 + NH_4^+ \Rightarrow C_5H_7O_2N + \frac{2}{Y_{Ac}}CH_3COOH$$
$$+\frac{4}{Y_{Ac}}H_2 + \frac{2}{Y_{Ac}}CO_2 + H^+ \qquad (4.11)$$

In the equation above, it can be accepted that the CO_2 is released as carbonic acid ($H_2CO_3^*$); again, due to the inclusion of the weak acid/base chemistry in the model, this will be automatically dissociated into the carbonate weak acid/base system species relevant to the pH.

Following the procedure above, equations can be derived for both high and low $\overline{pH}_2$ and the stoichiometry extracted. The stoichiometric relationships for acidogenesis can be summarised as follows:

Table 4.2: Stoichiometric relationship for acidogenesis under conditions of both low and high $\overline{pH}_2$

$C_6H_{12}O_6$	HAc	H_2	$H_2CO_3^*$	NH_4^+	H^+	Xa
moles	moles	moles	moles	moles	moles	moles
$-\frac{(1+\frac{5}{6}Y_{Ac})}{Y_{Ac}}$	$\frac{2}{Y_{Ac}}$	$\frac{4}{Y_{Ac}}$	$\frac{2}{Y_{Ac}}$	-1	1	1

Table 4.3: Stoichiometric relationship for acidogenesis under conditions of high $\overline{pH}_2$ only

$C_6H_{12}O_6$	HAc	H_2	HPr	NH_4^+	H^+	Xa
moles	moles	moles	moles	moles	moles	moles
$-\frac{(1+\frac{5}{6}Y_{Ac})}{Y_{Ac}}$	$\frac{1}{Y_{Ac}}$	$\frac{1}{Y_{Ac}}$	$\frac{1}{Y_{Ac}}$	-1	1	1

4.2.5.3 Acetogenesis

In acetogenesis, the acetogens convert propionic acid (HPr) generated in acidogenesis above to acetic acid (HAc). From Chapter 2, the stoichiometric equation for the acetogenesis reaction is given by:

$$CH_3CH_2COOH + 2H_2O \Rightarrow CH_3COOH + CO_2 + 3H_2 \quad (4.12)$$

Similar to acidogenesis, during acetogenesis growth of acetogens (X_P) will occur, with the synthesis of acetogenic bacteria given by:

$$3CH_3CH_2COOH + CO_2 + 2NH_3 \Rightarrow 2C_5H_7O_2N + 4H_2O + H_2 \quad (4.13)$$

Following the procedures detailed above for the acidogens, the combined equation for acetogenesis and acetogen growth can be developed and the stoichiometry extracted, to give:

Table 4.4: Stoichiometry for Acetogenesis

HPr	HAc	H_2	NH_4^+	X_P	H^+	$H_2CO_3^*$
moles	moles	moles	moles	moles	moles	moles
$-\frac{(1+\frac{3}{2}Y_{AP})}{Y_{AP}}$	$\frac{1}{Y_{AP}}$	$(\frac{1}{2}+\frac{3}{Y_{AP}})$	-1	1	1	$(\frac{1}{Y_{AP}}-\frac{1}{2})$

4.2.5.4 Hydrogenotrophic methanogenesis

From Chapter 2, the stoichiometric equation is given by:

$$CO_2 + 4H_2 \Rightarrow CH_4 + 2H_2O \quad (4.14)$$

Similar to the above, the hydrogenotrophic methanogenic bacteria (X_{HM}) synthesis equation is given by:

$$5CO_2 + 10H_2 + NH_3 \Rightarrow C_5H_7O_2N + 8H_2O \quad (4.15)$$

Applying the principles developed for the acidogenesis, the combined equations for hydrogenotrophic methanogenesis and associated growth can be developed and the stoichiometry extracted, to give:

Table 4.5: Stoichiometry for hydrogenotrophic methanogenesis

H_2	$H_2CO_3^*$	NH_4^+	H^+	X_{HM}	CH_4
moles	moles	moles	moles	moles	moles
$-\frac{(4+10Y_{HM})}{Y_{HM}}$	$-\frac{(1+5Y_{HM})}{Y_{HM}}$	-1	1	1	$\frac{1}{Y_{HM}}$

4.2.5.5 Acetoclastic methanogenesis

From Chapter 2, the stoichiometric equation for acetoclastic methanogenesis is as follows:

$$CH_3COOH \Rightarrow CH_4 + CO_2 \quad (4.16)$$

Similar to the above, the acetoclastic bacteria synthesis equation is given by:

$$5CH_3COOH + 2NH_3 \Rightarrow 2C_5H_7O_2N + 6H_2O \quad (4.17)$$

Applying the principles developed for the acidogenesis, the combined equations for acetoclastic methanogenesis and associated growth can be developed and the stoichiometry extracted, to give:

Table 4.6: Stoichiometry for acetoclastic methanogenesis

HAc^-	$H_2CO_3^*$	NH_4^+	H^+	X_{AM}	CH_4
moles	moles	moles	moles	moles	moles
$-\frac{(1+\frac{5}{2}Y_{AM})}{Y_{AM}}$	$\frac{1}{Y_{AM}}$	-1	1	1	$\frac{1}{Y_{AM}}$

4.2.5.6 Organism decay

In the model, growth of the four organism groups has been included. Accordingly, death/organism decay for each of the organism groups must be included also. In the death process, it is accepted that the organisms die releasing biodegradable particulate organics (COD_p) which are assumed to have the same formulation as the primary sludge. Also, the difference in N content between the biomass and primary sludge is released as ammonia (NH_3). Accordingly, the general stoichiometric relationship for the general biomass (X_x) is summarised as follows:

Table 4.7: Stoichiometry for the decay of biomass

X_x	$H_2CO_3^*$	NH3	CODp
moles	moles	moles	g COD
-1	0.5	0.762	160

The stoichiometry above applies to each organism group.

4.2.6 Process kinetics

Where possible, the different rate equations used were adapted from various literature sources to describe the reactions as accurately as possible. The rate equations chosen for each of the biological processes identified for inclusion above are described below.

4.2.6.1 Hydrolysis

With the exception of Hill and Bart (1977), up to now the rate of hydrolysis of particulate organic material has been modelled using first order kinetics. A number of researchers (e.g. Eastman and Ferguson, 1981; Gujer and Zehnder, 1983; Henze and Harremoës, 1983; Bryers, 1985; Pavlostathis and Giraldo-Gomez, 1991) used a simple first order equation dependent only on the available substrate concentration, namely:

$$-r_{COD_p} = k_h[COD_p] \qquad (4.18)$$

where:

k_h	=	first order kinetic rate constant
$[COD_p]$	=	biodegradable particulate COD concentration

However, the rate of hydrolysis is affected by temperature, pH, bacterial population, particle size, type of organic and soluble product concentration. Among these, at least the bacterial population plays a major role in regulating the rate of hydrolysis and should be included in some fashion in the rate of hydrolysis. Furthermore, application of the first order rate formulation has been found to give values for the first order rate constant that are situation specific, with the value varying with hydraulic retention time. Since the objective in this research project was to develop a kinetic model that would be applicable over a range of retention times, the first order approach was rejected.

In the modelling of activated sludge systems, Dold *et al.* (1980) used Levenspiel (1972) planar surface mediated reaction kinetics (also called Contois kinetics, Vavilin *et al.*, 1996) to model the hydrolysis/utilization of particulate slowly biodegradable COD. In application these kinetics gave reasonable predictions over a wide range of activated sludge system conditions with a single set of constants. Accordingly, this approach was followed here also for the anaerobic hydrolysis process. This gave the following process rate equation:

$$-r_{CODp} = \frac{k_{max} \cdot \frac{[COD_p]}{[X_a]}}{K_s + \frac{[COD_p]}{[X_a]}}[X_a] \qquad (4.19)$$

where:

k_{max}	=	maximum specific kinetic rate constant
K_s	=	half saturation constant
$[X_a]$	=	acidogenic biomass concentration
$[COD_p]$	=	biodegradable particulate COD concentration

4.2.6.2 Acidogenesis

As noted in Section 4.2.5.2 above, two equations for the degradation of glucose to propionic acid, acetic acid and hydrogen by acidogenic bacteria were employed. Firstly, under conditions of both low and high hydrogen partial pressure ($\overline{pH_2}$), a normal acidogenic reaction takes place, with products acetic acid, hydrogen and carbon dioxide. Noting that the process was to be formulated in terms of the growth of acidogens, the specific growth rate is a basic Monod equation (Gujer and Zehnder, 1983; Pavlostathis and Giraldo Gomez, 1991), and is given as follows:

$$r_{Xa} = \frac{\mu_{max}[COD_s]}{K_s + [COD_s]}\left(1 - \frac{[H_2]}{k_{H_2} + [H_2]}\right)[X_a] \qquad (4.20)$$

where:

μ_{max}	=	maximum specific acidogen growth rate constant
K_s	=	half saturation constant
$[X_a]$	=	acidogenic biomass concentration
$[COD_s]$	=	biodegradable soluble COD concentration
$[H_2]$	=	hydrogen concentration
$[k_{H2}]$	=	hydrogen inhibition constant

In the case of high hydrogen partial pressure conditions, in addition to the products acetic acid, hydrogen and carbon dioxide, propionate is also produced. For the propionate production process, the specific growth rate of the acidogens is also based on Monod kinetics:

$$r_{Xa} = \frac{\mu_{max}[COD_s]}{K_s + [COD_s]}\left(\frac{[H_2]}{k_{H_2} + [H_2]}\right).[X_a] \qquad (4.21)$$

where:

μ_{max}	=	maximum specific acidogen growth rate constant
K_s	=	half saturation constant
$[X_a]$	=	acidogenic biomass concentration
$[COD_s]$	=	biodegradable soluble COD concentration
$[H_2]$	=	hydrogen concentration
$[k_{H2}]$	=	hydrogen inhibition constant

To ensure that the above process only operates when the partial pressure of hydrogen is high, a switching function (non – competitive inhibition) is included in the formulation depended on the $\overline{p}H_2$. Further, to ensure that the rate of glucose utilization does not increase, the rate of acetate production (Eq. 4.20) must be reduced; this is done via a switching function dependent on $\overline{p}H_2$.

4.2.6.3 Acetogenesis

The propionate produced under high hydrogen partial pressure conditions, is degraded by acetogenic bacteria to produce acetate in a process called acetogenesis. The specific growth rate for acetogens is a simple Monod equation:

$$r_{Xp} = \frac{\mu_{max}.[Pr]}{K_s + [Pr]}\left(1 - \frac{[H_2]}{K_{H_2} + [H_2]}\right).[X_P] \qquad (4.22)$$

where:

μ_{max}	=	maximum specific acetogen growth rate constant

K_s = half saturation constant

$[X_P]$ = acetogenic biomass concentration

[Pr] = propionate concentration

Since the process only operates under low $\overline{pH}_2$ (Chapter 2) a switching function (non – competitive inhibition) is incorporated depending on the $\overline{pH}_2$.

4.2.6.4 Acetoclastic methanogenesis

Acetoclastic methanogenesis or acetate cleavage is the reaction where acetate is converted to methane and carbon dioxide. In the process, growth of acetoclastic methanogens occurs and the process is modelled in terms of this growth. The specific growth rate of the acetoclastic methanogens is as follows:

$$r_{X_{AM}} = \frac{\mu_{max}.[HAc]}{K_s + [HAc]}.[X_{AM}] \qquad (4.23)$$

where:

μ_{max} = maximum specific acetoclastic methanogen growth rate constant

K_s = half saturation constant

$[X_{AM}]$ = acetoclastic methanogen biomass concentration

[HAc] = acetic acid concentration

4.2.6.5 Hydrogenotrophic methanogenesis

Hydrogenotrophic methanogenic bacteria use hydrogen and carbon dioxide to form methane. The specific growth rate of this group methanogens is similar to that of the acetoclastic methanogens, and is as follows:

$$r_{X_{HM}} = \frac{\mu_{max}.[H_2]}{K_s + [H_2]}.[X_{HM}] \qquad (4.24)$$

where:

μ_{max} = maximum specific hydrogenotrophic methanogen

		growth rate constant
K_s	=	half saturation constant
$[X_{HM}]$	=	hydrogenotrophic methanogen biomass concentration
$[H_2]$	=	molecular hydrogen concentration

None of the rate equations above include any terms for the inhibition of organisms by inhibitory substances, except for H_2. This was done separately and will be discussed in Chapter 5.

4.2.7 Model presentation

In the mathematical model, the process rates and the stoichiometric relationships between the processes and the compounds are formulated mathematically, see above. However, the large number of complex interactions between compounds and processes makes visualization difficult. To aid understanding, the biological processes are presented in matrix format in Table 4.8. This format facilitates clear and unambiguous presentation of the compounds and processes and their interactions (Henze *et al.* 1987).

4.3 WEAK ACID/BASE CHEMISTRY

In anaerobic digesters weak acids and bases play an important role in establishing the pH and damping pH changes. The reaction scheme for the weak/acid base part of the model was taken from Musvoto *et al.* (1997), see Chapter 2, Table 2.1. The approach consists of a series of forward and reverse reactions describing all the weak acid/base components included in the model. A forward reaction for the dissociation and a reverse reaction for the reformation of products describe the interaction between each of the different weak acid/base species.

4.3.1 Weak acid/base chemistry rate equations

The rate equations used for the weak acid base chemistry were taken directly from Musvoto *et al.* (1997) (see Chapter 2 for a review), and are all first order rate equations of the form:

Table 4.8: Matrix representation of biological processes contained in conceptual model

Compound → / Process ↓	CODp	CODs	HAc	H_2	HPr	$H_2CO_3^*$	NH_4^+	NH_3	CH_4	H^+	X_a	X_{AM}	X_{HM}	X_P	Rate
Hydrolysis	-1	0.00521				-0.0046		0.0015							$\frac{\mu_{max}\frac{[COD_p]}{[X_a]}}{Ks+\frac{[COD_p]}{[X_a]}}[X_a]$
Acidogenesis (low pH_2)		$-\frac{1+\frac{5}{6}Y_{Ac}}{Y_{Ac}}$	$\frac{2}{Y_{Ac}}$	$\frac{4}{Y_{Ac}}$		$\frac{2}{Y_{Ac}}$	-1			1	1				$\frac{\mu_{max}[COD_S]}{Ks+[COD_S]}[X_a]$
Acidogenesis (high pH_2)		$-\frac{1+\frac{5}{6}Y_{Ac}}{Y_{Ac}}$	$\frac{1}{Y_{Ac}}$	$\frac{1}{Y_{Ac}}$	$\frac{1}{Y_{Ac}}$		-1			1	1				$\frac{\mu_{max}[COD_S]}{Ks+[COD_S]}\left(\frac{[H_2]}{k_{H_2}+[H_2]}\right)[X_a]$
Endogenous decay	160					0.5		0.762			-1				b_aX_a
Acetogenesis			$\frac{1}{Y_{AP}}$	$\frac{1}{2}+\frac{3}{Y_{AP}}$	$-\frac{1+\frac{3}{2}Y_{AP}}{Y_{AP}}$	$\frac{1}{Y_{AP}}-\frac{1}{2}$	-1			1				1	$\frac{\mu_{max}[Pr]}{Ks+[Pr]}\left(1-\frac{[H_2]}{k_{H_2}+[H_2]}\right)[X_P]$
Endogenous decay	160					0.5		0.762						-1	b_pX_P
Acetoclastic methanogenesis			$-\frac{1+\frac{5}{2}Y_{AM}}{Y_{AM}}$			$\frac{1}{Y_{AM}}$	-1		$\frac{1}{Y_{AM}}$	1		1			$\frac{\mu_{max}[HAc]}{Ks+[HAc]}[X_{AM}]$
Endogenous decay	160					0.5		0.762				-1			b_mX_m
Hydrogenotrophic methanogenesis				$-\frac{4+10Y_{HM}}{Y_{HM}}$		$-\frac{1+5Y_{HM}}{Y_{HM}}$	-1		$\frac{1}{Y_{HM}}$	1			1		$\frac{\mu_{max}[H_2]}{Ks+[H_2]}[X_{HM}]$
Endogenous decay	160					0.5		0.762					-1		b_HX_H
Units →	gCOD/ℓ	mole/ℓ													

$$r = K.[products] \quad (4.24)$$

The weak/acid base species included were the water, ammonia, inorganic carbon, acetate and propionate systems (the phosphate weak acid/base system was not included as its influence in the digester is small). For each interaction between the species of the system, two processes are used. One process is used to describe the kinetics of the forward weak acid/base dissociation, and another for the kinetics of the reverse reaction. In total 12 processes describe the weak/acid base system, see Table 4.9 below.

Table 4.9: Rate equations for weak/acid base chemistry (See Chapter 2, Table 2.1 for stoichiometry)

Process	**Rate equation**
Forward dissociation of NH_4^+	$K'_{fn}[NH_4^+]$
Reverse dissociation of NH_4^+	$K'_{rn}[NH_3][H^+]$
Forward dissociation of $H_2CO_3^*$	$K'_{fc1}[H_2CO_3^*]$
Reverse dissociation of $H_2CO_3^*$	$K'_{rc1}[HCO_3^-][H^+]$
Forward dissociation of HCO_3^-	$K'_{fc2}[HCO_3^-]$
Reverse dissociation of HCO_3^-	$K'_{rc2}[CO_3^{2-}][H^+]$
Forward dissociation of HAc	$K'_{fa}[HAc]$
Reverse dissociation of HAc	$K'_{ra}[Ac^-][H^+]$
Forward dissociation of water	K'_{fw}
Reverse dissociation of water	$K'_{rw}[H^+][OH^-]$
Forward dissociation of HPr	$K'_{fa}[HPr]$
Reverse dissociation of HPr	$K'_{ra}[Pr^-][H^+]$

As stated before, the principle requirement for the weak/acid base systems is the establishment of an accurate pH. All weak acid/base species that significantly influence the pH are included as compounds in the model including H^+ and OH^-, and hence the pH can be calculated directly via $pH = -\log(H^+) = -\log f_m.[H^+]$, see Chapter 2.

4.4 PHYSICAL PROCESSES – GAS EXCHANGE

In the anaerobic digester significant CO_2 is produced. This production has been modelled as $H_2CO_3^*$ species. The weak acid/base chemistry part of the model will distribute this species automatically depending on the prevailing pH. However, the carbonate weak acid/base species will tend to equilibrium also with CO_2 in the atmosphere, through gas exchange. Musvoto *et al.* (1997; 1998) also included CO_2 exchange in the model they developed. Their approach has been detailed in Chapter 2 and was followed here also.

Musvoto *et al.* included NH_3 gas exchange/stripping in their model also, and this was also included in the model application described in Chapter 3. However, in the model here NH_3 gas exchange was excluded as the prevailing pH (pH < 7.5) would cause the process to be insignificant. If required, its inclusion will not present undue difficulties.

Accepting the above, dissolution and expulsion of CO_2 are shown in Table 4.10; for stoichiometry, see Chapter 2, Table 2.1.

Table 4.10: The kinetics of dissolution/expulsion of CO_2.

Process	**Rate equation**
Dissolution of CO_2	K'_{fCO2} [CO_2 (g)]
Expulsion of CO_2 from solution	$K'_{rCO2}[H_2CO_3^*]$

In the model of Musvoto *et al.* generation and loss of CH_4 and H_2 were not included, since anaerobic biologically mediated processes did not form part of their model. In the model developed here, the anaerobic biological processes are an integral part of the model, and hence CH_4 and H_2 production and gas loss need to be included. This was done by including CH_4 and H_2 as gasses essentially dissolved in the bulk liquid.

In application of the model to steady state, $\overline{p}CO_2$ was calculated from the molar ratios of the gasses CO_2 and CH_4 produced (H_2 was not considered as its production is very much less than CO2 and CH4). Also, it was assumed that the gasses (CH_4, CO_2 and H_2) are dissolved species and leave with the effluent flow; in reality, the gasses

should leave via a separate flow. For the steady state situation, this assumption/simplification does not influence the simulated results, since the gas composition does not vary and is essentially the same in the separate gas flow or as "dissolved" gasses leaving via the effluent.

To check that this is true, as separate headspace reactor was included with a diffusive link to the main reactor, with gas (CO_2, CH_4 and H_2) loss to the headspace, and gas flow from the headspace. These simulated results were identical to those obtained with gasses leaving via the effluent.

4.5 COMBINED ANAEROBIC DIGESTION MODEL

In the section above, separate models gave been presented for:

- Biological processes (Table 4.8)
- Weak acid/base chemistry (Tables 4.9 and 2.1)
- CO_2 gas exchange (Tables 4.10 and 2.1)

Since these three models are kinetically based, they can be readily integrated to provide a single kinetic model for anaerobic digestion of sewage sludge. As noted earlier, this initial model is restricted to anaerobic digestion of primary sewage sludge. The interactions between the submodels take place through the common compounds in the model, in particular the various weak acid/base system species. Since H^+ is included explicitly as a compound in the model, the effect of the biological processes on pH (via $-\log.f_m.[H^+]$) can be directly determined. However, the direct influence of the pH on the biological processes was not included at this stage of model development; this will be addresses in Chapter 5 where digester failure is examined.

4.6 MODEL CONSTANTS

For the biological processes, values for stoichiometric constants have been derived above based on the reactions of the processes with the exception of organism yields. For the weak acid/base chemistry and CO_2 exchange processes, values for stoichiometric constants were taken unmodified from Musvoto *et al.* (1997) who

derived these from the appropriate chemical equations. What remains is to derive estimates for the appropriate kinetic constants and the organism yield stoichiometric constants. This will be done in the sections that follow. In deriving values for the constants, where possible these were obtained from the literature.

4.6.1 Constants for biological processes

The selection of biological processes constants from the literature is crucial in order to simulate the correct interaction between the various groups of organisms in the system. Ristow *et al.* (1999) did a thorough literature survey of constants used and the associated conditions. They concluded that the various parameters are dependent on organic substrate, the temperature of the system under investigation, the type of bioreactor used in the system, the pH, and that even constants measured under these identical conditions varied from one researcher to the next.

Sam-Soon *et al.* (1991) reported a similar variation from a similar survey. Variations of up to an order of magnitude were found. For example, the maximum specific growth rate for the acetogens (propionate utilisers) ranges from 0.155/d (Hill and Barth, 1977) to 1.4/d (Heyes and Hall, 1983).

In order to establish some sort of consistency, the values from one study were taken and adaptations made where necessary. The initial values were taken from the study by Sam-Soon *et al.* (1991) and adaptations made according to the survey of Ristow *et al.* (1999).

Table 4.11 lists the kinetic and stoichiometric yield constants for each of the biological reactions according to the different processes included.

Table 4.11 does not include kinetic constants for the hydrolysis process. Since a new formulation for this process rate was followed, appropriate values for kinetic constants could not be determined from the literature. These had to be determined through model application, see Chapter 5.

Table 4.11: Kinetic parameters used in the model

Bacteria	μ_{max}	Y	K_s	b
	d^{-1}	mole organism/mole substrate	mole substrate/l	d^{-1}
Acidogens	0.8	0.1179	0.000781	0.041
Acetogens	1.15	0.028958	0.0026786	0.015
Acetoclastic methanogens	0.3	0.01635	1e-006	0.037
Hydrogenotrophic methanogens	0.86	0.004088	2e-006	0.01

4.6.2 Kinetic constants for weak/acid base processes

Since the forward and reverse dissociation reactions are very rapid, the rates of these reactions cannot be measured. However, from a practical point of view, the exact value of the reaction rate is of little importance; the only requirement is that the reaction is effectively instantaneous. To ensure the reactions are virtually instantaneous , one of the rate constants ($K_r^{'}$) was given a very high theoretical value (new "equilibrium" reached in less than 10 s). To ensure that the kinetically established equilibrium corresponds to true equilibrium chemistry, the value for the other rate constant ($K_f^{'}$) was calculated through the relationship with the equilibrium constant (see Chapter 2). Taking the ammonia weak acid/base as an example, at equilibrium the rate of the forward and reverse reactions are equal:

$$r_f = r_r \tag{4.25}$$

Substituting for the rate formulation gives:

$$K_f^{'}.[NH_4^+] = K_r^{'}.[NH_3].[H^+]$$

$$\frac{K_f^{'}}{K_r^{'}} = \frac{[NH_3].[H_+]}{[NH_4^+]} = K_n^{'}$$

where:

$K_n^{'}$ = apparent equilibrium constant for the ammonia system.

The values for the reverse reaction rate constants were determined as above by Musvoto *et al.* (1997), and are listed in Table 4.12. The appropriate equilibrium constants are listed in Chapter 2, Tables 2.2 (a) and (b).

Table 4.12: Kinetic constants used in weak acid/base processes

Reverse dissociation reaction	
Symbol	**Value**
$K_m^{'}$	10^{12}(/s)
$K_{rc1}^{'}$	10^{7}(/s)
$K_{rc2}^{'}$	10^{10}(/s)
$K_{ra}^{'}$	10^{7}(/s)
$K_{rp}^{'}$	10^{7}(/s)
$K_{rw}^{'}$	10^{10}(/s)
$K_{rCO_2}^{'}$	10^{12}(/s)

4.7 CLOSURE

In this Chapter, an integrated two phase (aqueous/gas) biological, chemical and physical processes kinetic model has been developed. As noted earlier, even though the model essentially consists of three separate models (biological, weak acid/base chemistry and CO_2 gas exchange) integrated together, these models could not be developed as separate entities and the model evolved interactively through successful formulation and application.

What remains is to test the model formulated in this Chapter not only for the purpose of validation, but also to calibrate values for kinetic constants not available in the

literature, particularly those related to the hydrolysis process. This will be dealt with in Chapter 5.

CHAPTER 5

TWO PHASE BIOLOGICAL, CHEMICAL AND PHYSICAL PROCESSES KINETIC MODEL FOR ANAEROBIC DIGESTION OF SEWAGE SLUDGE: MODEL CALIBRATION AND VALIDATION

5.1 INTRODUCTION

In Chapter 4, based on a conceptual understanding of the anaerobic digestion of primary sludges drawn from the literature, a kinetic model has been developed that describes the two phase (aqueous/gas) biological, chemical and physical processes operative in the anaerobic digester. Where possible, values for constants in the model were extracted from literature. However, values for a number of constants were not available in the literature, particularly those associated with the hydrolysis process for which a new formulation has been developed. Furthermore, the developed model requires validation through application to experimental data.

In this Chapter, the proposed kinetic model will be applied to experimental data available in the literature, to calibrate those constants for which values are outstanding and to provide some evidence validating the model itself. Further, to enhance the usefulness of the model, it will be appropriately modified and applied to demonstrate digester failure.

5.2 DATA SET USED FOR MODELLING

In any calibration and validation exercise, the biggest obstacle is usually the quality of data available for application of the model. Not only is the accuracy of the measurements important, but also the specific parameters measured. The measured parameters must be sufficient to describe the influent as well as the effluent adequately.

Izzet *et al.* (1992) conducted a series of experiments aimed at identifying the effects of thermophilic heat pre-treatment on the anaerobic digestibility of primary sludge. In this investigation four lab – scale anaerobic digesters were operated. Two digesters were fed heat treated sludge, while the other two were fed untreated primary sludge. The digesters were run in parallel. By progressively reducing the retention times of the digesters, the difference in digestibility between heat treated and non-treated (primary) sludge was demonstrated. One of the digesters fed with primary sludge, was operated for a period of 211 days, during which the retention time were reduced as soon as stability of the digester was achieved, from 20 to 15, 12, 10 and finally 7 days. Digester stability was monitored by measuring pH, H_2CO_3* alkalinity, short chain fatty acids (SCFA) and gas production. As these parameters are all interlinked, a change in one would affect the others to a greater or lesser degree.

The averages of the data collected from the digester fed primary sludge, and the averages of the calculated parameters, are given in Table 5.1. These averages represent the behavioural characteristics of the digester operating under stable conditions for the relevant retention times. The data set and the number of parameters measured that could be used as input in the model included unusual, but useful measurements such as conductivity and $H_2CO_3^*$ alkalinity using the 5 point titration method of Moosbrugger *et al.* (1992).

5.3 MODEL CALIBRATION

In the development of the model in Chapter 4, a number of the constants could be found from the literature. However, since a new formulation was introduced for the hydrolysis process, values for appropriate constants could not be found in the literature. In particular, three aspects of the hydrolysis required calibration:

- Primary sludge stoichiometric formula
- Values for the maximum specific hydrolysis rate and half saturation constants
- Unbiodegradable particulate fraction of the primary sludge

This section describes quantification of these three aspects.

Table 5.1: Averages of data calculated form digesters fed with primary sludge

Retention	Total Solids		Volatile Solids				
Time	influent	Effluent	influent	added	effluent	removed	removed
(days)	(g/l)	(g/l)	(g/l)	(g/day)	(g/l)	(g/day)	(%)
7	31.308	19.405	25.971	51.942	14.601	22741	43.4
10	31.161	17.936	25.768	36.076	13.386	17335	47.7
12	29.977	17.453	24.727	28.684	12.264	14457	50.1
15	31.301	17.801	25.863	24.053	12.619	12317	50.9
20	31.554	16.922	25.690	17.983	12.131	9491	52.8

Retention	Non-volatile Solids			TKN		Free & Saline Ammonia	
Time	influent	Effluent	removed	influent	effluent	influent	effluent
(days)	(g/l)	(g/l)	(%)	(mg/l)	(mg/l)	(mg/l)	(mg/l)
7	5.337	4.805	9.0	1105	1041	196	371
10	5.392	4.550	14.5	1100	1039	203	409
12	5.250	5.188	1.4	1028	992	235	430
15	5.437	4.461	17.1	1075	976	221	404
20	5.865	4.791	17.6	1171	1157	244	511

Retention	COD					Conductivity	
Time	influent	Added	effluent	removed	removed	influent	effluent
(days)	(g/l)	(g/day)	(g/l)	(g/day)	(%)	(mS/m)	(mS/m)
7	42.906	85.811	23.530	38.818	44.9	208	284
10	42.354	59.295	20.852	30.453	50.6	216	299
12	39.714	46.068	19.148	23.994	51.6	252	354
15	42.367	39.401	19.969	20.663	52.3	224	323
20	42.570	29.799	18.741	16.680	55.4	271	407

Table 5.1(cont.): Averages of data calculated from digesters fed with primary sludge

Retention Time	SCFA (as HAc)		pH		Alkalinity (as $CaCO_3$)	
	influent	Effluent	influent	effluent	influent	effluent
(days)	(mg/l)	(mg/l)			(mg/l)	(mg/l)
7	1770	51	5.38	7.11	79	1853
10	1831	50	5.38	7.12	82	1903
12	2197	33	5.36	7.16	85	2068
15	1824	27	5.42	7.14	82	1994
20	2244	25	5.29	7.17	59	2110

Retention Time	Gas production	Carbon Dioxide	Methane
(days)	(l/day)	(%)	(%)
7	27.741	36.8	63.2
10	20.670	37.9	62.1
12	17.215	36.7	63.3
15	13.958	36.4	63.6
20	11.173	36.7	63.3

5.3.1 Influent primary sludge stoichiometric formulation

In the kinetic model, it is proposed that the primary sludge is hydrolysed to the intermediate compound glucose, see Chapter 4, Section 4.2. Since the stoichiometry of the subsequent products from complete anaerobic digestion of the glucose is well established and essentially fixed, the stoichiometric transformation of the primary sludge to the intermediate glucose is crucial. Accordingly, attention was focussed on this aspect.

As a starting point, the primary feed composition was assumed to be the same as generally accepted for activated sludge, namely $C_5H_7O_2N$ (WRC, 1984). However, since the output from the digester is a direct consequence of the input and the formulation $C_5H_7O_2N$ could not correctly reflect the output measured by Izzet *et al.*, this formulation was changed as described below.

Since measurements for TKN and free and saline ammonia (FSA) were done on the influent by Izzet *et al.*, (1992) (see Table 5.1), the organic nitrogen content of the primary sludge feed could be determined. This was done by calculating the organic nitrogen in the feed for the different retention times, from TKN – FSA. The resultant value expressed as a ratio of the measured COD remained fairly constant with decreasing retention time, and ranged from 0.00144 mole N/g COD to 0.00155 mole N/g COD. Accordingly, the average of 0.00149 mole N/g COD was taken as the organic nitrogen content of the feed sludge. However, changing the nitrogen content of the original formulation ($C_5H_7O_2N$), changes the molecular mass and thus also the COD value of the feed which was also available from direct measurement (Table 5.1). Through a process of iteration, the N value of the formula was changed and the new molecular mass and COD value calculated; these new values were then used to recalculate the N value of the formula from the measured N/COD ratio, and the calculation procedure repeated until convergence. In this manner, the formula for the primary sludge with the correct nitrogen content was established to be $C_5H_7O_2N_{0.265}$.

However, although the N and COD of this formulation above corresponded to measured values, in application of the model it was found that the C content (i.e. C/COD ratio) was inconsistent with measured results. Essentially, the C content of the influent primary sludge appears in the outputs CO_2 gas, CH_4 gas, dissolved carbonate weak acid/base species, and effluent organic C. Hence, there should be a balance between input and output C. Further, the carbonate weak acid/base species also plays a very important role in establishing a number of parameters such as pH, $H_2CO_3^*$ alkalinity, CO_2 gas produced in the process, etc. Therefore, in the proposed model it is vitally important to establish the C content of the influent as closely as possible. It was hoped that by means of ensuring a C mass balance as measured by Izzet *et al.*, i.e. tracking all the C leaving the system and equating this to the influent C, the carbon content of the original influent could be determined. In this process an inconsistency in the data measured by Izzet *et al.* was found. Three measurements relating to the carbonate weak acid/base species were not in agreement, i.e. the $H_2CO_3^*$ alkalinity, partial pressure of CO_2 ($\bar{p}CO_2$) and pH. These three parameters are all linked through the carbonate species equilibrium chemistry (Loewenthal *et al.*, 1989) as follows:

$$H_2CO_3^*Alk = \bar{p}CO_2.K_{CO_2}.10^{pH-pK_1'}(2x10^{pH-pK_2'}+1)+10^{pH-pK_w'}-\frac{10^{-pH}}{f_m} \qquad (5.1)$$

Where:

K_{CO_2}	=	Henry's law constant
pK_1', pK_2'	=	negative logarithm of carbonate weak acid/base species apparent equilibrium constants
pK_w'	=	negative logarithm of the apparent equilibrium constant for the water subsystem
f_m	=	monovalent activity coefficient

Accepting any 2 of the measurements by Izzet *et al.* on their systems and calculating the third parameter via Eq (5.1) above, the calculated value did not agree with the measured

value for that particular parameter. In examining the three parameters and their measurements, it was noted that the pH was not measured *in situ*. When a sample was taken to measure pH, it would have been supersaturated with respect to CO_2 and therefore a loss of CO_2 before measurement of the pH would have taken place. This would have resulted in an elevated pH reading, rendering the pH measurement unreliable. Accordingly, the $H_2CO_3^*$ alkalinity and $\bar{p}CO_2$ were taken as the more reliable measurements. However, initially it was accepted that only the $\bar{p}CO_2$ measurement was accurate.

The $\bar{p}CO_2$ for each retention time was taken as reasonable and the $H_2CO_3^*$ alkalinity calculated via Eq (5.1) for a range of pH values, from pH 6.5 to 7.5. From the calculated $H_2CO_3^*$ alkalinity, for each specific pH the total carbonate weak acid/base species concentration (C_T) was calculated as follows:

$$[CO_3] = \frac{H_2CO_3^* Alk - [OH^-] + [H^+]}{2 + \frac{[H^+]}{K_{c_2}}} \tag{5.2}$$

$$[HCO_3^-] = \frac{[CO_3^{2-}][H^+]}{K_{C2}} \tag{5.3}$$

$$[H_2CO_3] = \frac{[CO_3^{2-}][H^+]^2}{K_{C_1}.K_{C_2}} \tag{5.4}$$

$$C_T = [H_2CO_3^*] + [HCO_3^-] + [CO_3^{2-}] \tag{5.5}$$

The C_T above gave the inorganic carbon leaving the system as dissolved in the effluent flow. Together with the other carbon related measurements (i.e. CO_2 leaving as gas, CH_4, organic carbon in the effluent) the total carbon leaving the system could be calculated. From a mass balance, this must equal the carbon entering the system with the influent.

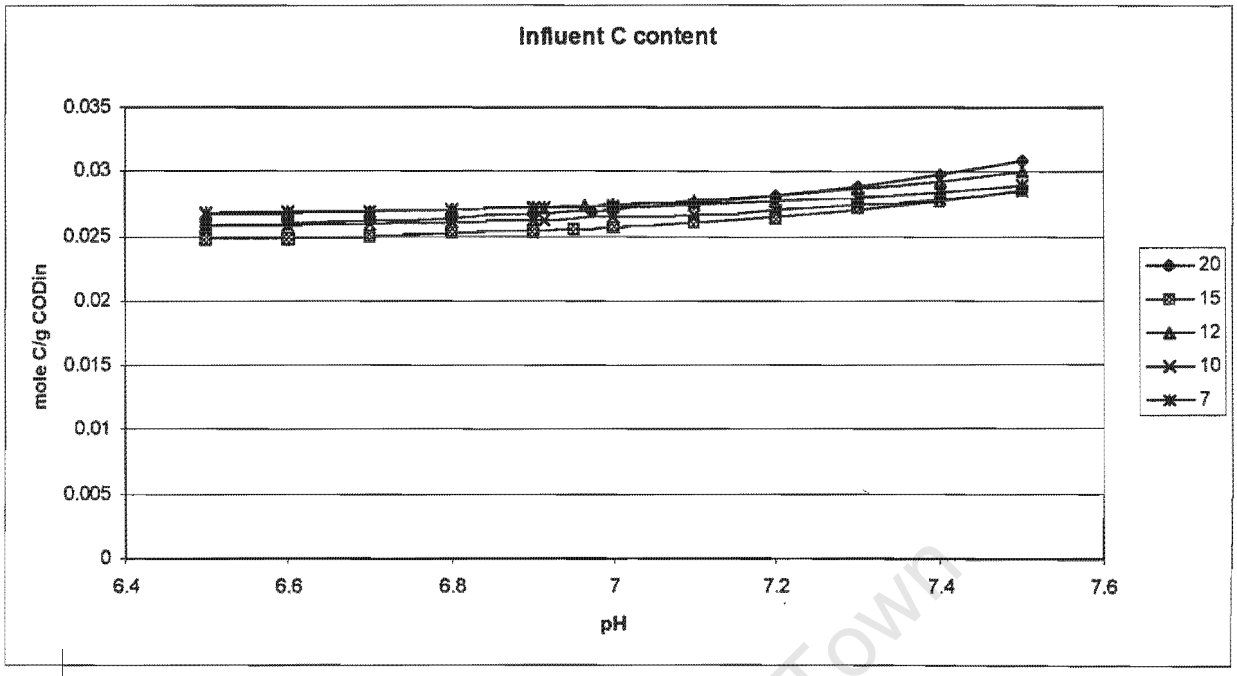

Figure 5.1: The Carbon content of the feed material (mole C/g COD) for the different retention times.

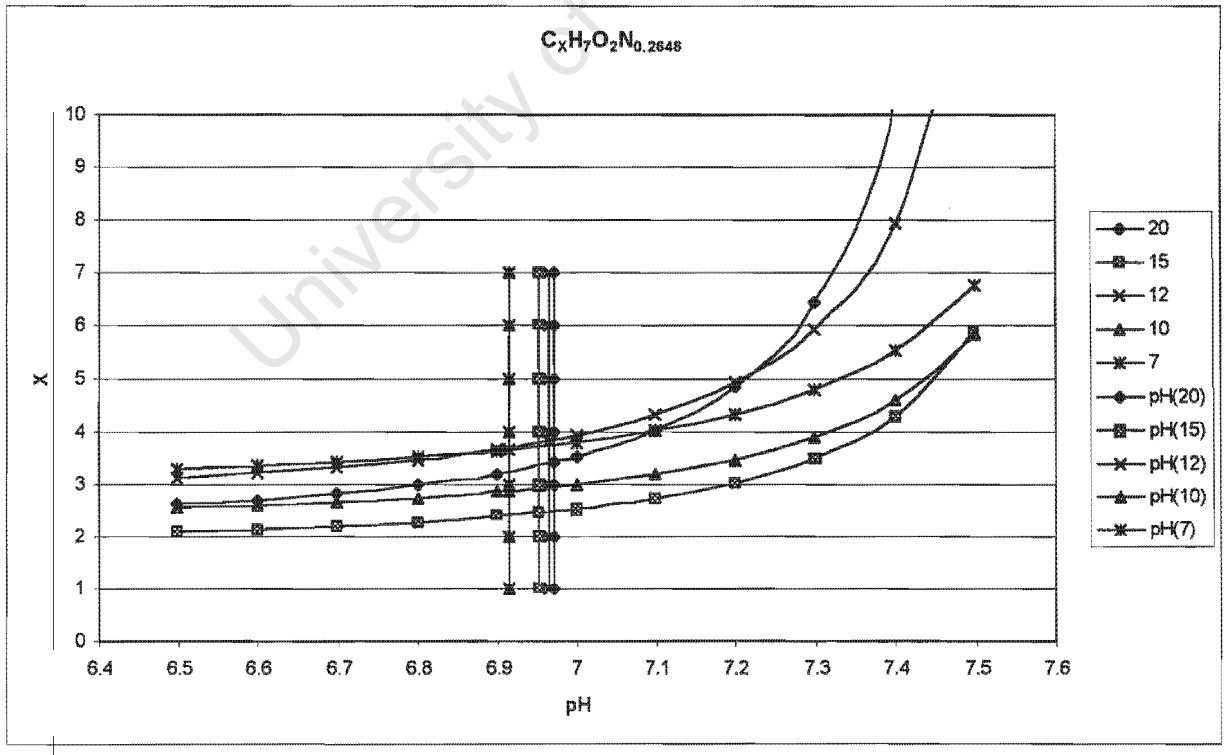

Figure 5.2: Influent formula over pH spectrum and associated calculated pH's.

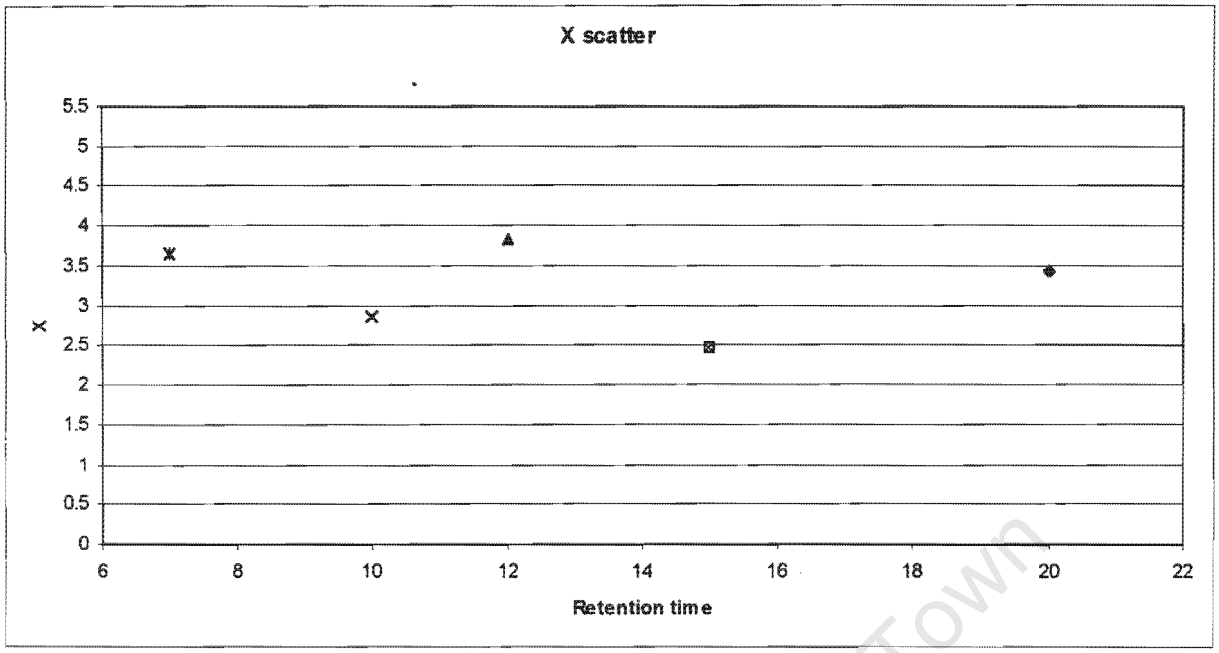

Figure 5.3: Scatter of X in the sludge formula $C_XH_7O_2N_{0.265}$ with increasing retention time.

Hence, the carbon in the influent could be calculated. This is expressed as the influent C/COD ratio for the various pHs and retention times in Fig. 5.1.

From Fig. 5.1, the C/COD values correlated closely over the whole spectrum of pH values for all the different retention times. Accepting the C/COD ratios in Fig. 5.1, these were used to calculate the moles of C in the formulation for primary sludge of $C_XH_7O_2N_{0.265}$. The values of X are shown plotted against pH for the different retention times in Fig 5.2, as the "exponential" type curves.

The curves relate the moles of C in the general formulation for primary sludge (X in $C_XH_7O_2N_{0.265}$) to a range of pH values in the reactor for the different retention times. To determine X, a true value for the reactor pH is required. As noted above, it was apparent the measured reactor pH values were in error and could not be used. However, the measured $H_2CO_3^*$ alkalinity is independent of the error in measured reactor pH, because $H_2CO_3^*$ alkalinity is not affected by CO_2 loss on sampling. Accordingly, the measured

$H_2CO_3^*$ alkalinity was accepted as reliable. Together with the measured $\bar{p}CO_2$, a calculated pH can be determined via Eq (5.1). For the different retention times these calculated pH values are shown plotted in Fig. 5.2 also, as the vertical lines. Where a vertical line (representing the true pH for a particular retention time) intersects the exponential line for the corresponding retention time, this represents the true state of the reactor, i.e. accepting $\bar{p}CO_2$ and $H_2CO_3^*$ alkalinity as correct and calculating the corresponding pH. The y – value at the intersection is the number of moles of C in the influent primary sludge formulation needed to achieve a C mass balance, i.e. the value for X in the formulation $C_XH_7O_2N_{0.265}$. The values of X, so derived, are plotted against retention time in Fig. 5.3; from Fig. 5.3, the value for X was accepted as 3.5. Substituting this into the general formulation for primary sludge, then the molecular weight and COD value of the sludge molecule will change. Accordingly, to retain the correct N/COD ratio in the primary sludge determined above, the N value in the formulation had to be changed also. This calculation gave the general formulation for the primary sludge used in the Izzet *et al.* (1992) experiments as $C_{3.5}H_7O_2N_{0.196}$. This formulation for primary sludge was accepted for all subsequent simulations of the Izzet *et al.* experiments. It is not certain whether the formulation will apply to primary sludges in general or not; this will have to be established through experimentation on a wider variety of primary sludges, by measuring COD, VSS, organic N and C content.

5.3.2 Hydrolysis rate constant

As noted in Chapter 4, to model sludge hydrolysis, a number of researchers (e.g. Eastman and Ferguson, 1981; Gujer and Zehnder, 1983; Henze and Harremoës, 1983; Bryers, 1985; Pavlostathis and Giraldo-Gomez, 1991) used a simple first order equation dependent only on the available substrate concentration, namely:

$$-r_{COD_p} = k_h[COD_p] \qquad (5.6)$$

where:

k_h = first order rate constant

$[COD_p]$ = concentration of particulate biodegradable organics

However, the rate of hydrolysis is affected by temperature, pH, bacterial population, particle size, type of organic and soluble product concentration. Among these, particularly the bacterial population should play a major role in regulating the rate of hydrolysis.

Recognising this, in Chapter 4 it was proposed to use Levenspiel (1972) planar surface saturation kinetics to model the hydrolysis rate, similar to that used to model the rate of SBCOD hydrolysis in activated sludge systems (Dold *et al.*, 1980; 1991; Henze *et al.*, 1987). This gave the hydrolysis rate formulation as:

$$-r_{CODp} = \frac{k_{max}\dfrac{[COD_p]}{[X_a]}}{K_s + \dfrac{[COD_p]}{[X_a]}}.[X_a] \qquad (5.7)$$

In the equation above, values are required for the maximum specific hydrolysis rate constant (k_{max}) and the half saturation constant (K_s). The data of Izzet *et al.* (1992) was used to derive values for these constants. It was decided to do this derivation in terms of the simple first order rate equation (Eq. (5.6)) above, so that the interrelationship between the first order and surface saturation reaction kinetics could be illustrated, and so that the conversion of data used to derive the first order rate constants to the new proposal could be demonstrated.

Initially the first order rate equation was accepted for hydrolysis. Setting up a mass balance for the system in terms of this equation gives:

$$V\frac{dCOD_p}{dt} = Q(COD_{p,in} - COD_{p,out}) - k_h.COD_{p,out}.V \qquad (5.8)$$

where:

V	=	volume of reactor
Q	=	flow through reactor
in, out	=	concentrations in the influent and effluent respectively

At steady state $\frac{dCOD_p}{dt} = 0$ and rearranging Eq (5.8) gives:

$$k_h = \frac{COD_{p,in} - COD_{p,out}}{R_h . COD_{p,out}} \quad (5.9)$$

where:

R_h	=	retention time in reactor

From the experimental data of Izzet *et al.* (1992), the influent and effluent total COD concentrations ($COD_{m,in}$ and $COD_{m,out}$ respectively) are available from measurement for each retention time. By accepting an unbiodegradable particulate COD fraction for the influent ($COD_{u,in}$ Section 5.3.3 below), then the biodegradable COD in the influent can be calculated ($COD_{p,in} = COD_{m,in} - COD_{m,out}$). Now, the measured effluent COD ($COD_{m,out}$) is made up of the unbiodegraded biodegradable particulates ($COD_{p,out}$), the unbiodegradable particulates ($COD_{u,out}$) and the organism biomass generated in the reactor. Since the unbiodegradable particulate COD remains unchanged in the system, its concentration in the effluent will equal its concentration in the influent, known from above. For the organism biomass COD in the effluent, the acidogen biomass dominates to the extent that with little error, the other biomass fractions can be neglected. This arises from the relatively high yield of the acidogens compared with the other organism groups (Y_{Ac} = 0.1179 mol/mol compared with < 0.03 mol/mol, Table 4.11). Accordingly, for the calculations here, only the acidogen biomass needs to be taken into account. A reasonable estimate for the concentration of acidogens in the effluent can be obtained by noting that:

$$[X_a] = Y_{Ac}(COD_{p,in} - COD_{p,out}) \quad (5.10)$$

where:

Y_{Ac} = acidogenic organism yield (mgCOD/mgCOD)

X_a = acidogen biomass concentration (mg COD/ℓ)

In Eq. (5.10), $COD_{p,in}$ is known but $COD_{p,out}$ is not. However, $COD_{p,out}$ can be estimated by noting that:

$$COD_{p,out} = COD_{m,out} - X_a - COD_{u,out} \quad (5.11)$$

where:

$COD_{m,out}$ = measured effluent COD

$COD_{u,out}$ = unbiodegradable particulate COD concentration in the effluent

= concentration in the influent, $COD_{u,in}$

Thus, solving Eqs. (5.10) and (5.11) simultaneously, the $COD_{p,out}$ and $[X_a]$ can be calculated for each retention time. Accordingly, k_h can be calculated for each retention time via Eq (5.9); values are listed in Table 5.2. The values for k_h were found to vary considerably for the different retention times (0.064/d to 0.12/d), and this illustrated the shortcoming in using a simple first order rate expression for hydrolysis.

Table 5.2: Values for the first order kinetic rate constant k_h.

Retention time	**k_h (d^{-1})**
7	0.117637
10	0.103117
12	0.089505
15	0.074776
20	0.063575

To derive estimates for k_{max} and K_s in Eq (5.7) above, this can be done in terms of the estimate derived for k_h above. Noting that the hydrolysis rate in terms of the two different rate expressions must be equal:

$$-r_{COD_p} = k_h[COD_p] = \frac{k_{max}\left(\frac{[COD_p]}{[X_a]}\right)[X_a]}{K_s + \left(\frac{[COD_p]}{[X_a]}\right)} \tag{5.12}$$

Rearranging Eq (5.12) gives:

$$k_h \frac{[COD_p]}{[X_a]} = \frac{k_{max}\left(\frac{[COD_p]}{[X_a]}\right)}{K_s + \left(\frac{[COD_p]}{[X_a]}\right)} = \mu \tag{5.13}$$

where:

μ = specific hydrolysis rate

In Eq (5.13) above, k_h , $COD_{p,out}$ (= COD_p) and $[X_a]$ are known from the calculations set out earlier, and k_{max} and K_s are unknown.

In order to determine values for the kinetic constants k_{max} and K_s, Eq (5.7) can be linearised in three different ways. These plots all yield a straight-line fit and the accuracy of estimation of k_{max} and K_s varies according to the fit.

Method 1

Eq (5.13) can be inverted and simplified according to the Lineweaver-Burk (double reciprocal) plot (Lehninger, 1973), resulting in:

$$\frac{[X_a]}{k_h[COD_p]} = \frac{K_s.[X_a]}{k_{max}.[COD_p]} + \frac{1}{k_{max}} \quad (5.14)$$

Therefore, by plotting $\frac{[X_a]}{k_h[COD_p]}$ versus $\frac{[X_a]}{[COD_p]}$ and fitting a linear line to the data, the slope of the line = $\frac{K_s}{k_{max}}$ and the y-intercept = $\frac{1}{k_{max}}$. Fig. 5.4 shows the resulting plot for the data of Izzet *et al.* (1992) with the best fit straight line, which gives an estimated k_{max} of 526.3 g COD_p/mole X_a and K_s of 657.1 g COD_p/mole X_a. Excluding the outliers identified in method 3 and again fitting a straight line (dashed line in Figure 5.4) through the data, changes the constants slightly to k_{max} = 526.3 g COD_p/mole X_a and K_s = 644.2 g COD_p/mole X_a. With the exclusion of the outliers, the R^2 value for the linear fit improved from 0.9212 (lower right hand corner) to 0.9968 (upper left hand corner).

Method 2

The second method involves dividing Eq (5.13) by $\frac{[COD_p]}{[X_a]}$ and then inverting, resulting in:

$$\frac{1}{k_h} = \frac{[COD_p]}{[X_a]}\frac{1}{k_{max}} + \frac{K_s}{k_{max}} \quad (5.15)$$

By plotting $\frac{1}{k_h}$ versus $\frac{[COD_p]}{[X_a]}$, and fitting a straight line through the data, the slope would give the value of $\frac{1}{k_{max}}$ and the y-intercept would give the value of $\frac{K_s}{k_{max}}$. Fig. 5.5 shows the plot of the data of Izzet *et al.* (1992) with the best fit linear line give the value for k_{max} of 625 g COD_p/mole X_a and for K_s of 839.9 g COD_p/mole X_a. However, the R^2 value obtained for the linear fit (lower right hand corner) is fairly poor (0.6785). By

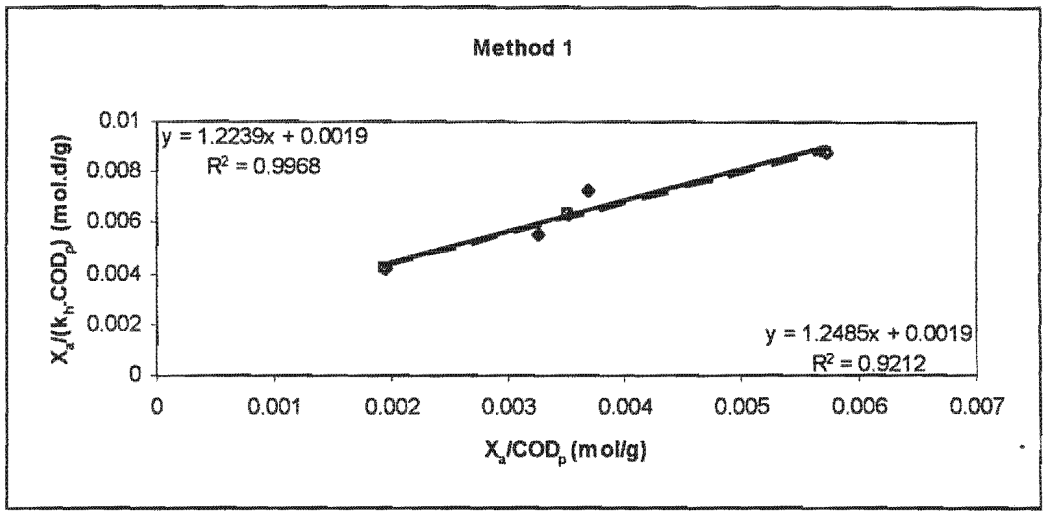

Figure 5.4: Plotting the data using the equation described in method 1.

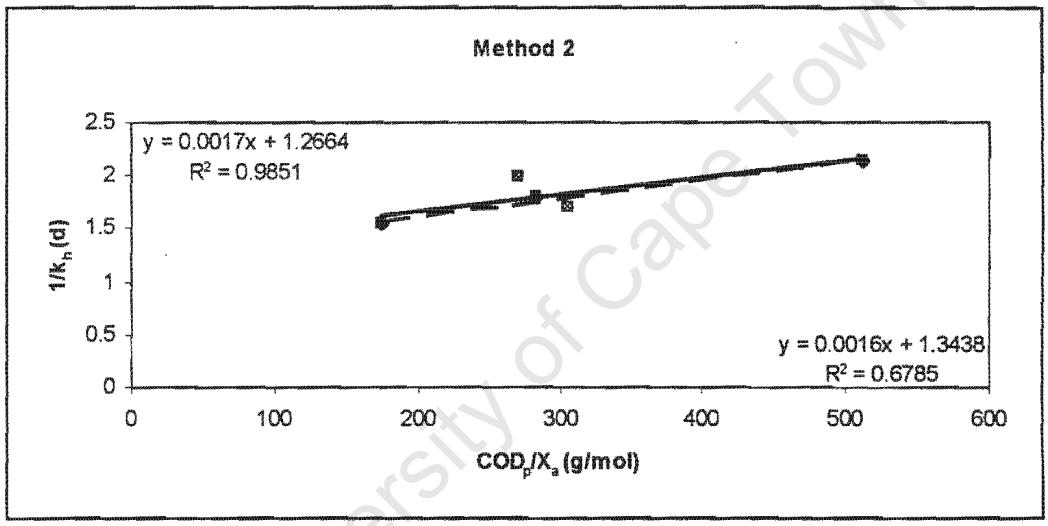

Figure 5.5: Plotting the data using the equation described in method 2.

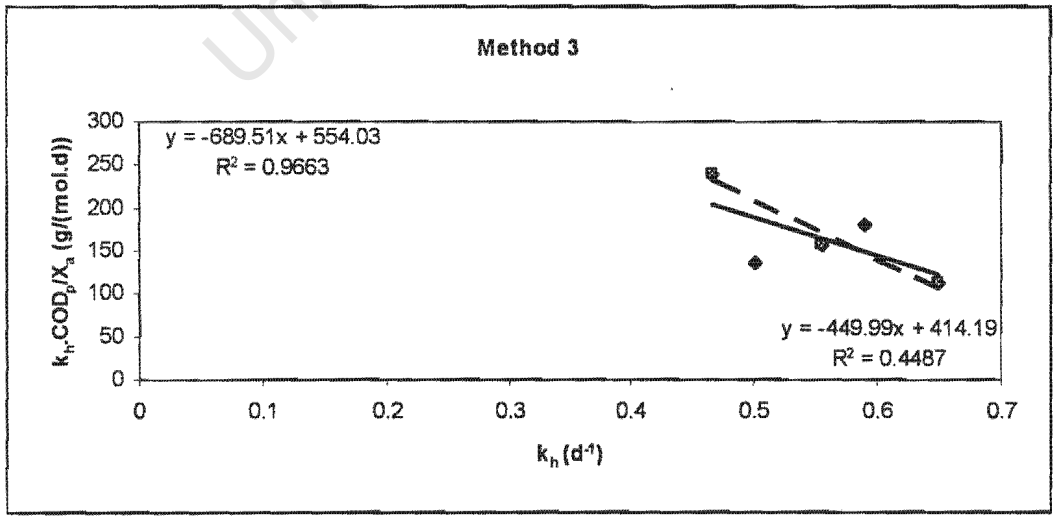

Figure 5.6: Plotting the data using the equation described in method 3.

excluding the outliers identified in method 3 and determining the best fit linear line (dashed line in Figure 5.5), the R^2 value can be improved considerably to a value of 0.9851. This yields the constants k_{max} = 588.2 g COD_p/mole X_a and Ks = 744.9 g COD_p/mole X_a.

Method 3

The Eadie-Hofstee linearization apparently magnifies departure from linearity that might not be apparent from a double-reciprocal plot (Lehninger, 1970). This plot is obtained from Eq (5.13) by multiplying both sides of the equation by k_{max}, and then simplifying to give Eq (5.16).

$$k_h \frac{[COD_p]}{[X_a]} = -K_s.k_h + k_{max} \qquad (5.16)$$

By plotting $k_h.\frac{[COD_p]}{[X_a]}$ against k_h, the best-fit linear line would give values for the slope = $-K_s$, the y-intercept = k_{max}, and the x-intercept = $\frac{k_{max}}{K_s}$. Fig. 5.6 shows the plot for the data of Izzet *et al.* (1992) with the best fit linear line. The values for k_{max} and K_s are 414.2 g COD_p/mol X_a and 450 g COD_p/mol X_a respectively. From this plot, the 10 and 15 day retention time data points can be identified as outliers. Fitting a linear line using all 5 data points, yielded an R^2 value of only 0.4487. Excluding the two outlier points improved the R^2 value considerably, to a value of 0.9663. The associated constants also compare much better with those obtained using methods 1 and 2 above. The constants are k_{max} = 554.03 g COD_p/mole X_a and K_s = 689.5 g COD_p/mole X_a.

For the three methods above, the value for k_{max} and K_s, without and with excluding the two outlier points, are listed in Table 5.3. With the different constants obtained, the specific hydrolysis rate (μ) can be calculated from:

$$\mu = \frac{k_{max}\dfrac{[COD_p]}{[X_a]}}{K_s + \dfrac{[COD_p]}{[X_a]}} \qquad (5.17)$$

Eq. (5.17) above is effectively a Monod type expression linking specific rate to substrate concentration ($\frac{[COD_p]}{[X_a]}$ here). Accordingly, plotting μ versus $\frac{[COD_p]}{[X_a]}$ yields a Monod - type graph. Using the various constants calculated above with the three different methods, the Monod – type plots are shown in Fig. 5.7. Also shown plotted are the data of Izzet *et al.* (1992), appropriately calculated via Eq. (5.7). From the plot it is evident that the constants derived via the three methods above yield virtually identical plots for low values of $\frac{[COD_p]}{[X_a]}$. It is in this region that most of the Izzet *et al.* data lies. As the $\frac{[COD_p]}{[X_a]}$ increases beyond about 500 g COD/mol X_a, the plots do diverge. Excluding the

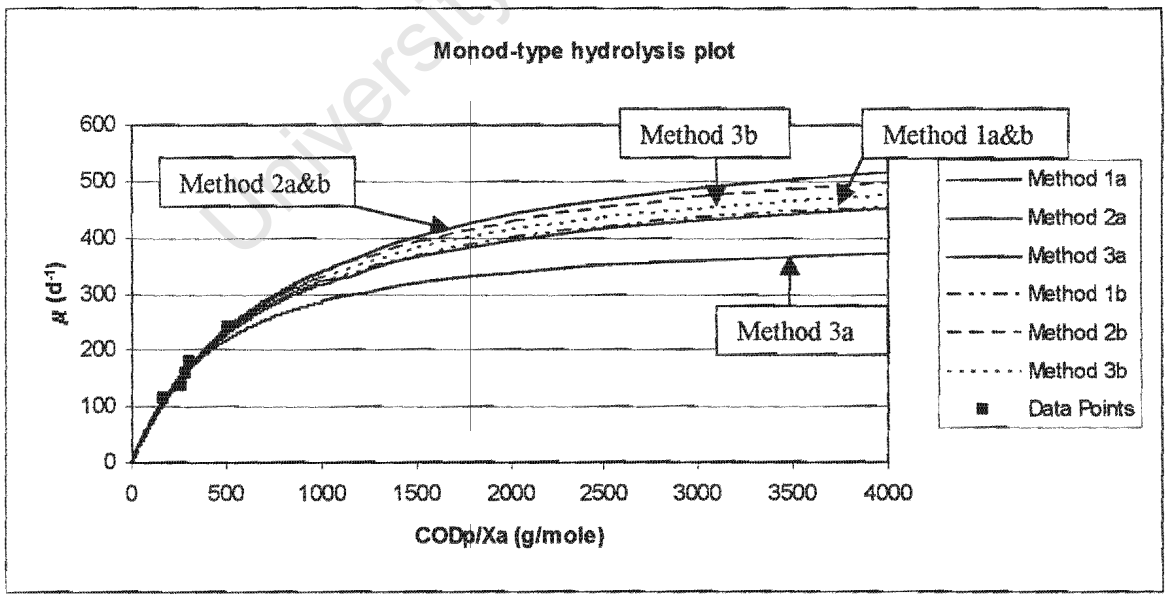

Figure 5.7: Monod – type plot of the constants obtained using 3 methods of linearization, (a) with all data points, (b) excluding the two outlier points.

outliers identified in method 3, the plots are much closer ((b) graphs in Fig. 5.7). In particular, the plot for the constants derived from method 3 is much closer to those from the other two methods (3 (a) to 3 (b) in Fig. 5.7).

Examining the fit of the curve to the actual experimental data of Izzet *et al.*, it is evident that, with the exception of method 3 (a) (i.e. with all data points), it is difficult to select which set of constants is superior. Accordingly, for simulating the Izzet *et al.* data, the average values for the data in Table 5.3 were calculated. However, in application, these values had to be changed slightly to improve the fit, to k_{max} = 650/d and K_s = 630 $gCOD_p/mol\ X_a$. This small change probably arises because the contribution of the non acidogen biomass to the effluent was not taken into account in the calculations above. To establish the values for the constants more precisely, data are required at higher $\frac{[COD_p]}{[X_a]}$, i.e. lower retention times.

Table 5.3: Summary of calculated constants for Hydrolysis

	All data points		Excluding outliers	
	K_s	k_{max}	K_s	k_{max}
	(g COD_p/mole X_a)	(d^{-1})	(g COD_p/mole X_a)	(d^{-1})
Method 1	657.1	526.3	644.2	526.3
Method 2	839.9	625	744.9	588.2
Method 3	450	414.2	689.5	554.03

5.3.3 Primary sludge unbiodegradable particulate fraction

In deriving values for the hydrolysis rate constants above, the data of Izzet *et al.* (1992) was used. This data includes the global COD measurements on the influent and effluent.

Initially, it was accepted that all the influent primary sludge was biodegradable. In plotting the experimental data on the Monod – type plot (Fig. 5.7 above), this caused that

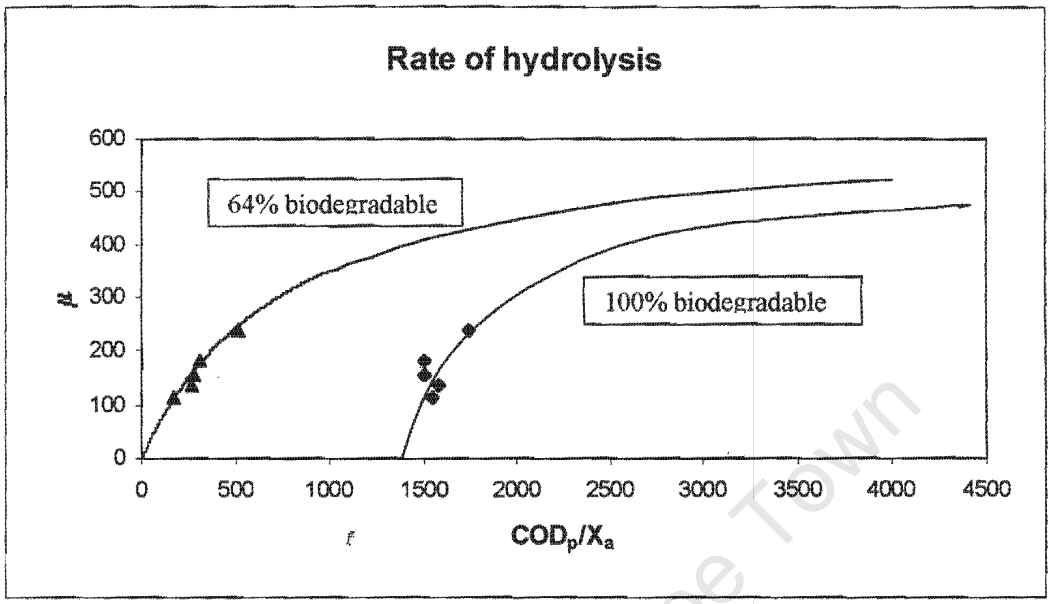

Figure 5.8: Monod – type curve fitted through the data of Izzet *et al.* (1992), accepting 100% biodegradable influent COD.

the curve fitting the data did not pass through the origin on the plot, but gave a $\mu = 0$ at some positive $\frac{[COD_p]}{[X_a]}$ value, for example see Fig. 5.8. This implied as expected, that the primary sludge contained unbiodegradable particulate organics. This was quantified by successfully changing the unbiodegradable particulate organic fraction of the primary sludge ($COD_{p,in}$ = measured COD – unbiodegradable COD) and replotting the data. In this fashion the unbiodegradable particulate fraction of the primary sludge was established, at 36% of the total COD. This value is the same as determined by O' Rourke *et al.* (1968) in their experimental investigation, which lends validity to the estimate.

5.4 MODEL VALIDATION

The model was validated through application to the data set of Izzet *et al.* (1992). Although the data were not collected specifically for the purpose of modelling, it is

sufficiently well defined for model validation. The data collected by Izzet *et al.* stretched over a period of 211 days. As noted earlier, the data were statistically processed and the average steady state data calculated, as given in Table 5.1. All simulations were done using AQUASIM ver. 2.0 (Reichert, 1994).

5.4.1 Input data

The input data to the model consisted of values for:

- System operational parameters – feed rate, reactor volume, temperature
- Influent compound concentrations
- Model kinetic and stoichiometric constants

5.4.1.1 System operational parameters

The systems operated by Izzet *et al.* (1992) were well controlled and defined. The system operational parameters are listed in Table 5.4.

Table 5.4: Operational parameters employed by Izzet *et al.* (1992).

Operational Parameter	Unit		Value
Temperature	°C		37
Volume	ℓ		14
Retention times	days		7, 10, 12, 15 and 20

5.4.1.2 Influent compound concentrations

Required as input are the concentrations of all the compounds included in the model, see Chapter 4, Tables 4.8 and 4.9. Available from direct measurement by Izzet *et al.* (1992) are the data listed in Tables 5.1.

The parameter serving as a main input value to the model is the measured COD entering the reactor. As described in Section 5.3.3 above, the unbiodegradable fraction for the primary sludge in the Izzet *et al.* experiments was determined to be 36% of the total measured COD, with the balance (64%) being biodegradable. In the model, the biodegradable fraction of the primary sludge in terms of COD units is hydrolysed to the intermediate glucose in terms of molar units. For this hydrolysis process, a stoichiometric formulation for the primary sludges is required. As noted in Section 5.3.1, the stoichiometric formula for primary sludge could not be obtained from the literature. Accordingly, a representative formula for the influent had to be deduced from influent organic N measurements and a C mass balance on the systems of Izzet *et al.*, as explained in Section 5.3.1 above. The formula established for the feed material was $C_{3.5}H_7O_2N_{0.196}$, and this was used for simulating the Izzet *et al.* systems.

For the simulations, available from direct measurements on the influent were $H_2CO_3^*$ alkalinity, pH and the short chain fatty acids and free and saline ammonia total weak acid/base species concentration. These values were accepted for simulations. However, as input to the model the specific weak acid/base species concentrations are required. As the conductivity of the feed had been measured and the temperature was known, the weak acid/base equilibrium constants could be determined (Loewenthal *et al.*, 1989; Musvoto *et al.*, 1998). The calculated equilibrium constants together with the influent pH and total weak acid/base species concentrations were used to speciate the weak acid/bases in the influent into their species concentrations. The pH and $H_2CO_3^*$ alkalinity was used to calculate the different carbonate weak acid/base species in the influent via Eqs (5.2) to (5.4) above.

It was assumed that no anaerobic organism biomass was present in the influent.

5.4.1.3 Model kinetic and stoichiometric constants

Required as input to the model are a large variety of stoichiometric and kinetic constants. These were determined as follows:

Weak acid/base aqueous chemistry:

- Values for "true" equilibrium constants were obtained from Musvoto *et al.* (1998), as listed in Chapter 4, Table 4.9 and Chapter 2, Table 2.2(a).
- With the measured conductivity (Table 5.1), converted internally in the model to an ionic strength value with the formula given by Loewenthal *et al.* (1989), the equilibrium constants above were corrected for ionic strength effects with the appropriate mono – , di – and tri – valent ion activity coefficients, as indicated in Chapter 2, Table 2.2(a), to give apparent equilibrium constants at $20^{\circ}C$.
- The apparent equilibrium constants were adjusted for temperature, as described in Chapter 2, Table 2.2(b).
- The specific rate constants for the reverse dissociation reactions of the weak acid/base (K_r) were taken from Musvoto *et al.* (1998; 2000c), Chapter 4, Table 4.12., but in times units /d due to instability in AQUASIM with time units /s. This change in time units does not influence the predictions as these rates are several orders of magnitude faster than the biological process rates.
- The specific rate constant for the forward dissociation reactions of the weak acid/bases (K_f) were calculated from the values for K_r above and the relationship with the apparent equilibrium constants, Chapter 2, Table 2.2(a).

Gas exchange:

- Although included in the model, NH_3 gas exchange was negligible due to prevailing pH. Accordingly, the value for the specific rate of NH_3 stripping (K'_{r,NH_3}, Table 2.3) was not of importance and the value from Musvoto *et al.* (1998, 2000c) was accepted unmodified, Chapter 2, Table 2.5.
- The value for the specific gas stripping rate constant for CO_2 (K'_{r,CO_2}, Table 4.10) had to be determined by calibration in the simulations. This is not unexpected, since this value will be influenced by the conditions prevailing in the reactor, e.g.

mixing. The rate of CO_2 gas dissolution (K'_{fCO_2}, Table 4.10) was calculated from K'_{rCO_2} via the relationship with Henry's law (Chapter 2, Section 2.4.2.1).

Biological processes:

Stoichiometric constants

- For the hydrolysis process, the stoichiometric formulation for the primary sludge developed in Section 5.3.1 above was adopted (the effect of changes in this formulation is demonstrated in the simulations), as well as the stoichiometric conversion to the intermediate glucose as developed in Chapter 4, Section 4.2.5.1.
- For the other biological processes, the stoichiometry as developed in Chapter 4 was accepted, with values for the organism yields (Acidogens – Y_{Ac}; acetogens Y_{AP}; acetoclastic methanogens – Y_{AM}; hydrogenotrophic methanogens – Y_{HM}) obtained from the literature, Chapter 4, Table 4.11.

Kinetic constants

- For the hydrolysis process, as noted in Section 5.3.2 above initially values for the kinetic constants (k_{max} and K_s) were the averages of the values derived from the data of Izzet *et al.* (1992) using three different linear curve fitting methods, i.e. k_{max} = 556/d and K_s = 693 $gCOD_p/mol\ X_a$. However, in application these values had to be changed slightly to improve the correlation between the predicted and measured data to k_{max} = 650/d and K_s = 630 $gCOD_p/mol\ X_a$; these changes are relatively minor.
- For the other biological processes, the values for the kinetic constants in the Monod formulations for growth/substrate utilization were obtained from the literature, Chapter 4, Table 4.11.
- For the biological processes describing death of the four organism groups, the values for the specific death rate constants were obtained from the literature, Chapter 4, Table 4.11.

Thus, effectively the only values for the kinetic and stoichiometric constants "calibrated" in the simulations were:

- K'_{rCO_2} - specific CO_2 gas stripping rate
- primary sludge stoichiometric formulation
- hydrolysis rate constants

In the simulations, values for the above constants were kept the same for all the retention times.

5.4.2 Output data

Several measurements were recorded that could serve as output to validate the model, see Table 5.1. The important measurements were gas production, $H_2CO_3^*$ alkalinity, acetic acid and pH, which were of particular importance to the inclusion of the weak acid/base systems. Other measurements used to validate the model included FSA and the partial pressure of carbon dioxide gas produced. The outputs from the model were compared to the measured data over the whole spectrum of retention times (7 days – 20 days).

5.4.2.1 Effluent COD

Since hydrolysis is in essence the starting process of the whole digestion process, great care was taken to ensure that the hydrolysis rate was correctly calibrated, see Section 5.3.2 above. This was to ensure that the correct quantity of organics enter the subsequent processes. In establishing the hydrolysis rate constants the unbiodegradable portion of the primary sludge was fixed at 36% (Section 5.3.3). The same inert fraction was also observed for the experimental investigation by O'Rourke *et al.* (1968). The inert material was taken as completely unbiodegradable and simply passed through the system unchanged. The effluent COD in the model was calculated as the sum of the inert material, the unutilized biodegradable COD and the biomass concentration grown in the system. These were compared to the measured effluent COD (Fig. 5.10); close agreement

was obtained. This close agreement demonstrates the superiority of the proposed hydrolysis kinetics over the simple first order kinetics used traditionally – with the proposed kinetics a single set of hydrolysis rate constants can accurately simulate the observed results over the range of retention times; with the simple first order kinetics a different constant is required for each retention time (Table 5.2).

To illustrate the various components making up the predicted effluent COD concentration, these are shown in Fig. 5.9.

From Fig. 5.9, the increase in unutilized biodegradable COD can be seen as the retention time decrease. This increase can be ascribed to the relative slow hydrolysis rate. Further, as noted in Chapter 2, under normal steady state operating conditions, conditions of low $\overline{pH}_2$ prevail causing low concentrations of acetogen organisms (X_p) to be present

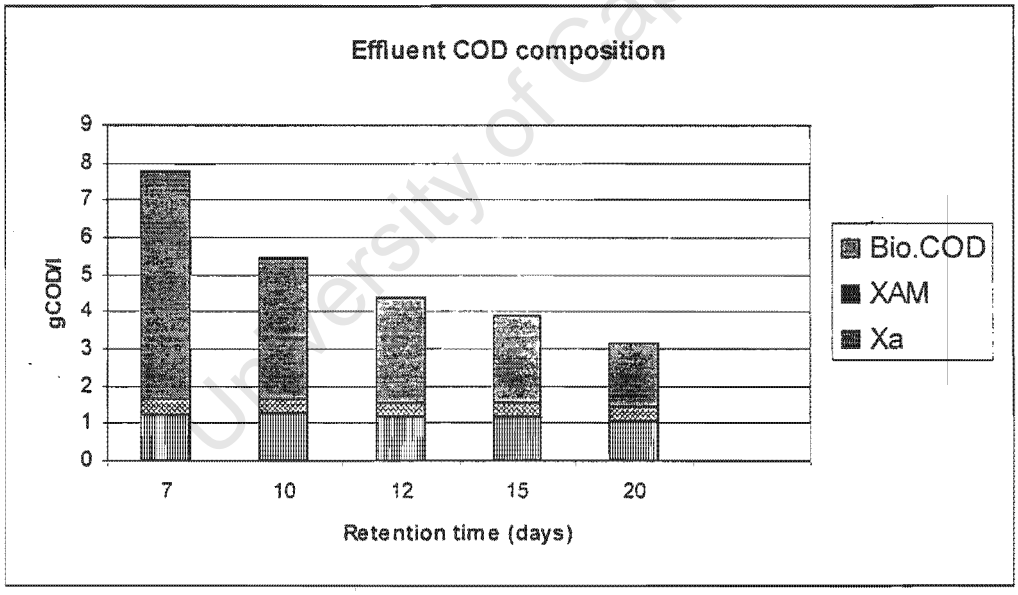

Figure 5.9: Compounds making up the effluent COD concentrations. For better representation of the other fractions, the unbiodegradable COD is not included. Also, X_{HM} and X_P are too small to show on the plot.

indicated by negligible acetogen growth due to the non – availability of propionate substrate. Of the biomass present, the acidogens dominate due to their relatively high

yield. This justifies neglecting the non – acidogen biomass fraction in the effluent in initially determining the hydrolysis rate constants (Section 5.3.2 above).

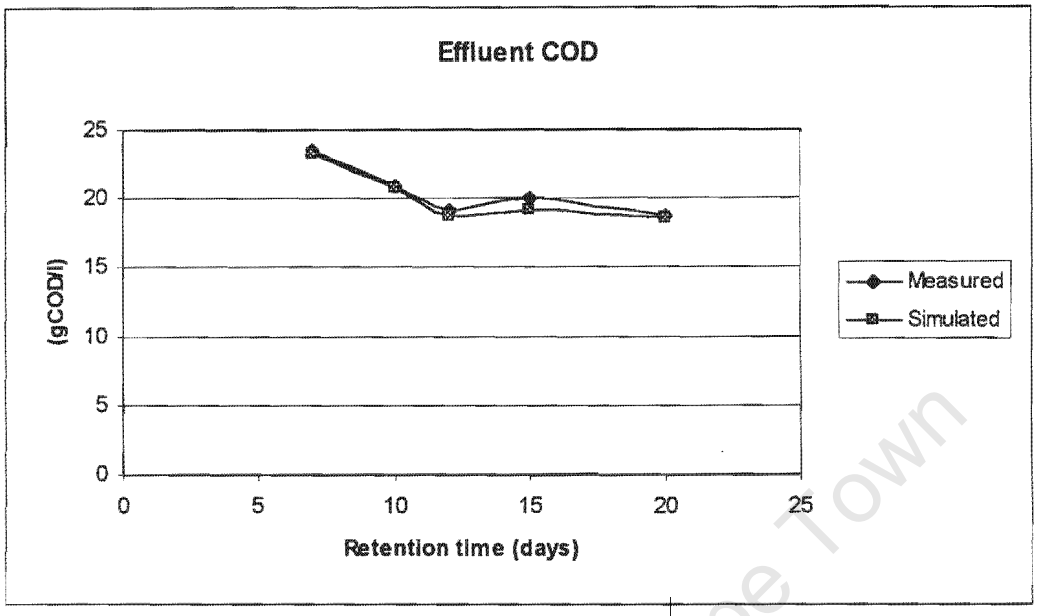

Figure 5.10: Predicted and measured effluent COD versus retention time for anaerobic digestion of primary sludge.

5.4.2.2 Free and Saline Ammonia (FSA)

For the initial model, the primary sludge formula $C_5H_7O_2N$ was accepted as a valid approximation of the organic material entering the system. However, in simulations with this formulation the concentration of FSA in the effluent was greatly overpredicted (Fig. 5.11); the simulated effluent FSA concentration, were almost 5 times higher than those measured. Clearly a major adjustment was needed and the decision was made to calculate the exact nitrogen content of the influent from the measured influent organic N concentration as detailed in Section 5.3.1 above. Together with the required C adjustment for a C mass balance, this gave the formulation for primary sludge of $C_{3.5}H_7O_2N_{0.196}$. The formula $C_5H_7O_2N$ was retained as representing the various active biomasses formed in the system. Incorporating the new primary sludge formula in the model improved the simulated results considerably (Fig. 5.12). However, the modelled output was still overpredicting the measured FSA. The experimental measurements on N were examined,

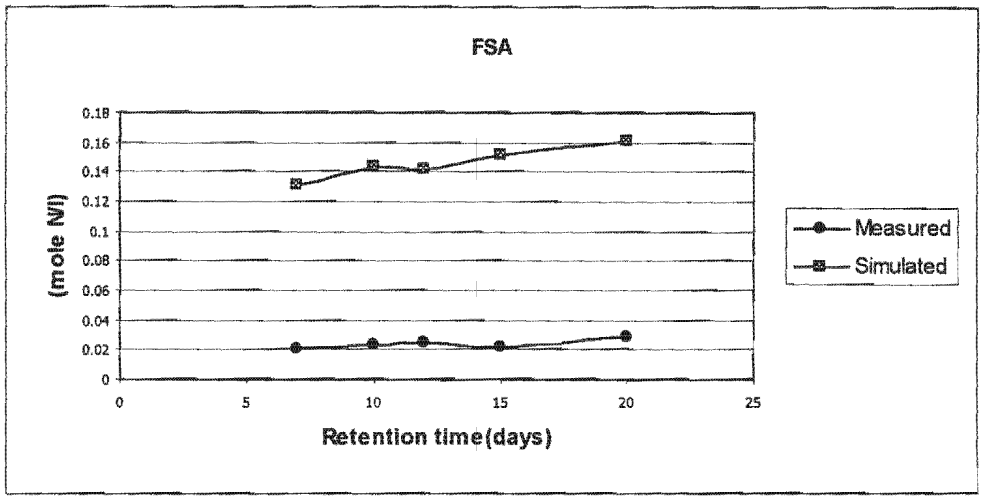

Figure 5.11: Comparison of FSA measurements in the effluent assuming initial sludge formula of $C_5H_7O_2N$.

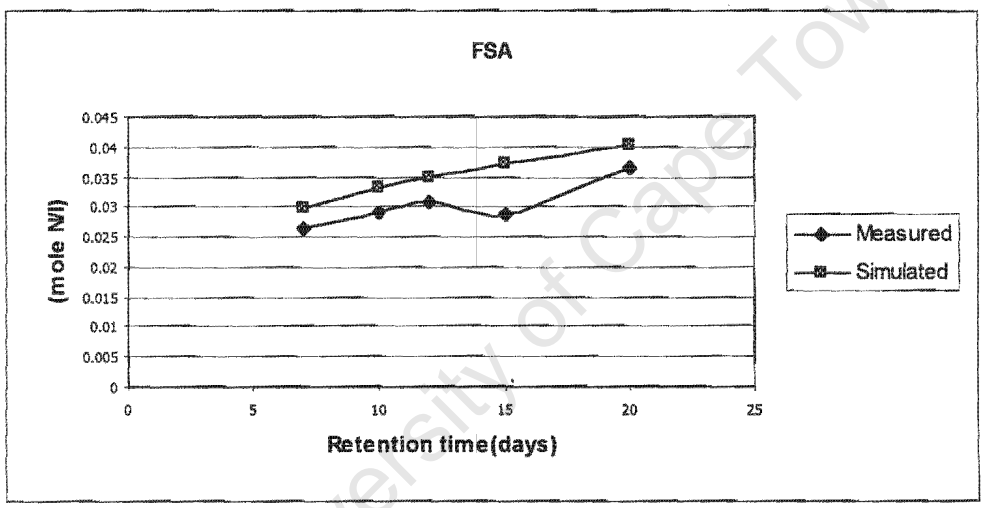

Figure 5.12: Comparison of FSA after adjusting the nitrogen content of the influent

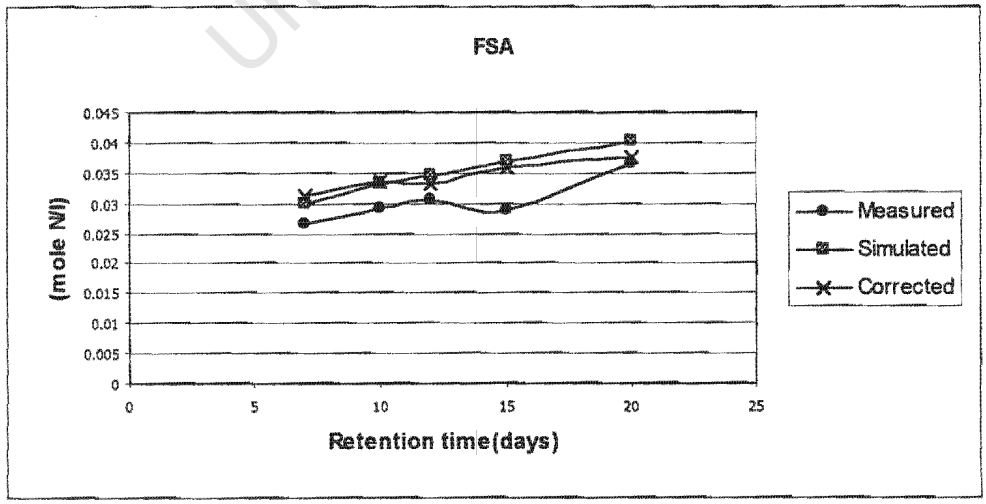

Figure 5.13: Comparison between simulated and corrected measurements

and it was established that a nitrogen mass balance had not been achieved across the system for all the different retention times. The N mass balances obtained ranged from 90-98%. Since the model is by necessity based on the mass balance principle, including N, closer correlation in the effluent FSA could only be achieved at the expense of organic N in the effluent. Accordingly, it was decided to correct the measured effluent FSA values by the amount of nitrogen missing from the nitrogen mass balance; this gave close correlation (Fig. 5.13).

5.4.2.3 Short Chain Fatty Acids (SCFA)

The SCFA included in the model are propionic and acetic acids. In the model, propionic acid is only generated significantly through acidogenesis under conditions of high $\overline{p}H_2$, and is converted to acetic acid through acetogenesis at low $\overline{p}H_2$. In all simulations the propionic acid concentrations were negligible, as is to be expected for completely mixed stable anaerobic digesters where low $\overline{p}H_2$ conditions prevail.

Acetic acid is generated through acidogenesis under low $\overline{p}H_2$ and serves as substrate subsequently for the acetoclastic methanogens. The measured effluent SCFA (accepted as acetic acid) in the experimental system were very low, typically less than 10^{-3} moles/ℓ. In the simulations it was not impossible to attain values quite as low for the SCFA. This arises because the SCFA are generated and utilized simultaneously; only with unrealistic high acetoclastic methanogenesis rates or low half saturation constant values can low acetic acid concentrations be achieved. However, the concentrations calculated in the model are acceptably close considering the very low % of the influent carbon that leaves via the effluent SCFA, and the same general trend seen in the measured values with change in retention time could be simulated (Fig. 5.14).

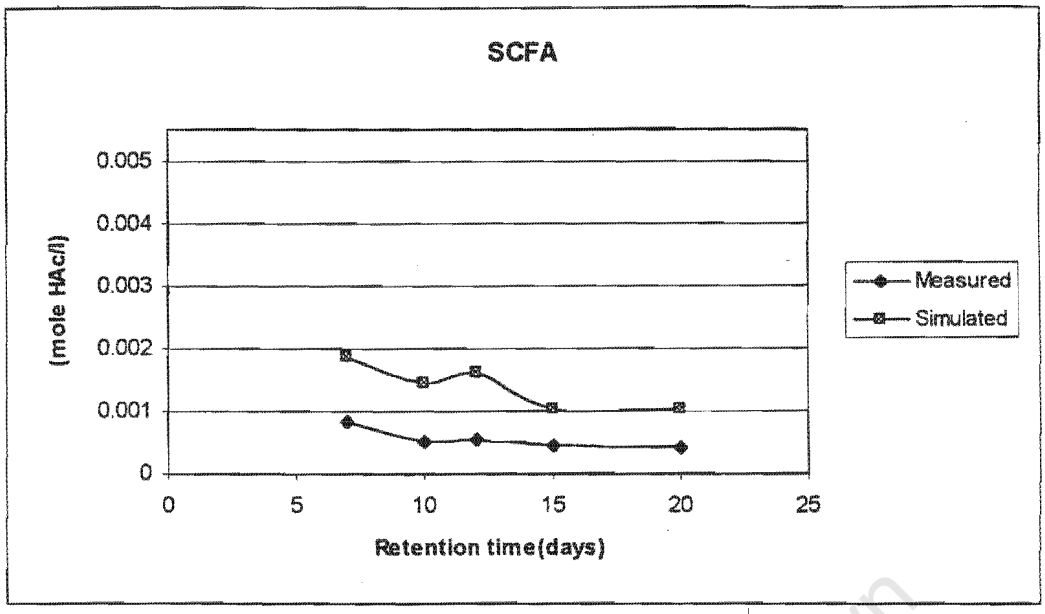

Figure 5.14: Comparison between modelled and measured SCFA output

5.4.2.4 Carbonate system and pH

Accepting the initial primary sludge formula of $C_5H_7O_2N$ during simulations, measurements relating to the carbonate weak acid/base system could not be accurately predicted. Initial simulations predicted the $H_2CO_3^*$ alkalinity too low, the partial pressure of CO_2 too high and the pH too low (Fig. 5.15). The carbon dioxide gas (CO_2) produced could be matched by changing the gas stripping rate used (obtained from Musvoto *et al.*, 1997).

As the model is based on a mass balance across the system, it was decided to calculate the true carbon content of the influent primary sludge and compare it with the formulation ($C_5H_7O_2N$) used. At closer inspection it was discovered that the experimental data of Izzet *et al.* (1992) showed an inconsistency in measurements relating to the carbonate weak acid/base system. As noted in Section 5.3.1 above, the C_T calculated using the pH and $H_2CO_3^*$ alkalinity, did not match the C_T calculated using for example the $\bar{p}CO_2$ and pH measurements. As a result of this inconsistency in the data a mass

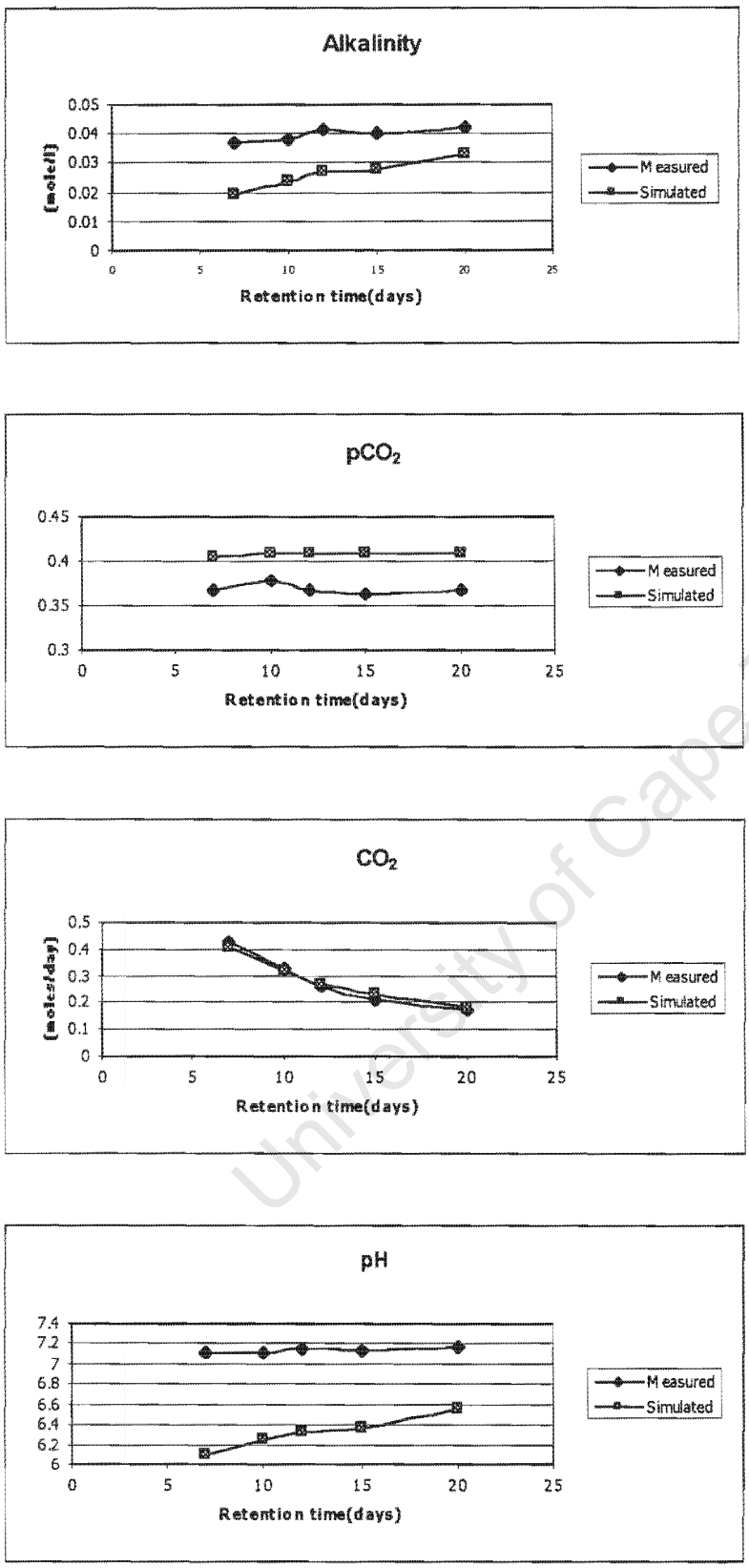

Figure 5.15: Comparison of carbonate output before changes to the influent sludge formula was made.

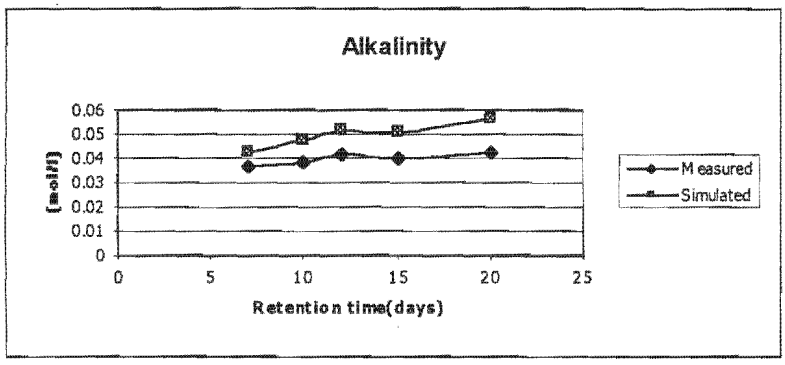

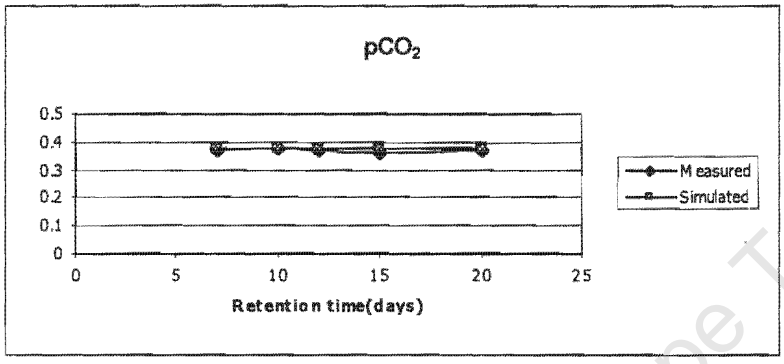

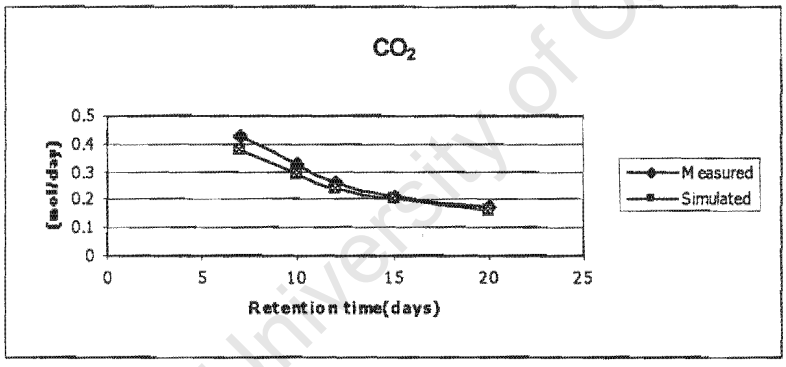

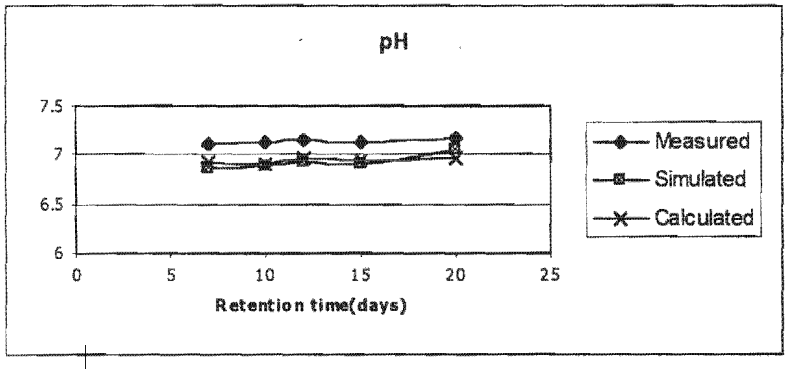

Figure 5.16(a): Comparison of output for the carbonate system after adjusting the sludge formula to $C_{3.5}H_7O_2N_{0.196}$.

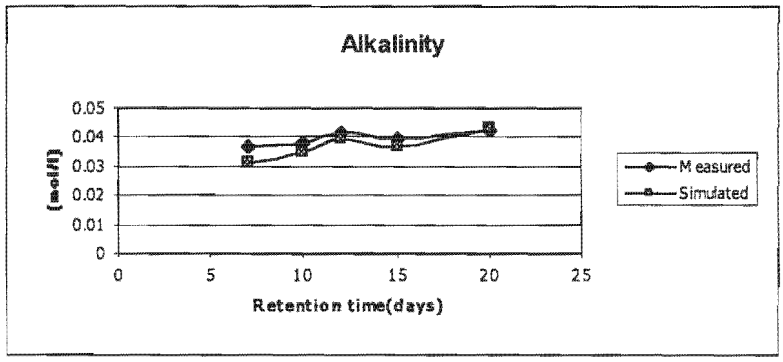

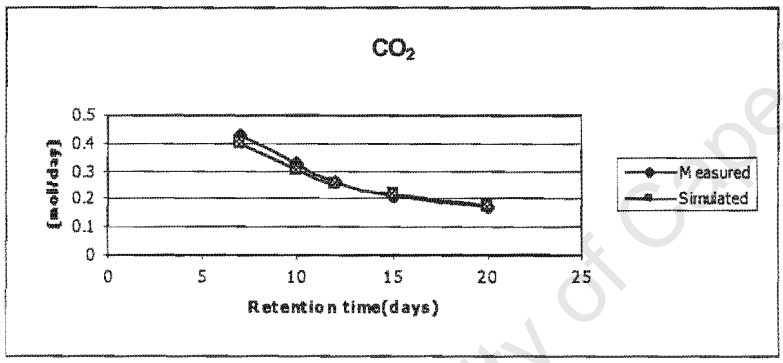

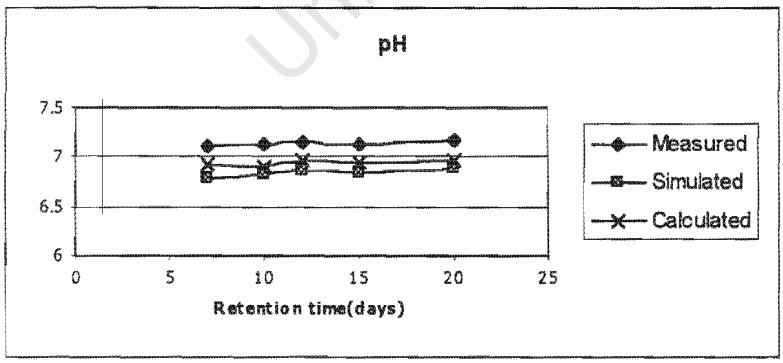

Figure 5.16(b): Comparison of output for the carbonate system after adding a small charge to the adjusted formula for the influent primary sludge.

balance across the system could not achieved. As described in Section 5.3.1 above, the $\bar{p}CO_2$ was taken as a true measurement and the $H_2CO_3^*$ alkalinity calculated for a range of pH values. A pH value was then calculated accepting the $\bar{p}CO_2$ and the $H_2CO_3^*$ alkalinity measurements; this indicated the influent primary sludge formula as $C_{3.5}H_7O_2N_{0.196}$.

Accepting the new sludge formula, simulated results closely matched experimental values (Fig. 5.16(a)). However, in the comparison there is a small deviation between measured and predicted $H_2CO_3^*$ alkalinity values. To improve this correlation a small negative charge can be added to the stoichiometric formulation for the primary sludge, to give $C_{3.5}H_{6.99945}O_2N_{0.196}^{0.00055-}$. Since this will cause H^+ to be taken up in the hydrolysis process, the predicted pH will decrease slightly as well as $H_2CO_3^*$ alkalinity while CO_2 gas evolution will increase, see Fig 5.16(b). No other parameters are affected by this change. In examining the data of Izzet *et al.* it was noted above (Section 5.3.1) that an inconsistency exists in the $\bar{p}CO_2$, $H_2CO_3^*$ alkalinity and pH measurements. It was concluded that the $H_2CO_3^*$ alkalinity and $\bar{p}CO_2$ were reliable, and these were used to calculate the corresponding pH (see Fig.5.16(a) and(b)). The small charge added to the primary sludge formulation improves the correlation between the predicted and the measured $H_2CO_3^*$ alkalinity, but the correlation between the calculated pH and the measured pH poorer. Therefore, it is not possible to make a definitive judgement as to whether the simulations with or without this small charge are superior.

5.4.2.5 Methane

With the adjustment above, the methane predicted by the model was consistently close to the experimental values measured by Izzet *et al.* (1992), see Fig 5.17. The methane production as predicted by the model accounts for about 60 to 65% of the total amount of gas produced, which is consistent with values found by other researchers in the literature for anaerobic digestion of primary sludge (e.g. Kiely *et al.*, 1996).

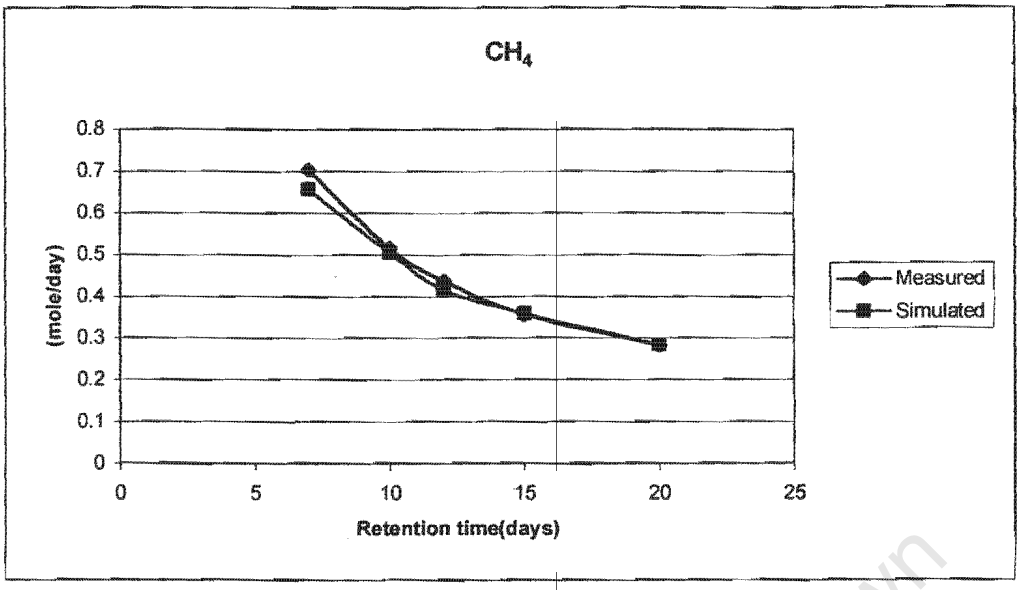

Figure 5.17: Comparison between measured and predicted values for methane output

5.4.3 Discussion

In this section, the proposed model has been applied to the data of Izzet *et al.* (1992) measured for anaerobic digestion of primary sludge for a range of retention times. Close correlation between measured and simulated results were obtained for all the measured data. In this model application it became evident that the stoichiometrical chemical formulation used for the primary sludge is crucial.

For the N, this could be determined from measurements on the influent TKN and FSA, as the organic N content of the primary sludge (TKN – FSA). However, for the C this had to be determined from a C mass balance on the experimental data. Accepting these, the formulation for the primary sludge was found to be $C_{3.5}H_7O_2N_{0.196}$. However, it is not certain whether this formulation is general or restricted to the Izzet *et al.* (1992) data. Recognising the importance of the formulation in the modelling efforts, clearly this is an area that requires further investigation. Further, it is recognised that the same data set was used to calibrate some constants in the model and to validate. Thus more extensive validation is necessary. Also, the application has been restricted to constant flow and load and steady state conditions; dynamic application also requires attention.

5.5 DIGESTER FAILURE

Having established above that the two phase biological, chemical and physical processes kinetic model provides a good description of the anaerobic digestion of primary sludge under stable conditions, the model could be used to explore the events that lead to digester failure. This was facilitated by the fact that the developed kinetic model integrates weak acid/base chemistry (and explicitly includes pH) with the biological processes.

From the literature review (Chapter 2), it is clear that a number of anaerobic digestion processes are very pH sensitive. Furthermore, since most of the influent substrate is converted to intermediate short chain fatty acids (SCFA) before conversion to methane, failure (even temporary) of one of the processes can readily lead to an accumulation of SCFA in the system. The accumulation of SCFA would cause the pH to decrease which in turn would severely impact the biological processes, and may lead to overall system failure.

In this section a brief look at the induction of failure in anaerobic digestion through modelling was taken, to illustrate potential usefulness of the kinetic model.

5.5.1 System of failure

Failure in anaerobic digesters can occur in a number of ways, but the main cause of failure in anaerobic digesters is described below.

Acetoclastic methanogens are probably the most sensitive organisms in the anaerobic process (Gujer and Zehnder, 1983) and are thus greatly influenced by the surrounding environment. It is believed that failure in anaerobic digestion usually starts with the inhibition of the acetoclastic methanogens. This can happen either by toxin or inhibitors in the feed material, a sudden shock load on the system or a drop in temperature as *Methanothrix soehngenii* has been reported to show extreme temperature sensitivity

in the feed material, a sudden shock load on the system or a drop in temperature as *Methanothrix soehngenii* has been reported to show extreme temperature sensitivity (Zehnder *et al.*, 1980). Any of these factors will slow down or inhibit the growth rate of the acetoclastic methanogens and cause acetic acid to accumulate in the digester. This accumulation will cause a decrease in pH. Both the acetoclastic methanogens and the hydrogenotrophic methanogens (e.g. *Methanobrevibacter arborphilus*) are pH sensitive, the latter also showing some sensitivity towards temperature changes. Accordingly, the drop in pH will slow down the acetoclastic and hydrogenotrophic methanogen growth, the latter of which will cause an increase in the hydrogen partial pressure ($\overline{p}H_2$) in the system.

An increase in $\overline{p}H_2$ will impact on the acidogenic process as described in Chapter 2, Section 2.2.2. Instead of producing acetic acid, the increase in $\overline{p}H_2$ will cause the acidogens to start producing propionic acid. As the acetogens (organisms responsible for the conversion of propionic acid to acetic acid) are inhibited by a rise in the $\overline{p}H_2$, the propionate will not be converted to acetate, causing the propionate concentration to increase causing a further build up of SCFA and resultant drop in pH, which will further influence the processes.

As can be gathered from the above description, the failure of anaerobic digesters has a "snowball effect" with various processes being influenced at the same time, with a build up of SCFA and the associated drop in pH being the primary features.

5.5.2 Modelling of failure in anaerobic digesters

Process inhibitions

Modelling of digester failure was mainly achieved by introducing a general non – competitive inhibition term of the form:

$$\left(1+\frac{[I]}{K_I}\right) \tag{5.18}$$

where:

[I] = concentration of the inhibitory compound

K_I = inhibition constant

This inhibition term (Eq. 5.18) was introduced into the general Monod kinetics describing the growth rate of the organism group inhibited by the particular compound as follows:

$$\frac{\mu_H . S_{bs}}{(K_{SH}+S_{bs})\left(1+\frac{I}{K_I}\right)} Z_{BH} \tag{5.19}$$

Inhibition of acetoclastic methanogens: The acetoclastic methanogens are inhibited by pH, and hence the inhibitory term in terms of pH (via $[H^+]$) was included in the growth rate formulation for this organism group:

$$\frac{\mu_{max,M}[HAc]}{(K_M+[HAc])\left(1+\frac{[H^+]}{K_{MI}}\right)} X_{AM} \tag{5.20}$$

Inhibition of hydrogenotrophic methanogens: The hydrogenotrophic methanogens are responsible for keeping the $\overline{p}H_2$ low, by utilizing H_2 as substrate. If they are also inhibited, this will inevitably slow down the conversion of H_2 to methane causing a rise in $\overline{p}H_2$. The hydrogenotrophic methanogens are pH neutrophiles and are inhibited at pH < 6.6 (Gujer and Zehnder 1983; Zehnder and Wuhrmann, 1977). Accordingly, the inhibitory term in terms of pH (via $[H^+]$) was also included in the growth rate formulation for this organism group:

$$\frac{\mu_{max,H}[H_2]}{(K_H+[H_2])\left(1+\frac{[H^+]}{K_{HI}}\right)}X_{HM} \qquad (5.21)$$

Inhibition of acetogens: Due to thermodynamics (Chapter 2), the acetogenic organism group is inhibited by a rise in the $\overline{p}H_2$. This will slow down the conversion of propionic acid to acetic acid, causing an accumulation of propionic acid in the digester. The effect of $\overline{p}H_2$ on acetogens has been included in the original formulation (Chapter 4):

$$\frac{\mu_{max,AP}[Pr]}{(K_{AP}+[Pr])}\left(1-\frac{[H_2]}{K_{H_2}+[H_2]}\right)[X_P] \qquad (5.22)$$

Table 5.5: Values of inhibition constants

Inhibition constant	Value
K_{MI}	1.15×10^{-6}
K_{HI}	0.00053
K_{H2}	4.5×10^{-7}

Gas loss

For the steady state simulations, with minimal error the gasses produced (CO_2, CH_4 and H_2) could be assumed to be "dissolved" and leave with the effluent. This was possible because the gas molar compositions remains constant. For simulation of the failure condition, the gas composition will change with time, and hence the assumption above may no longer be valid. Accordingly, the gas loss mechanism in the model were changed to more accurately reflect the real los of gasses to a separate gas flow stream. This was done as recommended by the IWA Task Group on anaerobic modelling with implementation in the computer programme Aquasim (Reichert, 1994):

A separate "headspace" reactor with volume 1 ℓ (as in the experimental system of Izzet *et al.*, 1992) was included, with a diffusive link to the main bioreactor. The compounds

$CO_2(g)$, $CH_4(g)$ and $H_2(g)$ were allowed to diffuse from the reactor to the headspace modelled using the Aquasim formulation:

$$r_{gas} = K_{LA,gas}(K_{H,gas}\overline{p}_{gas} - [S_{gas}]) \quad (5.23)$$

where:

r_{gas}	=	rate of gas diffusion across headspace/bioreactor link
$K_{LA,gas}$	=	specific gas exchange coefficient
	=	1000 /d for the 3 gasses
$K_{H,gas}$	=	Henry's law constant for the gas
$\overline{p}_{gas}$	=	partial pressure of the gas
	=	soluble gas concentration x RT
$[S_{gas}]$	=	concentration of gas in the bioreactor (mol/ℓ)

The partial pressure for the three gasses were calculated from the soluble concentrations in the headspace, using Daltons law of partial pressure (see above, and Chapter 2). The total pressure in the headspace is given by the sum of the partial pressures. The gas flow rate was calculated from proportional control loop with respect to atmospheric pressure, i.e.:

$$q_{gas} = K_p \frac{(P_{tot} - P_{atm})}{P_{atm}} V_{headspace} \quad (5.24)$$

where:

q_{gas}	=	gas flow rate (ℓ/d)
P_{tot}	=	sum of partial pressures
P_{atm}	=	atmospheric pressure
	=	1.013 bar
$V_{headspace}$	=	volume of headspace reactor
	=	1 ℓ

Accepting the more complex formulations for gas loss above, it was found that the predicted results were virtually identical to those wit the much simpler formulations where the gasses remains dissolved in solution and leave with the effluent flow. However, there might be digester failure conditions where the two approaches give divergent results. Accordingly, the more complex realistic formulation above was retained.

5.5.3 Modelling results

To simulate failure, the system of Izzet *et al.* at 15 days retention time was accepted. For this system, the model was run under stable digestion conditions to get steady state. Failure was then artificially induced by temporarily slowing down the growth rate of the acetoclastic methanogens for a short time interval of 3 days. Thereafter, the growth rate of the acetoclastic methanogens was increased to the original "steady state" value, and the simulation continued. Simulated results are shown in Figs. 5.18 to 5.21.

The short period of decreasing the acetoclastic methanogens maximum specific growth rate, had a very large effect due to non – utilization of acetic acid by acetoclastic methanogens: acetic acid concentration immediately increased sharply causing a concomitant drop in the pH (Fig 5.18). This drop in pH in turn inhibited the hydrogenotrophic methanogens causing $\overline{p}H_2$ to increase (Fig 5.20). This $\overline{p}H_2$ increase inhibited the acetogens and caused production of propionate in acidogenesis resulting in a delayed increase in propionate concentration (Fig. 5.18).

The decrease in concentration of both the acetoclastic and hydrogenotrophic methanogenic organism mass fractions can be seen from Fig. 5.19, coupled with an immediate increase in $\overline{p}H_2$ (Fig. 5.20). From Fig. 5.21, the decrease in gas production with the onset of failure is clearly illustrated.

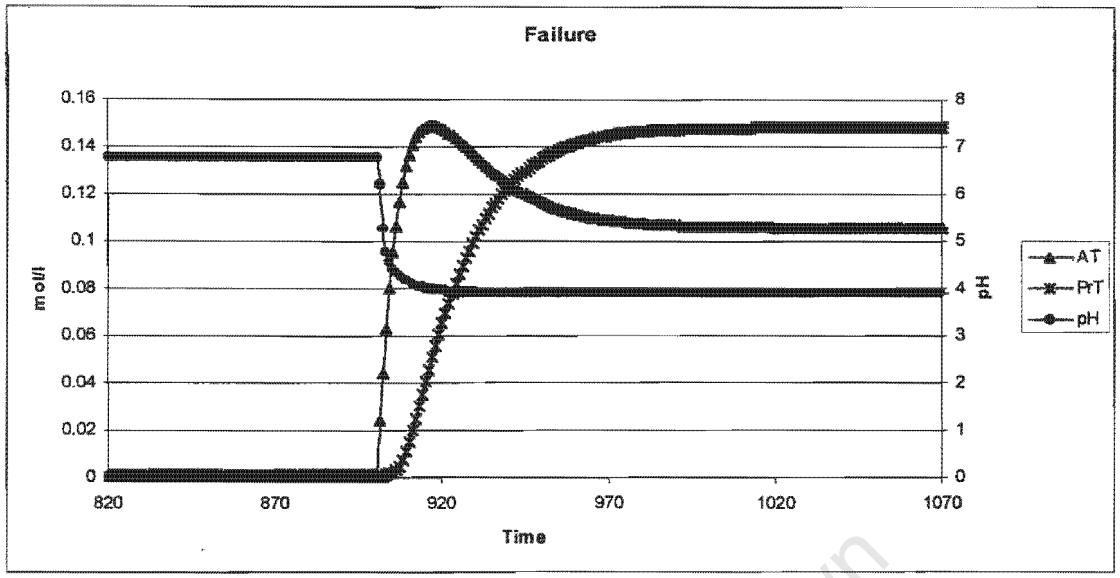

Figure 5.18: At induced failure the pH drop is shown with the increase in the SCFA's propionate and acetate.

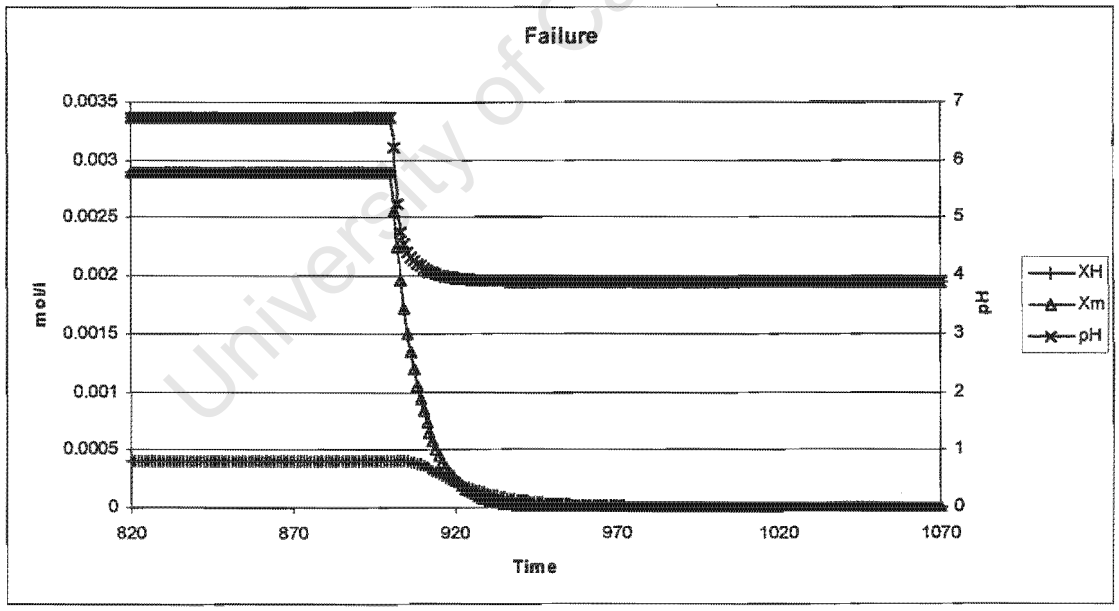

Figure 5.19: The drop in organism mass concentration with the drop in pH and the eventual washout of the acetoclastic -and hydrogenotrophic methanogens.

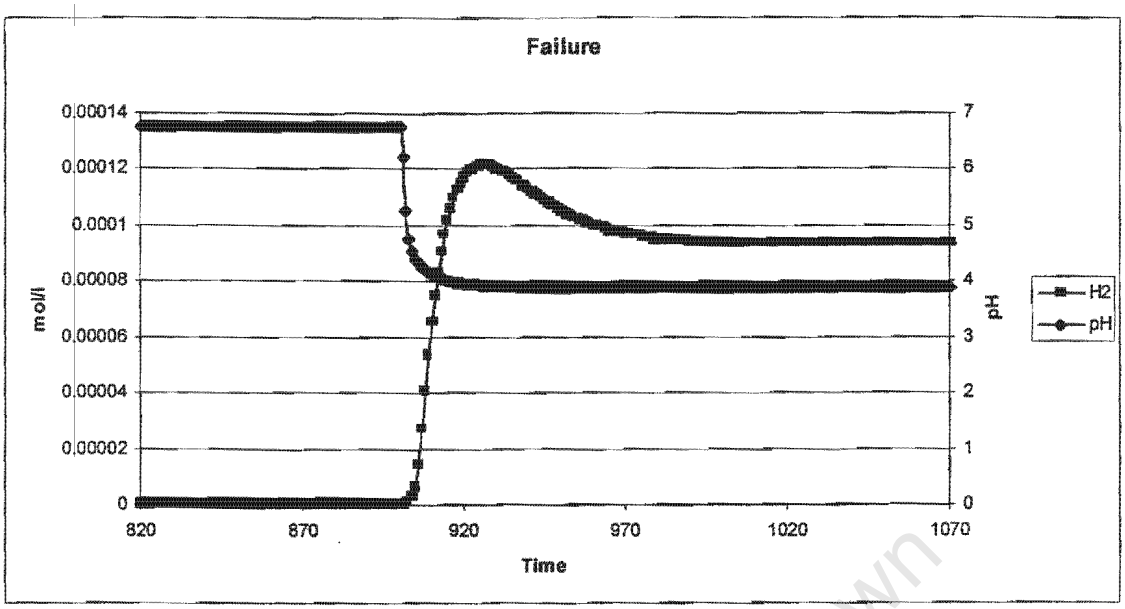

Figure 5.20: The rise in hydrogen partial pressure $\overline{p}H_2$ with drop in pH

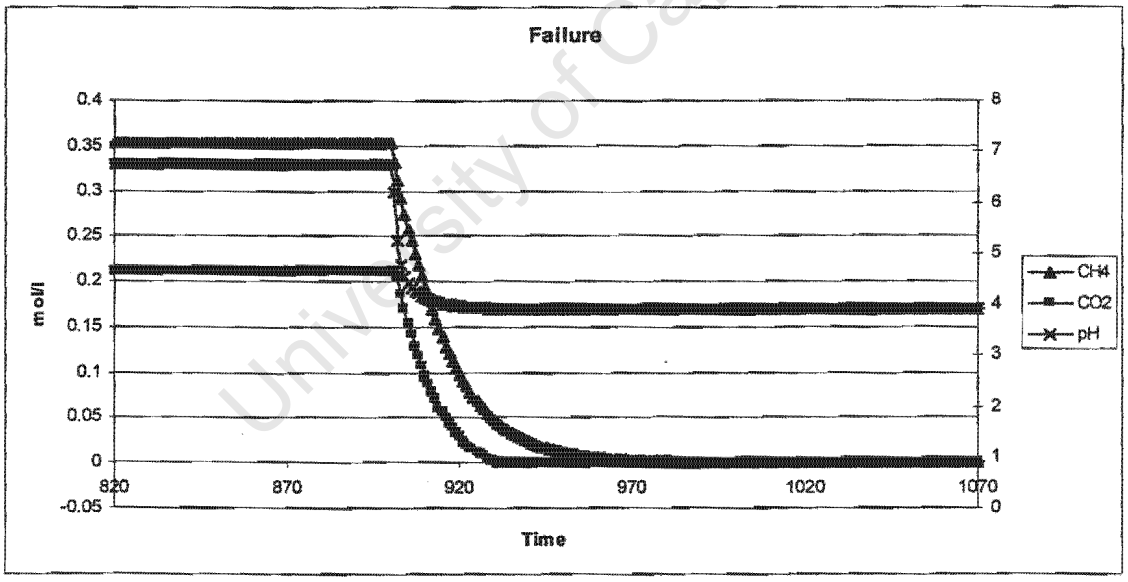

Figure 5.21: The drop in gas production during failure of the anaerobic digester process

These results indicate that the anaerobic digestion system is highly poised. Even a short duration inhibition of the acetoclastic methanogens causes the system to progress towards a state of failure. Furthermore, once the system starts towards failure it cannot recover by itself. For recovery, as widely reported in the literature (e.g. Moosbrugger *et al.*, 1993) pH control of the digester must be introduced. However, this will have to happen shortly after the onset of failure, for the process to be effective. As detection method for the onset of failure, effluent SCFA and gas production would seem appropriate parameters – these are widely applied in practise for monitoring digester performance.

5.6 CLOSURE

In this Chapter the two phase (aqueous/gas) integrated biological and physical processes kinetic model describing anaerobic digestion of primary sludge developed in Chapter 4 has been:

- calibrated, to determine constants not available from the literature
- validated, through application to the data set of Izzet *et al.* (1992) in the literature
- appropriately modified and applied to demonstrate the onset of anaerobic digester failure.

In the model calibration, values for most of the constants were found from the literature. However, since a new formulation was introduced for the hydrolysis process, three aspects of this required calibration:

- primary sludge stoichiometric formula
- values for the maximum specific hydrolysis rate and half saturation constants
- unbiodegradable particulate fraction of the primary sludge

To calibrate the above, the data of Izzet *et al.* (1992) was used. From a C mass balance on the Izzet *et al.* system, and from the measured influent organic N, the formulation for the primary sludge was determined to be $C_{3.5}H_7O_2N_{0.196}$. In model application, it became

evident that this stoichiometric formulation is crucial. It in effect determines the amount N and C contained in the influent per measured COD, and hence determines (i) the total N and C that leaves the system, (ii) the production of NH_3 in the hydrolysis and therefore H^+ consumption (alkalinity generation), (iii) the relative amounts of CH_4 and CO_2 in the gas, and (iv) the amount of inorganic C dissolved in the effluent.

It is not certain whether the formulation for primary sludge found in this investigation is general, or restricted to the Izzet *et al.* (1992) data. Clearly this is an area that requires further investigation.

Since a new kinetic formulation for hydrolysis based on Monod – type saturation kinetics (also termed planar surface saturation kinetics) was proposed to replace the more conventional first order kinetic equation, the rate constants had to be determined. This was done by calibrating the hydrolysis to the data set of Izzet *et al.* (1992). In this calibration, the advantages of the proposed kinetics over the first order type kinetics was clearly demonstrated. A single set of hydrolysis rate constants could be used for all retention times, compared to the first order approach where a different kinetic constant needed to be used for each retention time.

Interactively with the calibrations above, the unbiodegradable particulate fraction of the primary sludge in the Izzet *et al.* experiments was determined to be 36%. This value is the same as that determined by O'Rourke *et al.* (1968) for primary sludge in their investigation, which lends validity to the value.

Having calibrated the model, it was validated by application to the Izzet *et al.* (1992) data set. With a single set of model constants, close correlation between predicted and measured results was obtained for all retention times (7, 10, 12, 15 and 20 days), for

- effluent COD
- effluent free and saline ammonia (FSA)
- effluent short chain fatty acids (SCFA)

- effluent $H_2CO_3^*$ alkalinity
- effluent pH
- CO_2 gas production
- CH_4 gas production
- $\bar{p}CO_2$

These results lend substantive support to the validity of the model. However, it is recognized that partial calibration of the model was done using the same data set as for model validation. The model now requires application to a variety of literature data; this is an area for future attention.

Having shown that the model can accurately predict stable anaerobic digester behaviour, the model was modified to incorporate literature reported sensitivities of acetoclastic and hydrogenotrophic methanogens to pH. This proved possible since weak acid/base chemistry, particularly pH, were explicitly included in the model. The resultant model was then used to simulate digester failure, caused by temporary inhibition of the acetoclastic methanogens. The resultant failure process correlates well with observations reported in the literature. This demonstrates the usefulness of the developed kinetic model.

In closure, the two phase anaerobic digestion model, and the approach on which it is based, is a useful tool for research into, and design and operation of, anaerobic digestion systems, in which weak acid/bases significantly influence the behaviour. For research, the model can be used to focus attention on issues not obvious from direct experimentation. For design and operation, the model will allow identification of critical design and control parameters.

In future applications, the model needs to be extended to incorporate anaerobic digestion of waste activated sludges. This will require integration of three phase chemical processes (precipitation, ion pairing), i.e. integration of the model applied in Chapter 3

with that developed in this Chapter. Since both models are kinetically based and have weak acid/base chemistry in common, this should not present undue difficulty.

CHAPTER 6

CONCLUSIONS AND RECOMENDATIONS

6.1 RESEARCH OBJECTIVES

Application of anaerobic digestion to the stabilization of sewage sludges is widespread worldwide. However, the design, operation and control of anaerobic digesters treating sewage sludges still is largely based on experience, or empirical guidelines. To aid the design, operation and control of (and research into) anaerobic digestion, a mathematical model of the system would be an invaluable process evaluation tool. Recognising the potential usefulness of such a model, in this research project the principal aim was to:

- Develop a three phase (aqueous/gas/solid) kinetic model describing the anaerobic digestion of sewage sludges, which integrates the biological, chemical and physical processes.

To achieve the aim above, the research project was divided into two main phases:

- Development and evaluation of a kinetic model that describes the three phase chemical and physical processes possibly operative in the anaerobic digestion of sewage sludges, and

- Develop an integrated two phase (aqueous/gas) biological, chemical and physical processes model aimed at describing the anaerobic digestion system.

If the above two phases could be completed, then the two kinetic models could be readily integrated, to form a complete three phase model describing anaerobic digestion of sewage sludges. However, due to the lack of available comprehensive data in the

literature, and the constraints of time the integration of the two models falls beyond the scope of this research project.

6.2 PHASE I: THREE PHASE CHEMICAL AND PHYSICAL PROCESSES KINETIC MODEL

6.2.1 Phase I tasks

Musvoto *et al.* (1998; 2000a, b) have developed a kinetic model describing the aeration treatment of anaerobic digester supernatant (ADS). This model includes the three phase chemical and physical processes operative in such a treatment scheme. Since the model is based on kinetics, it can be readily integrated with a kinetic model describing the biological processes. Accordingly, it was decided to accept this model for this phase of the research project. However, the model was extensively evaluated against experimental data, and modified if necessary. The Cape Flats Wastewater Treatment Plant (Cape Town, South Africa) was experiencing mineral precipitation difficulties in unit processes treating sludges from the anaerobic digesters, e.g. in the centrifuges and pipelines. This presented an ideal opportunity to evaluate the Musvoto *et al.* (1998; 2000a, b) model, and to use the model to gain greater insight into the mineral precipitation problem at the Cape Flats Wastewater Treatment Plant. Thus, specific tasks identified for this phase were:

- Evaluating the kinetic model of Musvoto *et al.* (1998; 2000a,b), and
- Gaining insight into the mineral precipitation problem at the Cape Flats Wastewater Treatment Plant and providing possible solutions to resolving the problem.

6.2.2 Research approach

A series of experimental investigations were carried out on ADS drawn from the anaerobic digesters at the Cape Flats Wastewater Treatment Plant. These included batch aeration tests, pH controlled experiments and extended pH controlled experiments. The

kinetic model of Musvoto *et al.* (1998; 2000a, b) was then applied to the experimental results to address the tasks above.

6.2.3 Mineral precipitation at Cape Flats

From the results of this investigation the following conclusions on the mineral precipitation at Cape Flats Wastewater Treatment Plant could be made:

- The dominant mineral that precipitates is struvite. For the batch test conducted, struvite was dominant (516 mg/ℓ as $MgNH_4PO_4$ $6H_2O$ = 97% of mass of precipitant), followed by ACP (16.8 mg/ℓ as $Ca_3(PO_4)_2$ = 3% of the mass of precipitant), and negligible newberyite, calcite and magnesite precipitate. Similarly, for the extended pH change test, the dominant mineral that precipitates is struvite (217mg/ℓ as $MgNH_4PO_4$ $6H_2O$ = 99.8% of mass of precipitant), followed by very small amount of amorphous calcium phosphate (ACP) (0.36 mg/ℓ as $Ca_3(PO_4)_2$ = 0.2% of the mass of precipitant), and negligible newberyite, calcite and magnesite precipitate. These observations are similar to those of Musvoto *et al.* With the large volumes of ADS passing to the pelletization plant, this represents substantial precipitation potential.

- The precipitation of struvite is stimulated by the increase in pH when CO_2 is lost from the ADS. Within the anaerobic digester, the partial pressure of CO_2 is high due to anaerobic processes acting in the digester. When the ADS leaves the digester it comes into contact with atmospheric conditions where the partial pressure of CO_2 is much lower than inside the digester. This causes CO_2 loss from the ADS to the air, until equilibrium between the CO_2 concentration in the ADS and the air is reached. Loss of CO_2 can also be caused by pressure drops at pipe bends, pumps, etc. The loss of CO_2 represents an increase in acidity which means that the pH of the ADS will increase. This increase in pH causes struvite to become supersaturated, and hence it precipitates. Increasing the pH by addition

of NaOH also results in struvite precipitation and confirms that the increase in pH is the primary process driving the struvite precipitation.

- When the ADS leaves the digester, it is initially undersaturated with respect to struvite. Depending on the initial conditions in the ADS, significant struvite only starts precipitating when the pH increases above pH = 7.3 to 7.7. This indicates that if the pH of the ADS can be maintained below about 7.3 along the sludge treatment line, then significant struvite precipitation will not take place.

- With aeration, the critical pH for struvite precipitation is reached after 40 to 60 minutes aeration. However, this time will depend on a number of factors, including aeration rate, initial pH, buffer capacity, initial P and Mg concentrations, etc.

- With aeration, the loss of CO_2 from the ADS causes the pH to increase which stimulates struvite precipitation. Initially, the rate of CO_2 loss is rapid. However, as the partial pressure of CO_2 in the ADS approaches that in the atmosphere, the rate of CO_2 loss and consequent pH increase slows, and this effectively slows the rate of struvite precipitation with time. The maximum pH reached with aeration was about pH = 8. However, from about pH = 7.8 the rate of pH increase with time was very low, and consequently, the struvite precipitation effectively ceased. The pH = 7.8 was reached after about 80 minutes. However, this time will depend on a number of factors, including aeration rate, initial pH, buffer capacity, initial P and Mg concentrations, etc.

- The rate of struvite precipitation is very fast, so that essentially, in the aeration of the ADS from Cape Flats, struvite is at equilibrium between the precipitant and soluble species at all times. Thus, in this case the rate of struvite precipitation is not limited by the precipitation kinetics, but rather by the rate in increase in pH through aeration. The increase in pH is limited by the rate of CO_2 stripping.

- The amount of struvite that precipitates is limited by two factors: With aeration to increase pH, the struvite precipitating is limited by the final pH reached and the initial Mg concentration present - if the initial Mg concentration is increased, then more struvite precipitates. With addition of NaOH, the struvite precipitating is limited by the initial Mg concentration present - after precipitation the Mg concentration is very low, while significant concentrations of P and N are still present.

- The initial concentrations of P and Mg in the ADS were variable, with P ranging from 89 to 190 mgP/ℓ , and Mg from 29 to 67 mgMg/ℓ . This is probably indicative of the variable performance of the activated sludge system with regard to BEPR. The higher P concentrations are in agreement with values measured for anaerobically digested BEPR sludges in Johannesburg, at 150 to 250 mgP/ℓ (Pitman, 1995). Should BEPR become more reliable in the activated sludge system at Cape Flats, consistently higher P and Mg concentrations can be expected, with the resultant larger masses of struvite precipitating.

- The change in FSA due to struvite precipitation is insignificant compared with the amount of FSA present. Thus, FSA does not provide a reliable assessment of struvite precipitation, and will not limit the amount of struvite that potentially can precipitate.

- The increase in pH with aeration also stimulates precipitation of ACP. However, as noted above, the mass of ACP precipitating is relatively small compared with struvite. The ADS is initially undersaturated with respect to ACP, and ACP precipitation initiates only after the pH increases above 7.7.

- In running experiments on the ADS, the solids concentrations were so high that the ADS could not be effectively filtered. Accordingly, the ADS was allowed to settle for 5 days and the supernatant used for the experimental investigations. Accordingly, the effect of solids concentration on mineral precipitation could not

be evaluated, e.g. factors such as surface area for nucleation of minerals, inhibition or poisoning of crystal growth. However, the effect of solids is not expected to be significant, because theoretical modelling of the precipitation gave close correspondence with measured values.

- In the experimental investigation it was found that filtering samples through 0.45μm filters caused significant CO_2 loss, which resulted in increase in pH. To counter this, the samples should be acidified prior to filtration with these filters.

- The pH change tests provide a simple rapid method to assess struvite precipitation potential.

6.2.4 Model evaluation

To evaluate the kinetic model, the theoretical predictions from the model were compared with data collected in the extensive experimental investigation on this ADS. Keeping default values for the model constants suggested by Musvoto *et al.*, except for the struvite specific precipitation constant (which was increased form the default value of 300/d to 1000/d), close agreement was obtained between theoretically predicted and experimentally measured data. This would indicate that the kinetic model of Musvoto *et al.* adequately describes integrated three phase chemical and physical processes. The inherent value of such a model was clearly been demonstrated, by providing insight into the precipitation of minerals from ADS at the Cape Flats Wastewater Treatment Plant. From this deeper understanding, recommendations on controlling mineral precipitation (principally struvite) at this treatment plant could be identified.

6.3 PHASE II: TWO PHASE BIOLOGICAL, CHEMICAL AND PHYSICAL PROCESSES MODEL

6.3.1 Phase II tasks

Due to the availability of comprehensive data in the literature, it was decided to restrict the model to be developed to anaerobic digestion of primary sludge. From an

understanding of the processes operative in the anaerobic digester treating primary sludge, drawn from literature, required for inclusion in the two phase (aqueous/gas) kinetic model for anaerobic digesters are:

- biological processes
- chemical processes – weak acid/base chemistry
- physical processes – CO_2, CH_4, H_2 and NH_3 gas exchange

Accordingly in this phase the following specific tasks were identified:

- Develop a kinetic model for describing the biological processes operative in the anaerobic digestion of primary sewage sludges.
- Integrate the physical processes for CH_4 and H_2 gas exchange in the above model
- Integrate the weak acid/base chemistry and CO_2 gas exchange model developed by Musvoto *et al.*, (1997; 1998; 2000a, b) with the biological model above, for a complete description of the two phases in the anaerobic digestion of primary sewage sludges.
- Calibrate and validate the model using experimental data available in the literature.

6.3.2 Research approach

The proposed model was developed in stages. First, the biological processes kinetic model was set up. Then the weak acid/base chemistry kinetic model as developed by Musvoto *et al.* (2000) was integrated with the biological reactions. The complete model was then calibrated and validated against the experimental data set of Izzet *et al.* (1992). Finally, the model was modified and applied to examine anaerobic digester failure.

6.3.3 Biological processes kinetic model

The biological processes kinetic model was based on a modification and simplification of the Gujer and Zehnder (1983) reaction scheme. In setting up the biological processes kinetic model, of note were:

- The primary sludge was formulated as a generic organic representing the combined carbohydrates, lipids and proteins.

- The primary sludge was hydrolysed to the intermediate organic glucose, since the anaerobic pathways with glucose are well established.

- The effect of hydrogen partial pressure ($\overline{pH_2}$) on the anaerobic pathways was incorporated.

- With the exception of the hydrolysis process, formulations for the kinetic rates of the processes were in terms of the appropriate organism group growth rates.

- Where possible, formulations for the kinetic rates were drawn from literature.

- For the hydrolysis processes, the conventional first order rate formulation was rejected, and replaced by planar surface saturation kinetics, similar to that used for the hydrolysis of slowly biodegradable COD in activated sludge systems (Dold *et al.* 1980). This was to eliminate the shortcoming of the first order expression, of varying specific rate constants for different systems.

- The stoichiometry for the processes was developed from the established biochemical reactions.

6.3.4 Weak acid/base chemistry kinetic model

This section of the model was taken directly from that developed by Musvoto *et al.* (1998; 2000c). However, since propionic acid is a key intermediate in the anaerobic digestion process, this weak acid/base was added to the model, by following the approach of Musvoto *et al.* Also, the additional gasses CH_4 and H_2 and their gas loss were included (Musvoto *et al.* do not consider these gasses).

6.3.5 Model calibration

Where possible, values for model constants were drawn from the literature. However, due to the novel formulation of the hydrolysis process, three aspects required calibration:

- Stoichiometric formulation of the primary sludge
- Hydrolysis process maximum specific rate and half saturation constant.
- Unbiodegradable fraction of the primary sludge.

Values for these were determined from the experimental data set of Izzet *et al.* (1992). In this calibration exercise, it became evident that:

- The empirical stoichiometrical chemical formulation used for the primary sludge is crucial. This formulation in effect determines the amount N and C contained in the influent per measured COD, and hence determines (i) the total N and C that leaves the system, (ii) the production of NH_3 in the hydrolysis and therefore H^+ consumption (alkalinity generation), (iii) the relative amounts of CH_4 and CO_2 in the gas, and (iv) the amount of inorganic C dissolved in the effluent. For the N, this could be determined from measurements on the influent TKN and FSA, as the organic N content of the primary sludge (TKN – FSA). However, for the C this had to be determined from a C mass balance on the experimental data. Accepting these, the formulation for the primary sludge was found to be $C_{3.5}H_7O_2N_{0.196}$. However, it is not certain whether this formulation is general or restricted to the

Izzet *et al.* (1992) data. Recognising the importance of the formulation in the modelling efforts, clearly this is an area that requires further investigation.

- A single pair of hydrolysis rate constants could adequately describe the data of Izzet *et al.* (1992), see Section 6.3.6 below.
- The unbiodegradable fraction of the primary sludge in the Izzet *et al.* (1992) experiments was 36%. This corresponds to the value determined by O'Rourke *et al.* (1968) in an independent investigation.

6.3.6 Model validation

The model was validate by application to the data set of Izzet *et al.* (1992). From this application:

- With a single set of constants, close correlation could be achieved between predicted and measured results for:
  - effluent COD
  - effluent free and saline ammonia (FSA)
  - effluent short chain fatty acids (SCFA)
  - effluent $H_2CO_3^*$ alkalinity
  - effluent pH
  - CO_2 gas production
  - CH_4 gas production
  - $\overline{p}CO_2$

  This lends substantive support to validating the model.
- The advantage of the proposed planar surface saturation kinetics for the hydrolysis rate over the conventional first order kinetics was clearly demonstrated – with a single pair of hydrolysis rate constants the observed behaviour could be correctly predicted for all retention times (7 to 20 days), whereas the first order kinetics requires different rate constants for each retention time. This indicates that the proposed hydrolysis kinetics are more general.

- The interactions between the biological processes and weak acid/base chemistry could be correctly predicted for stable steady state operation of anaerobic digesters.
- It was recognized that the same data set was used for calibrating the hydrolysis process (Section 6.3.5 above) and validating the model. Accordingly it was proposed that future work should examine application of the model to other data sets in the literature. However, sufficiently comprehensive data sets are not readily available.

6.3.7 Digester failure

Having shown that the model can accurately predict stable anaerobic digester behaviour, the model was modified to incorporate literature reported sensitivities of acetoclastic and hydrogenotrophic methanogens to pH. This proved possible since weak acid/base chemistry, particularly pH, were explicitly included in the model. The resultant model was then used to simulate digester failure, caused by temporary inhibition of the acetoclastic methanogens. The resultant failure process correlates well with observations reported in the literature. This demonstrates the usefulness of the developed kinetic model.

6.4 FUTURE RESEARCH

From this investigation, the following areas can be identified for further research:

1. The principle aim in this research project was the development of an integrated three phase (aqueous/gas/solid) biological, chemical and physical processes kinetic model describing the anaerobic digestion of sewage sludges. The two main sections of this model were developed and evaluated separately:

    - Three phase chemical and physical processes model
    - Two phase (aqueous/gas) biological, chemical and physical processes model

What remains is to integrate these two sections and evaluate the resultant model against experimental data. Due to the constraints of time this integration of the two models was not undertaken in this research project. However, since both models are kinetically based and have the weak acid/base chemistry in common, the integration is not expected to present undue difficulty. The non – availability of sufficiently comprehensive data in literature may require the appropriate data to be gathered in an experimental investigation.

2. As the stoichiometric composition of the influent sewage sludge has a major influence on the products formed and is a major factor in the modelling of the anaerobic digestion process, further research should be conducted to establish whether the formulation derived for primary sludge ($C_{3.5}H_7O_2N_{0.196}$) is general, or restricted to the primary sludge used in the Izzet *et al.* (1992) experiments. Further, in extending application of the model to waste activated sludge a similar formulation for the sludge will have to be developed. However, more than likely the generally accepted formulation for waste activated sludge of $C_5H_7O_2N$ (WRC, 1984) will prove adequate.

3. With the aid of the model, the failure of anaerobic digesters was investigated theoretically. Digester failure should be investigated experimentally to confirm the failure mechanisms and to refine the model further in order to accurately predict failure and the conditions associated with failure.

APPENDIX A

EXPERIMENTAL RESULTS OBTAINED DURING EXPERIMENTS ON ANAEROBIC DIGESTER SUPERNATANT (ADS) FROM CAPE FLATS WASTEWATER TREATMENT PLANT

During the experimental investigation, the following tests were carried out:

(i) Batch aeration of (ADS)

(ii) pH change tests on ADS

(iii) Extended pH change tests on ADS

Table A.1: Detailed results for batch aeration of ADS from Cape Flats Wastewater Treatment Plant

Sample No.	Time (min)	Conduct. (mS/m)	pH	FSA-CMC (mgN/ℓ)	FSA-UCT (mgN/ℓ)	P (mgP/ℓ)	Ca (mgCa/ℓ)	Mg (mgMg/ℓ)	K (mgK/ℓ)	Na (mgNa/ℓ)	Fe (mgFe/ℓ)	$H_2CO_3^*$ Alkalinity (mg/ℓ as $CaCO_3$)	C_T (mg/ℓ as $CaCO_3$)	SCFA (mg/ℓ as HAc)
1	0	721	6.58	995	932	171	118	60.5	140	130	1.18	416	681	4465
2	5	773	6.58	1034	938	182	127	67.3	154	144	1.19	729	1193	3328
3	10	777	6.63	1069	879	186	125	66.4	156	146	1.1	464	727	3790
4	15	766	6.83	887	672	157	109	55.8	130	123	1.16	487	661	3772
5	20	766	7.05	995	890	172	120	63.3	149	153	1.1	365	444	3646
6	25	769	7.21	1037	932	179	119	66	156	146	NA	384	441	3765
7	30	754	7.37	1050	938	178	112	63.6	153	147	1.08	470	518	3716
8	35	750	7.48	1053	932	174	112	63	157	150	0.91	518	559	3578
9	39	753	7.55	1046	944	177	110	65.5	155	154	1.1	514	548	3813
10	45	740	7.6	1016	932	144	101	45.3	149	142	0.68	553	586	3540
11	50	743	7.59	1027	930	132	102	37.4	152	146	0.69	577	612	3378
12	58	700	7.59	965	784	114	105	30	152	164	NA	546	579	3192
13	65	710	7.61	1058	902	116	102	25	157	154	0.88	78	82	3096
14	71	716	7.67	1018	927	117	107	27	154	152	0.96	381	396	3726
15	81	720	7.76	1021	899	100	115	17	159	160	0.84	381	393	3821
16	90	718	7.84	1010	930	101	115	16.7	154	164	NA	665	686	3103
17	101	654	7.9	963	837	99	113	18.5	147	152	0.86	401	412	3483
18	111	704	7.96	971	916	97	104	16.9	146	145	2.3	468	479	3290
19	121	710	8	930	876	98	100	20.6	142	146	0.93	334	341	3591

Table A.2: Detailed results for pH change test, test set 3

Sample No.	pH	FSA (mgN/ℓ)	P (CMC) (mgP/ℓ)	P (CMC) (mgP/ℓ)	Ca (mgCa/ℓ)	Mg (mgMg/ℓ)	K (mgK/ℓ)	Na (mgNa/ℓ)	Fe (mgFe/ℓ)
1	2.0	1069	153	153	77	45	137	138	0.3
2	8.0	742	122	130	48	2.3	138	141	0.1
3	9.0	627	91	78	42	1.8	126	250	0.1

Table A.3: Detailed results for batch aeration of ADS from Cape Flats Wastewater Treatment Plant. Note that for samples 5 to 10, the pH was increased by addition of NaOH prior to filtration.

Sample No.	**Time** (min)	**Conductivity** (mS/m)	**pH**	**FSA** (mgN/ℓ)	**P** (mgP/ℓ)	**Ca** (CMC) (mgCa/ℓ)	**Mg** (UCT) (mgMg/ℓ)	**Mg** (CMC) (mgMg/ℓ)	**K** (mgK/ℓ)	**Na** (mgNa/ℓ)	**Fe** (mgFe/ℓ)
1	0	720	7.1	731	116	22.4	29.1	0.9	148	147	0.3
2	1		7.2	741	118	26.5		1.8	147	140	
3	53		7.4	653	120.5	25.6		2.2	148	144	
4	71		7.6	614	116	25.8		3.7	152	146	
5	81		7.8	748	113	29.2		2.6	148	145	
6	99		8	569	107.8	28.5		1.6	150	145	
7	115		8.2	692	105.7	26.5		0.7	149	145	
8	141		8.4	688	99.4	24.4		2.1	146	156	
9	181		8.7	716	95.2	22.6		0.9	142	269	
10			9	734	95.2	22.9	2.3	0.9	146	420	0.1

APPENDIX B

THE INTEGRATED PHYSICAL, CHEMICAL AND BIOLOGICAL MODEL PROGRAMMED INTO AQUASIM

In this appendix the integrated physical, chemical and biological model is listed as it was programmed into the computer simulation program AQUASIM (Reichert, 1994). A simulation of anaerobic digestion at 20 days sludge age is given as an example.

****

AQUASIM Version 2.0 (win/mfc) - Listing of System Definition

****

****
Variables
****

A:	Description:	Acetate species concentration
	Type:	Dyn. Volume State Var.
	Unit:	mol/l
	Relative Accuracy:	1e-006
	Absolute Accuracy:	1e-006
Ai:	Description:	Initial A- concentration
	Type:	Formula Variable
	Unit:	mol/l
	Expression:	Ka*ATi/(Hi+Ka)
Ain:	Description:	Acetate in the influent.
	Type:	Formula Variable
	Unit:	mol/l
	Expression:	0.0309578
Alkalinity:	Description:	H2CO3* Alkalinity
	Type:	Formula Variable
	Unit:	mol/l
	Expression:	2*CO3+HCO3+OH-H
AT:	Description:	Total acetate species concentration
	Type:	Formula Variable
	Unit:	mol/l
	Expression:	HAc+A
At:	Description:	Temperature constant for activity coefficients
	Type:	Formula Variable
	Unit:	
	Expression:	1.825e+006*(78.3*Tk)^(-1.5)
ATi:	Description:	Initial total acetate species concentration.
	Type:	Constant Variable
	Unit:	mol/l
	Value:	0.01
	Standard Deviation:	1
	Minimum:	0
	Maximum:	10
	Sensitivity Analysis:	inactive
	Parameter Estimation:	inactive
ba:	Description:	Decay constant for acidogens

	Type:	Constant Variable
	Unit:	d^-1
	Value:	0.041
	Standard Deviation:	0.01
	Minimum:	0
	Maximum:	1
	Sensitivity Analysis:	inactive
	Parameter Estimation:	inactive
bAP:	Description:	Decay constant for acetogens
	Type:	Constant Variable
	Unit:	d^-1
	Value:	0.015
	Standard Deviation:	0.001
	Minimum:	0
	Maximum:	1
	Sensitivity Analysis:	inactive
	Parameter Estimation:	inactive
bH:	Description:	Decay constant for hydrogenotrophic methanogens
	Type:	Constant Variable
	Unit:	d^-1
	Value:	0.01
	Standard Deviation:	0.001
	Minimum:	0.002
	Maximum:	0.015
	Sensitivity Analysis:	inactive
	Parameter Estimation:	inactive
bm:	Description:	Decay constant for acetoclastic methanogens
	Type:	Constant Variable
	Unit:	d^-1
	Value:	0.037
	Standard Deviation:	0.001
	Minimum:	0.03
	Maximum:	0.04
	Sensitivity Analysis:	inactive
	Parameter Estimation:	inactive
CH4:	Description:	Methane produced
	Type:	Dyn. Volume State Var.
	Unit:	mol CH4/l
	Relative Accuracy:	1e-006
	Absolute Accuracy:	1e-006
CH4i:	Description:	Initial CH4 value
	Type:	Constant Variable
	Unit:	mol /l
	Value:	0.4
	Standard Deviation:	0.001
	Minimum:	0
	Maximum:	2
	Sensitivity Analysis:	inactive
	Parameter Estimation:	inactive

CO2:	Description:	Carbon dioxide concentration
	Type:	Dyn. Volume State Var.
	Unit:	mol CO2/l
	Relative Accuracy:	1e-006
	Absolute Accuracy:	1e-006
CO2i:	Description:	Initial CO2 value
	Type:	Constant Variable
	Unit:	mol CO2/l
	Value:	0.2333
	Standard Deviation:	0.001
	Minimum:	0
	Maximum:	2
	Sensitivity Analysis:	inactive
	Parameter Estimation:	inactive
CO3:	Description:	CO3 species concentration.
	Type:	Dyn. Volume State Var.
	Unit:	mol/l
	Relative Accuracy:	1e-006
	Absolute Accuracy:	1e-006
CO3i:	Description:	Initial CO3 species concentration
	Type:	Formula Variable
	Unit:	mol/l
	Expression:	CTi*Kc1*Kc2/(Hi^2+Kc1*Hi+Kc1*Kc2)
CO3in:	Description:	CO3 species concentration in the influent
	Type:	Constant Variable
	Unit:	mol/l
	Value:	2.73222e-008
	Standard Deviation:	1
	Minimum:	0
	Maximum:	10
	Sensitivity Analysis:	inactive
	Parameter Estimation:	inactive
CODp:	Description:	Particulate biodegradable COD concentration
	Type:	Dyn. Volume State Var.
	Unit:	g COD/l
	Relative Accuracy:	1e-006
	Absolute Accuracy:	1e-006
CODpi:	Description:	Initial particulate COD concentration(Feed)
	Type:	Formula Variable
	Unit:	g COD/l
	Expression:	(1-Inert)*Feed_COD
CODpr:	Description:	Matched CODp output (+ Biomass)
	Type:	Formula Variable
	Unit:	g COD/l
	Expression:	CODp+(Xa+XH+Xm+XAP)*83.74*1.5678

CODpt:	Description:	Prediction of the measured CODp
	Type:	Formula Variable
	Unit:	g COD/l
	Expression:	3.4158-(Xa+XH+Xm)*83.744*1.5678
CODp_tot:	Description:	Total particulate COD concentration of feed material
	Type:	Formula Variable
	Unit:	g COD/l
	Expression:	CODp+CODp_unbio+(Xa+XAP+XH+Xm)*83.744*1.5678
CODp_unbio:	Description:	Unbiodegradable particulate COD concentration of feed material
	Type:	Formula Variable
	Unit:	g COD/l
	Expression:	Inert*Feed_COD
CODs:	Description:	Soluble COD concentration - glucose
	Type:	Dyn. Volume State Var.
	Unit:	mol glucose/l
	Relative Accuracy:	1e-006
	Absolute Accuracy:	1e-006
CODsi:	Description:	Initial soluble COD value
	Type:	Constant Variable
	Unit:	mol glucose/l
	Value:	0.0001106
	Standard Deviation:	0.001
	Minimum:	0
	Maximum:	2
	Sensitivity Analysis:	inactive
	Parameter Estimation:	inactive
CT:	Description:	Total carbonate species concentration
	Type:	Formula Variable
	Unit:	mol/l
	Expression:	H2CO3+HCO3+CO3
CTi:	Description:	Initial total carbonate species
	Type:	Constant Variable
	Unit:	mol/l
	Value:	0.005
	Standard Deviation:	1
	Minimum:	0
	Maximum:	10
	Sensitivity Analysis:	inactive
	Parameter Estimation:	inactive
fd:	Description:	Divalent activity coefficient
	Type:	Formula Variable
	Unit:	
	Expression:	10^(-At*2*(sqrt(mu)/(1+sqrt(mu))-0.3*mu))
Feed_COD:	Description:	COD value of feed material

	Type:	Constant Variable
	Unit:	g COD/l
	Value:	42.57
	Standard Deviation:	0.5
	Minimum:	39
	Maximum:	43
	Sensitivity Analysis:	inactive
	Parameter Estimation:	inactive
fm:	Description:	Monovalent activity coefficient
	Type:	Formula Variable
	Unit:	
	Expression:	10^(-At*(sqrt(mu)/(1+sqrt(mu))-0.3*mu))
ft:	Description:	Trivalent activity coefficient
	Type:	Formula Variable
	Unit:	
	Expression:	10^(-At*3*(sqrt(mu)/(1+sqrt(mu))-0.3*mu))
H:	Description:	H+ concentration
	Type:	Dyn. Volume State Var.
	Unit:	mol/l
	Relative Accuracy:	1e-006
	Absolute Accuracy:	1e-006
H2:	Description:	Hydrogen concentration
	Type:	Dyn. Volume State Var.
	Unit:	mol H/l
	Relative Accuracy:	1e-006
	Absolute Accuracy:	1e-006
H2CO3:	Description:	H2CO3 species concentration
	Type:	Dyn. Volume State Var.
	Unit:	mol/l
	Relative Accuracy:	1e-006
	Absolute Accuracy:	1e-006
H2CO3i:	Description:	Initial H2CO3 species concentration
	Type:	Formula Variable
	Unit:	mol/l
	Expression:	CTi*(Hi)^2/(Hi^2+Kc1*Hi+Kc1*Kc2)
H2CO3in:	Description:	H2CO3 concentration in the influent
	Type:	Constant Variable
	Unit:	mol/l
	Value:	0.008537778
	Standard Deviation:	1
	Minimum:	0
	Maximum:	10
	Sensitivity Analysis:	inactive
	Parameter Estimation:	inactive
H2i:	Description:	Initial H2 concentration
	Type:	Constant Variable

	Unit:	mol/l
	Value:	2.866e-005
	Standard Deviation:	0.001
	Minimum:	0
	Maximum:	2
	Sensitivity Analysis:	inactive
	Parameter Estimation:	inactive
H2PO4:	Description:	H2PO4 species concentration.
	Type:	Dyn. Volume State Var.
	Unit:	mol/l
	Relative Accuracy:	1e-006
	Absolute Accuracy:	1e-006
H2PO4i:	Description:	Initial H2PO4 species concentration
	Type:	Formula Variable
	Unit:	mol/l
	Expression:	PTi*Kp1*Hi^2/(Hi^3+Kp1*Hi^2+Kp1*Kp2*Hi+Kp2*Kp1*Kp3)
H3PO4:	Description:	H3PO4 species concentration
	Type:	Dyn. Volume State Var.
	Unit:	mol/l
	Relative Accuracy:	1e-006
	Absolute Accuracy:	1e-006
H3PO4i:	Description:	Initial H3PO4 species concentration
	Type:	Formula Variable
	Unit:	mol/l
	Expression:	PTi*Hi^3/(Hi^3+Kp1*Hi^2+Kp1*Kp2*Hi+Kp1*Kp2*Kp3)
HAc:	Description:	HAc species concentration
	Type:	Dyn. Volume State Var.
	Unit:	mol HAc/l
	Relative Accuracy:	1e-006
	Absolute Accuracy:	1e-006
HAci:	Description:	Initial HAc species concentration
	Type:	Formula Variable
	Unit:	mol HAc/l
	Expression:	Hi*ATi/(Hi+Ka)
HAcin:	Description:	Influent HAc concentration
	Type:	Constant Variable
	Unit:	mol/l
	Value:	0.006442169
	Standard Deviation:	1
	Minimum:	0
	Maximum:	10
	Sensitivity Analysis:	inactive
	Parameter Estimation:	inactive

HCO3:	Description:	HCO3 species concentration
	Type:	Dyn. Volume State Var.
	Unit:	mol/l
	Relative Accuracy:	1e-006
	Absolute Accuracy:	1e-006
HCO3i:	Description:	Initial HCO3 species concentration
	Type:	Formula Variable
	Unit:	mol/l
	Expression:	CTi*Kc1*Hi/(Hi^2+Kc1*Hi+Kc1*Kc2)
HCO3in:	Description:	Influent HCO3 concentration
	Type:	Constant Variable
	Unit:	mol/l
	Value:	0.001185072
	Standard Deviation:	1
	Minimum:	0
	Maximum:	10
	Sensitivity Analysis:	inactive
	Parameter Estimation:	inactive
Hi:	Description:	Inital H+ concentration
	Type:	Formula Variable
	Unit:	mol/l
	Expression:	10^(-pHi)
HPO4:	Description:	HPO4 species concentration
	Type:	Dyn. Volume State Var.
	Unit:	mol/l
	Relative Accuracy:	1e-006
	Absolute Accuracy:	1e-006
HPO4i:	Description:	Initial HPO4 species concentration
	Type:	Formula Variable
	Unit:	mol/l
	Expression:	PTi*Kp1*Kp2*Hi/(Hi^3+Kp1*Hi^2+Kp1*Kp2*Hi+Kp1*Kp2*Kp3)
HPr:	Description:	HPr species concentration
	Type:	Dyn. Volume State Var.
	Unit:	mol/l
	Relative Accuracy:	1e-006
	Absolute Accuracy:	1e-006
H_feed:	Description:	Concentration of H+ in the feed material
	Type:	Formula Variable
	Unit:	mol/l
	Expression:	10^(-pH_feed)
Inert:	Description:	Inert Fraction of Influent COD.
	Type:	Constant Variable
	Unit:	
	Value:	0.36
	Standard Deviation:	1

	Minimum:	0
	Maximum:	10
	Sensitivity Analysis:	inactive
	Parameter Estimation:	inactive
Ka:	Description:	Equilibrium constant for acetate species
	Type:	Formula Variable
	Unit:	
	Expression:	10^(-pKa)/(fm^2)
KAP:	Description:	Acetogenesis half saturation constant
	Type:	Constant Variable
	Unit:	mol Pr/l
	Value:	0.0026786
	Standard Deviation:	0.0001
	Minimum:	0
	Maximum:	1
	Sensitivity Analysis:	inactive
	Parameter Estimation:	inactive
Kc:	Description:	Acidogenesis half saturation constant
	Type:	Constant Variable
	Unit:	mol glucose/l
	Value:	0.000781
	Standard Deviation:	1e-006
	Minimum:	0
	Maximum:	1
	Sensitivity Analysis:	inactive
	Parameter Estimation:	inactive
Kc1:	Description:	Equilibrium constant for carbonate species
	Type:	Formula Variable
	Unit:	
	Expression:	10^(-pKc1)/fm^2
Kc2:	Description:	Equilibrium constant for carbonate species
	Type:	Formula Variable
	Unit:	
	Expression:	10^(-pKc2)/fd
KCO2:	Description:	Constant for CO2 dissolution/ expulsion
	Type:	Formula Variable
	Unit:	
	Expression:	KHCO2*R*Tk
Kfa:	Description:	Rate of dissociation of acetate
	Type:	Formula Variable
	Unit:	
	Expression:	Kra*Ka
Kfc1:	Description:	Rate of dissociation of carbonate

	Type:	Formula Variable
	Unit:	
	Expression:	Krc1*Kc1
Kfc2:	Description:	Rate of dissociation of carbonate
	Type:	Formula Variable
	Unit:	
	Expression:	Krc2*Kc2
KfCO2:	Description:	Rate of CO2 dissolution.
	Type:	Formula Variable
	Unit:	
	Expression:	KrCO2*KCO2
Kfn:	Description:	Rate of dissociation of ammonia
	Type:	Formula Variable
	Unit:	
	Expression:	Krn*Kn
Kfp1:	Description:	Rate of dissociation of phosphate
	Type:	Formula Variable
	Unit:	
	Expression:	Krp1*Kp1
Kfp2:	Description:	Rate of dissociation of phosphate
	Type:	Formula Variable
	Unit:	
	Expression:	Krp2*Kp2
Kfp3:	Description:	Rate of dissociation of phosphate
	Type:	Formula Variable
	Unit:	
	Expression:	Krp3*Kp3
Kfpr:	Description:	Rate of dissociation of propionate
	Type:	Formula Variable
	Unit:	
	Expression:	Krpr*Kpr
Kfw:	Description:	Rate of dissociation of water
	Type:	Formula Variable
	Unit:	
	Expression:	Krw*Kw
KH:	Description:	Hydrogenotrophic methanogenesis half saturation constant
	Type:	Constant Variable
	Unit:	mol H/l
	Value:	2e-006
	Standard Deviation:	1e-005
	Minimum:	0
	Maximum:	1
	Sensitivity Analysis:	inactive
	Parameter Estimation:	active
KH2:	Description:	Hydrogen inhibition constant
	Type:	Constant Variable

	Unit:	mol H/l
	Value:	0.000625
	Standard Deviation:	1e-005
	Minimum:	0
	Maximum:	1.2
	Sensitivity Analysis:	inactive
	Parameter Estimation:	inactive
KHCO2:	Description:	Henry's law constant
	Type:	Formula Variable
	Unit:	mol/l.atm
	Expression:	10^(-pKCO2)
Km:	Description:	Acetoclastic methanogenesis half saturation constant
	Type:	Constant Variable
	Unit:	mol HAc/l
	Value:	1e-006
	Standard Deviation:	0.0001
	Minimum:	0
	Maximum:	0.006
	Sensitivity Analysis:	inactive
	Parameter Estimation:	active
Kn:	Description:	Equilibrium constant for ammonia
	Type:	Formula Variable
	Unit:	
	Expression:	10^(-pKn)
Kp1:	Description:	Equilibrium constant for phosphate
	Type:	Formula Variable
	Unit:	
	Expression:	10^(-pKp1)/(fm^2)
Kp2:	Description:	Equilibrium constant for phosphate
	Type:	Formula Variable
	Unit:	
	Expression:	10^(-pKp2)/fd
Kp3:	Description:	Equilibrium constant for phosphate
	Type:	Formula Variable
	Unit:	
	Expression:	10^(-pKp3)*fd/(ft*fm)
Kpr:	Description:	Equilibrium constant for propionate
	Type:	Formula Variable
	Unit:	
	Expression:	10^(-pKpr)/(fm^2)
Kra:	Description:	Constant for backwards reaction of acetate
	Type:	Formula Variable
	Unit:	s-1
	Expression:	1e+007
Krc1:	Description:	Reverse dissociation constant for carbonate

	Type:	Formula Variable
	Unit:	s-1
	Expression:	1e+007
Krc2:	Description:	Constant for backwards reaction of carbonate
	Type:	Formula Variable
	Unit:	s-1
	Expression:	1e+010
KrCO2:	Description:	Kinetic constant for CO2 dissolution/expulsion
	Type:	Constant Variable
	Unit:	s-1
	Value:	1e+012
	Standard Deviation:	1
	Minimum:	0
	Maximum:	1e+012
	Sensitivity Analysis:	inactive
	Parameter Estimation:	active
Krn:	Description:	Constant for backwards reaction of ammonia
	Type:	Formula Variable
	Unit:	s-1
	Expression:	1e+012
Krp1:	Description:	Constant for backwards reaction of phosphate
	Type:	Formula Variable
	Unit:	s-1
	Expression:	1e+008
Krp2:	Description:	Constant for backwards reaction of phosphate
	Type:	Formula Variable
	Unit:	s-1
	Expression:	1e+012
Krp3:	Description:	Constant for backwards reaction o phosphate
	Type:	Formula Variable
	Unit:	s-1
	Expression:	1e+015
Krpr:	Description:	Constant for backwards reaction of propionate
	Type:	Formula Variable
	Unit:	s-1
	Expression:	1e+007
Krw:	Description:	Constant for backwards reaction of water
	Type:	Formula Variable
	Unit:	s-1
	Expression:	1e+010

ks:	Description:	Half Saturation constant for hydrolysis
	Type:	Constant Variable
	Unit:	mg COD/mol Xa
	Value:	630
	Standard Deviation:	1
	Minimum:	50
	Maximum:	1400
	Sensitivity Analysis:	inactive
	Parameter Estimation:	inactive
Kw:	Description:	Apparent equilibrium constant for water
	Type:	Formula Variable
	Unit:	
	Expression:	10^(-pKw)/fm^2
mu:	Description:	Ionic Strength
	Type:	Formula Variable
	Unit:	
	Expression:	0.000168*SC
mu_max:	Description:	Maximum rate of hydrolysis
	Type:	Constant Variable
	Unit:	d^-1
	Value:	650
	Standard Deviation:	1
	Minimum:	600
	Maximum:	850
	Sensitivity Analysis:	inactive
	Parameter Estimation:	inactive
mu_maxA:	Description:	Maximum rate constant for acidogenesis
	Type:	Constant Variable
	Unit:	d^-1
	Value:	0.8
	Standard Deviation:	0.1
	Minimum:	0.7
	Maximum:	1
	Sensitivity Analysis:	inactive
	Parameter Estimation:	inactive
mu_maxAP:	Description:	Maximum rate constant for acetogenesis
	Type:	Constant Variable
	Unit:	d^-1
	Value:	1.15
	Standard Deviation:	0.01
	Minimum:	0
	Maximum:	1.5
	Sensitivity Analysis:	inactive
	Parameter Estimation:	inactive
mu_maxH:	Description:	Maximum rate constant for hydrogenotrophic methanogens
	Type:	Constant Variable

	Unit:	d^-1
	Value:	0.4
	Standard Deviation:	0.1
	Minimum:	0
	Maximum:	2
	Sensitivity Analysis:	inactive
	Parameter Estimation:	active
mu_maxM:	Description:	Maximum rate constant for acetoclastic methanogens
	Type:	Constant Variable
	Unit:	d^-1
	Value:	0.3
	Standard Deviation:	0.01
	Minimum:	0
	Maximum:	5
	Sensitivity Analysis:	inactive
	Parameter Estimation:	active
NH3:	Description:	NH3 species concentration
	Type:	Dyn. Volume State Var.
	Unit:	mol NH3/l
	Relative Accuracy:	1e-006
	Absolute Accuracy:	1e-006
NH3i:	Description:	Initial NH3 subspecies concentration
	Type:	Formula Variable
	Unit:	mol/l
	Expression:	Kn*NTi/(Hi+Kn)
NH3in:	Description:	Influent NH3 concentration
	Type:	Constant Variable
	Unit:	mol/l
	Value:	3.35095e-006
	Standard Deviation:	1
	Minimum:	0
	Maximum:	10
	Sensitivity Analysis:	inactive
	Parameter Estimation:	inactive
NH4:	Description:	NH4 species concentration
	Type:	Dyn. Volume State Var.
	Unit:	mol/l
	Relative Accuracy:	1e-006
	Absolute Accuracy:	1e-006
NH4i:	Description:	Initial NH4 subspecies concentration
	Type:	Formula Variable
	Unit:	mol/l
	Expression:	Hi*NTi/(Hi+Kn)
NH4in:	Description:	Influent NH4 concentration
	Type:	Constant Variable
	Unit:	mol/l
	Value:	0.013552205

	Standard Deviation:	1
	Minimum:	0
	Maximum:	10
	Sensitivity Analysis:	inactive
	Parameter Estimation:	inactive
NT:	Description:	Total ammonia species concentration
	Type:	Formula Variable
	Unit:	mol/l
	Expression:	NH4+NH3
NTi:	Description:	Initial total species concentration for N
	Type:	Constant Variable
	Unit:	mol/l
	Value:	0.004
	Standard Deviation:	1
	Minimum:	0
	Maximum:	10
	Sensitivity Analysis:	inactive
	Parameter Estimation:	inactive
OH:	Description:	OH- concentration
	Type:	Dyn. Volume State Var.
	Unit:	mol/l
	Relative Accuracy:	1e-006
	Absolute Accuracy:	1e-006
OHi:	Description:	Initial concentration of OH molecules
	Type:	Formula Variable
	Unit:	mol/l
	Expression:	Kw/Hi
parCO2:	Description:	Partial pressure of CO2
	Type:	Formula Variable
	Unit:	
	Expression:	CO2/(CO2+CH4)
pH:	Description:	Calculated pH value
	Type:	Formula Variable
	Unit:	
	Expression:	-log10(H*fm)
pHi:	Description:	Initial pH value
	Type:	Constant Variable
	Unit:	
	Value:	6.5
	Standard Deviation:	1
	Minimum:	0
	Maximum:	10
	Sensitivity Analysis:	inactive
	Parameter Estimation:	inactive
pH_feed:	Description:	pH of the feed material
	Type:	Constant Variable

	Unit:	
	Value:	5.29
	Standard Deviation:	1
	Minimum:	0
	Maximum:	10
	Sensitivity Analysis:	inactive
	Parameter Estimation:	inactive
pKa:	Description:	pK constant for ammonia
	Type:	Formula Variable
	Unit:	
	Expression:	1170.5/Tk-3.165+0.0134*Tk
pKc1:	Description:	pK constant for the carbonate system
	Type:	Formula Variable
	Unit:	
	Expression:	3404.7/Tk-14.8435+0.03279*Tk
pKc2:	Description:	pK constant for the carbonate system
	Type:	Formula Variable
	Unit:	
	Expression:	2902.4/Tk-6.498+0.02379*Tk
pKCO2:	Description:	Henry's law constant for the CO2 dissolution/expulsion
	Type:	Formula Variable
	Unit:	
	Expression:	-2025.3/Tk-0.0104*Tk+11.365
pKn:	Description:	pK constant for nitrogen
	Type:	Formula Variable
	Unit:	
	Expression:	2835.8/Tk-0.6322+0.00123*Tk
pKp1:	Description:	pK constant for the phosphate system
	Type:	Formula Variable
	Unit:	
	Expression:	799.3/Tk-4.5535+0.01349*Tk
pKp2:	Description:	pK constant for the phosphate system
	Type:	Formula Variable
	Unit:	
	Expression:	1979.5/Tk-5.3541+0.01984*Tk
pKp3:	Description:	pK constant for the phosphate system
	Type:	Formula Variable
	Unit:	
	Expression:	12.023
pKpr:	Description:	pK constant for propionate
	Type:	Formula Variable
	Unit:	

	Expression:	1170.5/Tk-3.165+0.0134*Tk
pKw:	Description:	pK constant for water
	Type:	Constant Variable
	Unit:	
	Value:	14
	Standard Deviation:	1
	Minimum:	13
	Maximum:	15
	Sensitivity Analysis:	inactive
	Parameter Estimation:	inactive
PO4:	Description:	PO4 species concentration
	Type:	Dyn. Volume State Var.
	Unit:	mol/l
	Relative Accuracy:	1e-006
	Absolute Accuracy:	1e-006
PO4i:	Description:	Initial PO4 species concentration
	Type:	Formula Variable
	Unit:	mol/l
	Expression:	PTi*Kp1*Kp2*Kp3/(Hi^3+Kp1*Hi^2+Kp1*Kp2*Hi+Kp1*Kp2*Kp3)
Pr:	Description:	Pr subspecies concentration
	Type:	Dyn. Volume State Var.
	Unit:	mol/l
	Relative Accuracy:	1e-006
	Absolute Accuracy:	1e-006
PrT:	Description:	Total propionate species concentration
	Type:	Formula Variable
	Unit:	mol/l
	Expression:	HPr+Pr
PT:	Description:	Total phosphate species concentration
	Type:	Formula Variable
	Unit:	mol/l
	Expression:	H3PO4+H2PO4+HPO4+PO4
PTi:	Description:	Initial total species concentration for phosphate species
	Type:	Constant Variable
	Unit:	mol/l
	Value:	0.003
	Standard Deviation:	1
	Minimum:	0
	Maximum:	10
	Sensitivity Analysis:	inactive
	Parameter Estimation:	inactive
Q_in:	Description:	Influent flow
	Type:	Constant Variable
	Unit:	1/d
	Value:	0.7

	Standard Deviation:	0.1
	Minimum:	0.6
	Maximum:	2
	Sensitivity Analysis:	inactive
	Parameter Estimation:	inactive
R:	Description:	Universal gas constant
	Type:	Constant Variable
	Unit:	l.atm/K.mol
	Value:	0.0820575
	Standard Deviation:	1
	Minimum:	0
	Maximum:	10
	Sensitivity Analysis:	inactive
	Parameter Estimation:	inactive
SC:	Description:	Specific Conductivity
	Type:	Constant Variable
	Unit:	mS/m
	Value:	407
	Standard Deviation:	1
	Minimum:	0
	Maximum:	500
	Sensitivity Analysis:	inactive
	Parameter Estimation:	inactive
t:	Description:	time
	Type:	Program Variable
	Unit:	Days
	Reference to:	Time
Tc:	Description:	Temperature in degrees C
	Type:	Constant Variable
	Unit:	C
	Value:	37
	Standard Deviation:	1
	Minimum:	0
	Maximum:	100
	Sensitivity Analysis:	inactive
	Parameter Estimation:	inactive
Tk:	Description:	Temperature in Kelvin
	Type:	Formula Variable
	Unit:	K
	Expression:	Tc+273.15
Xa:	Description:	Acidogenic biomass concentration
	Type:	Dyn. Volume State Var.
	Unit:	mol organisms/l
	Relative Accuracy:	1e-006
	Absolute Accuracy:	1e-006
Xai:	Description:	Initial acidogenic biomass concentration
	Type:	Constant Variable
	Unit:	mol org/l
	Value:	0.008317

	Standard Deviation:	0.1
	Minimum:	0
	Maximum:	1
	Sensitivity Analysis:	inactive
	Parameter Estimation:	inactive
XAP:	Description:	Acetogenic organism mass concentration
	Type:	Dyn. Volume State Var.
	Unit:	mol org/l
	Relative Accuracy:	1e-006
	Absolute Accuracy:	1e-006
XAPi:	Description:	Initial acetogenic organism mass concentration
	Type:	Constant Variable
	Unit:	mol org/l
	Value:	0.0001778
	Standard Deviation:	0.0001
	Minimum:	0
	Maximum:	1
	Sensitivity Analysis:	inactive
	Parameter Estimation:	inactive
XH:	Description:	Hydrogenotrophic methanogen biomass concentration
	Type:	Dyn. Volume State Var.
	Unit:	mol organisms/l
	Relative Accuracy:	1e-006
	Absolute Accuracy:	1e-006
XHi:	Description:	Initial concentration of hydrogenotrophic organisms mass
	Type:	Constant Variable
	Unit:	mol org/l
	Value:	0.0003067
	Standard Deviation:	0.001
	Minimum:	0.0001
	Maximum:	0.1
	Sensitivity Analysis:	inactive
	Parameter Estimation:	inactive
Xm:	Description:	Acetoclastic methanogen organism mass concentration
	Type:	Dyn. Volume State Var.
	Unit:	mol organisms/l
	Relative Accuracy:	1e-006
	Absolute Accuracy:	1e-006
Xmi:	Description:	Initial concentration of acetoclastic biomass
	Type:	Constant Variable
	Unit:	mol org/l
	Value:	0.0007956
	Standard Deviation:	0.0005
	Minimum:	0.0005
	Maximum:	0.0015

```
                Sensitivity Analysis: inactive
                Parameter Estimation: inactive
--------------------------------------------------------------------------
Y_Ac:           Description:          Yield of acidogens
                Type:                 Constant Variable
                Unit:                 mol org/mol glucose
                Value:                0.1179
                Standard Deviation:   0.001
                Minimum:              0.11
                Maximum:              0.22
                Sensitivity Analysis: inactive
                Parameter Estimation: inactive
--------------------------------------------------------------------------
Y_AM:           Description:          Yield of acetoclastic methanogens
                Type:                 Constant Variable
                Unit:                 mol org/mol HAc
                Value:                0.01635
                Standard Deviation:   0.001
                Minimum:              0.01
                Maximum:              0.02
                Sensitivity Analysis: inactive
                Parameter Estimation: inactive
--------------------------------------------------------------------------
Y_AP:           Description:          Yield of acetogenic organisms
                Type:                 Constant Variable
                Unit:                 mol org/mol Pr
                Value:                0.028958
                Standard Deviation:   0.001
                Minimum:              0
                Maximum:              1
                Sensitivity Analysis: inactive
                Parameter Estimation: inactive
--------------------------------------------------------------------------
Y_HM:           Description:          Yield of hydrogenotrophic
                                      methanogens
                Type:                 Constant Variable
                Unit:                 mol org/mol H2
                Value:                0.004088
                Standard Deviation:   0.0001
                Minimum:              0.004
                Maximum:              0.005
                Sensitivity Analysis: inactive
                Parameter Estimation: inactive
**************************************************************************
```



```
**************************************************************************
Processes
**************************************************************************
Acetoclastic_methanogenesis:
                Description:          Degradation of acetic acid to
                                      methane
                Type:                 Dynamic Process
                Rate:                 mu_maxM*HAc*Xm/(Km+HAc)
```

```
                Stoichiometry:
                  Variable : Stoichiometric Coefficient
                  HAc : -(1+5/2*Y_AM)/Y_AM
                  H2CO3 : 1/Y_AM
                  NH4 : -1
                  CH4 : 1/Y_AM
                  Xm : 1
                  H : 1
-------------------------------------------------------------------------
Acetogenesis:   Description:          Acetogenic conversion of propionate
                                       to HAc
                Type:                 Dynamic Process
                Rate:                 mu_maxAP*Pr*XAP/(KAP+Pr)*(1-(H2/(KH
                                      2+H2)))
                Stoichiometry:
                  Variable : Stoichiometric Coefficient
                  HAc : 1/Y_AP
                  H2 : (1/2+3/Y_AP)
                  HPr : -(1+3/2*Y_AP)/Y_AP
                  H2CO3 : (1/Y_AP-1/2)
                  NH4 : -1
                  XAP : 1
                  H : 1
-------------------------------------------------------------------------
Acetogenic_decay:
                Description:          Endogenous decay


                Type:                 Dynamic Process
                Rate:                 bAP*XAP
                Stoichiometry:
                  Variable : Stoichiometric Coefficient
                  CODp : 160
                  NH3 : 0.762
                  Xa : -1
                  H2CO3 : 0.5
-------------------------------------------------------------------------
Acidogenesis_highH:
                Description:          Acidogenesis of glucose to
                                      propionic and acetic acid under
                                      high pH2


                Type:                 Dynamic Process
                Rate:                 mu_maxA*CODs*Xa/(Kc+CODs)*(H2/(KH2+
                                      H2))
                Stoichiometry:
                  Variable : Stoichiometric Coefficient
                  CODs : -(1+5/6*Y_Ac)/Y_Ac
                  H2 : 1/Y_Ac
                  NH4 : -1
                  Xa : 1
                  HPr : 1/Y_Ac
                  HAc : 1/Y_Ac

                  H : 1
-------------------------------------------------------------------------
```

```
Acidogenesis_lowH:
                Description:          Acidogenesis of glucose to acetic
                                      Acid under low pH2
                Type:                 Dynamic Process
                Rate:                 mu_maxA*CODs*Xa/(Kc+CODs)
                Stoichiometry:
                  Variable : Stoichiometric Coefficient
                  CODs : -(1+5/6*Y_Ac)/Y_Ac
                  HAc : 2/Y_Ac
                  H2 : 4/Y_Ac
                  H2CO3 : 2/Y_Ac
                  NH4 : -1
                  Xa : 1
                  H : 1
-------------------------------------------------------------------------
Acidogenic_decay:
                Description:          Endogenous decay
                Type:                 Dynamic Process
                Rate:                 ba*Xa
                Stoichiometry:
                  Variable : Stoichiometric Coefficient
                  CODp : 160
                  NH3 : 0.762
                  Xa : -1
                  H2CO3 : 0.5
-------------------------------------------------------------------------
AM_decay:       Description:          Endogenous decay
                Type:                 Dynamic Process
                Rate:                 bm*Xm
                Stoichiometry:
                  Variable : Stoichiometric Coefficient
                  CODp : 160
                  NH3 : 0.762
                  Xm : -1
                  H2CO3 : 0.5
-------------------------------------------------------------------------
bdisC1:         Description:          Backward dissociation of HCO3
                Type:                 Dynamic Process
                Rate:                 Krc1*HCO3*H
                Stoichiometry:
                  Variable : Stoichiometric Coefficient
                  H2CO3 : 1
                  HCO3 : -1
                  H : -1
-------------------------------------------------------------------------
bdisC2:         Description:          Backward dissociation of CO3
                Type:                 Dynamic Process
                Rate:                 Krc2*CO3*H
                Stoichiometry:
                  Variable : Stoichiometric Coefficient
                  HCO3 : 1
                  CO3 : -1
                  H : -1
-------------------------------------------------------------------------
bdisHA:         Description:          Backwards dissociation of A-
                Type:                 Dynamic Process
```

```
                Rate:                   Kra*A*H

                Stoichiometry:
                  Variable : Stoichiometric Coefficient
                  HAc : 1
                  A : -1
                  H : -1
-------------------------------------------------------------------------
bdisN:          Description:            Backwards dissociation of NH3
                Type:                   Dynamic Process
                Rate:                   Krn*NH3*H
                Stoichiometry:
                  Variable : Stoichiometric Coefficient
                  NH4 : 1
                  NH3 : -1
                  H : -1
-------------------------------------------------------------------------
bdisP1:         Description:            Backward dissociation of H3PO4
                Type:                   Dynamic Process
                Rate:                   Krp1*H2PO4*H
                Stoichiometry:
                  Variable : Stoichiometric Coefficient
                  H3PO4 : 1
                  H2PO4 : -1
                  H : -1
-------------------------------------------------------------------------
bdisP2:         Description:            Backward dissociation of HPO4
                Type:                   Dynamic Process
                Rate:                   Krp2*HPO4*H
                Stoichiometry:
                  Variable : Stoichiometric Coefficient
                  H2PO4 : 1
                  HPO4 : -1
                  H : -1
-------------------------------------------------------------------------
bdisP3:         Description:            Backward dissociation of PO4
                Type:                   Dynamic Process
                Rate:                   Krp3*PO4*H
                Stoichiometry:
                  Variable : Stoichiometric Coefficient
                  HPO4 : 1
                  PO4 : -1
                  H : -1
-------------------------------------------------------------------------
bdisPr:         Description:            Backwards dissociation of Pr-
                Type:                   Dynamic Process
                Rate:                   Krpr*Pr*H
                Stoichiometry:
                  Variable : Stoichiometric Coefficient
                  HPr : 1
                  Pr : -1
                  H : -1
-------------------------------------------------------------------------
bdisW:          Description:            Backwards dissociation of water
                Type:                   Dynamic Process
                Rate:                   Krw*OH*H
```

```
                Stoichiometry:
                  Variable : Stoichiometric Coefficient
                  OH : -1
                  H : -1
-------------------------------------------------------------------------
DisCO2:         Description:          Dissolution of CO2
                Type:                 Dynamic Process
                Rate:                 KrCO2*parCO2*KHCO2
                Stoichiometry:
                  Variable : Stoichiometric Coefficient
                  CO2 : -1
                  H2CO3 : 1
-------------------------------------------------------------------------
ExpCO2:         Description:          Expulsion of CO2 from solution
                Type:                 Dynamic Process
                Rate:                 KrCO2*H2CO3
                Stoichiometry:
                  Variable : Stoichiometric Coefficient
                  CO2 : 1
                  H2CO3 : -1
-------------------------------------------------------------------------
fdisC1:         Description:          Forward dissociation of H2CO3
                Type:                 Dynamic Process
                Rate:                 Kfc1*H2CO3
                Stoichiometry:
                  Variable : Stoichiometric Coefficient
                  H2CO3 : -1
                  HCO3 : 1
                  H : 1
-------------------------------------------------------------------------
fdisC2:         Description:          Forward dissociation of HCO3
                Type:                 Dynamic Process
                Rate:                 Kfc2*HCO3
                Stoichiometry:
                  Variable : Stoichiometric Coefficient
                  CO3 : 1
                  HCO3 : -1
                  H : 1
-------------------------------------------------------------------------
fdisHA:         Description:          Forward dissociation of HA
                Type:                 Dynamic Process
                Rate:                 Kfa*HAc
                Stoichiometry:
                  Variable : Stoichiometric Coefficient
                  HAc : -1
                  A : 1
                  H : 1
-------------------------------------------------------------------------
fdisN:          Description:          Forward dissociation of NH4+
                Type:                 Dynamic Process
                Rate:                 Kfn*NH4
                Stoichiometry:
                  Variable : Stoichiometric Coefficient
                  NH4 : -1
                  NH3 : 1
                  H : 1
-------------------------------------------------------------------------
```

```
fdisP1:         Description:          Forward dissociation of H3PO4
                Type:                 Dynamic Process
                Rate:                 Kfp1*H3PO4
                Stoichiometry:
                  Variable : Stoichiometric Coefficient
                  H3PO4 : -1
                  H2PO4 : 1
                  H : 1
-------------------------------------------------------------------------
fdisP2:         Description:          Forward dissociation of H3PO4
                Type:                 Dynamic Process
                Rate:                 Kfp2*H2PO4
                Stoichiometry:
                  Variable : Stoichiometric Coefficient
                  H2PO4 : -1
                  HPO4 : 1
                  H : 1
-------------------------------------------------------------------------
fdisP3:         Description:          Forward dissociation of HPO4
                Type:                 Dynamic Process
                Rate:                 Kfp3*HPO4
                Stoichiometry:
                  Variable : Stoichiometric Coefficient
                  HPO4 : -1
                  PO4 : 1
                  H : 1
-------------------------------------------------------------------------
fdisPr:         Description:          Forward dissociation of HPr
                Type:                 Dynamic Process
                Rate:                 Kfpr*HPr
                Stoichiometry:
                  Variable : Stoichiometric Coefficient
                  HPr : -1
                  Pr : 1
                  H : 1
-------------------------------------------------------------------------
fdisW:          Description:          Forward dissociation of water
                Type:                 Dynamic Process
                Rate:                 Kfw
                Stoichiometry:
                  Variable : Stoichiometric Coefficient
                  OH : 1
                  H : 1
-------------------------------------------------------------------------
HM_decay:       Description:          Endogenous decay
                Type:                 Dynamic Process
                Rate:                 bH*XH
                Stoichiometry:
                  Variable : Stoichiometric Coefficient
                  CODp : 160
                  NH3 : 0.762
                  XH : -1
                  H2CO3 : 0.5
-------------------------------------------------------------------------
Hydrogenotrophic_methanogenesis:
                Description:          Conversion of H2 to methane
                Type:                 Dynamic Process
```

```
                Rate:                   mu_maxH*H2*XH/(KH+H2)
                Stoichiometry:
                  Variable : Stoichiometric Coefficient
                  H2 : -(4+10*Y_HM)/Y_HM
                  H2CO3 : -(1+5*Y_HM)/Y_HM
                  NH4 : -1
                  CH4 : 1/Y_HM
                  XH : 1
                  H : 1
-------------------------------------------------------------------------
Hydrolysis:     Description:            Particulate hydrolysis to soluble
                                        COD
                Type:                   Dynamic Process
                Rate:                   (mu_max*CODp/Xa)/(ks+CODp/Xa)*Xa
                Stoichiometry:
                  Variable : Stoichiometric Coefficient
                  CODp : -1
                  CODs : 0.00521
                  NH3 : 0.00149281
                  H2CO3 : -0.00459268
                  H : 0.00055
*************************************************************************
```



```
*************************************************************************
Compartments
*************************************************************************
Anaerobic_Reactor:
                Description:
                Type:                   Mixed Reactor Compartment
                Compartment Index:      0
                Active Variables:       A, CH4, CO2, CODp, CODs, H2, HAc, P
                                        r, Xa, XAP, XH, Xm, CO3, H, H2CO3,
                                        H2PO4, H3PO4, HCO3, HPO4, NH3, NH4,
                                         OH, PO4, HPr
                Active Processes:       bdisHA, bdisN, bdisP1, bdisP2, bdis
                                        P3, bdisW, fdisHA, fdisN, fdisP1, f
                                        disP2, fdisP3, fdisW, bdisC1, fdisC
                                        1, fdisC2, bdisC2, Acetoclastic_met
                                        hanogenesis, Acetogenesis, Acetogen
                                        ic_decay, Acidogenesis_highH, Acido
                                        genesis_lowH, Acidogenic_decay, AM_
                                        decay, DisCO2, ExpCO2, HM_decay, Hy
                                        drogenotrophic_methanogenesis, Hydr
                                        olysis, bdisPr, fdisPr
                Initial Conditions:
                  Variable(Zone) : Initial Condition
                  HAc(Bulk Volume) : HAci
                  NH3(Bulk Volume) : NH3i
                  H(Bulk Volume) : Hi
                  NH4(Bulk Volume) : NH4i
                  A(Bulk Volume) : Ai
                  CO3(Bulk Volume) : CO3i
                  H2CO3(Bulk Volume) : H2CO3i
```

```
    H2PO4(Bulk Volume) : H2PO4i
    H3PO4(Bulk Volume) : H3PO4i
    HCO3(Bulk Volume) : HCO3i
    HPO4(Bulk Volume) : HPO4i
    OH(Bulk Volume) : OHi
    PO4(Bulk Volume) : PO4i
    pH(Bulk Volume) : pHi
    CH4(Bulk Volume) : CH4i
    CO2(Bulk Volume) : CO2i
    CODs(Bulk Volume) : CODsi
    H2(Bulk Volume) : H2i
    Xa(Bulk Volume) : Xai
    XAP(Bulk Volume) : XAPi
    XH(Bulk Volume) : XHi
    Xm(Bulk Volume) : Xmi
    CODp(Bulk Volume) : CODpi
  Inflow:                Q_in
  Loadings:
    Variable : Loading
    CODp : (1-Inert)*Feed_COD*Q_in
    H : H_feed*Q_in
    CO3 : CO3in*Q_in
    H2CO3 : H2CO3in*Q_in
    HCO3 : HCO3in*Q_in
    HAc : HAcin*Q_in
    NH3 : NH3in*Q_in
    NH4 : NH4in*Q_in
    A : Ain*Q_in
  Volume:                14
  Accuracies:
    Rel. Acc. Q:         0.001
    Abs. Acc. Q:         0.001
    Rel. Acc. V:         0.001
    Abs. Acc. V:         0.001
*******************************************************************************
```



```
*******************************************************************************
Definitions of Calculations
*******************************************************************************
calc1:          Description:
                Calculation Number:    0
                Initial Time:          0
                Initial State:         given, made consistent
                Step Size:             1
                Num. Steps:            300
                Status:                active for simulation
                                       inactive for sensitivity analysis
*******************************************************************************
```

```
*****************************************************************************
Plot Definitions
*****************************************************************************
Ac:             Description:          Acetate concentration
                Abscissa:             Time
                Title:                Ac-
                Abscissa Label:       days
                Ordinate Label:       mol/l
                Curves:
                  Type : Variable [CalcNum,Comp.,Zone,Time/Space]
                  Value : A [0,Anaerobic_Reactor,Bulk Volume,0]
-----------------------------------------------------------------------------
Alkalinity:     Description:          H2CO3* Alkalinity
                Abscissa:             Time
                Title:                Alkalinity
                Abscissa Label:       days
                Ordinate Label:       mol/l
                Curves:
                  Type : Variable [CalcNum,Comp.,Zone,Time/Space]
                  Value : Alkalinity [0,Anaerobic_Reactor,Bulk Volume,0]
-----------------------------------------------------------------------------
AT:             Description:          Total acetic acid species concentra
                                      tion
                Abscissa:             Time
                Title:                AT
                Abscissa Label:       days
                Ordinate Label:       mol HAc/l
                Curves:
                  Type : Variable [CalcNum,Comp.,Zone,Time/Space]
                  Value : AT [0,Anaerobic_Reactor,Bulk Volume,0]
-----------------------------------------------------------------------------
CH4:            Description:
                Abscissa:             Time
                Title:                CH4
                Abscissa Label:       days
                Ordinate Label:       mol CH4/l
                Curves:
                  Type : Variable [CalcNum,Comp.,Zone,Time/Space]
                  Value : CH4 [0,Anaerobic_Reactor,Bulk Volume,0]
-----------------------------------------------------------------------------
CO2:            Description:          Plot of the CO2 concentration
                Abscissa:             Time
                Title:                CO2
                Abscissa Label:       days
                Ordinate Label:       mol CO2/l
                Curves:
                  Type : Variable [CalcNum,Comp.,Zone,Time/Space]
                  Value : CO2 [0,Anaerobic_Reactor,Bulk Volume,0]
-----------------------------------------------------------------------------
CODp:           Description:
                Abscissa:             Time
                Title:                Biodegradable CODp
                Abscissa Label:       days
```

```
                Ordinate Label:       g COD/l
                Curves:
                  Type : Variable [CalcNum,Comp.,Zone,Time/Space]
                  Value : CODp [0,Anaerobic_Reactor,Bulk Volume,0]
-------------------------------------------------------------------------
CODpt:          Description:          Particulate COD in effluent
                Abscissa:             Time
                Title:                CODp + Biomass
                Abscissa Label:       days
                Ordinate Label:       g COD/l
                Curves:
                  Type : Variable [CalcNum,Comp.,Zone,Time/Space]
                  Value : CODpt [0,Anaerobic_Reactor,Bulk Volume,0]
-------------------------------------------------------------------------
CODp_tot:       Description:          Total amount of particulate COD
                Abscissa:             Time
                Title:                Total CODp
                Abscissa Label:       days
                Ordinate Label:       g COD/l
                Curves:
                  Type : Variable [CalcNum,Comp.,Zone,Time/Space]
                  Value : CODp_tot [0,Anaerobic_Reactor,Bulk Volume,0]
-------------------------------------------------------------------------
CODp_unbio:     Description:          Unbiodegradable particulate COD
                Abscissa:             Time
                Title:                CODp_unbio
                Abscissa Label:       days
                Ordinate Label:       g COD/l
                Curves:
                  Type : Variable [CalcNum,Comp.,Zone,Time/Space]
                  Value : CODp_unbio [0,Anaerobic_Reactor,Bulk Volume,0]
-------------------------------------------------------------------------
CODs:           Description:          Plot of soluble COD concentration
                Abscissa:             Time
                Title:                CODs
                Abscissa Label:       days
                Ordinate Label:       mol glucose/l
                Curves:
                  Type : Variable [CalcNum,Comp.,Zone,Time/Space]
                  Value : CODs [0,Anaerobic_Reactor,Bulk Volume,0]
-------------------------------------------------------------------------
CT:             Description:          Total carbonate species
                Abscissa:             Time
                Title:                CT
                Abscissa Label:       days
                Ordinate Label:       mol/l
                Curves:
                  Type : Variable [CalcNum,Comp.,Zone,Time/Space]
                  Value : CT [0,Anaerobic_Reactor,Bulk Volume,0]
-------------------------------------------------------------------------
FSA:            Description:
                Abscissa:             Time
                Title:                FSA
                Abscissa Label:       days
                Ordinate Label:       mol/l
                Curves:
                  Type : Variable [CalcNum,Comp.,Zone,Time/Space]
```

```
                Value : NT [0,Anaerobic_Reactor,Bulk Volume,0]
-------------------------------------------------------------------------
H2:             Description:          H2 concentration
                Abscissa:             Time
                Title:                H2
                Abscissa Label:       days
                Ordinate Label:       mol H2/l
                Curves:
                  Type : Variable [CalcNum,Comp.,Zone,Time/Space]
                  Value : H2 [0,Anaerobic_Reactor,Bulk Volume,0]
-------------------------------------------------------------------------
HPr:            Description:          Propionic acid
                Abscissa:             Time
                Title:                Propionic Acid
                Abscissa Label:       days
                Ordinate Label:       mol/l
                Curves:
                  Type : Variable [CalcNum,Comp.,Zone,Time/Space]
                  Value : HPr [0,Anaerobic_Reactor,Bulk Volume,0]
-------------------------------------------------------------------------
NH3:            Description:          NH3 subspecies concentration
                Abscissa:             Time
                Title:                FSA
                Abscissa Label:       days
                Ordinate Label:       mol NH3/l
                Curves:
                  Type : Variable [CalcNum,Comp.,Zone,Time/Space]
                  Value : NH3 [0,Anaerobic_Reactor,Bulk Volume,0]
-------------------------------------------------------------------------
NH4:            Description:          NH4 subspecies concentration
                Abscissa:             Time
                Title:                NH4
                Abscissa Label:       days
                Ordinate Label:       mol NH4/l
                Curves:
                  Type : Variable [CalcNum,Comp.,Zone,Time/Space]
                  Value : NH4 [0,Anaerobic_Reactor,Bulk Volume,0]
-------------------------------------------------------------------------
parCO2:         Description:          partial pressure of CO2
                Abscissa:             Time
                Title:                parCO2
                Abscissa Label:       days
                Ordinate Label:       pCO2
                Curves:
                  Type : Variable [CalcNum,Comp.,Zone,Time/Space]
                  Value : parCO2 [0,Anaerobic_Reactor,Bulk Volume,0]
-------------------------------------------------------------------------
pH:             Description:          pH
                Abscissa:             Time
                Title:                pH
                Abscissa Label:       days
                Ordinate Label:
                Curves:
                  Type : Variable [CalcNum,Comp.,Zone,Time/Space]
                  Value : pH [0,Anaerobic_Reactor,Bulk Volume,0]
-------------------------------------------------------------------------
PrT:            Description:          Total propionate species concentrat
```

```
                                ion
                Abscissa:       Time
                Title:          PrT
                Abscissa Label: days
                Ordinate Label: mole Pr/l
                Curves:
                  Type : Variable [CalcNum,Comp.,Zone,Time/Space]
                  Value : PrT [0,Anaerobic_Reactor,Bulk Volume,0]
-------------------------------------------------------------------------
Xa:             Description:    Acidogenic organism concentration
                Abscissa:       Time
                Title:          Xa
                Abscissa Label: days
                Ordinate Label: mole acidogenic organisms/l
                Curves:
                  Type : Variable [CalcNum,Comp.,Zone,Time/Space]
                  Value : Xa [0,Anaerobic_Reactor,Bulk Volume,0]
-------------------------------------------------------------------------
XAP:            Description:    Acetogenic organism concentration
                Abscissa:       Time
                Title:          Acetogenic organism concentration
                Abscissa Label: days
                Ordinate Label: mol org/l
                Curves:
                  Type : Variable [CalcNum,Comp.,Zone,Time/Space]
                  Value : XAP [0,Anaerobic_Reactor,Bulk Volume,0]
-------------------------------------------------------------------------
XH:             Description:    HP organism concentration
                Abscissa:       Time
                Title:          Hydrogenotrophic methanogens
                Abscissa Label: days
                Ordinate Label: mol XH/l
                Curves:
                  Type : Variable [CalcNum,Comp.,Zone,Time/Space]
                  Value : XH [0,Anaerobic_Reactor,Bulk Volume,0]
-------------------------------------------------------------------------
Xm:             Description:    AM organism concentration
                Abscissa:       Time
                Title:          Acetoclastic methanohens
                Abscissa Label: days
                Ordinate Label: mol Xm/l
                Curves:
                  Type : Variable [CalcNum,Comp.,Zone,Time/Space]
                  Value : Xm [0,Anaerobic_Reactor,Bulk Volume,0]
*************************************************************************
```

```
*************************************************************************
Calculation Parameters
*************************************************************************
Numerical Parameters:    Maximum Int. Step Size:  1
                         Maximum Integrat. Order: 5
                         Number of Codiagonals:   1000
                         Maximum Number of Steps: 1000
```

```
------------------------------------------------------------------------------
                          Fit Method:               secant
                          Max. Number of Iterat.:   100
******************************************************************************
```

REFERENCES

Abbona F, Lündager Madsen HE and Boistelle R (1982). Crystallisation of two magnesium phosphates, struvite an newberyite: effect of pH and concentration. J. Cryst. Growth, **57**(1): 6 – 14.

Abbona F, Lündager Madsen HE and Boistelle R (1986). The initial phases of calcium and magnesium phosphates precipitated from solutions of high to medium concentrations. J. Cryst. Growth, **74**: 592 – 602.

Abbona F, Lündager Madsen HE and Boistelle R (1988). The final phases of calcium and magnesium phosphates precipitated from solutions of high and medium concentration. J. Cryst. Growth, **89**: 581 – 602.

Arvin E (1983). Observations supporting phosphate removal by biologically mediated chemical precipitation – A review. Water Sci. Technol., **15**: 43 – 63.

Betts F, Blumenthal NC and Posner AS (1981). Bone mineralization. J. Cryst. Growth, **53**: 63 – 73.

Blumenthal NC, Betts F and Posner AS (1977). Stabilisation of Amorphous Calcium Phosphate by Mg and ATP. Calcif. Tiss. Res., **23**: 245 – 250.

Borgerding J (1972). Phosphate deposits in digestion systems. J. Water Pollut. Control Fed., **44**(5): 813 – 819.

Butler JN (1964). *Ionic Equilibrium – A Mathematical Approach.* Addison – Wesley Publishing Co. Inc., Reading, Massachusetts.

Chugtai A, Marshall R and Nancollas GH (1968). Complexes in calcium phosphate solutions. J. Phys. Chem., **71**(1): 208 – 211.

Costello DJ, Greenfield PF and Lee PL (1991). Dynamic modelling of a single high rate anaerobic reactor. Part 2. Model verification. Wat. Res. **25**:859 - 871

Cout D, Gennon G, Ranzini M and Romano P (1994). Anaerobic co-digestion of municipal sludges and industrial organic wastes. In: Proceedings of the 7th International Symposium on Anaerobic Digestion. Johannesburg, South Africa.

Dold PL, Ekama GA and Marais GvR (1976). A general model for the activated sludge process. Prog. Water Technol. **12**(6): 47 – 77.

Dold PL, Wentzel MC, Billing AE, Ekama GA and Marais GvR (1991). Activated Sludge Simulation Programs. Published by Water Research Commision, PO Box 824, Pretoria 0001, South Africa.

Dubourguier HC, Prensier G, Samain E and Albagnac G (1985). Granular methanogenic sludge. In: Palz W, Coombs J and Hall DO (Eds). *Energy from biomass.* Elsevier Applied Science Publishers, 542 – 546.

Ferguson JF and McCarthy P (1971). Effects of carbonate and magnesium on calcium phosphate precipitation. Environ. Sci. and Tech. **5**(6): 534 – 540.

Friend JFC, Loewenthal RE (1992). Stasoft III – Chemical Conditioning of Low and Medium Salinity Waters. TT 53/92, ISBN 1 874858 30 6, Water Research Commision, P O Box 824, Pretoria, 0001, RSA

Gujer W and Zehnder AJB (1983). Conversion processes in anaerobic digestion. Wat. Sci. Tech. **15**(8/9): 127 – 167.

Gunn DJ (1976). Mechanisms for the formation and growth of ionic precipitates from aqueous solution. Faraday Discuss. Chem. Soc., **61**: 133 – 134.

Henze M, Grady CPL (Jr), Gujer W, Marais GvR and Matsuo T (1987). Activated Sludge Model No. 1. IAWPRC Scientific and Technical Report No.1, IAWPRC, Londen.

Heughebaert JC and Nancollas GH (1984). Kinetics of crystallisation of octacalcium phosphate. J. Phys. Chem., **88**: 2478 – 2481.

Hill DT and Barth CL (1977). A dynamic model for simulation of animal waste digestion. Technical Contribution No. 1318. Journal WPCF October 1977: 2129 – 2143.

Hoffmann RJ (1972). Phosphorus removal in the modified activated sludge process. Research Report W22, Dept. of Civil Eng., Univ. of Cape Town, Rondebosch 7700, South Africa.

Hoffmann RJ and Marais GvR (1977). Phosphorus Removal in the Modified Activated Sludge Process. Research Report W22, Dept. of Civil Eng., Univ. of Cape Town, Rondebosch 7701, South Africa.

Huser BA, Wuhrmann K and Zehnder AJB (1982). Methanothrix Soehngenii gen. nov. sp. nov., a new acetotrophic non-hydrogen oxidising methane bacterium., Arch. Microbio. **132**: 1 – 9.

Izzet HB, Wentzel MC and Ekama GA (1992). The effect of thermophilic heat treatment on the anaerobic digestibility of primary sludge. Research Report W76, Univ. of Cape Town, Dept. of Civil Eng. Rondebosch 7701, Cape, South Africa.

Jenkins D, Menar AB and Ferguson JF (1972). Recent studies of calcium phosphate precipitation in wastewaters. In: Applications of New Concepts of Physical –

Chemical Wastewater Treatment (Eckenfelder WW and Cecil LK Eds). Prog . Water Technol., **1**: 211 – 230.

Jewell WJ (1987). Anaerobic sewage treatment. Environmental Science and Technology., **21**: 14 – 21.

Jones DT and Woods DR (1986). Acetone-Butanol fermentation revisited. Microb. Rev., **50**(4): 474 – 524.

Kaspar HF and Wuhrmann K (1987). Kinetic parameters and relative turnovers of some important catabolic reactions in digesting sludge. Appl. Environ. Microbiol., **36**: 1 – 7.

Kayhanian M and Tchobanoglous G (1992). Pilot investigation of an innovative two-stage anaerobic digestion and aerobic composting process for the recovery of energy from the organic fraction of MSW. In: Proceedings of the 5th International Symposium on Anaerobic Digestion. Venice, Italy.

Kiely G, Tayfur G, Dolan C and Tanji K (1997). Physical and mathematical modelling of anaerobic digestion of organic wastes. Wat. Res. **31**(3): 534 – 540.

Koutsoukos P, Amjad Z, Tomson MB and Nancollas GH (1980). Crystallisation of calcium phosphates. A constant composition study. J. Am. Chem. Soc., **27**: 1553 – 1557.

Laubscher ACJ (2000). Operational problems in a UASB system treating distillery wastewaters. MSc. Thesis, Univ. of Cape Town, Dept of Civil Eng., Rondebosch 7700, Cape Town, South Africa

Lehninger AL, (1972). *Biochemistry.* Worth Publishers Inc., 70 Fifth Avenue, New York, N Y 10011.

Loewenthal RE and Marais GvR (1976). *Carbonate Chemistry of Aquatic Systems – Theory and application.* Ann Arbor Science Publishers, P O Box 1425, Ann Arbor, Michigan 48106, USA.

Loewenthal RE, Wiechers HNS, Marais GvR (1986). *Softening and stabilization of municipal waters.* Published by Water Research Commission, P O Box 824, Pretoria 0001, South Africa, 4.32 – 4.35.

Loewenthal RE, Ekama Ga and Marais GvR (1989). Mixed weak acid/base systems: Part I – Mixture characterisation. Water SA **15**(1): 3 – 24.

Loewenthal RE, Wentzel MC, Ekama GA and Marais GvR (1991). Mixed weak acid/base systems: Part II – Dosing estimation, aqeous phase. Water SA **17**(2): 107 – 122.

Loewenthal RE, Kornmuller URC and van Heerden EP (1994). Struvite precipitation in anaerobic treatment systems. *Water Sci. Technol.* **30**(12): 107 – 116.

Mamais D, Pitt PA, Cheng YW, Loiacono J and Jenkins D (1994). Determination of ferric chloride dose to control struvite precipitation in anaerobic sludge digester. Water Environ. Res., **66**(7).

Massé DI and Droste RL (1999). Comprehensive model of anaerobic digestion of swine manure slurry in a sequencing batch reactor. Wat. Res. **34**(12): 3087 – 3106.

McCarty PL (1974). Anaerobic Processes. Proceedings of the Birmingham shortcourse on design aspects of biological treatment. International association of water pollution research, Birmingham, England.

McCarty PL (1981). *One hundred years of anaerobic treatment. In: Anaerobic Digestion*, DE Hughes *et al.* (Eds). Elsevier Biomedical Press, Amsterdam, 3 - 22.

Mcinerney MJ, Bryant MP and Stafford DA (1979). In: *Anaerobic Digestion.* (Eds). DA Stafford, BI Wheatly and DE Hughes. Applied Science Publishers Ltd., Ripple Road, Barking, Essex, England.

McInerney MJ and Bryant MP (1981). Basic principles of bioconversions in anaerobic digestion and methanogenesis. In: *Biomass Conversion Processes for Energy and Fuels.* SR Sofer and OR Zaborsky (Eds.). Plenum-Press, New York.

Meyer JL and Eanes ED (1978). A thermodynamic analysis of the amorphous to crystalline calcium phosphate transformation. Calcf. Tiss. Res., **25**: 59 – 68.

Mohajit KK, Bhattarai E, Taiganides EP and Yap BC (1989). Struvite deposits in pipes and aerators. Biol. Wastes, **30**: 133 – 147.

Moosbrugger RE, Wentzel MC, Ekama GA and Marais GvR (1992). Simple titration procedures to determine $H_2CO_3^*$ alkalinity and short chain fatty acids in aqueous solutions containing known quantities of ammonium, phosphate and sulphide weak acid/bases. Published by Water Research Commission, P O Box 824, Pretoria 0001, South Africa.

Moosbrugger RE, Wentzel MC, Ekama GA and Marais GvR (1993). Weak acid/bases and pH control in anaerobic systems – A review. Water SA, **19**(1): 1 – 10.

Moutin T, Gal JY, El Hlouani H, Picot B and Bontoux J (1992). Decrease of phosphate concentration in a high rate pond by precipitation of calcium phosphate: Theoretical and experimental results. Water Res. **26**(11): 1445 – 1450.

Mullin JW (1972). *Crystallisation.* Londen, Butterworths.

Munz C and Roberts PV (1989). Gas and liquid – phase mass transfer resistances of organic compounds during mechanical surface aeration. Water Res **23**(5): 589 – 601

Murray K and May PM (1996). Joint Expert Speciation System (JESS). An international computer system for determining chemical speciation in aqueous and non-aqueous environments. Supplied by Murdoch University, Murdoch 6150, Western Australia and the Division of Water Technology, CSIR, PO Box 395, Pretoria, South Africa.

Musvoto EV, Wentzel MC, Loewenthal RE and Ekama (1997). Kinetic-based model for weak acid/base systems. Water SA **23**(4) 311 – 322.

Musvoto EV (1998). Mathematical modelling of integrated chemical, physical amd biological treatment of wastewaters. Ph.D Thesis, Univ of Cape Town, Dept of Civ. Eng., Rondebosch 7700, Cape Town, South Africa.

Musvoto EV, Wenzel MC, Ekama GA and Loewenthal RE (1998). Mathematical modelling of integrated chemical, physical and biological treatment of wastewaters. Research Report W97, Univ. of Cape Town, Dept. of Civil Eng., Rondebosch 7701, Cape, South Africa.

Musvoto EV, Wentzel MC, Loewenthal RE and Ekama GA (2000a). Integrated chemical – physical processes modelling – I. Development of a kinetic – based model for mixed weak acid/base systems. Wat. Res. **34**(6): 1857 – 1867.

Musvoto EV, Wentzel MC, Loewenthal RE and Ekama GA (2000b). Integrated chemical – physical processes modelling – II. Simulation aeration treatment of anaerobic digester supernatants. Wat. Res. **34**(6): 1868 – 1880.

Musvoto EV, Ekama GA, Wentzel MC and Loewenthal RE (2000c). Extension and application of the three – phase weak acid/base kinetic model to the aeration treatment of anaerobic digester liquors. Water SA **26**(4): 417 – 438.

Nancollas GH and Pirdie N (1964). The kinetics of crystal growth. Chem. Soc., Quarterly Reviews, **18**: 1 – 20.

Nordstrom DK, Plummer NL, Langmuir D, Busenberg E, May HM, Jones BF and Parkhurst DL (1990). Revised chemical and equilibrium data for major water – mineral reactions and their limitations. Am. Chem. Soc., **416**: 398 – 413

O'Rourke JT (1968). Kinetics of anaerobic treatment at reduced temperatures. Dissertion, Department of Civil Engineering, Stanford University.

Pavliostathis SG and Giraldo-Gomez E (1991). Kinetics of anaerobic treatment. Wat. Sci. Tech. **24**(8): 35 - 59.

Pitman AR (1995). Practical experiences with biological nutrient removal on full-scale plants in South Africa. Presented at International Konferenz Zur Vermehrten Biologischen Phosphorelimination, Hanover, Germany.

Reichert P (1994). AQUASIM – A tool for simulation and data analyses of aquatic systems. Water Sci. and Technol., **30**(2): 21 – 30.

Reichert P, Schultness R and Wild D (1995). The use of AQUASIM for estimating parameters of activated sludge models. Water Sci. Technol., **31** (2): 135 – 147.

Ristow NE (1999). The modelling of a Falling Sludge Bed Reactor using AQUASIM. MSc. Thesis, Univ. of Cape Town, Dept. Chem. Eng., Rondebosch 7700, Cape Town, South Africa.

Roques H and Girou A (1974). Kinetics of the formation conditions of carbonate tartars. Water Res., **8**: 907 – 920.

Sam-Soon PALNS, Loewenthal RE, Wentzel MC and Marais GvR (1990a). Growth of biopellets on glucose in upflow anaerobic sludge bed (UASB) systems. Water SA **16**(3) 151 – 164.

Sam-Soon PALNS, Wentzel MC, Dold PL, Loewenthal RE and Marais, GvR (1991). Mathematical modelling of upflow anaerobic sludge bed (UASB) systems treating carbohydrate waste waters. Water SA **17**(2): 91 – 106.

Scott WD, Wrigley TJ, and Webb KM (1991). A computer model for struvite solution chemistry. Talanta, **38**(8): 889 – 895.

Sillen LG and Martell AE (1964). *Stability constants of metal ion complexes.* Special publications, The Chemical Society, London.

Standard Methods (1985). *Standard Methods for the Examination of Water and Wastewater.* 16th Edn. APHA, AWWA & QPCF, New York.

Stumm W and Morgan JJ (1970). *Aquatic chemistry.* Wiley Interscience.

Stumm W and Morgan JJ (1981). *Aquatic chemistry.* Wiley Interscience.

Taylor AW, Frazier AW and Gurney EL (1963). Trans. Faraday Soc., **59**: 1580.

Thauer RK, Jungermann K and Decker K (1977). Energy conservation in chemotropic anaerobic bacteria. Bact. Rev., **41**: 100 – 180.

Van Haandel AC, Ekama GA and Marais GvR (1992). The activated sludge process Part 3 – Single sludge denitrification. Water Res. **15**: 1135 – 1152.

Vavilin VA and Lokshina Lya (1996). Modeling of volatile fatty acids degradation kinetics and evaluation of microorganism activity. Biores. Tech. **57**(1):69 – 80.

Verbeek RMH and Devenyns JAH (1992). The kinetics of dissolution of octalcium phosphate II. The combined effects of pH and solution Ca/P ratio. J. Cryst Growth, **121**: 335 – 348.

Wiechers HNS, Loewenthal RE and Marais GvR (1980). Lime treatment of wastewater: Development and application of a simple graphical technique for predicting the chemical composition of lime – treated secondary effluent. Prog. Water Technol. **12** (Toronto): 347 – 358.

Wolin MJ (1974). Metabolic interaction among intestinal micro-organisms. Am. Journ. Clin. Nutr., **24**: 1320 – 1328.

Wood HG (1982). *Of oxygen, fuels and living matter, Part 2*. G. Semenza (Ed). John Wiley and Sons, New York.

Zehnder AJB, Huser BA, Brock TD and Wuhrmann K (1980). Characterising of an acetate decarboxylating non-hydrogen oxidizing methane bacteria. Arch. Microbiol. **124**: 1 – 11.

Zehnder AJB and Wuhrmann K (1977). Physiology of a Methanobacterium strain AZ. Arch. Mikrobiol. **III**: 199 – 205.